American
Petroleum
Institute

STEP
Strategies for Today's
Environmental Partnership

A GUIDANCE MANUAL FOR MODELING HYPOTHETICAL ACCIDENTAL RELEASES TO THE ATMOSPHERE

Health and Environmental Sciences Department
Publication Number 4628
November 1996

STEP

Strategies for Today's
Environmental Partnership

One of the most significant long-term trends affecting the future vitality of the petroleum industry is the public's concerns about the environment. Recognizing this trend, API member companies have developed a positive, forward-looking strategy called STEP: Strategies for Today's Environmental Partnership. This program aims to address public concerns by improving our industry's environmental, health and safety performance; documenting performance improvements; and communicating them to the public. The foundation of STEP is the API Environmental Mission and Guiding Environmental Principles.

API ENVIRONMENTAL MISSION AND GUIDING ENVIRONMENTAL PRINCIPLES

The members of the American Petroleum Institute are dedicated to continuous efforts to improve the compatibility of our operations with the environment while economically developing energy resources and supplying high quality products and services to consumers. The members recognize the importance of efficiently meeting society's needs and our responsibility to work with the public, the government, and others to develop and to use natural resources in an environmentally sound manner while protecting the health and safety of our employees and the public. To meet these responsibilities, API members pledge to manage our businesses according to these principles:

- To recognize and to respond to community concerns about our raw materials, products and operations.
- To operate our plants and facilities, and to handle our raw materials and products in a manner that protects the environment, and the safety and health of our employees and the public.
- To make safety, health and environmental considerations a priority in our planning, and our development of new products and processes.
- To advise promptly, appropriate officials, employees, customers and the public of information on significant industry-related safety, health and environmental hazards, and to recommend protective measures.
- To counsel customers, transporters and others in the safe use, transportation and disposal of our raw materials, products and waste materials.
- To economically develop and produce natural resources and to conserve those resources by using energy efficiently.
- To extend knowledge by conducting or supporting research on the safety, health and environmental effects of our raw materials, products, processes and waste materials.
- To commit to reduce overall emission and waste generation.
- To work with others to resolve problems created by handling and disposal of hazardous substances from our operations.
- To participate with government and others in creating responsible laws, regulations and standards to safeguard the community, workplace and environment.
- To promote these principles and practices by sharing experiences and offering assistance to others who produce, handle, use, transport or dispose of similar raw materials, petroleum products and wastes.

A Guidance Manual For Modeling Hypothetical Accidental Releases to the Atmosphere

Health and Environmental Sciences Department

API PUBLICATION NUMBER 4628

PREPARED UNDER CONTRACT BY:

JAMES H. MOSER, PH.D.
JAMES MOSER RESEARCH, INC.
PO BOX 898
CYPRESS, TX 77410-0898

NOVEMBER 1996

American
Petroleum
Institute

FOREWORD

API PUBLICATIONS NECESSARILY ADDRESS PROBLEMS OF A GENERAL NATURE. WITH RESPECT TO PARTICULAR CIRCUMSTANCES, LOCAL, STATE, AND FEDERAL LAWS AND REGULATIONS SHOULD BE REVIEWED.

API IS NOT UNDERTAKING TO MEET THE DUTIES OF EMPLOYERS, MANUFACTURERS, OR SUPPLIERS TO WARN AND PROPERLY TRAIN AND EQUIP THEIR EMPLOYEES, AND OTHERS EXPOSED, CONCERNING HEALTH AND SAFETY RISKS AND PRECAUTIONS, NOR UNDERTAKING THEIR OBLIGATIONS UNDER LOCAL, STATE, OR FEDERAL LAWS.

NOTHING CONTAINED IN ANY API PUBLICATION IS TO BE CONSTRUED AS GRANTING ANY RIGHT, BY IMPLICATION OR OTHERWISE, FOR THE MANUFACTURE, SALE, OR USE OF ANY METHOD, APPARATUS, OR PRODUCT COVERED BY LETTERS PATENT. NEITHER SHOULD ANYTHING CONTAINED IN THE PUBLICATION BE CONSTRUED AS INSURING ANYONE AGAINST LIABILITY FOR INFRINGEMENT OF LETTERS PATENT.

CONTRACTOR'S ACKNOWLEDGMENTS

The author wishes to recognize and thank the following people for their contributions of time and expertise during this study and for their support in the development of this document. Many technical and editorial contributions were made which enhanced the content of the Manual as well as its organization:

Mr. K. W. Steinberg, Exxon Research & Engineering, Chair, Air Modeling Task Force of the American Petroleum Institute

Howard Feldman, API Staff, Health and Environmental Science Department; and these members of the Air Modeling Task Force: **Doug N. Blewitt,** Amoco Corporation, **Richard W. Carney,** Phillips Petroleum Company, **Mark W. Deese,** Phillips Petroleum Company, **David J. Fontaine,** Chevron Research & Technology, **Lee K. Gilmer,** Texaco Research, **Marvin Hertz** (dec.), Shell Development Company, **John A. King,** Shell Development Company, **Gilbert Jersey,** Mobil Research & Development, **George Lauer,** ARCO, **Robert L. Peace, Jr.,** Unocal Corporation, **Jerry Hill,** Bechtel Corporation.

Richard M. Gustafson, Texaco Inc, also a member of the API Air Modeling Task Force, contributed significantly to the content and presentation of thermodynamic as well as fluid dynamic concepts in Chapter 3 on Source Modeling.

Frank L. Worley, Jr., Ph.D., P.E., Professor of Chemical Engineering at the University of Houston, who significantly contributed to the Manual's development by reviewing the initial manuscript in its entirety. In addition, he provided significant insight and knowledge for the design and modeling of water spray mitigation barriers.

Ronald L. Petersen, Ph.D., Vice President of Cermak Peterka Petersen, Inc., who provided much information and references on physical modeling of dispersion and mitigation of accidental releases, and contributed to the chapter on meteorology.

Robert N. Meroney, Ph.D., Professor of Engineering, Fluid Mechanics and Wind Engineering, Colorado State University, who provided significant assistance in the presentation of methods for incorporating the effects of contaminant removal and jet-induced air entrainment by water spray barriers and physical barriers into the dispersion modeling process.

The instruction and assistance of **Peter T. Roberts,** Shell Research Ltd., Thornton Research Centre, England, in the proper usage of HGSYSTEM for modeling the effect of removal- and/or physical-type plume mitigation barriers for the hydrogen fluoride release/dispersion/mitigation simulation which was greatly appreciated.

Most of all, I wish to thank and compliment **Carol O. Moser** of James Moser Research, Inc., for her major efforts of data processing, graphing simulation results, desk-top publishing, editing and proofreading. Her technical and editorial support greatly facilitated the development of this document; her assistance was invaluable.

PREFACE

This manual presents methods for modeling hypothetical accidental releases of fluids into the atmosphere from petroleum process operations. Given a particular type of release (e.g., pipe break, evaporating pool) and the chemicals or petroleum fractions involved, methods for modeling the release and subsequent dispersion phenomena are treated in a step-wise, comprehensive manner. The reader is presumed to be technically oriented, but not a specialist in the various disciplines represented.

Release phenomena, germane meteorological concepts, and after-the-fact mitigation countermeasures are presented for ready reference in this document. First, fluid dynamic and thermodynamic procedures best used to calculate flow rates and initial fluid states for a material being released into the atmosphere are given in some detail, including numerical examples. Next, the essential information required to characterize the atmosphere for dispersion modeling is presented, along with recommended default parameters. Lastly, available quantitative methods for incorporating vapor cloud mitigation methods into the dispersion modeling are presented.

To demonstrate how a number of the modeling procedures can be implemented, detailed simulation of eight hypothetical release scenarios are presented. The assumptions made, the calculation and/or selection of appropriate modeling parameters, use of several well-known modeling programs, and graphical presentation of results obtained are discussed.

It is not possible to present all the information that might be required for the various disciplines involved; however, extensive references are provided.

TABLE OF CONTENTS

CHAPTER ONE: Introduction

CHAPTER TWO: Overview of Release/Dispersion Processes and Demonstration Scenarios

CHAPTER THREE: Source Modeling

Contents

Chapter 3 (continued)

Contents

Chapter 3 (continued)

CHAPTER FOUR: **Meteorology**

CHAPTER FIVE: **Mitigation Countermeasure Modeling**

Contents

Chapter 5 (continued)

CHAPTER SIX: **Analysis and Simulation of Release Scenarios**

1: Hydrogen Sulfide from Unlit Flare Stack

2: Hydrogen Sulfide and Carbon Dioxide from a Safety Relief Stack

3: Supercritical Propane Pipe Hole Release

Contents

Chapter 6 (continued)

4: Oil Well Blowout

5: Liquified Chlorine Tank Truck Accident

6: Ammonia Hose or Pipe Break

7: Hydrogen Chloride Pipe Break

8: Evaporating Pool of Liquid Benzene

Contents

Chapter 8 (continued)

APPENDIX II: **Overview of Scenario Modeling Programs**

FIGURES AND TABLES

I. Figures

Chapter 2: ***Overview of Release/Dispersion Processes and Demonstration Scenarios***

Chapter 3: ***Source Modeling***

Chapter 4: ***Meteorology***

Chapter 5: ***Mitigation Countermeasure Modeling***

Chapter 6: ***Scenario 1***

Figures and Tables

Figures (continued)

Chapter 6: ***Scenario 2***

Chapter 6: ***Scenario 3***

Chapter 6: ***Scenario 4***

Chapter 6: ***Scenario 5***

Chapter 6: ***Scenario 6***

Chapter 6: ***Scenario 7***

Chapter 6: ***Scenario 8***

Figures and Tables

II. Tables

Tables (continued)

Chapter 6: ***Scenario 8***

Appendix II: ***Overview of Scenario Modeling Programs***

III. Example Boxes

Chapter 3: ***Source Modeling***

NOMENCLATURE

NOMENCLATURE

Symbol	Quantity	SI Units of Measure[a]
L	Length	meters, m
M	Mass	kilogram, kg
F	Force	newton, N
τ	Time	seconds, s
E	Energy	joules, J
T	Temperature	kelvin, K
P	Pressure	Pascal (derived)
kmol[b]	Moles	kilogram molecular weight

a: If blank, the quantity is dimensionless, a fraction, or a count.

b: "mol" is defined as one gram molecular weight.

Symbol	Description	Units of Measure
A	Throat area, pool area, etc.	L^2
$\mathbf{A_s}$	Effective area for air entrainment by sprays	L^2
B	Buoyancy factor for evaporation	
$\mathbf{C_p}$	Heat capacity at constant pressure (+ subscripts **l** or **v**)	E/[M•T]
$\mathbf{C_D}$	Discharge coefficient	
$\mathbf{C_I}$	Cloudiness index	
c	Concentration	M/L^3
D	Diameter (e.g, orifice, evaporating pool)	L
d	Ordinary differential operator	
E	Energy	E/M
$\mathbf{E_{int}}$	Internal energy	E/M
$\mathbf{E_{kin}}$	Kinetic energy	E/M
$\mathbf{E_{pot}}$	Potential energy	E/M
$\mathbf{F_N}$	Nozzle flow number for Equation 5-1	
FDF	Finite duration factor	
$\mathbf{f_{n\,s}}$	Mole fraction in cloud entering spray barrier	
$\mathbf{f_s}$	Mole fraction in cloud leaving spray barrier	
$\mathbf{f_{rm}}$	Mole fraction released material	
$\mathbf{f_v}$	Mole fraction vapor (or weight for pure component)	
G	Mass flux	$M/[L^2 \bullet \tau]$
$\mathbf{G_{max}}$	Maximum mass flux	$M/[L^2\tau]$
G'	Normalized mass flux, Leung/Epstein model	$M/[L^2\tau]$
g	Gravitational constant (= 9.807 m/s^2)	L/τ^2
H	Enthalpy	E/M
h	Heat transfer coefficient, air-to-pool	$E/[T\tau]$
$\mathbf{h_f}$	Vapor barrier fence height	L
$\mathbf{h_l}$	Liquid head	L
hpool	Height of evaporating pool	L
K	Equilibrium vapor/liquid mole fraction ratio (Chapter 3)	
K	Empirical nozzle constant (Chapter 5)	
k	Specific heat ratio	
k	von Karman's constant (0.41)	
$\mathbf{k_c}$	Convective mass transfer coefficient	L/τ

Nomenclature

Symbol	Description	Units of Measure
k_s	Thermal conductivity of ground	E/[LTτ]
L	Length of water curtain, Equation 5-1	L
L_{ns}	Lateral spray nozzle separation distance	L
M	Molecular weight	M/kmol
M	Momentum flow rate per unit length of barrier	F/L
m	Number of spray nozzles	
N_{Pr}	Prandtl number	
N_{Re}	Reynolds number	
N_s	Number of chemical species	
N_{Sc}	Schmidt number	
N_{sh}	Sherwood number	
n	Number of intervals, samples	
n_{mol}	Number of moles	
ndf	Number of degrees of freedom (Phase Rule)	
P	Pressure	F/L^2
$\mathcal{P}$	An intensive property, a variable quantity	
p	Exponent in wind speed power law	
Q	Amount of heat	E
q	Heat rate	E/τ
R	Ideal gas constant	[F•L]/[kmol•T]
Ri	Release Richardson Number	
r	Evaporating pool radius	L
r	Pressure ratio (defined with various subscripts)	
r_c	Critical pressure ratio	
S	Entropy	E/[M•T]
s	Downwind dimension of spray barrier	L
T	Temperature	T
t	Time	τ
tol	Numerical equation solution tolerance	
U	Volumetric flow rate	L^3/τ
u	Velocity of fluid	L/τ
u_f	Air entrainment velocity	L/τ
u_f	Wind speed at vapor barrier fence height	L/τ
u_{wind}	Wind speed	L/τ
u_*	Friction velocity	L/τ
V	Volume	V
v	Specific volume (volume per unit mass)	L^3/M
v_c^m	Specific molal volume (volume per mole)	$L^3/kmol$
W	Mass	M
w	Mass flow rate	M/τ
X	Evaporation surface roughness correction factor	none
x	Downwind distance	L
x_i	Mole fraction of a component in the liquid phase	
y	Crosswind distance	L

Nomenclature

Symbol	Description	Units of Measure
y_i	Mole fraction of a component in the vapor phase	
z	Vertical distance (elevation)	L
z_l	Liquid head	L
z_{meas}	Wind speed measurement height	L

Greek and Other Letters

α_1	Void fraction (fraction vapor in a vapor/liquid stream)	
α	Before/after concentration ratio for barriers	
α_T	Thermal diffusivity	L^2/τ
γ	Convergence filter or "accelerator"	
Δ	Finite difference operator	
∂	Partial differential operator	
κ	Fraction material remaining in the plume after curtain	
ε	Scrubbing (removal) efficiency fraction	
ϵ	Error of equation solution	
$\epsilon_{\uparrow\downarrow}$	Radiation emissivity (average)	none
ζ	Heat flux	$E/[L^2\tau]$
η	Number of phases in equilibrium	
Θ	Heat of conduction factor	$E/[L^2\tau^{1/2}]$
λ	Monin-Obukov length	L
λ_T	Thermal conductivity	$E/[LT\tau]$
μ	Absolute viscosity	Pa•s (pressure/time)
ξ	Vapor barrier fence porosity	
ν	Kinematic viscosity of the vapor in air	L^2/τ
ρ	Density	M/L^3
$\sigma_x, \sigma_y, \sigma_z$	Atmospheric dispersion coefficients	L
σ	Surface tension	FL/L
σ_{sb}	Stefan-Boltzman constant	$E/[L_2T_4]$
Φ	Monin-Obukov length function	
ϕ	Downward pointing spray correlation parameter	
ϕ_S	Sun angle	degrees
χ	Mass fraction	
ψ	Rain out mass fraction	
Ω	Net work (includes expansion)	E
Ω_{shaft}	Shaft work	E
ω	Correlating parameter for Leung/Epstein model	
$\mathfrak{C}$	Molecular diffusivity of the vapor in air	L^2/τ
$\mathfrak{h}$	Henry's Law constant	P

Subscripts

*	denotes friction velocity
▼	low superheat
1.25	wind speed at 1.25 meters elevation
2	stagnant reservoir (flow models)
	orifice throat (flow models)

Nomenclature

Symbol	Description	Units of Measure
3	atmosphere (flow models)	
a	atmospheric	
avg	average	
BP	bubble point temperature	
b	mitigation barrier location	
bulk	bulk property, pseudo-pure component	
c	critical (temperature, pressure, volume)	
DP	dew point temperature	
e	air entrainment	
i	component index	
int	internal (energy)	
j	phase index	
key	key component in a mixture	
kin	kinetic	
l	liquid phase	
lh	liquid head	
lv	liquid-to-vapor, heat of vaporization	
max	maximum (choked)	
ms	mean value specific to entropy calculations	
N	Maximum value of index n	
NBP	Normal boiling point	
n	index, count	
ns	for the plume (= cloud), just before entering the spray	
p	initial plume (except for C_p)	
pool	evaporating pool	
pot	potential (energy)	
pxs	plume cross-section entering the spray	
rev	reversible process	
rm	released material	
s	saturation conditions	
s	spray interaction surface	
sat	saturated	
sauter	Sauter mean particle diameter	
si	spray impact area	
spray	after the spray	
surf	surface value	
T	thermal	
v	vapor phase	
vap	of vaporization	
wind	wind	
x	for downwind distance axis	
y	for crosswind distance axis	
z	for vertical distance (elevation)	
↓	Into the pool	
↑	Upward out of the pool	

CHAPTER 1

CHAPTER ONE

Introduction

The purpose of this Guidance Manual is to provide methodologies for consequence analysis purposes. That is, given a potential or after-the-fact set of circumstances for the accidental release of a chemical fluid into the atmosphere (the *"scenario"*), what are the appropriate methods to estimate spatial and time dependent concentrations of the material over a particular geographical area?

Scenarios may be generated within the hazard analysis parts of overall risk assessment studies. Techniques such as HAZOPS, fault tree, and "what if" analyses are used to discover potential hazardous situations which lead to an accidental release. Concentrations predicted for an identified release scenario may then be used to estimate possible impact of the shock waves and thermal damage from vapor cloud explosions, or potential toxic effects. The impact of toxic dispersed vapor clouds requires interpretation by specialists such as toxicologists and industrial hygienists. Thus the person or persons doing the source/release and dispersion modeling must interact "upstream" with those doing hazard analyses and with those "downstream" who interpret health or flammability aspects.

The modeling methodologies presented and recommended are intended for use in risk assessment studies for refinery/chemical plants during design or operation as well as for emergency response planning purposes. Also, available quantitative or semi-quantitative methods for mitigating a release after or during its occurrence are discussed. The product of any modeling exercise is an estimate of concentrations of the released material over a potentially affected geographic area so that possible toxic and/or flammability impact can be estimated. Modeling procedures are recommended on the basis of applicability to the particular situation being considered, required accuracy of results, simplicity, and availability of computer codes. If comparable modeling methods are available, they are discussed and used selectively in the example release scenarios. The calculational procedures and computer programs discussed are in the public domain. To limit the extent of the demonstrative simulation work, only SLAB, HGSYSTEM and DEGADIS program systems were used.

The release/dispersion scenarios described and exemplified are hypothetical; that is, they do not describe any particular accident that has occurred, nor a known situation for which an accident is liable to occur. However, the treatment and examples are realistic, for they have been drawn from the experience and knowledge of many technical personnel working in industry, government and academia. Calculational procedures used and recommended are well-accepted and are state-of-the-art in terms of readily available methods in the public domain; for example, the calculations for initial fluid release amount/flow rate and its concomitant physical state use standard chemical engineering methods, including thermodynamic and physical property estimation. Additionally, the turbulent jet and dense gas atmospheric dispersion models are based on atmospheric boundary layer theory and other physical principles; the models have been extensively evaluated against small and large scale experiments.

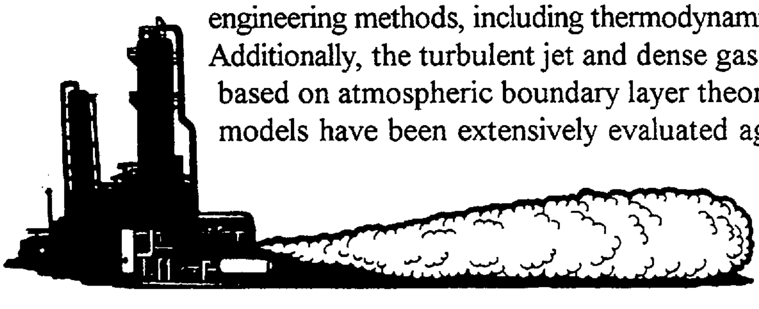

This Manual does not cover the origination of release scenarios, nor the interpretation of concentration estimates, except to demonstrate the concepts. These factors should be established separately for each individual modeling application. Effects criteria, such as flammability limits and references to toxic materials, toxicities, or toxic concentrations levels, *(concentration of concern)*, are used only to impart a sense of reality to the various examples and should not be used without review. Estimation and/or interpretation of possible toxic effects of model-predicted chemical concentrations are outside the scope and purpose of this Manual. The sidebar suggests a method for selection of flammability limit concentrations if no other information is available and/or for screening purposes.

The scope of the manual does not include model development and evaluation. Use of a specific modeling program for a type of application does not imply that program is particularly recommended. In general, problems encountered by the author in using a program were made known to the program author.

Flammability Criteria

Published flammability limits are determined in the laboratory by means of experiments in which the fuel/air concentrations are uniform and precisely known. Thus measured, the lower flammability limit ("LFL") for most hydrocarbons ranges from about 2% to 6% by volume. So, to be conservative, a LFL of 2% can be taken as a nominal, global value for the purposes of this Guidance Manual.

Actually, the concentration at any point and time in a real cloud, such as that being considered here, will be highly variable. There will be "fingering," "holes," and other inhomogeneities caused by terrain, structures and general turbulence.

*In a number of field tests, it has been found that peak concentrations are generally about twice that of average concentrations in vapor clouds. On this basis, the LFL of 1% should be considered for general use. However, dispersion models do not predict concentrations more accurately than a factor of 2 at best. For these reasons, a range of concentrations for the lower flammability limits must be considered. Therefore, for these purposes, **if a model calculates a released material concentration less than 0.5%v, the corresponding real cloud will be taken as non-flammable.***

Also, an upper flammability limit need not be considered, as it must be for a closed system. With a cloud, there is always an "edge" in which a flammable mixture exists, thus the cloud can be ignited if the edge encounters an ignition source.

Manual Organization

Chapter 2 of the Manual provides an overview of phenomena which must be considered in defining release/dispersion scenarios. The phenomena involved are discussed qualitatively so that the applicability of modeling methods described in later chapters can be appreciated. Eight representative scenarios are described for the purpose of previewing types of problems, which will be analyzed, simulated and discussed in Chapter 6.

Chapter 3 provides working methods for estimating the rates and physical states of released substances on entering the atmosphere. Because chemical engineering thermodynamics is extensively used, a working overview to this subject provides the basic concepts involved, as well as references to sources of physical and thermodynamic data required for the calculations. Calculational methods follow for releases from process equipment (valves, openings in vessel walls, sudden vessel failure, etc.). The releases may form "clouds" consisting of vapor, and vapor plus liquid aerosols. In some cases, evaporating pools of liquids may be formed on water or ground surfaces. The best, *practical*, calculational methods are presented for the current state-of-the-art. The results of these calculations are needed as parameters for the atmospheric dispersion models.

Chapter 4 provides an brief overview of meteorological phenomena which affect vapor cloud transport and dispersion as well as descriptions of associated characterization parameters used in dispersion modeling. Recommendations are made for selection of parameter values.

Chapter 5 describes mitigation of accidental releases into the atmosphere from the standpoint of modeling after-the-fact actions with estimates of their effectiveness. This information can be used with dispersion modeling to help in the selection and design of mitigation measures.

Chapter 6 presents the purposes, statement, analysis, simulation methods and results for eight release scenarios. Recommendations are made within each presentation for selection and analysis of modeling parameters for the problem at hand.

The *Nomenclature* (follows the Table of Contents) lists the symbols with their generalized units-of-measure used in the Manual. The *SI* units-of-measure system is used for all equations and examples. The three modeling program systems use various mixtures of the metric system units; conversions to and from SI units by the user are implied. ★

Appendix I summarizes the suggested default values for selected modeling parameters.

Appendix II is an overview of the features and input data requirements of the three modeling program systems, SLAB, HGSYSTEM and DEGADIS. These are used for demonstrating the modeling techniques and typical results for the demonstration scenarios in Chapter 6. User's Manuals should be consulted for detailed descriptions of program theory, operation, data requirements, file formats, and results generated.

Appendix III contains listings of germane modeling program input and intermediate result files referenced in the time dependent release simulation of Scenario 7 of Chapter 6.

Quick References

In addition to the Table of Contents and the Subject Index, several techniques have been used to aid the reader in locating particular information or methods to use in modeling applications. Chapters 3 through 5 each have a *Quick Reference* text box showing the page and/or equation where a particular subject or algorithm is most directly discussed.

In the scenario descriptions of Chapter 6, a text box summarizes the major *Release Attributes* by which the scenario's type and principal parameters may be readily identified. A *RECAP* summarizes the parameters used in the modeling. Additional methods, noted in the introduction of that chapter, are also used to aid quick referencing.

Equations which are primarily used for calculations have the symbol ✧ appended to the equation number.

Conventions

Within each chapter, tables, figures and equations are each numbered sequentially from the top of the chapter. If reference to these items is made from one chapter to another, the chapter number is prefixed. For example, Figure 3-12 is the 12th figure in Chapter 3. Pages are numbered according to *Chapter number-Page number*. To avoid confusion, the tables and figures for each scenario in Chapter 6 are prefixed by Sn, where n is the scenario number and S designates "Scenario." For example, Figure S6-2 denotes the second figure in Scenario 6.

★ Perry's Chemical Engineering Handbook, Sixth Edition, Chapter 1, contains a complete definition of the SI quantities, the relationships between them, and tables of conversion factors to other units-of-measure systems. This will be called "Perry's Sixth" for brevity. See *References* for further information on the handbook.

References, listed after Chapter 8, are presented according to chapter number. Within a chapter, a particular reference is made according to *author [reference number].* If a citation is made from within one chapter to a reference listed under another chapter heading, the chapter number is prefixed.

Terminology

Not all of the terminology used in this field is precisely defined or used. In this manual, "*substance*" is used to denote a pure chemical, chemical mixture, or other material which can or might be released to the atmosphere. "*Fluid*" is used for a substance capable of flowing, which may be gas, liquid, a gas/liquid mixture or aerosol suspension, or even a suspension containing solids in a flowing stream.

It is common practice to use the term "*vapor cloud*" for any visible or invisible body of substance moving with, and/or through, the atmosphere. Such a cloud may actually contain released liquid (in addition to its vapor) or even suspensions of solid particles. Although "*plume*" may most often refer to elevated releases from stack, it is used herein also for ground level or vapor clouds. "*Gas blanket*" is sometimes used to describe a surface level, dense vapor cloud in the early stages of its release. These terms are used more or less synonymously in this manual to mean the bounded, fluid entity of released substance (mixing with air) flowing through the atmosphere.

The symbol "ppm" refers to parts-per-million by volume [mole] in the gas, unless otherwise stated. Also, if at all possible, standard mathematical symbols as in the disciplinary literature are used for the parameters and variables. However, the same symbol or letter is often used in this text for many different items; this can be very confusing. Therefore, to help minimize possible misinterpretations, some different-than-standard symbols are used.

Subject Index Development

The subject index is based upon Chapters 1 - 6 and Appendix II. Not every appearance of a particular word or phrase is listed; a usage which is of minor importance does not appear in the index. The Nomenclature, References, Appendix I and Appendix III are not indexed.

In Chapter 6 demonstration scenario simulations, the words/phrases *pressure, temperature, wind speed,* and *stability class* are not indexed because they appear a large number of times in the text for each scenario.

CHAPTER 2

CHAPTER TWO

Overview of Release/Dispersion Processes and Demonstration Scenarios

The Overall Modeling Process

Every modeling study involves six major steps:

1. State the objective(s) of the study, including consideration of the material and mechanism, or *scenario*, by which it could be released. A scenario may also define initial ranges for parameters to be studied, such as release rates and modes, meteorology, etc.;
2. Devise or select appropriate release/dispersion modeling method(s);
3. Calculate the source parameters such as the amount released or mass flow rate(s) as well as physical state(s) of the released fluid for the next step;
4. Model the initial transport and mixing of the fluid with the atmosphere;
5. Model the transport and dispersion of the formed plume or cloud in the atmosphere; this produces concentration estimates over the space and time of interest; and
6. Document the work and report the results in a clearly understandable manner.

The goal of a modeling study is to answer the question: "What are the safety implications of a particular hypothetical release?" This must be considered in light of the local area involved, *e.g.*, population density, structures, terrain, weather, etc. In a real study, **Step 1** above must address the local situation.

Given the objective and the hypothesized circumstances of a release, modeling methods can be selected in **Step 2** to best (or adequately) represent the scenario. Sometimes, particular phenomena can only be modeled in a very approximate, or bounding, manner because of lack of a valid model, experimental information, time allowed to do the study, etc. In such situations, it may be necessary to modify originally chosen scenarios to fit the available resources. Since modeling of an entire scenario often requires sequential use of submodels, results from a particular model may change or influence the choice and use of following model(s).

Calculation of release rates/amounts via **Step 3** may be fairly straightforward. In some cases, the rate may be given as a result of a preceding risk analysis or "what if" study. However, most of the time these values will need to be calculated by accepted engineering methods and thermodynamics.

After the fluid enters the atmosphere, a *"transition"* modeling method may be required as **Step 4** to define the initial mixing of the fluid with the air. This will represent phenomena such as cooling of the cloud or jet by gas expansion, state phase changes, etc. A common example is a fluid at high temperature and pressure being released through a hole. Intense mixing, which occurs in jets, can markedly affect downwind concentration results when compared with the case where a jet is not formed.

Step 5 is the final dispersion modeling process for a scenario. For example, the selection of a particular dispersion model will be based upon whether an elevated plume proceeds into the "far field" under the influence of wind and atmospheric dispersion phenomena, or whether a dense gas cloud is formed from an area source, or perhaps where a jet is ignited to flare. These models, which may be steady state or time dependent, will generate concentration isopleths (constant value loci) over the geographical area and time of interest.

Step 6, documenting the work and proper presentation of the results, is very important. The manner of presentation should be designed with the background of the intended audience in mind. The presentation of results by means of extensive tables of numbers, *e.g.,* concentration vs. downwind distance, is usually very ineffective. Well-prepared plots and other figures designed with the intended audience in mind are preferred.

Near vs Far Field Modeling

Consider the release of a fluid for which the plume or cloud remains near the ground as it travels downwind. Close to the source, the detailed "mechanism" by which the fluid leaves its containment to form a plume at atmospheric pressure must be modeled to obtain accurate concentration estimates. For example, release of a turbulent jet will immediately entrain large amounts of air. On the other hand, at sufficiently long downwind distances, the amount of air entrained into the plume by the turbulent jet becomes insignificant relative to the amount subsequently entrained by atmospheric mixing processes.

Therefore, the term ***near field*** is generally used to mean the area close to a source where the details of the release mechanism phenomena still *significantly affect* the concentrations. The term ***far field*** denotes the area beyond the near field.

If a particular modeling application is concerned only with the far field, it may be possible to simplify the modeling procedures. To estimate the approximate distance for the beginning of the far field, modeling with and without detailed source effects can be used; the distance at which plume centerline concentration curves approach each other is the beginning of the far field as a first approximation; the far field is where the original substance concentration becomes less than about 1/1000 of the release concentration.

Note that the above definitions apply only to releases occurring near the ground (or sea) for which the plume remains near the ground. For elevated plumes, the near versus far field concept is not as useful. Plume rise has a significant effect on all calculated ground-level concentrations.

To summarize, *if near field receptor locations are of interest for ground level releases:*

- The mechanism of the release source effects should be modeled (*e.g.,* for released chemicals the particular reactions and phase equilibria should be appropriately modeled);
- Time dependent modeling should be used if the release is of short duration (varies rapidly with time).

If far field receptor locations are of interest for ground level releases:

- Concentrations are functions of release rate only, not the specific mechanism of the release (*e.g.,* once chemical reactions and phase equilibria effects disappear in the far field, inert gas thermodynamics may be used in the modeling);
- Steady state modeling of finite duration releases may often be used with appropriate correction for concentration averaging time with respect to travel time.

Mitigation effects on the cloud can be important, particularly if pollutant is removed from the cloud. However, air entrainment which dilutes the pollutant concentrations in the cloud are generally only important in the near-field. Cloud mitigation systems are discussed in Chapter 5 and Scenario 7 of Chapter 6.

Release-to-Dispersion Phenomena

The phenomena associated with an accidental release of a petroleum or chemical material into the atmosphere and its subsequent dispersion is, in general, a complex process. To properly model the final dispersion process, which is primarily controlled by atmospheric forces, all release phenomena must be appropriately modeled so the correct release rates and fluid states are used for dispersed concentration estimates. Without this, serious over- and under-predictions can be obtained.

Figure 1 broadly summarizes most of the sequences of processes, or paths, through which a discharged material can pass until its dispersion is controlled completely by atmospheric boundary layer phenomena. (Key words or phrases corresponding to the boxes in the figure are shown in bold type below.)

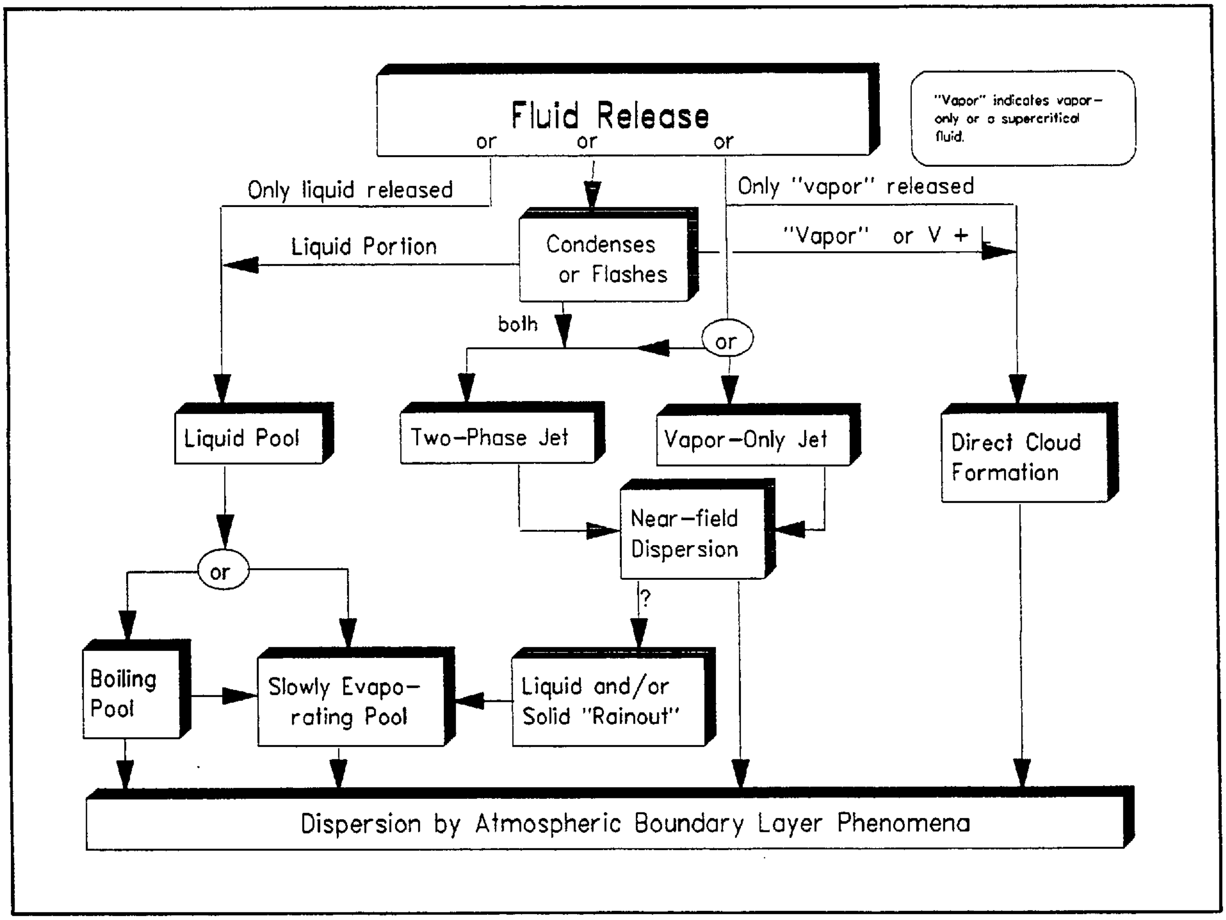

Figure 1. Paths to Air Dispersion near the release point.

Starting at the top of the figure, the fluid★ release may be from a bursting, or large, opening in a vessel, or from a valve, a small hole in a vessel or pipe, and so forth. If the fluid is a liquid superheated above its normal boiling point, it will flash to form a **vapor/liquid mixture**; this is a high energy process, so much or all of the liquid may remain suspended in the gas phase as an **aerosol** of very fine droplets. If the fluid is condensable vapor, the cooling caused by expansion from storage to atmospheric pressure may cause a liquid phase to form. This liquid may remain all suspended as an aerosol, or some can "**rain out**" to form a **pool**.

If the fluid is released at high pressure through a hole, nozzle, orifice or pipe-end, a **turbulent jet** will be formed. Turbulent jets rapidly mix the fluid with the air. Thermodynamic processes mentioned above are also acting. Thus dispersion in the near source is primarily controlled by these mechanisms. However, for a vertical release, the plume will bend over to an extent, depending upon its density relative to air. A **dense gas, ground level cloud** may be formed by the plume sinking to the ground.★★

If the original fluid is below its boiling point at atmospheric pressure (*i.e.*, its normal boiling point), is a non-boiling solution, is a cryogenic liquid, or is a liquid formed by condensation from the adiabatic release, a pool of liquid may be formed upon release. (The cases where all the fluid is absorbed by the ground or drops to the bottom of a water body are not treated in this Manual.) Pool evaporation may occur by two modes: 1) **Boiling evaporation** takes place if the ground is, and remains, warmer than a liquid which is below its normal boiling point; 2) mass-transfer limited **slow evaporation** occurs from the turbulent action of the wind over the surface of a liquid or solution which is a non-boiling liquid. Since the boiling process requires heat, a spill may start as a boiling liquid, but as the ground is cooled, the evaporation may become mass transfer limited.

Finally, the released cloud becomes subject to dispersion by **atmospheric** turbulence, as indicated in the lowest box in the figure. If an elevated jet-plume is formed above the ground, its velocity will slow to the wind speed, and the temperature and density of the plume will asymptotically approach that of air. If the jet directly impacts the ground, the cloud formed will spread horizontally and then disperse in the atmosphere. If the cloud is from a boiling pool, *usually* a dense cloud is formed, which will initially spread due to its density, and then disperse downwind through normal atmospheric processes. For surface area releases in which the emission rate is small enough not to affect significantly the density of the air at the source, a neutrally buoyant cloud will be formed at ground level and disperse through normal atmospheric processes.

It is common practice to refer to all the modeling processes above the bottom box in Figure 1 as "source modeling," while the dispersion by atmospheric-only process is often called "dispersion modeling."

Demonstration Scenarios

Eight hypothetical release scenarios have been developed to demonstrate methods recommended for modeling. These scenarios were selected to encompass many of the paths shown in Figure 1, and to demonstrate the atmospheric variables required (to estimate concentrations) for a given situation.

Table 1 summarizes the source/release, interpretation, boundary layer, and attributes for all eight

---

★ "Fluid" refers to gas-only, liquid-only, vapor plus liquid and/or solid mixtures (aerosols), etc. The material may be a pure chemical or a multicomponent system.

★★ "Ground" will be generally used to denote the earths's surface, either sea or ground.

scenarios.

In the following descriptions, only minimum details are given. Full scenario descriptions, their analyses, simulation results, and summary discussions are provided in Chapter 6. Excerpts from Figure 1 show the particular analysis path for each scenario; those scenarios with similar paths are grouped in a single figure.

Table 1. Summary of Scenario Attributes

No.	SCENARIO
8	Liquid benzene from tank bottom outlet
7	Anhydrous HCl vapor jet - water spray mitigation
6	Ammonia loading hose or pipe break
5	Liquified chlorine tank truck accident
4	Oil well blowout
3	Supercritical propane pipe hole release
2	H2S in CO2 from safety relief stack
1	H2S from unlit flare stack

ATTRIBUTE	1	2	3	4	5	6	7	8
SOURCE CHARACTERIZATION								
Release method:								
"Hole" (orifice, nozzle, pipe-end, etc.)	X	X	X	X		X	X	X
Vessel burst					X			
Area flux								X
Flow rate given	X	X		X				
Released fluid state:								
Liquid						X		
Vapor	X	X			X		X	
Liquid + Vapor				X	X			
Supercritical fluid			X					
Chemical reactions:								
Time characterization:								
Steady state	X	X	X	X				X
Finite					X	X	X	
Short transient (fast decay)							X	
TRANSITIONAL								
Turbulent Jet:								
Vertical upwards orientation	X	X		X				
Horizontal orientation			X			X	X	
Other orientation								
Pools, ponds, etc. (areas):								
Boiling ("cryogenic")								
Non-boiling					X			X
ATMOSPHERIC ATTRIBUTES								
(Flat, level terrain assumed.)								
Cloud or plume elevation:								
On the surface				X	X	X	X	X
Elevated	X	X	X	X				
Roughness type:								
Rural		X		X	X			
Urban						X		X
Industrial	X					X	X	X
Other			X					
Stability:								
Stable	X	X		X	X	X	X	
Neutral	X	X	X	X		X		X
Unstable	X	X		X				
INTERPRETATION								
Averaging time:								
Instantaneous			X			X	X	
1 minute	X	X		X		X		
10 minute								X
Other					X	X		
Hazard type:								
Toxic	X	X		X	X	X	X	X
Flammable			X	X				X

Scenario 1: Hydrogen Sulfide from Unlit Flare Stack

This scenario demonstrates the effects of two important variables on the dispersion behavior of vertically-directed turbulent jets (plumes): 1) the *momentum*, which is the product of the initial fluid mass flow rate and its density; and 2) the *atmospheric conditions*, which govern the wind speed and air density. In addition, the method for treating a multi-component gas release using the properties of a pseudo-pure component gas will be shown.

For a hazard analysis, maximum ground level concentrations of H_2S are to be estimated for a range of potential pressure relief valve discharges of sour process gas from a 26.8 m tall flare stack. Flared gas has greatly increased plume buoyancy as well as air dilution rates compared with the non-burned gas. Of concern here is the possibility that the released gas is not ignited or that the flame goes out, thus causing potentially hazardous concentrations of H_2S at ground level.

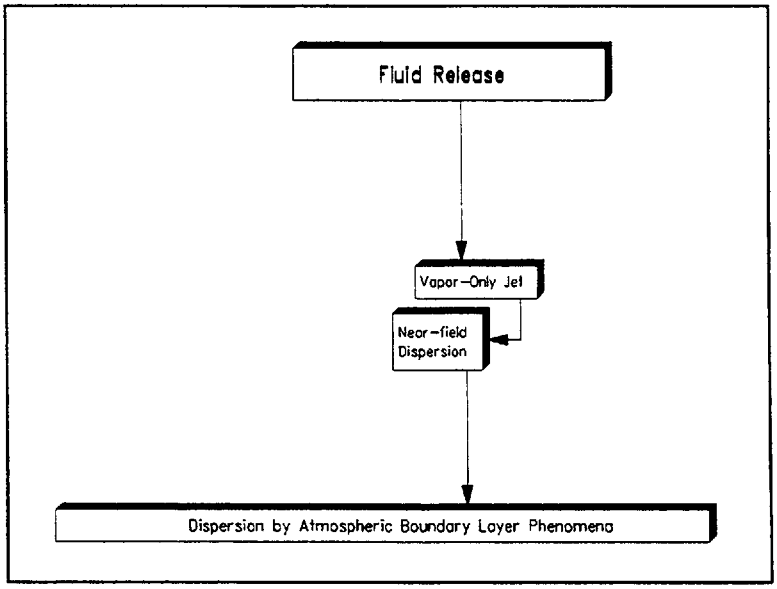

Figure 1. Release paths for Scenarios 1, 2, and 3.

The design maximum flow rate for the stack is 16 kg/s, the minimum flow rate is 1.6 kg/s, the flow regime is non-choked, and the stack exit temperature is 300K. The exit diameter of the stack is 0.20 m. The chemical composition of the stack gas, which contains methane, ethane, propane and hydrogen sulfide is given.

The process unit is in a large oil refinery surrounded by urban and suburban areas with trees.

Scenario 2: Hydrogen Sulfide and Carbon Dioxide from a Safety Relief Stack

For an oil field located in a rural area, secondary recovery operations use carbon dioxide as the flooding agent to maintain reservoir pressure. The separation plant produces a recycled stream containing about 1.3%v H_2S with the balance being essentially all CO_2. This stream is representative of the gas discharged to a new safety relief stack being designed for the unit. The maximum flow rate of 12 kg/s is to be used to estimate the required stack height and exit diameter. For the diameter calculations, assume an internal pressure of 70 kPa (gauge) at 275 K.

For this example, assume that the ground level concentrations for H_2S and CO_2 should not exceed 10 ppm and 2.0 %v, respectively, on an averaging time basis of 60 seconds.

Scenario 3: Supercritical Propane Pipe Hole Release

Supercritical propane at 340 K and 7.0 MPa is heated in a gas-fired process preheater to a temperature of 540 K. Assume that the pressure in the outlet line is the same as for the feed line, and that a 19 mm diameter hole can develop from some type of failure on either line. Either hole would be about 3 meters above grade. How far downwind could a vapor cloud remain flammable? The most likely ignition source is about 15 m from the heater. Could the jet's vapor be ignited if it happened to be directed towards the ignition source?

Scenario 4: Oil Well Blowout

The 0.35 m diameter well casing of a sour crude production well breaks off at ground level to cause a blowout which spews oil and gas vertically into the air at about 23,000 kg/hr. The temperature of the mixture just before discharge into the atmosphere is 316 K (108 F). It is expected that the discharge would continue at this rate for some time, perhaps several days, before it could be shut off. The results of the crude assay analysis and flash calculation are known. From these, the H_2S concentration in the vapor phase of the released fluid is about 12%v.

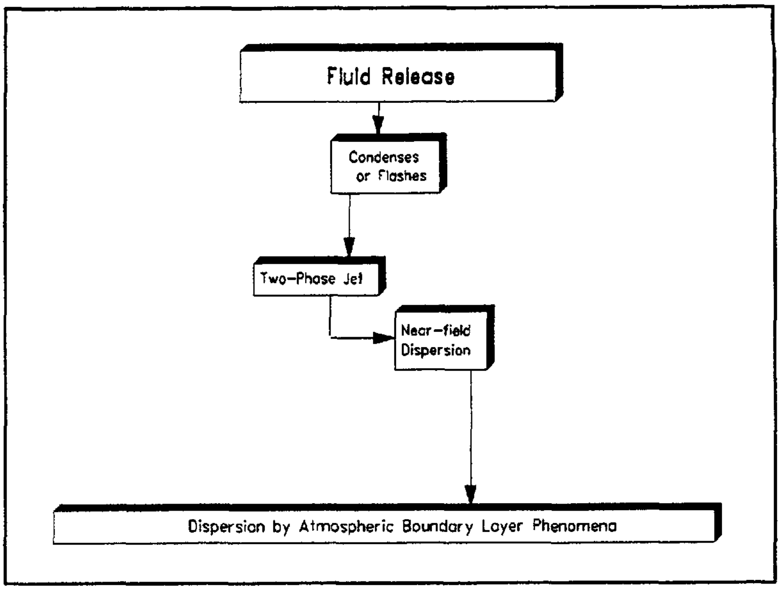

Figure 1. Release paths for Scenarios 4, 6, and 7.

Dispersion modeling is required to estimate "worst case" estimates of H_2S concentrations vs the radial distance from the well. Or, stated another way, what would be the radius from the source for which the H_2S concentration would always be less than 10 ppm, for all expected meteorological conditions?

The meteorological conditions typical for the location are hot, humid days when the atmosphere becomes very unstable during the day, with maximum instability occurring in the early afternoon. At night, the earth cools to cause stable conditions. Daytime winds and cloud cover produce neutral stability conditions.

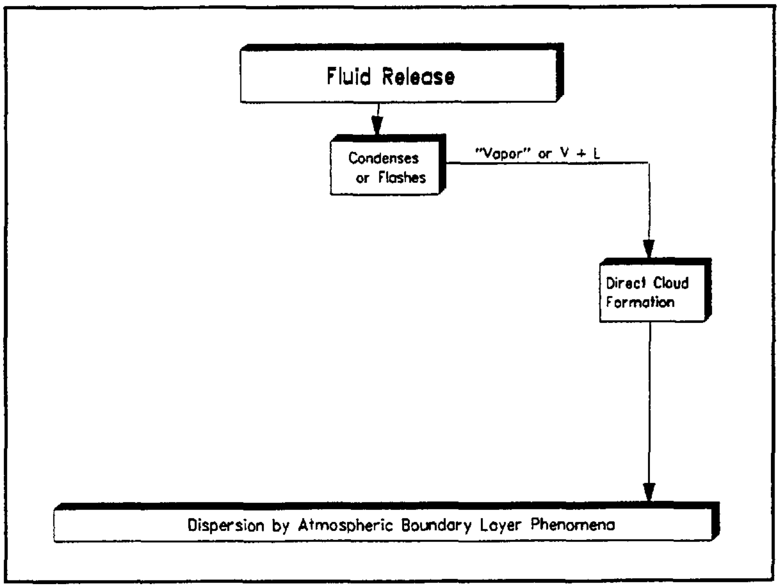

Figure 1. Release path for Scenario 5.

Scenario 5: Liquified Chlorine Tank Truck Accident

On a partly cloudy night with light winds, a tank truck, filled with liquid chlorine to its full 16 metric ton capacity, jack-knifes, then overturns in tall grass adjacent to the highway. The tank ruptures and empties in 30 minutes in a manner so that the rapidly expanding fluid forms a cloud of vapor and liquid aerosol as it enters the atmosphere. No liquid pool forms. Assume that the internal tank storage temperature equals the ambient temperature, 303 K. For this locale in the Midwest prairie/farm country, forecasts call for daytime high temperatures of 303 K with winds from 4 to 8 m/s with moderate insolation and minimum nighttime temperatures near 293 K with winds ranging from calm to 3 m/s with less than 40% (< 3/8) cloud cover.

To assist emergency response personnel, estimates of downwind chlorine concentrations along with the areas potentially affected are required.

Scenario 6: Ammonia Hose or Pipe Break

As part of a study to design the site of a new railroad tank car and tank truck ammonia loading facility for a very large refinery/chemical plant complex, the hazard analysis indicates the consequences of hose breakage or accidental disconnection that should be investigated. The hose end could whip around to discharge liquid ammonia in any direction, or the pipe to which the hose was connected could discharge the stream in any direction.

Upstream automatic control systems are being designed so that if a release such as this occurs, flow can be stopped quickly (several minutes or less). To assist the control system designers in deciding the maximum automatic shut-off time, a modeling study was requested to estimate the effect of shut-off time, and therefore release duration, on downwind cloud travel from the facility.

Assume the ammonia is stored in pressure vessels which are in temperature equilibrium with the surroundings, and that the pipes and hoses have inside diameters of 5 cm.

Demonstrate how different release durations and associated averaging times can affect analysis results.

Scenario 7: Hydrogen Chloride Pipe Break

This exercise demonstrates typical procedures that may be used to model water spray barrier mitigation effects by means of a ground level hydrogen chloride plume release. The presentation differs from other scenarios in this chapter in that it is a step-by-step presentation of methods, rather than an analysis and solution of a given problem. These methods are, in general, applicable to the removal of other chemicals and/or the use of other barriers (*e.g.*, steam curtains, vapor fences) provided their specific effects can be quantified.

Scenario 8: Evaporating Pool of Liquid Benzene

During construction operations, an outlet line on the bottom of a benzene storage tank is sheared off. The discharge continues for 30 minutes before it is stopped. The diked tank is located in the tank farm of a large refinery/chemical plant complex surrounded by urban and suburban populated areas. The minimum distance from this particular tank through the complex to the company fence line is 195 meters. Tank size and information needed for discharge rates as well as dike dimensions are given. Assume the potential release occurred in the morning of a warm day

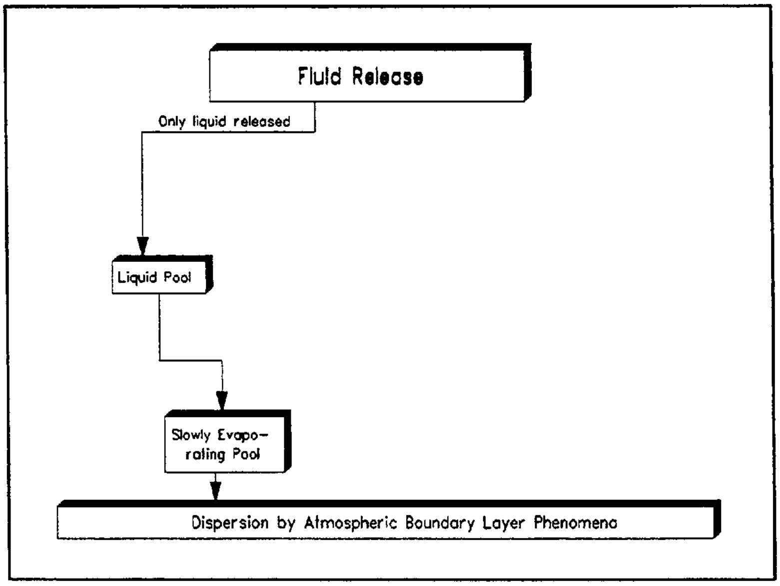

Figure 1. Release path for Scenario 8.

with full cloud cover.

Required are estimates of downwind maximum concentrations of benzene as comparative plume areas shown by 1 and 50 ppm benzene concentration isopleths. The effect of wind speed is also of interest. A 10-minute averaging time needs to be used for all concentration estimates.

CHAPTER 3

CHAPTER THREE

Source Modeling

Overview

This chapter presents methods for calculating release rates and fluid conditions for substances accidentally released to the atmosphere; this information is required by atmospheric dispersion models to calculate downwind chemical concentrations. The *substances* may be pure chemical compounds or mixtures thereof, and the fluid stream may be vapor, liquid, or a suspension of a vapor and a liquid ("aerosols"). Parameters needed to characterize a released substance are: Source type (*e.g.*, jet, evaporating pool, "instantaneously" formed cloud★), mass flow rate, physical state (vapor, liquid, or both), stream temperature and composition. Parameters can be estimated by methods drawn from Chemical Thermodynamics and Fluid Mechanics.

Commonly used calculational methods, with overviews of background theory, are presented. Derivations of most equations are not provided; references are given so the methods may be expanded or modified to suit specific circumstances which are beyond the scope of this Manual. Concepts applicable to systems in thermodynamic equilibrium are reviewed, starting with phase equilibria.

Methods for obtaining and/or calculating generally required physical and thermodynamic properties of gas and liquid phases are presented. For releases involving large flow rates, such as rapid flow through a hole, or an instantaneous rupture of a vessel containing supercooled fluids, the thermodynamic equilibrium and fluid momentum concepts for calculation of flow rates are presented. Finally, methods for calculation of evaporation rates from boiling and non-boiling pools are discussed. Example calculations for the various methods are given.

Release Characterization Complexities

Most incidents start with a substance being released from containment, owing to either failure of the storage vessel or pipe, or an abnormal discharge from an engineered device such as a relief valve, vent stack, or other device. Superheated liquids will expand into the atmosphere as a cooled vapor and/or liquid stream, and if both, usually an aerosol cloud. Liquids with normal (atmospheric) boiling points below their storage temperature will form evaporating pools on the ground. If the container fails by means of a relatively small opening, the mass flow rate through this "hole" can be estimated by well-known equations, provided the temperature, pressure, and physical properties are known (*e.g.*, liquid or gas density). For a chemical system involving vaporizable components, vapor/liquid equilibria calculations are required to calculate the relative amounts of the vapor and liquid phases, as well as to establish instantaneous phase compositions. Physical and thermodynamic properties are temperature, pressure, and composition dependent.

★ Releases in which all of the available substance is released into the atmosphere in less than roughly one minute are often called "instantaneous" releases.

Also, as flow continues to decrease the amount of stored substance, the pressure and temperature (and composition, if applicable) in the vessel will change to satisfy conservation of mass and energy. In some applications, these time dependent changes should be considered in modeling a specific release scenario.

Most release scenarios can be modeled by assuming that the processes involved are *reversible and in thermodynamic equilibrium*, considering the large uncertainties of scenario definitions and dispersion models. Although this assumption is generally not true in the strict sense, some processes are so fast that equilibrium calculations provide adequate results. Also, use of this assumption may be the only way estimates can be obtained, because sufficient detailed knowledge of the phenomena is rarely available for more accurate calculations.

Units of Measure

The SI units-of-measure system is used for all calculations in this manual; see Smith and Van Ness [8], Perry's Sixth [6]. A list of all symbols with units-of-measure is presented in the *Nomenclature* which precedes Chapter 1. The SI *pascal* unit of pressure is primarily used, but other common units are often used in scenario discussions (1 atm = 14.7 psia = 101,325 Pa = 0.101 MPa). When pressure in pascals is used in the various equations involving energy balances, the gravitational constant, $g = 9.807\ \text{m/s}^2$, usually does not appear explicitly because of SI definitions. In other units-of-measure systems, such as English and Metric, g appears explicitly. Finally, because of common usage, degrees Celsius and atmospheres, for temperature and pressure, respectively, will often be used in example problems and release scenarios throughout the Manual.

Phase Equilibria

A frequent calculational problem is: "Given the composition of a system, its temperature and pressure, what are the relative amounts of vapor and liquid, and what are the compositions of each phase?" The methodology of solution is called "VLE" (for Vapor-Liquid Equilibrium) or a "flash" calculation. The general methods for calculating phase equilibria are beyond the scope of this discussion. However, introductory methods to solve this problem for "well-behaved" substances (*e.g.*, certain hydrocarbons at low pressure) are presented to give an overview of the techniques involved. Further, these equations can be used in some accidental release modeling applications. For comprehensive information on this subject, please refer to texts such as Smith & Van Ness, Chapter 13. Reid, Prausnitz and Poling [7] also provides a table of references.

Phase Rule

A *phase* is a homogeneous region of matter. A gas or mixture of gases, a liquid or liquid solution, and a solid crystal are examples of phases. A phase need not be continuous; examples of homogeneous phases are a *gas* (*e.g.*, CO_2) dispersed as bubbles in a *liquid* (soda water), and *liquid* droplets suspended in a vapor cloud. Abrupt changes in physical properties occur in the interface between phases. Consider a vessel containing one or more phases in thermodynamic equilibrium; the relative amount and composition of each phase remain constant with time, and all phases have the same temperature and pressure. The *phase rule* governs the number of *intensive* variables which can be independently specified – the *number of degrees of freedom (ndf)*. (Intensive properties are those which are independent of the extent of the system and of the individual phases.) The phase rule for non-reacting systems is

$$ndf = N_{cs} - \eta + 2 \qquad (1)✧$$

where N_{cs} = number of species and η = number of phases in the system.

For the case of a single substance, or "pure component," $N_{cs} = 1$. Thus if the system contains only liquid or vapor, *but not both*, then *ndf* = 2. This means that both temperature and pressure may be specified (manipulated), as long as another phase does not appear. However, suppose *pure liquid is in equilibrium with its vapor*, then $\eta = 2$ and *ndf* = 1. This means that either temperature or pressure may be specified (manipulated), *but not both*. That is, if temperature is specified, then the pressure of the gas phase above the liquid in the vessel is the *vapor pressure* at that temperature.

For multicomponent systems, $N_{cs} > 1$ and the degrees of freedom increase, so more knowledge (*e.g.*, independent equations) must be applied to completely specify the state of a system. Some examples are shown in the box.

Phase Rule Examples

Degrees of Freedom	Number of Species	Number of Phases	Allowed Specifications, Typical Situations
ndf =	N_{cs} −	$\eta + 2$	
2	1	1	Can specify T and P; *e.g.*, for vapor only
1	1	2	Specify T or P; Use vapor pressure curve for non-specified variable
2	2	2	Specify T and P, then the phase compositions are determined.
3	3	2	Specify T and P, the mole fraction of one component in a phase may be set.

The degrees of freedom determines the number of independent equations which must be solved to find the phase compositions and overall vapor/liquid mole ratio. Also, for example, if temperature is an unknown variable, another relation such as the overall vessel energy balance must be invoked [Smith & Van Ness, p 362 *et seq*].

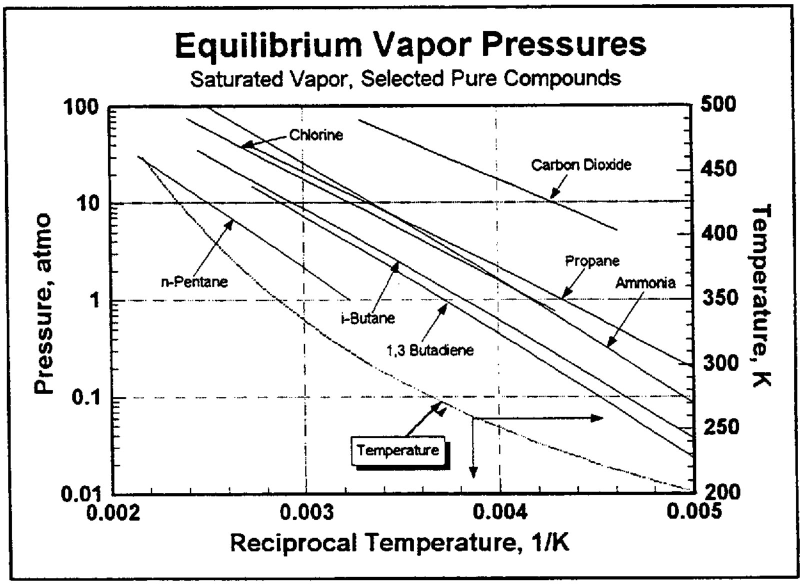

Figure 1.

Pure Component Systems

For a pure substance contained in a vessel, specification of either temperature or pressure determines whether the single phase is liquid or vapor. *Figure 1* shows vapor pressure vs temperature plots for several pure chemical compounds. At constant pressure (*e.g.*, the atmosphere), all of a given substance is vapor at temperatures to the right of its curve, and it is all liquid to the left. The temperature at which the vapor pressure equals 1 atm is called the *Normal* boiling point (T_{NBP}).

As shown in Figure 1, the example plots of the logarithm of the equilibrium ("saturation") pressures (P_s) vs the reciprocal of absolute temperatures ($1/T$) gives straight or nearly straight lines for the ranges shown. For vaporization at low pressures, the Clausius/Clapeyron equation [Smith & Van Ness p. 182] may be used to relate the vapor pressure to the temperature and the latent heat of vaporization (ΔH_{lv}):

$$\Delta H_{lv} = -R\left(\frac{d\ln P_{sat}}{d(1/T)}\right) \tag*{(2)✧}$$

The derivation of this equation assumes the gas is ideal and that molar volume of the liquid is negligible with respect to that of the vapor. (The SLAB dense gas dispersion model uses this equation.) If the pressure (temperature) is high enough for the gas to be significantly non-ideal, the Clapeyron equation (not presented) should be used using numerical solution techniques.

Multicomponent Vapor-Liquid Equilibria

Almost all substances in industrial applications are multicomponent streams. If a stream consists of one major component, with small amounts of other components ("trace" substances)★, then it can be thermodynamically treated as a pure component. For multicomponent streams that can form vapor and liquid, there may be a range of pressures (at constant temperature) in which liquid and vapor co-exist. An example is shown in *Figure 2.* It shows temperature (T) vs. phase concentrations for a two component mixture. Shown are the mole fractions of component 1 in the liquid and vapor phases, x_1 and y_1, respectively. (Because the sum of mole fractions of all components in a phase must always sum to 1, x_2 and y_2 can be found by difference; this is in accordance with the phase rule.) The horizontal dashed line shows the liquid and vapor composition in equilibrium at 80 C; the liquid phase is at its bubble point and the vapor phase is at its dew point for this particular pressure.

Heat of Vaporization Example

The SLAB dense gas dispersion model is to be used in an application concerned with the release of chlorine to the atmosphere. The latent heat of vaporization, a required input parameter if a two phase system is possible in the turbulent jet expansion, can be estimated from Figure 3-1 as follows: Using the finite difference approximation,

$$slope = \frac{d\ln P_{sat}}{1/T} \cong \frac{(\ln P_1) - (\ln P_2)}{(1/T_1) - (1/T_2)} = \frac{\ln 18 - \ln 1.6}{0.003 - 0.004} = -2420.$$

The ideal gas constant in SI units is 8313 (Pa - K - kg - m - Joules), thus the approximate heat of vaporization is:

$$\Delta H_{lv} = -R \cdot slope = (-8313)\cdot(-2420) = 20.12\,MJ/kg.$$

SLAB requires J/kgmol; dividing the above value by the molecular weight of chlorine, 70.91, gives <u>283 KJ/kgmol</u>.

Raoult's Law connects the vapor and liquid concentrations for ideal gases in equilibrium with ideal solutions:

$$P_i = x_i P_{sat,i} = y_i P \tag{3}$$

★ "Small" usually means less than about 1%. The concentration(s) of trace compounds are such that the physical, chemical and thermodynamic properties of the major component *of interest* are not significantly affected.

That is, the partial pressure of the component in the vapor (P_i) is proportional to its mole fraction in the liquid times its pure component, saturated vapor pressure value. Because the partial pressures must sum to the total pressure (P),

$$\sum_i y_i P = P \sum_i y_i = P \bullet 1 \quad . \tag{4}$$

The vapor/liquid equilibrium "K-value" is defined as

$$\frac{y_i}{x_i} \equiv K_i \quad . \tag{5}$$

For non-ideal systems, the K-values depend on composition, and the vapor and liquid mole fractions are multiplied by concentration dependent vapor and liquid phase *activity coefficients*. These coefficients are obtained by empirical correlations developed from measured data, and their use is beyond the scope of this chapter.

In some applications, the full curve of Figure 2 does not exist in the ranges of temperature, pressure and composition conditions of interest. For example, the solubility of a gas in a solute is very low. In that case, *Henry's Law* may be used:

$$P_1 = \mathcal{H}_1 x_1 \tag{6}$$

in which subscript 1 denotes the solute, and $\mathcal{H}_1$ is the Henry's law constant, which may be a strong function of temperature. Note that the constant is found by extrapolation of solubility data to infinite dilution; activity coefficients are applied when the concentration becomes great enough to be significant. For this situation, special techniques must be used in setting up the VLE equations to be solved.

Discussion

The following VLE methods should be useful for understanding the types of governing sets of equations; an example solution of a simple, well-behaved VLE problem is presented later. For accidental release modeling purposes, the required accuracies of solution are less than those needed for typical chemical engineering design purposes. That is, applications which involve pure components, or mixtures of substances may be solved by ideal gas and ideal liquid assumptions. In general, these substances will be of

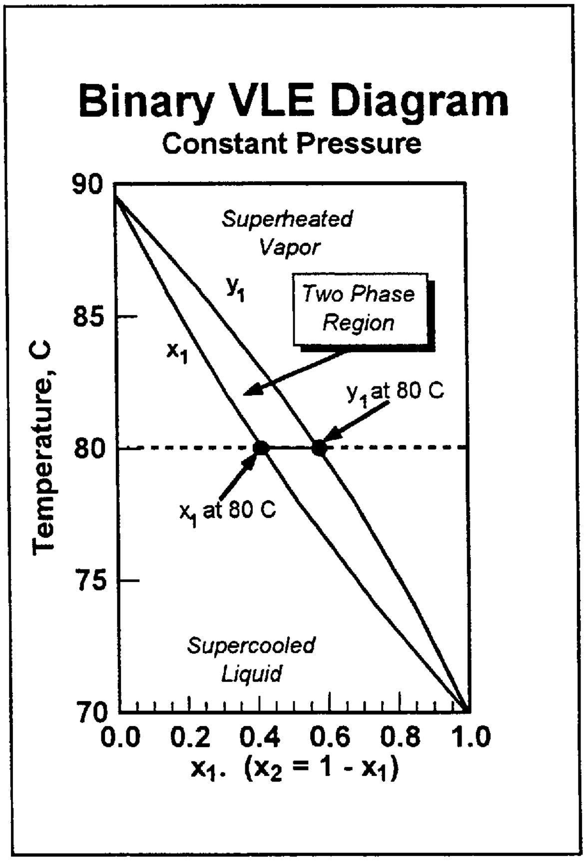

Figure 2.

low molecular polarity, such as hydrogen-saturated hydrocarbons, and the vessel will be at low pressures. As the compounds become more polar, molecular interaction increases (as may pressure), thus mixing and compositional effects must be accounted for. Thus, to obtain adequate accuracy, more complete thermodynamic equations are used which employ liquid and vapor component *concentration activity coefficients*; these are based on measured deviations from ideality. The best advanced methods are based on *equations of state* which, in some way, account for molecular size and attraction (*i.e.*, the ideal gas law does not).

Because VLE calculations for real streams are complex and require a database of characterizing parameters for all substances of interest, computer programs are used. Many organizations, such as petroleum and chemical companies as well as process engineering organizations, have stand-alone VLE computer programs. Programs are available from several vendors. Process engineering flowchart simulation programs usually contain complete thermodynamic and physical properties for substances, and may be used just to obtain VLE solutions along with physical properties.

The VLE concepts discussed here are limited to constant temperature and pressure applications. In the more general problem, temperature and/or pressure is unknown, so, in addition to the conservation of mass equation, energy and/or momentum balance equations must be used for implicit specification of these variables. For example, a stream of constant bulk composition and mass in equilibrium at conditions $[T_1, P_1]$ isenthalpically changes to $[T_2, P_2]$, with T_1, P_1, and P_2 being known. A VLE calculation is performed for the mixture from which the enthalpy (H_1) is directly calculated. Then, T_2 is iteratively adjusted by the algorithm until the specific enthalpy (H_2) matches the first value, H_1. Of course, for the general case, the VLE computational part of the computer program must always determine the number and kind of phases existing before proceeding with the flash calculation. This is usually done by calculation of the dew point temperature (T_{DP}) and the bubble point temperature (T_{BP}); if a trial solution for T_2 is between T_{DP} and T_{BP}, then a two-phase solution exists. Smith & Van Ness has complete discussions on these topics, including detailed computational flow charts for bubble and dew temperature/ pressure calculations.

Ideal VLE (Flash) Calculations. Consider a multicomponent mixture for which the temperature, pressure and overall (bulk) composition are known for N_{cs} chemical species (components). The moles (mass) of each component must be equal to the sum of the moles in the vapor and liquid phases:

$$z_i(n_v + n_l) = y_i n_v + x_i n_l \tag{7}$$

where z_i = mole fraction of i^{th} component for the total system ("bulk"), n_v = total moles in the vapor phase, and n_l = total moles in the liquid phase. This equation may be put on a single total mole basis by dividing it by the quantity $n_v + n_l$ to obtain:

$$z_i = y_i f_v + x_i f_l \tag{8}$$

where f_v = mole fraction vapor and f_l = mole fraction liquid in the system. By definition,

$$f_v + f_l = 1 \tag{9}$$

Substitution of Equations 7 and 8 into 9 and rearranging yields

$$x_i = \frac{z_i}{[f_v(K_i - 1) + 1]} \qquad (10)$$

To maintain material balance in the liquid phase,

$$\sum_i x_i = 1 \qquad (11)$$

must be satisfied. (Summations with respect to I are always made over all N_{cs} unless otherwise stated.) Thus, given the z_i and K_i values (the latter are generally known as a function of temperature), the problem is to find f_v while satisfying Equation 11. However, a real solution to the set of equations (10 and 11) does not exist if two phases do not exist; *e.g.*, as depicted in Figure 2.

If the system is just at the *dew point* of the vapor, then $f_v = 1$; substituting this into Equation 10 and then the result into Equation 11 yields

$$\sum_i \frac{z_i}{K_i} \leq 1 : \quad \textit{True for all vapor} \qquad (12)✧$$

In the preceding, equality holds at the dew point (saturated vapor), and if the summation is less than 1, the system is all superheated vapor. Equations equivalent to 10 to 12 may be derived using f_l and y_i from which it may be shown that if the system is at or below the *bubble point* of the liquid (thus the system is all liquid), then

$$\sum_i z_i K_i \leq 1 : \quad \textit{True for all liquid} \qquad (13)✧$$

For chemical systems for which the K-values are very weakly dependent upon concentrations, the non-linear Equations 10 and 11 may be numerically solved for f_v with Newton's Method. Define the error for the j^{th} iteration for Equation 11 to be

$$\epsilon_j = 1 - \sum_i x_{i,j} \qquad (14)$$

the value of which is to be reduced below some small constant, *tol.* Given a positive, real value for $f_{v,j}$, an improved value can be calculated by Newton's Method by

$$f_{v,j+1} = f_{v,j} + \gamma \cdot \left[\frac{\epsilon_j}{(d\epsilon / df_v)_j} \right] \qquad (15)$$

where γ is a convergence "accelerator" or "filter" coefficient ($0.1 < \gamma \leq 1$). From Equations 10 and 11, the derivative in Equation 15 is

$$\left(\frac{d\epsilon}{df_v}\right)_j = -\sum_i \frac{z_i\,(K_i\ -1)}{[f_{v,j}\,(K_i\ -)\ +\ 1]^2} \tag{16}$$

Flash Calculation Algorithm

Using the above equations for a stream in which the K-values are independent of phase compositions, and are known for the given temperature and pressure, the equilibrium amount of liquid and vapor, as well as their compositions, may be found. The following algorithm assumes that a two phase solution exists.

1. Given the bulk composition (*z*-values) and the K-values, choose a starting value for f_v. Use 0.9 if no other information is available; do not use a value near zero or else the algorithm may march into zero or negative territory. Assign $j = 1$ and *tol* (a very small number, *e.g.*, 1E-06).
2. Calculate ϵ_j by Equations 10, 11, and 12, and the derivative by Equation 16.
3. If $\epsilon_j < tol$, then go to Step 5, else go to Step 4.
4. Calculate an improved value, f_{v+1}, by Equation 17, and go to Step 2.
5. The solution is complete. Calculate the vapor component mole fractions by Equation 7, if required.

An example flash calculation for a three component system is presented on the next page.

Multicomponent Vapor-Liquid Equilibrium Calculation Examples

For three components in the bulk mixture; constant K-values

Typographical Note:
Given constant values are shown in italic type.
Values of special interest are shown in bold type.
Calculated values are given in non-italic type.

Component	**1**	**2**	**3**	Component Sums	
K-value K	*0.10*	*0.50*	*10.00*		
Case 1: The mixture is all liquid					
Bulk mole fraction z	*0.99*	*0.01*	*0.01*	1	
z/K quotient =	9.90	0.01	0.00	**9.911**	= Sum(z/K) < 1 for all vapor: FALSE
zK product =	0.10	0.00	0.05	**0.152**	= Sum(zK) < 1 for all liquid: TRUE
Case 2: The mixture is all vapor					
Bulk mole fraction z	*0.01*	*0.01*	*0.99*	1	
z/K quotient =	0.05	0.01	0.10	**0.159**	= Sum(z/K) < 1 for all vapor: TRUE
zK product =	0.00	0.00	9.90	**9.903**	= Sum(zK) < 1 for all liquid: FALSE
Case 3: Vapor and liquid phases exist in equilibrium					
Bulk mole fraction	***0.20***	***0.30***	***0.50***	1	***<< These bulk mole fractions are used in the VLE calculation below.***
z/K quotient =	2.00	0.60	0.05	**2.65**	= Sum(z/K) < 1 for all vapor: FALSE
zK product =	0.02	0.15	5.00	**5.17**	= Sum(zK) < 1 for all liquid: FALSE

Vapor-Liquid Equilibrium Calculations for Case 3:

Terms and equations are developed from left to right. See Equations 10 to 16.

Equation 15 Filter = 0.2

Iteration No.	Fraction Vapor fv	Mole fraction in liquid, x(i) (Equation 10) Component 1	2	3	Sum x(i)	Error of Eq. 14	Derivative terms for Equation 16 Component 1	2	3	Neg. Error Derivative Eq. 16	Error/ Err. Der. Quotient Eq. 15	Filtered fv Correction Eq. 15
Initial guess	*0.9*	1.0000	0.5455	0.0549	1.600400	***-0.60040***	-4.986150	-0.495868	0.054341	5.427676	-0.110618	**-0.022124**
1	**0.877876**	0.9528	0.5347	0.0562	1.543658	***-0.54366***	-45.389822	-0.476508	0.056800	45.809530	-0.011868	**-0.002374**
2	**0.875503**	0.9432	0.5336	0.0563	1.533066	***-0.53307***	-0.444799	-0.474498	0.057073	0.862224	-0.618246	**-0.123649**
3	**0.751854**	0.6186	0.4807	0.0644	1.163650	***-0.16365***	0	-0.385141	0.074600	0.310541	-0.526984	**-0.105397**
4	**0.646457**	0.4783	0.4433	0.0733	0.994868	**0.00513**	0	-0.327497	0.096802	0.230695	0.022246	**0.004449**
5	**0.650906**	0.4829	0.4447	0.0729	1.000525	**-5.254E-04**	0	-0.329660	0.095675	0.233986	-2.245E-03	**-4.491E-04**
6	**0.650457**	0.4824	0.4446	0.0729	0.999950	**5.036E-05**	0	-0.329441	0.095788	0.233653	2.155E-04	**4.310E-05**
7	**0.650500**	0.4825	0.4446	0.0729	1.000005	**-4.859E-06**	0	-0.329462	0.095777	0.233685	-2.079E-05	**-4.158E-06**
8	**0.650496**	0.4824	0.4446	0.0729	1.000000	**4.685E-07**	0	-0.329460	0.095778	0.233682	2.005E-06	**4.010E-07**
9	**0.650496**	0.4824	0.4446	0.0729	1.000000	**-4.517E-08**	0	-0.329460	0.095778	0.233682	-1.933E-07	**-3.866E-08**
10	**0.650496**	0.4824	0.4446	0.0729	1.000000	**4.356E-09**	0	-0.329460	0.095778	0.233682	1.864E-08	**3.728E-09**

Note that the process has converged to three significant figure accuracy in five iterations, and to five significant figure accuracy in seven iterations. Also, the ninth iteration has converged to within the number of digits used by the computer (about 8). If further iterations are continued, then the solution will probably stabilize at the above solution, within the computational real number word size.

The value of the convergence filter coefficient must be chosen to obtain a valid solution, i.e., $0 <$ fraction vapor < 1. For this example, a coefficent between about 0.15 and 0.35 works. The validity of solution should always be checked in this manner.

Fluid Properties

Volumetric Properties of Pure Fluids.

The calculation of release rates into the atmosphere, and the state of the fluid (liquid, vapor, or both) requires certain physical properties (*e.g.*, density) and thermodynamic quantities (*e.g.*, internal energy, enthalpy, entropy). The latter quantities are derived from volumetric and thermal data. Quantitative knowledge of the pressure-volume-temperature ("PVT") relationship for a pure component or a mixture is key to understanding and calculating phase existence, phase equilibria, flow rates, and fluid expansion parameters into the atmosphere. The basic concepts and equations of state are summarized below. The last section of this Fluid Properties part provides general references from which property values and estimation methods may be obtained.

Homogeneous substances are *liquids, vapors*, or *solids* for which physical and thermodynamic properties are markedly different between the three states for a given chemical compound. However, the differences in properties become indistinguishable at the *critical point*. The critical point is determined experimentally, and is characterized by the critical temperature (T_c) and critical pressure (P_c). Above this point, the substance is totally homogeneous and is neither liquid or gas or solid; it is called a *supercritical fluid*. These fluids are beyond the scope of this chapter, as are solids.

The Virial Equation of State for Gases. It has been experimentally determined that the PV product for a pure gas is more nearly constant, at a constant temperature, than for either P or V alone. A form of the generalized empirical *Virial* equation of state for gases is:

$$\frac{PV}{RT} = Z = 1 + k_1 P + k_2 P^2 + k_3 P^3 + \dots \tag{17}$$

where P is the *pressure*, V is the volume per mole, R is the *ideal gas constant* (8314.4 for SI units), T is the absolute temperature, Z is the *compressibility factor*, and k_1, k_2, k_3 are constants, termed the *virial coefficients*. This is the basis for the *ideal gas law*, for it has been determined that as P tends to zero, the PV product tends to the same value for all gases in the limit (at a constant temperature). A number of useful correlations have been developed in which the compressibility factor is presented as a function of pressure along isothermal curves for pure gases and mixtures. The *API Technical Data Book*, Vol. I [2] contains graphical compressibility factor data for many petroleum-type hydrocarbons.

The Ideal Gas Law. As pressure is decreased, all terms on the right hand side of the preceding equation except for the first approach zero, so in the limit $Z = 1$, thus $PV = RT$, where the constant R is based on one mole of the substance. For n moles, the ideal gas law is

$$PV = n\,RT \tag{18}$$ ✧

from which molal and mass density may be readily derived. The ideal gas is generally used in all atmospheric dispersion programs. For calculation of current vessel contents ("holdups"), and flow through pipes and orifices, the ideal gas law *may* provide sufficient accuracy *for these purposes* if the system is not near the critical point.

Cubic Equations of State. Polynomial equations cubic in molar volume have been found the simplest of those capable of well representing both liquid and vapor behavior; this dual phase applicability is required for general thermodynamic use. Some well-known equations have been developed by *van der Waals, Redlich/Kwong, Soave, Benedict-Webb-Rubin* and *Peng/Robinson.* Solution of the cubic equations with concomitant calculation of physical and thermodynamic properties are iterative and usually require computer methods. In some process simulator programs used to obtain properties for release modeling, the user may be required to select the equation of state method. Descriptions can be found in references [3,5,7,8].

Generalized Correlations for Liquids. Because of the uncertainties in modeling accidental releases, where the major uncertainties are specification of the release scenarios and stochastic variations caused by atmospheric processes, the *variation* of liquid specific volume (reciprocal density) with temperature and pressure should not be significant in many applications. For example, hydrocarbons will change volume by about 1 to 2 percent with change of 10 degrees kelvin. Thus it may be sufficient to use a single average value, taken from tables or correlations for the temperature range of interest. Also, liquid specific volume is usually a weak function of pressure, so this variation can often be neglected. If the temperature range of interest is large, it might be necessary to fit a simple linear or quadratic function of temperature to tabulated densities. Densities for multicomponent liquids can often be obtained from general purpose VLE/physical properties computer programs.

If liquid density data is not available for a particular compound, Rackett's equation (Smith and Van Ness, p. 97) is probably the simplest available. The specific molal volume for a saturated pure liquid is found by

$$V^m_{sat} = V^m_c Z_c^{(1-T_r)^{0.2857}} \tag{19}$$

where V^m_c is the critical molal volume, Z_c is the compressibility calculated from the ideal gas law using the critical volume, temperature, and pressure, and T_r is the reduced temperature (T/T_c). Critical constants are given for selected compounds in Smith and Van Ness, Appendix B, and for an extensive number of compounds in Appendix A of Reid, Prausnitz and Poling [7]. The latter authors present (p.67) a modified form of the above equation which is accurate, but requires an additional, empirically fitted constant unique to each compound. Smith and Van Ness also discuss the Lydersen et al correlation, which is also based upon corresponding states with which the reduced density is found graphically for given reduced temperatures and pressures. Reid, Prausnitz and Poling present several other, more complex methods designed for accurate liquid density estimation over wide ranges of temperature and pressure.

Thermodynamic Properties

The *primary* thermodynamic properties are pressure (P), volume (V), temperature (T), internal energy (E★), and entropy (S). These quantities may be related through the first and second laws of thermodynamics by means of differential equations for particular applications. For convenience, three additional properties have been defined:

$$\begin{aligned} \textit{Enthalpy}:&\ H = E + PV \\ \textit{Helmholtz energy}:&\ A = E - TS \\ \textit{Gibbs energy}:&\ G = H - TS \end{aligned} \tag{20}$$

★ Smith and Van Ness use the symbol U.

These quantities, and/or differential quantities *derived* from them, are used to develop sets of equations to represent particular applications (*e.g.*, a VLE calculation).

In release applications, *heat capacities* are often involved. The *heat capacity at constant pressure* is defined as

$$C_p = \left(\frac{\partial H}{\partial T} \right)_P \qquad (21)\diamond$$

and the *heat capacity at constant volume* is defined as

$$C_V = \left(\frac{\partial E}{\partial T} \right)_V \qquad (22)$$

These important parameters are required for the calculation heat content and temperatures of mixtures from individual component values, adiabatically expanded gas properties, and flashing choked flow rates, for examples.

Experimentally obtained values of specific or molal volumes, enthalpies, and entropies as functions of temperature and pressure are available in the literature and computerized databases for many substances. For some of these substances, heat capacities at constant pressure can be found. Heat capacities at constant volume are seldom found in the literature, but may be derived from the other available quantities. If, for example, the enthalpy for a substance is available as a function of temperature at a given pressure, then the data may be fitted to an empirical equation, and Equation 21 used to calculate the temperature slope (C_p) at a particular temperature, or, more simply, finite differences can be used to calculate the approximate value from a table.

As will be seen, the ratio $k = C_p/C_v$ is used in certain equations to calculate choked flow. For ideal gases *only*,

$$C_v = C_p - R \qquad (23)$$

If the gas departs significantly from ideality, spurious values can be obtained by using the preceding equation. (*e.g.*, $C_V < 0$). If k is not available from reliable sources, a value of 1.4 is recommended for screening purposes in release scenario modeling.

Other Properties

Viscosity. For calculations involving the flow of fluids through pipes and other devices where frictional energy losses need be considered, the *viscosity* (v) fluid property is required; examples are pipe flow and pool evaporation. Viscosity is defined as the ratio of shearing stress divided by a velocity gradient, so its dimensions[★] are $F\tau/L^2$; the *poise* is 0.1 Pa•s. The *kinematic viscosity* is the ratio of viscosity to density with units $L^2\tau$.

Perry's Sixth, Chapter 3, has nomographs for obtaining the viscosities of a number of pure compound gases and liquids. A number of estimation methods for gas viscosities, based on molecular theory of gases coupled with empirical correlations, are available; their number and

---

[★] See *Nomenclature* for dimension symbols.

complexity are beyond the scope of this chapter [Reid, Prausnitz and Poling, Chapter 9]. Estimation methods for liquids are generally empirical and are based on correlations which relate the logarithm of viscosity to temperature or reciprocal absolute temperature. Reid, Prausnitz and Poling combined experimental correlation parameters from three sources which may be used to *interpolate* viscosities of pure compounds with experimental temperature ranges; these are presented in their Table 9-8.

Those authors also discuss the Grunberg and Nissan method which uses binary functional molecular group parameters for estimating the viscosity of mixtures. Also, the Teja and Rice method based on a Corresponding States treatment for mixture compressibility factors is described. The latter authors showed that their method gave about the same accuracies as the Grunberg and Nissan method for nonpolar-nonpolar and nonpolar-polar systems. The Teja and Rice method gave good accuracies for polar-polar mixtures, but the Grunberg and Nissan form should not be used for these mixture types.

Molecular Diffusivity. This parameter ($\mathfrak{C}$) characterizes the rate of molecular diffusion of chemical species in a phase. In the applications discussed here, it is used in the calculation of evaporation rates of substances from liquid pools. Its dimensions are M^2/τ. Reid, Prausnitz and Poling discuss a number empirical and theoretically-based methods for estimating diffusion coefficients (diffusivities) which are too extensive to be mentioned here. However, for modeling evaporation release scenarios, diffusivities of single pure compounds in air are all that may be required. Perry's Sixth (Table 3-256) lists values for a number of organic compounds; for the accuracy required, it may suffice to use the value of an analogous compound from this or other sources.

Surface Tension. This parameter (σ) characterizes the tangential forces acting in the liquid surface and is defined as the force exerted per unit length of surface; commonly-used dimensions are dynes/centimeter. This parameter is used in models involving aerosol formation and spreading of liquids on plane surfaces. Aerosol formation is discussed further under *Evaporation*.

For estimating the surface tensions of pure compounds, Reid, Prausnitz and Poling recommend the Corresponding States method described in their Chapter 12 for non-hydrogen bonded liquids. For hydrogen-bonded liquids, they recommend the Macleod-Sugden form. The data collection of Jasper [5b] has experimental surface tensions of many liquids. They also recommend the Macleod-Sugden equation form for nonaqueous mixtures; this method was originally developed for pure nonpolar compounds. If the solubility of the organic compound in water is low, the Szyszkowski equation, as developed by Meissner and Michaels, is recommended by Reid, *et al.*

For estimating the surface tensions of binary organic-aqueous mixtures, they recommend the method of Tamura, Kurata, and Odani.

Mixture Bulk Properties, Pseudo-Pure Components and Average Values

Fluid modeling equations for flow rates, mass, energy and momentum balances are based on single-value *bulk* properties for the released substance, *e.g.*, liquid and vapor density, enthalpy, entropy, specific heat, and viscosity. In an actual release, bulk intensive properties may be changing with time and distance (travel time) along the stream/vapor cloud path. These changes can be caused by composition changes in mixtures (evaporating and/or reactive liquids) as well as by pressure and temperature changes of the fluid stream. Computer modeling programs designed to treat multicomponent vapor and liquids contain thermodynamic - fluid properties subprograms which calculate fluid properties based upon temperature, pressure and composition for each instant or step during the solution of algebraic and/or differential equations. These property calculations use accurate, non-ideal condition estimation methods. However, many stand-alone dispersion programs handle the released fluid (vapor or liquid) as a pure compound (component), with user-supplied, constant property values and parameters, *e.g.*, molecular weight (M) and heat capacity (C_p). Such constant values are also required for simplified modeling estimates with desk calculators and computerized spreadsheets. These constant values are often called *"pseudo-pure component"* properties.

To calculate a pseudo-pure component property, $\mathcal{P}$, for a multicomponent vapor or liquid at constant temperature and pressure, the following equation can often be used:

$$\mathcal{P} = \sum_{i} f_i \mathcal{P}_i, \qquad i = 1,\ 2, \ldots N_{cs} \tag{24}$$

where $\mathcal{P}_I$ is the corresponding property for the i^{th} component, f_i is the mole (or mass) fraction concentration of the i^{th} component; the summation is made over all N_{cs} components in the mixture. It is exact for molecular weights. Nonlinear mixing effects for hydrocarbons are small, but as the polarity of compounds increase, mixing effects become larger; aqueous-polar mixtures have very large mixing effects. For release and dispersion modeling purposes, the preceding equation is applicable for specific volumes (= reciprocal densities), and thermodynamic properties such as enthalpy, entropy, internal energy, and Gibbs energy. This equation is generally *not* applicable for surface tension and transport properties such as viscosity and diffusivity.

Example Calculation of Pseudo-Pure Component Properties

Column =	2	3	4	5	6	7
Compound	Mole Percent	M = Molecular Weight	Col. 2 * Col. 3	Weight % = Col. 4 / Sum Col. 4	C_p KJ/[kg•K]	Col. 5 * Col. 6
Methane	14.6	16.04	234.2	6.1	2.30	14.13
Ethane	10.6	30.07	318.7	8.4	1.86	15.58
Propane	71.6	44.09	3156.8	82.8	0.99	81.73
H2S	3.2	32.02	102.5	2.7	1.08	2.91
Totals	100.0		3812.2	100.0		114.36

Pseudo pure component values

Bulk M = Sum Col. 4 / 100 = 38.12

Bulk C_p = Sum Col. 7 / 100 = 1.14 KJ/[kg•k]

The box above shows how several psuedo-pure component properties were calculated for Scenario 1 in Chapter 6. If a dispersion modeling program is used with pseudo-pure component properties, the dispersed concentration at downwind locations will be reported on the basis of the released mixture. If the dispersed concentration of a particular (*"key"*) component is required, calculate it by:

$$c_{key} = f_{key}\, c_{bulk} \tag{25}✧$$

where f_{key} is the mole fraction of the key in the released material, c_{bulk}, is the model reported downwind concentration (mole fraction = volume fraction) of the released material, and c_{key} is the downwind concentration of the key component. This equation assumes constant relative concentrations among the mixture's components. This calculation is also shown in the box.

Modeling often requires *averaging* of certain properties over temperature and/or pressure, and concentrations at given downwind locations over time intervals. Given a quantity $\mathcal{P}(x)$ which is a known function of the independent variable x, the average value of the quantity over the linear interval x_1 to x_2 is

$$\bar{\mathcal{P}} = \frac{\int_{x_1}^{x_2} \mathcal{P}(x)\, dx}{x_2 - x_1} \tag{26}$$

for the continuous case, and,

$$\bar{\mathcal{P}} = \frac{\sum_i \mathcal{P}(x_i)\, \Delta x_i}{x_2 - x_1}, \qquad i = 1, 2, \ldots n \tag{27}$$

for the finite difference case of n intervals. If the x-interval is constant, the preceding equation reduces to

$$\bar{\mathcal{P}} = \frac{1}{n} \sum_i \mathcal{P}_i \tag{28}$$

To select average values for a particular substance's property, particularly over a large range of temperature or pressure, and the property varies significantly (*i.e.*, over 20 percent), a plot can help decide the best method of averaging. Heat capacities are often available as polynomial functions of temperature; thus the integral form above can be used directly.

General References

Desktop References. *Perry's Chemical Engineering Handbook* [6] contains tables in Chapter 3 of physical, thermodynamic, and transport properties for many commonly-encountered chemical compounds. The same chapter also presents a number of property estimation methods and correlations, in both nomograph and equation form. This is a good book to start looking for (constant) property values required by simple release rate calculations (*e.g.*, choked flow of ideal gases; discussed later) and required by public domain dense gas dispersion programs (*e.g.*, heats of vaporization and boiling points).

Reid, Prausnitz and Poling's *The Properties of Gases and Liquids* [7], presents a critical review of various estimation procedures for essentially all of the properties of interest in release modeling, and recommends the best methods. Equations are given for each procedure, usually with example calculations along with comparisons of estimated vs. experimental values. Appendix A of that book contains parameters such as molecular weights, normal boiling points, critical temperatures, pressures and volumes, constants for nonideal equations of state, heat capacities temperature coefficients, and standard enthalpies and Gibbs energies of formation for 618 pure compounds. Many of the method descriptions and recommendations presented in the following overviews were taken from this reference.

Smith and Van Ness also describe many property estimation methods.

The *Technical Data Book—Petroleum Refining* from the American Petroleum Institute [2] is available in three loose leaf binders as well as in computerized form for both the English and Metric measurement systems. To quote the API Publications catalog [2]:

> "The *Technical Data Book* is a comprehensive manual of physical and thermodynamic data and correlations on behavior of hydrocarbons and hydrocarbon mixtures for use in process design. It contains over 1000 pages and includes 15 chapters on general data, characterization of fractions, ASTM-TBP-EFV relationships, critical properties, vapor pressure, density, thermal properties, vapor-liquid equilibria, water solubility, surface tension, viscosity, thermal conductivity, diffusivity, and combustion."

The catalog also lists a number of other publications on physical properties of pure compounds and petroleum fractions.

AIChE's Design Institute of Physical Property Data (DIPPR®) has developed a large database containing evaluated and screened data for pure chemical compounds as well as for binary mixtures [4]. (This information is also available on-line; see later.) Gess, Danner and Nagvekar's *Thermodynamic Analysis of Vapor-Liquid Equilibria: Recommended Models and a Standard Data Base*, [5] which provides practical methods for using a limited number of experimental data points to interpolate and extrapolate VLE-required properties to other conditions. This book also contains definitive summary descriptions of the equations used in generalized VLE algorithms, equations of state, data fitting methods, consistency tests, guidelines for selections of models, and an extensive set of references on these subject. In addition, generic Fortran programs and subroutines for evaluation of VLE data and methods are provided on floppy disc with the book. Also, see Danner and Daubert's *Manual for Predicting Chemical Process Design Data* [3].

On-Line Computer Services. The Chemical Abstract Service's *STN International* network provides direct online access to over 160 scientific and technical databases [9]. *Table 1* lists those databases of most interest. Personal computer software is available from STN which greatly simplifies data searches and information retrieval to user files. STN also has a literature search service which will obtain information, such as chemical property data, most expeditiously if only a few such requirements are anticipated.

Technical Database Services, Inc., provides online interactive service for a number of databases containing physical, thermodynamic, safety, environmental and regulatory data for chemicals [10]. Examples of interest are DIPPR, DETHERM®, DDB®, and PPDS2; all contain thermophysical and phase equilibria properties for pure components and mixtures, as well as interpolation and estimation methods. Customer assistance is available for literature searching, physical property estimation and VLE calculations by means of their PC and on-line software.

Process Flowchart Simulators. Process flowchart simulation programs, available commercially or within petroleum, chemical, and process engineering companies, have comprehensive capabilities for thermodynamic and fluid mechanics computations for pure compounds and multicomponent mixtures which include VLE, flow rates through pipes, orifices and other devices. These programs contain large databases for process stream property retrieval and estimation; detailed stream and component properties can be output to a file or printer. Such properties may be used directly in release and dispersion simulation programs and/or to develop pseudo-pure component properties. References and advertisements for commercially available programs may be found in the current chemical engineering literature.

Table 1. STN Databases

Symbol	Database	Contents
DIPPR	Design Institute for Physical Property Data	Over 1,200 organic compounds
CHEMLIST	Regulated Chemicals Listings	U.S. and Canadian chemicals
HODOC	*CRC Handbook of Data on Organic Compounds*	25,500 compounds
JANAF	Joint Army-Navy-Air Force	Thermochemical data for > 1,100 plus organic substances with 1 or 2 carbons
NISTFLUIDS	NISTFLUIDS (National Institute. of Standards and Technology)	Critically evaluated properties for 12 industrial fluids.
NISTTHERMO	Tables of Chemical Thermodynamic Properties (National Institute. of Standards and Technology)	Thermochemical property data for over 8,000 inorganic and small organic molecules.

Thermodynamics of Fluid Depressurization

Basic Premises and Equations

As discussed by Smith and Van Ness, two assumptions can be made to simplify the application of thermodynamic principles to flow processes:

1. Fluid flow is unidirectional through any cross section (differential slice) of a conduit (or vapor cloud along its axis of flow) where thermodynamic, kinetic, and dynamic properties are assigned or evaluated.
2. Within a cross section, properties do not vary with the direction perpendicular to flow.

The first premise rules out countercurrent and/or recirculating flows in the phenomena to be addressed. The second eliminates the need to model velocity, temperature, concentration, etc. profiles through cross sections; this greatly simplifies the formulation of modeling equations. The second assumption is often called "plug flow," or "top hat flow profile." Considering other modeling uncertainties (*e.g.*, scenario definition and atmospheric processes) associated with the purposes of this manual, calculations made with these assumptions should be sufficiently accurate.

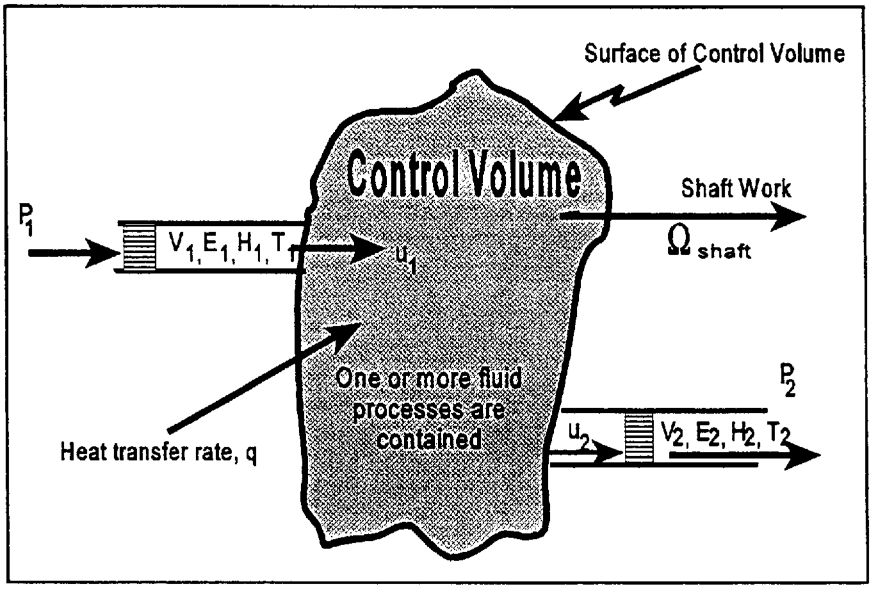

Figure 3.

Overall equations for conservation of mass, energy, and momentum are applied to *control volumes* or *process envelopes* which are equivalent to thermodynamic closed systems. Such equations are often called "*macroscopic shell balances*." The control volume can have flow entrances and exits corresponding to physical equipment, for which the control volume surface is placed perpendicular to the flow to impose the above two assumptions. Net flows of heat energy (q) and shaft work (Ω_{shaft}) can enter or exit the control volume at any point. A control volume example is shown in *Figure 3*. For example, a control volume may contain a process as simple as flow through an orifice or it may be as complex as a chemical process unit composed of many pipes, heat exchangers, compressors, etc, and with many entrances and exits.

Conservation of Mass. For any process, the conservation of mass equation for flow processes contained within a control volume is:

$$\left\{\begin{array}{c}\textit{Accumulation rate of}\\ \textit{mass within the}\\ \textit{control volume}\end{array}\right\} = \left\{\begin{array}{c}\textit{Net in mass}\\ \textit{flow rate at}\\ \textit{entrances}\end{array}\right\} - \left\{\begin{array}{c}\textit{Net out mass}\\ \textit{flow rate at}\\ \textit{exits}\end{array}\right\} \tag{29}$$

The term on the left side the equation reflects the change with time for a dynamic system, *e.g.*, the change in total contents ("holdup") of a vessel for which the control volume coincides with the vessel volume. Using W for mass, w for mass flow rates, the change of total mass holdup in the control volume with time is

$$\frac{dW}{dt} = w_1 - w_2 \tag{30}$$

for which the numerals 1 and 2 denote the entrances and exits of the control volume, respectively. Also, the mass flow rates at entrances and exits are

$$w = \rho u A \tag{31}$$

where ρ is the average fluid density, u is the average velocity, and A is the cross-sectional area. Substitution of the preceding into Equation 30 yields the general *continuity equation*:

$$\frac{dW}{dt} = \Delta(\rho u A) \tag{32}$$

where Δ denotes the difference between all exit and entrance streams.

Methods for calculating flow rates are limited in this Manual to the special *steady state* application of the above equations, for which it is assumed that there is no net change in the mass holdup of the control volume over time; *e.g.*, $dW/dt = 0$. Time dependent evaporation from pools usually requires consideration of holdup. Relationships concerning holdup cannot be deduced from models which assume a steady state process on the basis of such mass balance equations alone; additional information is needed which is not available from non-time dependent equations.

Conservation of Energy. An analogous procedure to the above for mass can be applied to the conservation of energy around a control volume or an open system:

$$\left\{\begin{array}{c}\textit{Accumulation rate}\\ \textit{of energy within}\\ \textit{control volume}\end{array}\right\} = \left\{\begin{array}{c}\textit{Net (in-out) energy}\\ \textit{transport rate for}\\ \textit{control volume}\end{array}\right\} + \left\{\begin{array}{c}\textit{Net heat transport}\\ \textit{rate, } q\textit{, in across}\\ \textit{the control surface}\end{array}\right\} - \left\{\begin{array}{c}\textit{Net power out,}\\ W^{I}\textit{, across the}\\ \textit{control surface}\end{array}\right\} \tag{33}$$

The left-most term is the rate of change of energy with time of the total internal energy within the control volume. Associated with each flowing stream are three forms of energy: internal, kinetic (stream velocity), and potential (elevation above a datum level). The heat term can contain contributions from radiative, conductive (through solids) and convective heat transfer (flowing streams).

Again, the above time dependent, general equation can be simplified with the *steady state assumption* for which there is no accumulation of energy in the control volume with time.

General Steady State Energy Balance. Referring to Equation 33, with zero accumulation rate and the rightmost term transposed to the left side of the equality, the macroscopic energy balance around a closed system of fluid of unit mass may be written as (Smith & Van Ness)

$$Q - \Omega = \Delta E_{int} + \Delta E_{kin} + \Delta E_{pot} \tag{34}$$

where

ΔE_{int} = change in internal energy,

ΔE_{kin} = change in kinetic energy = $\Delta(wu^2/2g)$,

ΔE_{pot} = change in potential energy = $\Delta(wzg/g)$,

Q = heat transferred across the system boundary,

Ω = net work for system = Ω_{shaft} + expansion or pressure work, and,

Ω_{shaft} = shaft work[★].

Note that heat, Q, must be transferred across the system boundaries, and that both heat Q and work Ω are path dependent. Unlike the other terms in the above equation, ΔE_{int}, ΔE_{kin}, and ΔE_{pot}, which only depend upon the change in initial and final states of the fluid, heat transferred into a system, and work performed on or by a system, depend upon the thermodynamic history of the fluid.

Next, take this same unit mass, and assume it is flowing, but draw a process envelope around it, as in Figure 3. There are pressure forces on the fluid, and these forces do work. The upstream forces do work on the fluid system. The downstream pressure forces do work on the surroundings. The kinetic energy change of a unit mass of fluid between the inlet and the outlet is

$$\Delta E_{kin} = \tfrac{1}{2}u_2^2 - \tfrac{1}{2}u_1^2 = \tfrac{1}{2}\Delta u^2 \tag{35}$$

In this equation u is the average fluid velocity, defined as the volumetric flow rate (U) divided by the cross-sectional area (A). The potential energy change of a unit mass of fluid between the inlet and outlet is

$$\Delta E_{pot} = z_2 g - z_1 g = g\Delta z \tag{36}$$

where z_2 and z_1 are the elevations of the outlet and inlet, respectively. Equation 34 now becomes

$$Q - \Omega = \Delta E_{int} + \tfrac{1}{2}\Delta u^2 + g\Delta z \tag{37}$$

The force exerted on the upstream face of the inlet stream is P_1A_1, and the work done by this force in pushing the cylinder into the apparatus is

$$\Delta E_1 = P_1 A_1 \frac{V_1}{A_1} = P_1 V_1 \tag{38}$$

[★] Smith and Van Ness use U for internal energy and W for work, different symbols are used here to avoid conflicts.

This is the work done *on* the system by the surroundings. Correspondingly, the work done *by* the system on the surroundings as the fluid leaves the exit is

$$\Delta E_2 = P_2 A_2 \frac{v_2}{A_2} = P_2 v_2 \tag{39}$$

Because ΔE_{int} represents *all* the work done by the unit mass of fluid, it is equal to the sum of the shaft work and the entrance and exit work quantities:

$$E_{int} = \Omega_{shaft} + P_2 v_2 - P_1 v_1 \tag{40}$$

Combining the above equation with Equation 37 and rearranging yields

$$\Delta E_{int} + \Delta(Pv) + \tfrac{1}{2}\Delta u^2 + g\Delta z = Q - \Omega_{shaft} \tag{41}$$

For a unit mass, enthalpy is defined by

$$\Delta H = \Delta E_{int} + \Delta(P v) \tag{42}$$

Also

$$\Delta(Pv) = v\Delta P + P\Delta v \tag{43}$$

Solving the Equation 3-42 for ΔE_{int} and substituting into Equation 3-41 yields:

$$\Delta H + \tfrac{1}{2}\Delta u^2 + g\Delta z = Q - \Omega_{shaft} \tag{44}✧$$

(Smith & Van Ness, p. 216). *Equation 44 is the* ***first law of thermodynamics for a steady state flow process;*** all terms are expressions of energy per unit mass in the SI system of units (Joules or multiples thereof). All of the terms may be significant depending upon the circumstances of the application. However, many hazardous substance releases involve a large flow rate of a compressible fluid. This usually involves a large depressurization. For a compressible fluid, this large depressurization results in a decrease in density, which for piping of constant or moderately changing diameter results in a corresponding change in velocity. Also typically, unless the pipe system is very long, contact with the pipe is brief enough that heat transfer through the pipe wall is small or negligible. Many problems involve flows under choked conditions, in which the substance is at the speed of sound in the fluid at the end (or restricted part) of the pipe. This results in typical velocities for two phase fluids on the order of 50 meters/second, and for gases of several hundred meters/second. For moderate length pipe systems, the contact period is on the order of a few seconds or less, insufficient to transfer a large amount of heat through the pipe wall. Finally, for the sake of simplicity, assume there is no shaft work, and potential energy changes are negligible compared to kinetic energy changes. The final, simplified energy balance is:

$$\Delta H + \Delta E_{kin} = 0 \tag{45}$$

To have an isenthalpic situation, (ΔH=0), there can be no significant change in kinetic energy. This is an assumption in developing Joule-Thompson expansion coefficients; adiabatic depressurization without an appreciable change in kinetic energy. *Thus, an isenthalpic, or Joule-Thompson type path is* ***inappropriate*** *for a situation in which a substantial change in kinetic energy occurs to a releasing fluid, typical of a gas or flashing liquid release from high pressures.*

To better model flow systems with significant kinetic energy changes, reversible and irreversible processes are defined: "A process is *reversible* when its direction can be reversed at any point by an infinitesimal change in external energy" (Smith and Van Ness, page 39). That is, energy losses, such as from friction and mixing, are *not* incurred which cannot be recovered should the flow process be reversed. An *irreversible* process is one for which the restoring energy is finite, *e.g.*, constant. An example of an irreversible process is the steady state depressurization of a flowing stream into the atmosphere for which it is assumed that no mixing with–, or heat transfer to–, the atmosphere occurs. The restoring force is the constant atmospheric pressure.

Entropy is defined as

$$\Delta S = \int_{T_1}^{T_2} \frac{d\underset{\sim}{Q}_{rev}}{T} dT \tag{46}$$

where

T = system temperature, (subscripts 1 and 2 denote initial and final states), and,

$\underset{\sim}{Q}_{rev}$ = heat amount change occurring during the differential temperature change, dT, if the thermodynamic path is reversible.

Smith and Van Ness (pp 155-156) show that the total work for an adiabatic irreversible process which goes from State 1 to State 2, coupled with the reversible restoration process is

$$\Omega = \Omega_{irr} + \Omega_{rev} = \underset{\sim}{Q}_{rev} = \int_2^1 d\underset{\sim}{Q}_{rev} \, . \tag{47}$$

(Note that the integral in the above equation is negative for the *reversible* restoration process.) Since the original irreversible process is adiabatic, the total entropy change for this process is $\Delta S_{total} = S_2 - S_1 > 0$. Thus, ΔS_{total} is always positive for any process, and it *approaches* zero in the limit when the process becomes reversible. This is a statement of the second law of thermodynamics which can be written as

$$\Delta S \geq 0 \, . \tag{48}$$

Hence, by definition, an isentropic process (ΔS = 0) is reversible and adiabatic. It is also an idealization which can never be attained in practice. But it is a useful concept for modeling real processes on an *a priori* basis. Often, a flow process can be sufficiently well-modeled by ignoring energy losses such as friction and other work. Also, the efficiency of a process (*e.g.*, a turbine expander) can be evaluated by using the isentropic process (100% efficiency) as the basis.

It follows that use of the first law of thermodynamics (Equation 44) coupled with the assumption of constant entropy will give more accurate results for rapidly expanding depressurizing releases than by assuming constant enthalpy: the former should be used if the appropriate thermodynamic data can be obtained.

Superheated Gases

A gas is *superheated* if its temperature is above its dew point at the given pressure. If the gas is released to atmospheric pressure, and its temperature is sufficiently high, then it will not condense during the expansion process. In many release applications, non-condensing gas discharges may be approximated by assuming that the gas is ideal. Because the energy of an ideal gas, by definition, is independent of volume (and therefore pressure), Equation 21 reduces to

$$C_p = \frac{dH}{dT} . \tag{49}$$

Thus for a change from State 1 to State 2,

$$\Delta H = \int_{T_1}^{T_2} C_p(T)\, dT . \tag{50}$$

where $C_P(T)$ is the heat capacity function over the temperature range of interest. Often, C_p may be assumed constant over a particular temperature range of interest, or as a simple mean. For applications involving entropy, the mean value is best calculated by

$$C_{P,ms} = \frac{\int_{T_1}^{T_2} [C_P(T)/T]\, dT}{ln(T_2/T_1)} \tag{51}$$

in which the subscript *ms* denotes the *mean value specific to entropy calculations*. Usually, these can be obtained as polynomial functions of *T* from property databases such as DIPPR, and the order can be as high as six. If C_P can be taken as constant over the temperature range of interest, then that value can be used directly as $C_{P,ms}$ in Equations 50 and 52.

The general equation for entropy change for an ideal gas is (Smith and Van Ness, p. 153):

$$\Delta S = C_{P,ms}\, ln \frac{T_2}{T_1} - R\, ln \frac{P_2}{P_1} . \tag{52}$$

(For simplicity, subscript *ms* will be dropped in the following; it is to be understood.) Assuming isentropic expansion, Equation 52 equals zero, and can be rearranged to

$$\frac{T_2}{T_1} = \left(\frac{P_2}{P_1}\right)^{R/C_P} \tag{53}$$

Because $R = C_P - C_V$ (Equation 23), it may be shown that

$$\frac{R}{C_P} = \frac{k-1}{k} \tag{54}$$

where $k = C_P/C_V$ as before. Thus Equation 53 can be written as

$$\frac{T_2}{T_1} = \left(\frac{P_2}{P_1}\right)^{(k-1)/k}$$

(55)✧

These equations are useful in the calculation of quantities associated with expanding or contracting gases such as orifice throat temperatures for choked gaseous flow, the temperatures of a jet expanded to atmospheric pressure, and for calculating the densities of homogeneous multiphase mixtures (see following).

Two Phase Fluid Densities

The density of a two phase homogeneous fluid is calculated by combining the specific (or molal) phase volumes according to mass (or mole) fractions. Thus, $v = 1/\rho$, where v is specific or molal volume (*e.g.*, m^3/kg), and ρ is the corresponding density (*e.g.*, kg/m^3). That is,

$$v_{lv} = f_v v_v + f_l v_l$$

(56)✧

Then the homogeneous mixture, or aerosol, density is

$$\rho_{lv} = \frac{1}{v_{lv}}$$

(57)✧

Instantaneous Flashing Releases

When a substance is contained as a liquid at temperatures above its normal boiling point, the pressure will be equal to or greater than its vapor pressure at that temperature. The relative amount of “liquefied gas” vs “saturated liquid” contained in the pipe or vessel can be estimated by VLE calculations. Consider the case in which a vessel contains vapor and liquid in thermodynamic equilibrium, and *only the liquid phase* is suddenly exposed to atmospheric pressure. This could be caused by a

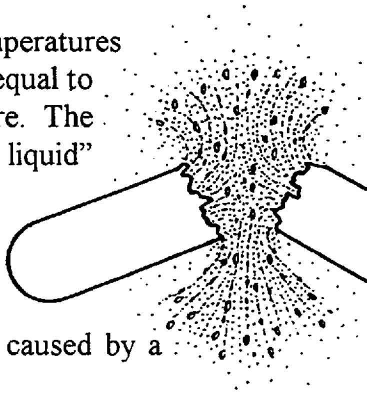

"catastrophic" rupture★ of the vessel, or by the liquid flowing from an orifice or other outlet below the liquid surface. If it is assumed that the initial expansion is adiabatic, that air does not mix with the expanding stream, and that the process is reversible, then the relative amount of vapor existing in the fully expanded substance may be calculated by an *isentropic energy balance.*

Let *State 1* be for the vessel ("reservoir") contents at temperature and pressure T_1 and P_1; these are often called "stagnation" conditions. Let *State 3* be for the liquid and vapor in thermodynamic equilibrium at its atmospheric boiling point (T_3, P_3)★★. The entropy balance is

$$\Delta S = S_1 - S_3 = 0 \tag{58}$$

With *v* and *l* subscripts representing liquid and vapor, and *f* their mole fractions at State 3, and because

$$f_l + f_v = 1 \qquad (59)✧$$

then, the entropy of the liquid plus vapor at state 3 is

$$S_{lv,3} = (1 - f_v) S_{l3} + f_v S_{v3} \tag{60}$$

Flashing Liquid. For liquid-only expansion, the entropy for State 1 is $S_{l,1}$, thus Equation 58 becomes

$$S_{l1} = S_{l3} - f_v S_{l3} + f_v S_{v3} \tag{61}$$

Solving the preceding equation for f_v, the fraction of vapor in the fluid at atmospheric pressure is

$$f_v = \frac{S_{l1} - S_{l3}}{S_{v3} - S_{l3}} \qquad (62)✧$$

The denominator in the preceding equation is the entropy of vaporization, ΔS_{vap} at atmospheric temperature and pressure and the numerator is the difference of entropies between the two states. (Example calculations are shown later.) *This equation should be used in cases where a saturated liquid is released.*

Vapor Condensation. If only the (saturated) vapor phase (in the infinite reservoir) is exposed to atmospheric pressure, using the same assumptions as for the liquid above, then it may be similarly shown that

---

★ The vessel bursts or fails all at once.

★★ State 2 will be used later for choked flow throat conditions.

$$f_v = \frac{S_{v1} - S_{l3}}{S_{v3} - S_{l3}} \qquad (63)✧$$

This equation is important; *it should be used to estimate the fraction of condensed liquid in a released saturated vapor stream;* e.g., a pressure relief valve on the vapor side of a fractionator reflux drum, with or without the valve outlet connected to the flare header system.

Approximate Isenthalpic Methods. If the kinetic energy involved in an expansion is neglected, as discussed in a previous section, then an isenthalpic balance can be used to calculate the vapor fractions for the two types of expansions specified above. That is,

$$\Delta H = H_1 - H_3 = 0 \qquad (64)$$

and, for the *flashing liquid,*

$$f_v = \frac{H_{l1} - H_{l3}}{H_{v3} - H_{l3}} = \frac{\Delta H_l}{\Delta H_{vap}} \qquad (65)$$

and for the *condensing vapor,*

$$f_v = \frac{H_{v1} - H_{l3}}{H_{v3} - H_{l3}} = \frac{H_{v1} - H_{l3}}{\Delta H_{vap}} \qquad (66)$$

If it is assumed that the molal heat capacity of the liquid ($C_{p,l}$) is constant, and defining $\Delta T = T_1 - T_3$, then Equation 66 becomes

$$f_v = \frac{C_{p,l} \Delta T}{\Delta H_{vap}} \qquad (67)$$

For most applications, C_p varies with temperature; the integral forms, Equations 65 and 66, are more correct. Equation 67 is often used in dispersion modeling programs which treat two-phase releases, as well as being cited in a number of "how to" manuals in the present literature.

The next page presents a detailed example of these calculations for chlorine. Although the enthalpy vs entropy results are not very different in this particular example, it is recommended that entropy always be used if possible.

Example for Instantaneous Flashing Release

Columns 1 - 9 in the table below contain the thermodynamic values for chlorine given in Perry's Sixth, page 3-184. The reference values were converted to SI units. The first, italicized, bolded row of numbers is for the normal boiling point at one atmosphere pressure and corresponds to State 3 in the text. Any of the following rows may be selected for the initial State 1, for example that underlined for a temperature of 37.78 degrees C.

Columns 10 and 11, enthalpies and entropies of vaporization, were found by difference of the column pairs [7-6], [9-8], respectively. The approximations for C_p in Column 12 were found by dividing the enthalpy difference from two adjoining rows in Column 10 by the temperature difference between the same rows for Column 1.

Columns 13 and 14 were therefore found directly from Equations 65 and 62 for enthalpy and entropy, respectively. For Column 15, the C_p values contained in the Column 12 were averaged; this value of 70,408 kg/kmol was used in Equation 67 with the Column 10 vaporization enthalpy values to calculate the vapor fractions.

Thus for a reservoir containing chlorine liquid under pressure (10.53 atm) at 37.78 C, if the pressure is dropped adiabatically to 1 atm, the temperature of the expanded, homogeneous two-phase mixture will drop to -34.05 C (the normal boiling point of chlorine) and will contain 0.212 and 0.788 mass fractions of vapor and liquid, respectively. This result is for the entropy-based calculation, Column 14.

Referring to Columns 13 and 14, the fractions vaporized as calculated by the enthalpy and entropy equations, respectively, increasingly diverge as the storage temperature becomes higher, as expected. Comparing Columns 13 and 15 for enthalpy, the differences in fraction vaporized are not very different over most of the temperature range. This is because the enthalpy is almost a linear function of temperature until the critical point is approached. For other compounds, and multicomponent systems, this may not be true.

Chlorine Data from Perry's Sixth, page 3-184

Calculated Values for Flashing Liquid

1	2	3	4	5	6	7	8	9	10	11	12	13	14	15
Temperature		Pressure	Molal Volume m³/kmol		Enthalpy kJ/[kmol•K]		Entropy kJ/[kmol•K]		Enthalpy of Vaporization	Entropy of Vaporization	Finite Difference ΔH/ΔT	Mass Fraction Vaporized		
kelvin	celsius	Atmo	Liquid	Vapor	Liquid	Vapor	Liquid	Vapor				per H Eq. 65	per S Eq. 62	per C_p Eq. 67
T	T	P	v_l	vv	H_l	H_v	S_l	S_v	H_v-H_l	S_v-S_l	$C_{p,l}$	f_f	f_f	f_f
239.10	***-34.05***	***1.000***	***0.0454***	***19.2386***	***16,855,409.9***	***37,253,771.2***	***129,921.41***	***215,219.45***	***20,398,361.3***	***85,298.04***	*{Not applicable for the initial row}*			
244.26	-28.89	1.247	0.0458	15.6972	17,210,034.9	37,402,218.9	131,376.20	214,031.87	20,192,184.0	82,655.67	68,711	0.017	0.017	0.018
255.37	-17.78	1.939	0.0467	10.4515	17,972,066.4	37,710,660.2	134,404.53	211,716.09	19,738,593.8	77,311.55	68,623	0.055	0.053	0.056
266.48	-6.67	2.894	0.0477	7.2200	18,735,747.2	38,005,906.1	137,314.11	209,637.82	19,270,158.9	72,323.71	68,667	0.092	0.087	0.095
277.59	4.44	4.168	0.0487	5.1483	19,506,025.8	38,281,359.0	140,134.61	207,767.38	18,775,333.3	67,632.77	68,857	0.130	0.120	0.133
288.71	15.56	5.824	0.0498	3.7640	20,281,252.6	38,537,018.9	142,836.36	206,075.08	18,255,766.4	63,238.71	69,062	0.168	0.151	0.171
299.82	26.67	7.922	0.0511	2.8141	21,064,726.5	38,766,288.1	145,478.73	204,501.53	17,701,561.7	59,022.80	69,327	0.206	0.182	0.210
310.93	37.78	10.531	0.0525	2.1421	21,861,395.7	38,965,867.8	148,032.03	203,046.74	17,104,472.1	55,014.71	69,694	0.245	0.212	0.248
322.04	48.89	13.718	0.0539	1.6552	22,672,909.7	39,130,809.7	150,525.95	201,651.33	16,457,900.0	51,125.38	70,142	0.285	0.242	0.287
333.15	60.00	17.553	0.0556	1.2939	23,505,866.2	39,254,516.1	153,019.87	200,285.62	15,748,649.9	47,265.74	70,712	0.326	0.271	0.325
344.26	71.11	22.112	0.0575	1.0204	24,368,512.2	39,330,389.4	155,484.10	198,949.59	14,961,877.2	43,465.48	71,444	0.368	0.300	0.363
355.37	82.22	27.474	0.0596	0.8096	25,270,744.2	39,345,234.1	157,978.03	197,583.87	14,074,489.9	39,605.84	72,376	0.413	0.329	0.402
366.48	93.33	33.719	0.0621	0.6432	26,227,407.0	39,282,556.2	160,531.33	196,129.08	13,055,149.2	35,597.75	73,573	0.459	0.359	0.440
377.59	104.44	40.941	0.0651	0.5100	27,263,242.0	39,119,263.8	163,173.70	194,585.23	11,856,021.8	31,411.53	75,150	0.510	0.390	0.479
388.71	115.56	49.231	0.0690	0.3997	28,412,886.9	38,807,523.6	166,023.89	192,774.16	10,394,636.8	26,750.27	77,253	0.567	0.423	0.517
399.82	126.67	58.695	0.0745	0.3054	29,752,214.9	38,251,669.5	169,230.36	190,517.76	8,499,454.7	21,287.40	80,246	0.632	0.461	0.555
410.93	137.78	69.442	0.0846	0.2151	31,510,495.2	37,116,869.4	173,386.90	187,014.39	5,606,374.2	13,627.50	85,289	0.718	0.510	0.594
416.48	143.33	75.340	0.1012	0.1514	33,121,977.3	35,441,060.0	177,127.78	182,709.41	2,319,082.7	5,581.63	91,703	0.797	0.553	0.613
417.16	144.01	76.082	0.1238	0.1239	34,269,972.7	34,269,972.7	179,859.21	179,859.21	At critical temperature.					

Flow Rate Estimation

Introduction

Many accidental releases occur from three types of discharges:

1. Through a relatively thin-walled hole or small rupture in a vessel or pipe wall.
2. From valves, which have very short piping lengths, if any, from their closure mechanisms to their surroundings, e.g., a pressure relief valve discharging to a larger vent pipe than its inlet, or with a very short outlet pipe.
3. Pipes (tubing), in which flow through significant lengths involve energy losses from friction, elbows, bends, valves, flow measuring venturis or orifices, etc.

Various flow regimes may be encountered, such as laminar ("Bernoulli") flow of vapors and liquids, critical ("choked") flow of vapors and liquids, and two phase flow. For the purposes of this manual, the first two types of discharges listed above can often be treated with the same equations, differing only in selection of discharge coefficients and/or effective orifice area. Thus, calculations for flow through a frictionless, thin-edged orifice will be presented with appropriate distinctions made for valves. Subsequently, a qualitative overview of pipe flow rate estimation is presented.

For any one fluid discharge from a vessel or pipe, it can usually be assumed that the position of the outlet on a vessel or pipe, and its orientation with respect to the direction the discharge is known. That is, from external knowledge, the initial state of the substance to be discharged is either liquid, vapor or both. Given this, then the rates and other quantities needed or derived from the source can be estimated. For example, suppose an insulated pressurized vessel is 90 %v liquid full, there is no current inflow or outflow, then a hole develops or a valve opens at the vessel height corresponding to 40 %v liquid full. Initially, liquid will flow from the hole, and as it does, vaporization will occur in the vessel as the liquid level decreases; this will cool the vessel contents. When the level gets to the hole, liquid and vapor will flow, but at a decreased rate compared with the liquid-only situation. Liquid and vapor will continue to flow (because of boiling, frothing and sloshing of the dense phase) until the fluid mixture cools to its boiling point or the vessel becomes essentially empty. Appropriate modeling of this process is very complex and requires extensive computation. On the other hand, it may be adequate to assume that the hole is at the top or bottom of the vessel (or on associated piping) and that either vapor or liquid flows at the initial conditions; this assumption generally gives worst case results from the atmospheric dispersion standpoint. Estimation of flow rates from pipes and piping systems is beyond the scope of this Manual. However, the *Flow from Pipes* section which follows the *Flashing Choked Flow* section in this Manual provides starting references for this subject. Quantitative flow rate estimation is limited to situations which can be treated by frictionless orifice theory.

Maximum flow through valves depends upon the internal geometry of the body/moving part (plug, butterfly, gate) assembly which controls the fluid flow. However, in the *limit*, the absolute maximum flow rate is that calculated for a sharp-edged, circular orifice for cases where the inlet flow is not limited and the resistance to flow at the outlet is very low. The same is true for short pipes (pipes less than about 100 mm in length) [Leung, 30]. For example, consider a pressure relief valve connected to the top of a pressure vessel by means of a sufficiently large diameter short pipe, and the valve outlet is connected to a large diameter flare header. Another example would be a drain valve near the bottom of a hydrocarbon storage tank. Each requires different treatment to best estimate the fluid flow rate through them.

For many accidental release scenarios, in which worst-case estimates of maximum flow rates are required, it is usually sufficient to use the upper-bound assumption of a sharp-edged orifice to estimate the discharge rate. Conversely, the hole area or diameter may be similarly calculated if the flow rate is postulated.

All the equations given in detail below are generally based on isentropic flow, as discussed in preceding sections. A basic reference for flow through venturi tubes, orifices, and nozzles is Perry's Sixth, pages 5-12 to 5-17. For valves, catalogs containing sizing equations (e.g., equivalent orifice areas) and parameters are available from valve manufacturers. Also, API Recommended Practice 520 [13], Coker's article [16], and Leung's article [18], all on the sizing and selection of pressure relief devices, can be used in a reverse manner to estimate flow through existing equipment.

Critical Pressure Ratio

The *critical pressure ratio* is used to characterize the choked vs. non-choked flow regimes:

$$r_c = \frac{P_2}{P_1} \qquad (68)\diamond$$

Figure 4 shows nomenclature conventions. The "reservoir" is assumed to contain a large fluid volume compared with the rate of flow through the hole, and, if a single phase, is homogeneous in temperature and composition. If the downstream, or external, pressure (P_3) is less than the pressure calculated for the throat (P_2) by means of the critical pressure ratio (r_c), then the flow regime is called "critical," or "choked," and the flow rate is independent of the external pressure P_3. If the downstream pressure is greater than the throat pressure as determined by the critical pressure ratio, but less than the upstream pressure, then the flow is called "non-critical" or "non-choked" because the flow rate *is* dependent on the external pressure, P_3.★

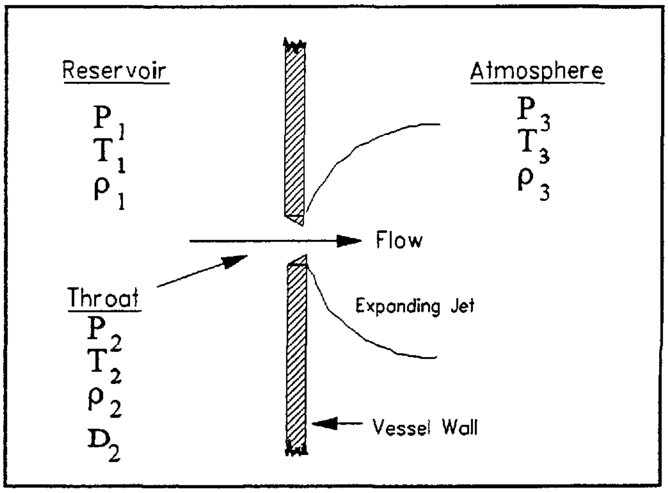

Figure 4. Definitions

For an *ideal gas* flowing through a frictionless orifice and for which no downstream mechanical hindrance to the expanding jet exists, the *critical pressure* ratio is

$$r_c = \frac{P_2}{P_1} = \left(\frac{2}{k+1}\right)^{k/(k-1)} \qquad (69)\diamond$$

for which

★ In this Manual, the terms "non-choked" and "choked" will be used instead of "sub-critical" and "critical," respectively, to avoid confusion with the use of "critical" for certain thermodynamic quantities; e.g., critical temperature.

$$k = \frac{C_p}{C_v} \qquad (70)✧$$

and C_p and C_v are the heat capacities at constant pressure and constant volume, respectively. For many gases at relatively low pressures (not near the critical point), k will range between about 1.1 and 1.8. For these values, r_c equals 0.585 and 0.469, respectively. Therefore, as a **"rule of thumb,"** *if the downstream (atmospheric) pressure is less than roughly half the upstream pressure, the flow will be choked.* If the ratio is near 0.5, then it might be a good idea to calculate r_c. However, for actual pressures very near the critical pressure ratio, the equations for choked vs. non-choked flow give similar values.

A General Model for Choked Flow

Referring to Equation 44, assume that flow through an orifice is adiabatic (Q and Ω_{shaft} are zero) and that there are no gravity effects ($g\Delta z = 0$), then

$$\begin{aligned} \tfrac{1}{2}\Delta u_2^2 &= \Delta H, \qquad or, \\ \tfrac{1}{2}(u_2^2 - u_1^2) &= H_2 - H_1 \end{aligned} \qquad (71)$$

for which subscript 1 is for the reservoir and *2* is for the throat. If the reservoir is stagnant, i.e., $u_1 = 0$, then

$$\tfrac{1}{2}u_2^2 = \Delta H \qquad (72)$$

This equation states that the kinetic energy of the flowing gas in the orifice throat must equal the change in enthalpy *per unit mass* of flowing gas. The equation provides an upper bound for the *flux* (G = mass flow rate per unit cross-sectional area) which is related to the velocity in the throat by

$$G = u_2\rho_2 \qquad (73)$$

where ρ_2 = density of the fluid in the throat. Equations 72 and 73 may be combined to yield:

$$G = \rho_2\sqrt{2(H_1 - H_2)} \qquad (74)✧$$

The choked flow rate is that for which the mass flux, G, is *maximum* with respect to throat pressure:

$$\left(\frac{\partial G}{\partial P_2}\right)_S = 0 \qquad (75)✧$$

for which the subscript S denotes constant entropy. The maximum, choked mass flow rate (w_{max}) is calculated from the throat area (A_2) by means of

$$w_{max} = G_{max} A_2$$

(76)✧

Equations 72 through 75 comprise a generalized choked flow algorithm, or model, wherein Equation 74 is to be solved subject to Equation 75 using an accurate (non-ideal) thermophysical properties method. This model will give the best results, subject to the applicable scope and accuracy of the thermophysical properties method as well as the stated assumptions, and is equally applicable to homogeneous, multiphase and supercritical systems. If the iterative solution process "passes near" the thermodynamic critical point, the extreme sensitivity of some physical property parameters to small pressure changes may inhibit convergence of the algorithm. It was found by the author that the Fibonacci search method was particularly effective for solving the above maximization problem for a number of single- and multi-component systems.

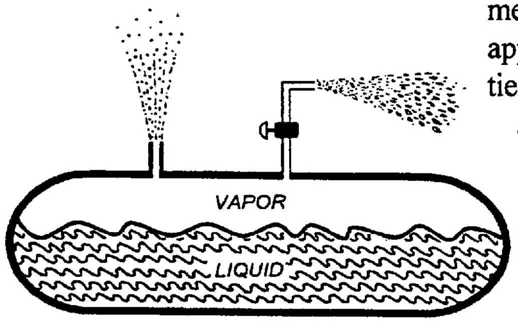

The above model serves as a basis for models designed for specific applications, such as for ideal gases and flashing choked flow. Actual computed flows will be less than the ideal, for the entropy changes will be positive and nonzero, and to various extents. Thus a *discharge coefficient* is often used to empirically correct for the non-ideality. However, nozzles can be tapered to achieve near-isentropic flow, and thus high efficiency.

Note that u_2 ***defines*** the speed of sound for the fluid at the throat conditions. Also, if a maximum for G with respect to throat pressure does not exist, the flow is non-choked.

Choked Flow of an Ideal Gas

In many applications, and particularly for screening studies, simplified equations can be obtained from the above general starting point by assuming that the gas is ideal. For this case, the choked mass flow rate through an orifice is

$$w_{max} = C_D A_2 \sqrt{k\left(\frac{P_1}{v_1}\right)\left(\frac{2}{k+1}\right)^{(k+1)/(k-1)}}$$

(77)✧

Here,

C_D = discharge coefficient, and

v_1 = specific volume of fluid in reservoir (volume per unit mass).

Substitution of the ideal gas equation (18) into Equation 77 yields

$$w_{max} = C_D A_2 P_1 \sqrt{k \left(\frac{M}{RT_1} \right) \left(\frac{2}{k+1} \right)^{(k+1)/(k-1)}} \quad (78)$$

where M = molecular weight of the gas. (Also, if SI units-of-measure are not used, the quantities in the square root symbol of the mass flow rate equations presented above and below should by multiplied by the gravitational constant, g = 9.807 m/s^2.)

However, Equation 77 (which uses specific volume molal directly) should be used for estimating choked flow rates for any gas below the critical point, unless a more rigorous method can be implemented, or the gas can be treated as ideal, for the factor involving k is not sensitive. For best results, values for the specific volume (v_1) and the specific heat ratio (k) should be obtained from the literature (e.g., Perry's Sixth) from experimental values, from thermophysical properties algorithms for real systems, etc. As a last resort use:

$$C_v = C_p - R \quad (79)$$

to calculate k; this applies strictly to an ideal gas. If a gas departs significantly from ideality, very spurious results can be obtained by using this equation (e.g., $C_v < 0$). *For screening purposes, use* $k = 1.4$ *for default.*

The coefficient of discharge (C_D) is used to empirically "calibrate" a particular shape and/or type of orifice, nozzle or valve, etc. Depending upon the device and its service, discharge coefficients can range from about 0.2 to 1.0. Graphs giving C_D values for specific applications may be found in standard engineering handbooks and references cited therein, e.g., Perry's Sixth, pp 5-13 to 5-16. For valves, the manufacturer's literature provides effective areas (A_2) as well as discharge coefficients. *For default screening purposes, use* $C_D = 0.6$ *and assume a circular hole.*

Non-Choked Gas Flow

The practical working equation for weight rate of gas discharge, adopted by the ASME Research Committee on Fluid Meters is [6, p. 5-12]:

$$w = C_D \Upsilon A_2 \sqrt{2(P_1 - P_3)\rho_1} \quad (80)✧$$

This "Bernoulli" type equation is applicable to discharge from the orifice or valve to the open atmosphere for which the critical pressure ratio (Equation 69) is not exceeded. The factor Υ accounts for the change in gas density as it expands adiabatically from the reservoir pressure P_1 to atmospheric pressure P_3:

$$\Upsilon = \sqrt{r^{2/k}\left(\frac{k}{k-1}\right)\left(\frac{1-r^{(k-1)/k}}{1-r}\right)} \tag{81}$$

in which

$$r = P_3/P_1 \tag{82}$$

These equations assume the entire exit stream is not mechanically restricted. If the flow is so restricted (*e.g.*, a pipe casing), then the β factor must be incorporated according to the reference. Some modeling programs may assume that the expansion factor, Υ, is close to 1.0, but this assumption may introduce additional estimation error. For example, if $r = 0.6$ and $k = 1.4$, then $\Upsilon = 0.75$.

Non-Flashing Liquid Flow

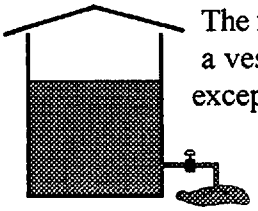

The flow of a liquid, stored below its boiling point temperature, through a hole in a vessel can be calculated by the same equation (80) as for non-choked gas flow, except the expansion factor Υ is unity; i.e.,

$$w = C_D A_2 \sqrt{2(P_1 - P_3)\rho_l} \tag{83}$$

For this, the total internal vessel pressure at the discharge point (P_1) is the sum of the liquid head (P_{lh}) and any imposed pressure on the surface of the liquid, such as atmospheric air or an inert gas pad for which this "vapor" pressure is therefore known and controlled:

$$P_1 = P_{lh} + P_{vapor} \tag{84}$$

The liquid head pressure is

$$P_{lh} = \Delta z_l \rho_l g \tag{85}$$

in which Δz_l is the vertical height of the liquid above the release point. Equation 83 is often called a "Bernoulli" equation.

Example Gas Flow Rate Calculations

Constants	***Chlorine***		
Temperature	T	kelvin	300
Molecular weight	M	--	70.91
Ideal gas constant	R	SI	8314.4
Atmo. pressure	P_3	Pa	101325
Discharge coefficient	C_D	--	0.6
Throat diameter	D_2	m	0.010
Cp/Cv	k		1.4
Throat area (Calc'd.)	A_2	m^2	7.854E-05

Both the choked and non-choked equations are used for actual choked and non-choked flow conditions to show the differences in results. The values for the incorrect combinations have been stricken out.

Parameters		**Case =**	**1**	**2**	**3**	**4**
Reservoir Pressure	P_1	Pa	506,625	151,988	506,625	151,988
Reservoir pressure	P_1	atm	5.0	1.5	5.0	1.5
Critical pressure ratio	r_c		0.528	0.528	0.528	0.528
ratio = P_3/P_1			0.200	0.667	0.200	0.667
Type of flow per critical pressure ratio			Choked	Non-choked	Choked	Non-choked
Type of flow equation			Choked	~~Choked~~	~~Non-choked~~	Non-choked
Flow equation No.			69	69	71-73	71-73
r = P_3/P_1 for Upsilon (Eq, 72)					0.200	0.667
Adiabatic expansion factor (Bernoulli)					0.4023	0.8022
Reservoir gas density	ρ_1	kg/m^3	14.40	4.32	14.40	4.32
Mass flow rate	w_{max}	***kg/s***	***0.0872***	~~***0.02615***~~	~~***0.0648***~~	***0.0705***

Flashing Liquid Flow

When a liquid, stored under pressure above its boiling point, is exposed through a hole to a region of lower pressure, such as the atmosphere, it will flash as it flows. The two phase mixture will have a much higher specific volume than the liquid, so the flow will be choked. The extent of flow limitation (compared with non-boiling liquid flow, Equation 83) depends upon the degree of “subcooling” below the VLE equilibrium temperature of the substance in the vessel.★ If the liquid temperature is relatively close to its atmospheric boiling point (*low subcooling*), vapor will be formed before the liquid reaches the final exit position. If the liquid temperature is low enough below its normal boiling point so that essentially no vapor is formed before the fluid reaches the final exit position, it is said to be in the *high subcooling* region. For accidental release modeling purposes, it is important to estimate the release rate of these “liquefied” substances as accurately as possible; if the non-boiling liquid "Bernoulli" equation (83) is used for a flashing liquid, the flow rate will be significantly overestimated. Below, the three most useful algorithms for

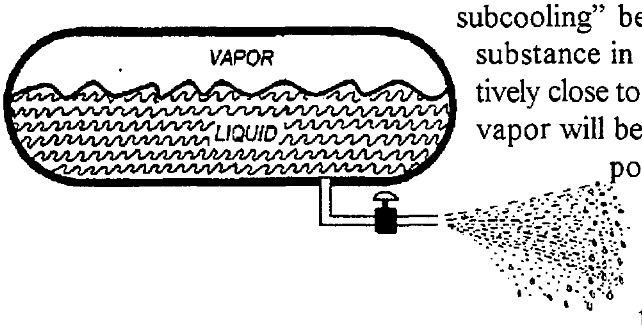

★ For these discussions, as in all preceding, it is assumed each phase in the reservoir, or container from which the substance is being released, is homogeneous in temperature and composition, and the phases are in temperature and composition equilibrium. This is the basis of the Homogeneous Equilibrium Model (“HEM”).

flashing liquid choked flow rates are summarized, followed by recommendations for accidental release modeling. Note that all algorithms presented are simplified procedures for pure components only.

A number of methods for estimating flow rates of flashing liquids through orifices and valves have evolved; the latest of interest have been developed by the AIChE Design Institute for Emergency Relief Systems (DIERS) [17,18,19]. Methods given in API Recommended Practice 521 [13] and by Fauske's 1965 method adopted by Cude (1975) [32] are not considered because they lack sound theoretical bases and/or are not validated by comparison with experimental data. The DIERS models, based upon extensive experimental data, can account for two phase slip (different velocities for vapor and liquid) for different flow regimes from the vessel, such as vapor-only, frothing, etc. The Homogeneous Equilibrium Model ("HEM"), in which it is assumed that the phases are in thermodynamic equilibrium (no phase velocity slippage), is the basis for several of the simpler DIERS modeling programs. Coker [16] and Simpson [16b] present simplified methods based upon the HEM for sizing pressure relief valves; these equations may be used in a reverse manner to estimated two phase flow rates from valves and orifices.

The following simplified calculational methods are based on the HEM concept, which has been recommended by AIChE-DIERS for emergency relief sizing design. According to Leung and others he referenced [30], these methods should be valid for flow passages of at least 50-100 mm in length, which are closely approached in most industrial type relief devices. The methods are presented below in historical order. *HEM-based flows are lower than those based on the more refined models which consider phase slip.*

Fauske and Epstein [20,24] state that if the stagnation pressure (P_1) is substantially larger than the vapor pressure corresponding to the stagnation temperature (T_1), the all-liquid Bernoulli *type* flow equation can be assumed to calculate the flow rate. Thus, restating Equation 83 in terms of mass flux (Equation 76), replacing P_3 with the saturation vapor pressure, P_s and dropping the subscript max denoting maximum flux:★

$$G = C_D\sqrt{2(P_1 - P_s)\rho_{l,1}} \qquad (86)\diamond$$

(This will be called the "Vapor Pressure Limited Flux.") However, as subcooling approaches zero, i.e., P_1 approaches P_s, those authors use the following approximate equation for *low quality flashing liquids*★★ (low subcooling):

$$G \cong \frac{\Delta H_{lv}}{\Delta v_{lv}}\left(\frac{1}{TC_{pl}}\right)^{1/2} \qquad (87)$$

in which T is the normal boiling point if discharge is to the atmosphere. The preceding equation is a reasonable approximation as long as the vapor mass fraction obeys

---

★ The symbol P_s will be used for saturated vapor pressure of the pure component at stagnation temperature T_1 to avoid conclusion with other usages; also this is consistent with the references.

★★ *Quality* of a vapor/liquid mixture refers to the relative amount of vapor vs. liquid and is the mass fraction of vapor (f_v). The symbol x is often used for this parameter.

$$f_v < \frac{P_3 v_{lv}}{\Delta H_{lg}^2} \bullet C_{pl} T_{NBP} \qquad (88)$$

On the basis of five example pure compounds, Fauske and Epstein found that Equation 87 gives good mass flux estimates if the void fractions (volumetric fractions vapor, Equation 99) corresponding to the mass fraction vapor in the right-hand-side of Inequality 88 are less than roughly 0.90. For propylene, this limit corresponds to a quality less than about 0.28.

To calculate flows for the transition region from subcooled to saturated stagnation conditions, where the above inequality is violated, Fauske and Epstein suggested using the sum of the squares of Equations 86 and 87, viz,

$$G = C_D \sqrt{2(P_1 - P_s)\rho_{l,1} + \left(\frac{\Delta H_{lv}}{\Delta v_{lv}}\right)^2 \left(\frac{1}{TC_{pl}}\right)} \qquad (89)$$

This will be called the "Fauske/Epstein Combined Equation." Example calculations are presented later.

Leung and Grolmes [32] developed a method for calculating choked flow of flashing liquids based upon an approximate two-phase, pure component equation of state and basic isentropic thermodynamics as discussed earlier. The single independent parameter of the equation of state is defined as

$$\omega = \frac{C_{pl} T_1 P_s}{v_l} \left(\frac{\Delta v_{lv}}{\Delta H_{lv}}\right)^2 \qquad (90)✧$$

in which Δv_{lv} is the difference in vapor and liquid specific volumes, ΔH_{lv} is heat of vaporization, and all properties are for the stagnation temperature T_1. Defining the ratio

$$r_s = \frac{P_s}{P_1} \qquad (91)$$

and the *critical pressure ratio*

$$r_c = \frac{P_2}{P_1} \qquad (92)✧$$

these authors found an exact transcendental equation★ relating r_c to ω and r_s (shown later in Leung's 1992 method) along with the critical (choked) mass flux equation

---

★ A *transcendental* equation has no analytic solution; it must be solved numerically.

$$G = r_c \left(\frac{P_1 \rho_l}{\omega r_s} \right)^{½} \qquad (93)$$

The equation for the critical pressure ratio, required by the above flux equation, must be solved numerically to obtain solutions over all variable ranges. Leung and Grolmes also pursued a short cut solution for r_c which used a second-order Taylor series expansion. The resulting quadratic expression in r_c yielded the following explicit solution

$$r_c = r_s \left(\frac{2\omega}{2\omega - 1} \right) \left[1 - \sqrt{1 - \frac{1}{r_s} \left(\frac{2\omega - 1}{2\omega} \right)} \right] \qquad (94)$$

(Choked flux calculated by the preceding two equations will be called "Leung/Grolmes low subcooling" flux.) As in the Fauske/Epstein method, the properties for the above two equations are evaluated at the stagnation conditions. For Equation 94 to have a real solution, the following inequality must be satisfied:

$$r_s \geq \frac{2\omega - 1}{2\omega} \qquad (95)$$

This criterion distinguishes between the *low subcooling region* where the inequality is satisfied and the *high subcooling region* where it is not. In the former, the fluid attains flashing prior to reaching the choked location, while for the latter, no vapor is formed until the choked location is reached. For the high subcooling region, Leung and Grolmes show that the Vapor Pressure Limited Flux, Equation 86 applies, and that the critical pressure ratio is r_s. Example results for these calculations are presented later.

Leung and Grolmes tested this algorithm against the very extensive *tabulation* for homogeneous critical flow of water *calculated* from the generalized model by Hall and Czapary [22] in the entire subcooled inlet regime. They found that the entire subcooled liquid inlet regime, the transitional critical pressure ratio (Equation 94) was in excellent agreement with their computational results. Using the transcendental equation for the critical pressure ratio in the low subcooling region, the fluxes calculated by this model agreed well with the tabulated results in both high and low subcooling regions. Standard errors for differences between the two methods agreed within roughly 2%. As the stagnation temperature approaches the thermodynamic critical temperature, agreement becomes poorer.

Leung 1992 [30] published a newer generalized HEM-based correlation (based on the preceding work and other [28,29]) designed to estimate flashing choked flow of initially two phase mixtures, as well as subcooled liquids. This capability is desirable for pressure relief device sizing applications which can encounter frothing and foaming flows from reactors and other process equipment. Because it is difficult, on an *a priori* basis, to specify such detail of two phase flow in accidental release scenarios, the following discussion of this algorithm (and the equations therein) is primarily *limited to initially liquid-only fluid states*. If flows for initially two phase flashing fluids must be calculated, please see Leung's paper; the expansion of the algorithm is fairly simple.

With the above restriction, the so-called ω *correlating parameter* for saturated conditions is calculated by Equation 90 which is reproduced here:

$$\omega = \frac{C_{pl} T_1 P_s}{v_l} \left(\frac{\Delta v_{lv}}{\Delta H_{lv}} \right)^2 \qquad (90)✧$$

The normalized mass flux is defined as

$$G' = \frac{G}{\sqrt{P_1 \rho_1}} \qquad (96)✧$$

The generalized solutions are divided into the low and high subcooling regions as before by the inequality:

$$r_s \geq \frac{2\omega}{1 + 2\omega} \qquad (95)$$

where $r_s = P_s / P_1$ as before, in the low subcooling region where this inequality is satisfied, the normalized mass flux is given by

$$G' = \frac{\left\{ 2(1 - r_s) + 2 \left[\omega r_s \ln\left(\frac{r_s}{r} \right) - (\omega - 1)(r_s - r) \right] \right\}^{1/2}}{\omega \left(\frac{r_c}{r} - 1 \right) + 1} \qquad (97)$$

where $r = P_1/P_3$ and the critical pressure ratio, r_c is found by iterative solution of the transcendental equation

$$\frac{\left(\omega + \frac{1}{\omega} - 2 \right)}{2 r_s} r_c^2 - 2(\omega - 1) r_c + \omega r_s \ln\left(\frac{r_c}{r_s} \right) + \frac{3}{2} \omega r_s - 1 = 0 \qquad (98)$$

As before, in the high subcooling region where inequality 95 is not satisfied, the vapor pressure limited flux equation applies:

$$G = C_D \sqrt{2 (P_1 - P_s) \rho_{l,1}} \qquad (86)$$

and the critical pressure ratio is again equal to r_s:

$$r_c = \frac{P_s}{P_1} \qquad (92)$$

The results for this algorithm were tested by Leung against the same Hall and Czapary data as before with excellent agreement.

Comparison of Methods

To illustrate the relative "behavior" of the three methods for estimating flashing choked flow rates, mass flux calculations were made over a range of liquid heads and for two storage (stagnation) temperatures. The non-flashing liquid Bernoulli type equation results are shown for comparison. Using chlorine for this example, the physical properties shown in the preceding *Example for Instantaneous Flashing Release* (page 28) were fitted to smooth interpolating functions of temperature; the multiple correlation coefficients for all properties were all greater than 0.997. The liquid heads from the surface of the liquid down to the release level in the closed, static vessel to which an exit device would be attached were varied from zero to ten meters. Considering the normal boiling point of chlorine, 238.55 kelvin (-34.6 C), curves of mass flux vs. liquid head were obtained for 250 and 290 kelvin stagnation temperatures. *Table 2* shows the r_s values and corresponding minimum liquid heads required for high subcooling. *Figures 5a and 5b* present the curves. Note that curves are shown only for their liquid head ranges of valid existence (e.g., the Leung/ Grolmes low subcooled flux for 250 kelvin does not exist).

At 250 kelvin (Figure 5a), the curves for the three flashing choked flow methods are close to each other because subcooling exists essentially over the whole liquid head range. At 290 kelvin (Figure 5b), the Fauske/Epstein Combined Equation curve is higher than the others for flashing flow, the Vapor Limited Flow Equation for high subcooling applies for both the Leung/Grolmes and Leung 1992 methods for liquid heads greater than about 2 m. The Leung/Grolmes low subcooling curve makes a smooth transition to the high subcooling curve from zero to 2 meters. The Leung 1992 low subcooling flux is significantly lower; this anomalous behavior is unexplained.

Table 2.

Minimum r_s Ratios and Liquid Chlorine Heads vs. Stagnation Temperatures (Leung 1992 Method)

Stagnation Temperature T_1 kelvin	Minimum r_s for high subcooling	Minimum Liquid Head r_s m
238.56	0.9869	0
240	0.9863	0.10
250	0.9824	0.19
260	0.9777	0.35
270	0.9725	0.57
280	0.9666	1.12
290	0.9600	1.84

Leung states that for reduced temperatures ($T_r = T/T_c$) above 0.9, or reduced pressures (P/P_c) above 0.5, the correlation tends to underestimate mass flux. In Figure 3 of his 1986 paper [29], Leung shows normalized mass flux and critical pressure ratio curve families in which separate curves are drawn for reduced temperatures from 0.90 to 0.99. The higher the reduced temperature and ω, the larger the divergence.

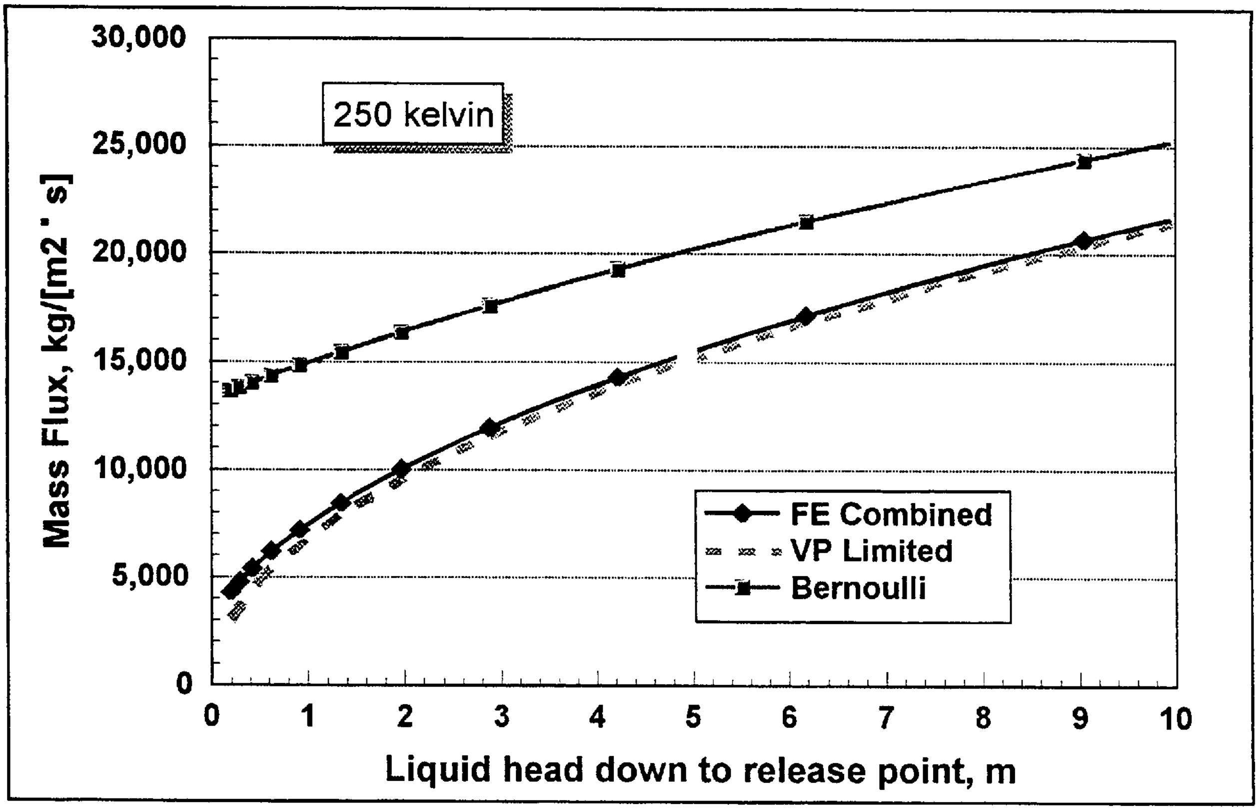

Figure 5a. Chlorine example flashing choked flow rates for 250 kelvin.

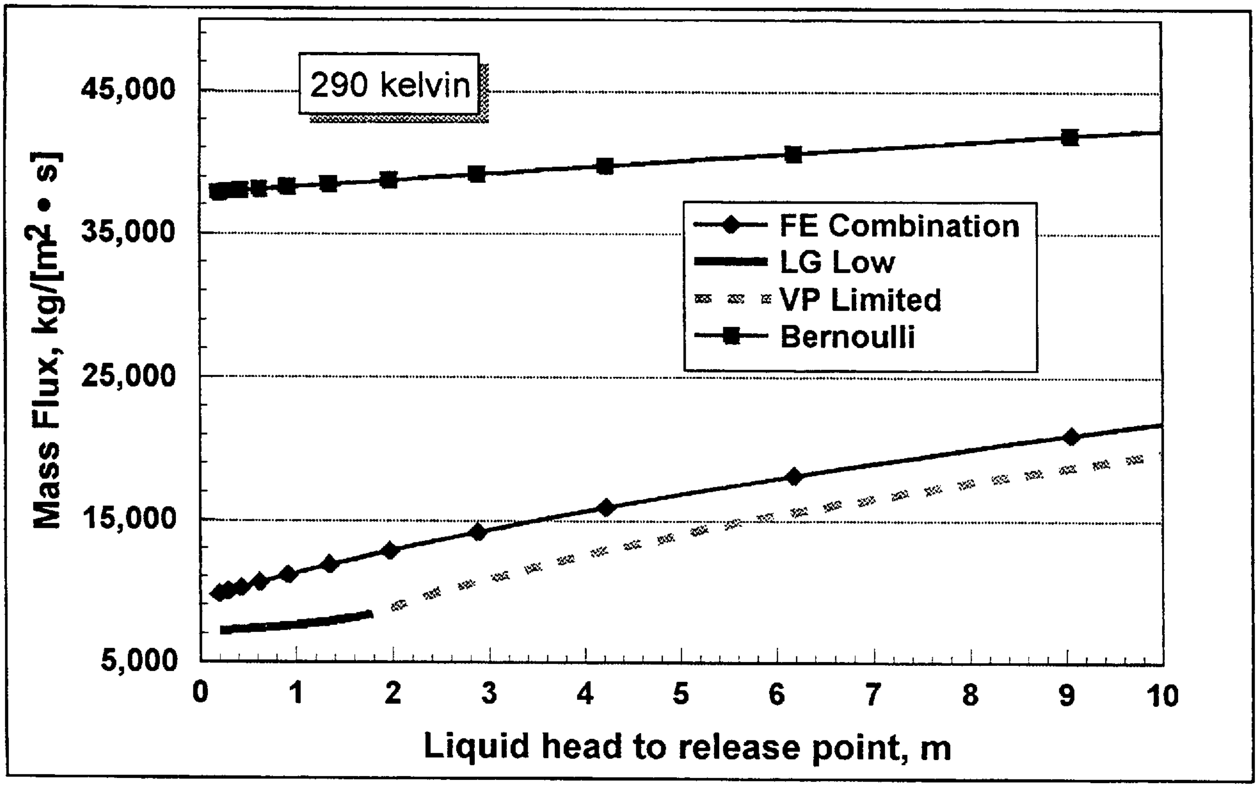

Figure 5b. Chlorine example flashing choked flow rates for 290 kelvin.

In release modeling work, worst case scenarios are used, such as flow from the lowest possible release point in an almost liquid-full storage tank. Thus high subcooling should apply for most cases, in which the Vapor Pressure Limiting Equation should be used, according to the Leung 1992 and Leung/ Grolmes criteria. For this, the user should check the limiting criterion and select a large enough liquid head accordingly. If the total pressure for the release indicates low subcooling, but the physical dimensions involved in a particular application do not allow large enough liquid heads, an artificially high total pressure (P_l) should be used; this will give "worst case" estimations. For the chlorine example, Table 3 shows the minimum liquid heads required by the Leung 1992 criterion (Inequality 95) vs stagnation temperatures so required.

Conclusions. The Fauske/Epstein Combined equation appears to be an *ad hoc* suggestion and no comparison with data was cited by those authors. The Leung/Grolmes and Leung 1992 correlations appear to differ little, except at high liquid heads and high stagnation temperatures (high subcooling). Leung and Grolmes, and Leung (1992) state that by using the critical pressure ratio from the transcendental Equation 98, calculated fluxes all agreed well with the Hall and Czapary data. Because the Leung 1992 correlation is an "upgrade" of the earlier work with Grolmes, it can be recommended.

Figures 6 and *7* are the Figures 3 and 5 dimensionless design charts provided by Dr. Leung from his 1992 CEP paper[★] Figure 6 can be used to quickly estimate flashing choked flows of subcooled liquids after calculation of the independent variables ω and r_s from stagnation conditions. Note that the "bounding" mass flux curve, from which the "ω tails" depend, are for high subcooling calculated by the Vapor Limited Flux equation. *Flow rate estimates made by use of this graph should be sufficiently accurate for the purposes of the manual.* Figure 7 relates non-flashing two phase flow to flashing liquid flow for cases wherein the fluid being released may be subcooled or a two phase mixture according to the HEM. For this, the parameter α_l is the volumetric fraction of vapor or void fraction, of the fluid at the release point. Given the mass fraction vapor (4), then

$$\alpha = \frac{f_v v_v}{(1 - f_v) v_l + f_v v_v} \tag{99}$$

where subscript *l* would denote stagnation conditions. Also in the design chart figures, we have used $\omega' = \alpha_1 + \omega$. This chart can be used for frothing or foaming type releases. Note that if $\alpha_l = 0$ and $\omega = 1$, the correlation mass flux equation reduces to that for gas-only choked flow (Equation 77). Leung points out that the correlation is only applicable to a pure component fluid, strictly speaking. However, he found that if multicomponent mixtures contain compounds of boiling range within about 100 degrees kelvin, the pseudo-pure component approach appears to give good results. For wider boiling range mixtures, he stated that the pseudo-pure component approach tends to underestimate the mass flux.

In summary, the above correlations can be used as simplified methods for accidental release modeling as first approximations, considering the constraints on parameter ranges (*e.g.*, screening studies). If higher accuracy estimates are required, i.e., the released fluid is near or above its critical point, or for wide boiling range mixtures, generalized models (*e.g.*, Equations 74 and 75) should be used with appropriate thermophysical properties capabilities.

[★] For consistency, certain of Leung's symbols have been changed in this text; namely, he used η for ratios, subscript *o* for stagnation, and subscript f_g for vaporization, whereas *r*, *1*, and *lv* are used here, respectively.

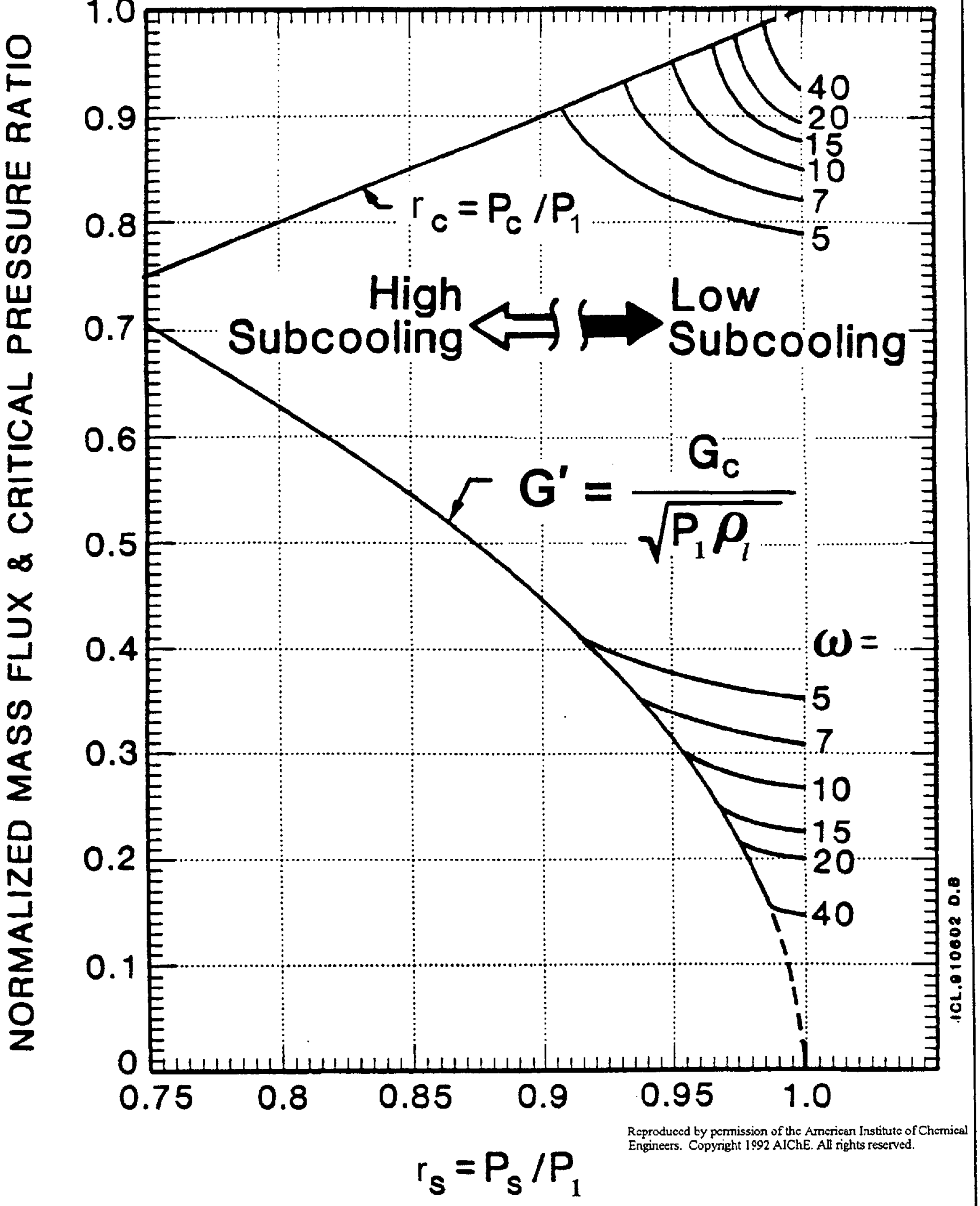

Reproduced by permission of the American Institute of Chemical Engineers. Copyright 1992 AIChE. All rights reserved.

Figure 6. Design chart for flashing liquid flow (Leung 1992).

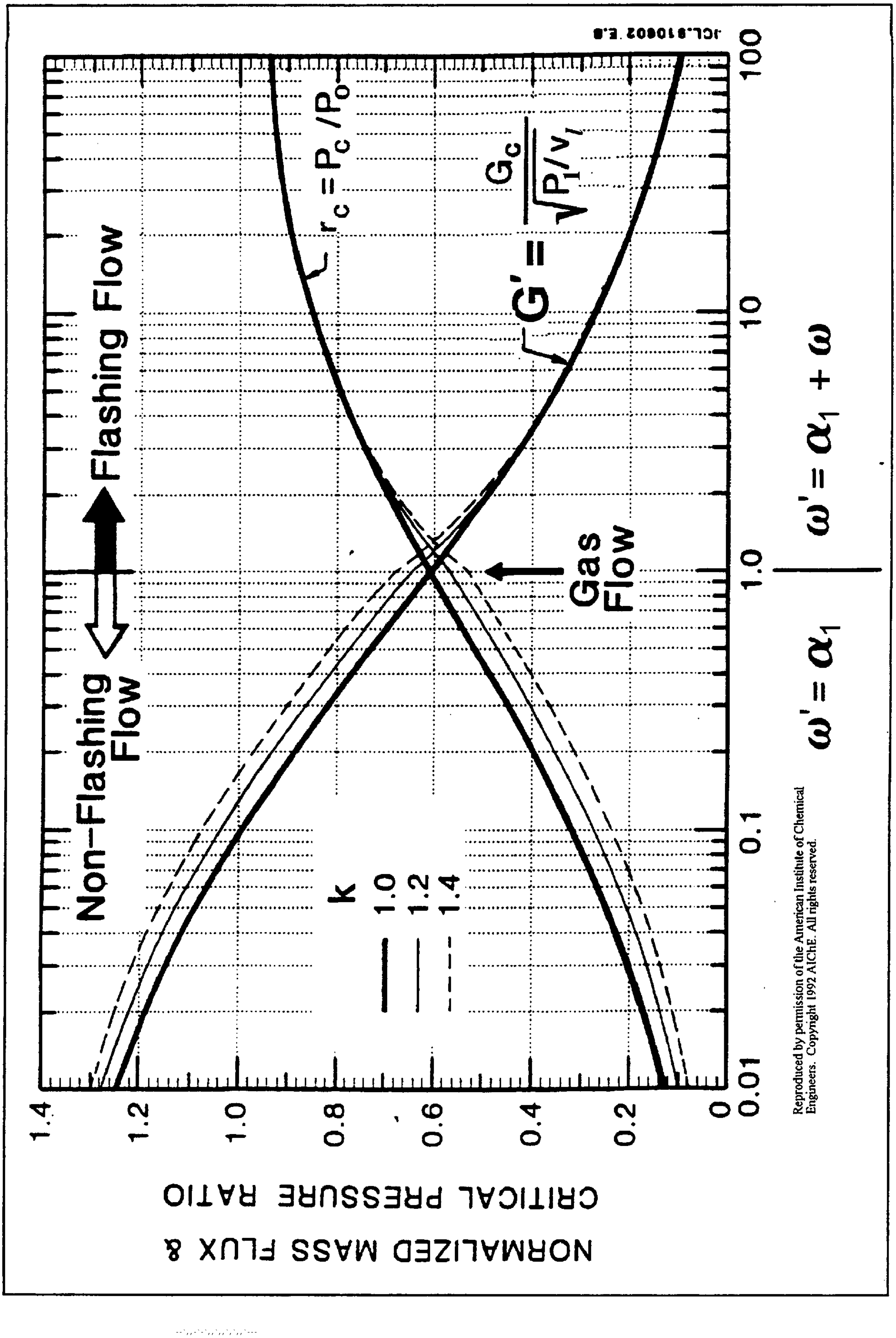

Reproduced by permission of the American Institute of Chemical Engineers. Copyright 1992 AIChE. All rights reserved.

Figure 7. Design chart for non-flashing two phase and flashing choked flow.

The following example is for the flashing choked flow of liquid chlorine from an orifice; the critical pressure ratio an mass flux were found graphically from Figure 6 preceding. Note that the derived values are listed in the order found. Entropies and densities were taken from the fitted equations as in previous examples.

Example: Liquid Chlorine Flashing Choked Flow Rate

Constants	Symbol	Units	Value	Reference
Molecular weight	M	NA	70.91	
Gravitational constant	g_c	SI	9.807	
Stagnation (Reservoir) Parameters				
Temperature	T_1	kelvin	290.0	Given
Vapor entropy	S_{v1}	J/[kg·K]	2909.8	Fitted data
Liquid Entropy	Sl1	J/[kg·K]	2016.8	Fitted data
Liquid head (1.0 meter)	Δz	Pa	13,811	Given
Vapor pressure	P_s	Pa	608,652	Fitted data
Pressure at orifice	P_1	Pa	622642	$P_s + \Delta z$
Heat of vaporization	Δp_s	J/kg	250,629	Fitted data
Liquid specific volume	v_l	m^3/kg	7.104E-04	Fitted data
Vapor specific volume	v_v	m^3/kg	0.05168	Fitted data
Specific heat of liquid, const. P	C_{pl}	J/[kg·K]	1166.0	Fitted data
Leung's correlating parameter	ω		12.0	By Equation 90
Pressure ratio	r_s		0.978	By Equation 91
The following two quantities were then read from Figure 6 using r_s and ω.				
Normalized mass flux	G'		0.26	Equation 96 defines
Critical pressure ratio	r_c		0.89	Equation 92 defines
Mass flux	G	kg/[m^2·s]	7,698	Equation 96
Orifice diameter	D_2	m	0.010	Given
Orifice area	A_2	m^2	7.854E-05	Circle
Discharge coefficient	C_D		0.6	Given
Choked mass flow rate	w_{max}	**kg/s**	**0.3628**	**= $C_D A_2 G$**

Flow from Pipes

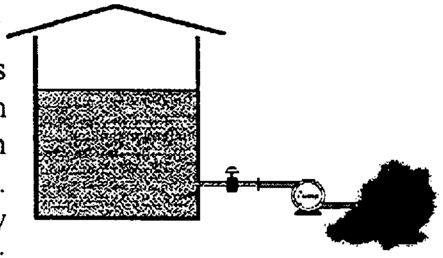

Accidental release modeling often requires estimation of vapor and liquid flow rates from broken pipes, open valves connected to pipes, etc. Often an application is concerned with discharge to a flare header piping system, which may contain long pipe runs, several liquid knockout vessels or devices, etc. Flow of fluid through a pipe, or piping network, is initially determined by the inlet pressures from pumps and/or vessels; fluid temperatures affect density and viscosity. As the fluid flows through the pipes, energy loss influences the flow rate due to pipe wall roughness, bends and elbows, pipe elevation changes, constrictions, liquid flashing, etc. The technology for calculating such flows has been developed over many years and is beyond the scope of this Manual. However, a few comments and references follow. Beyond that, it is recommended that knowledgeable engineering advice be sought.

Smith and Van Ness (page 220) give an equation for the maximum fluid velocity in a pipe of constant cross section; we note that this equation is equivalent to those given above for choked flow through orifices. In both situations, the maximum flow rate *is* the speed of sound in the fluid, as noted before. The following is quoted from those authors: "However, the speed of sound is the maximum value that can be reached in a conduit of constant cross section, provided the entrance velocity is subsonic. The sonic velocity must be reached at the *exit* of the pipe. If the pipe length is increased, the mass flow rate decreases so the sonic velocity is still obtained at the outlet of the lengthened pipe." When the pipe becomes very long, as in a catastrophic failure of a high pressure pipeline, the phenomena become very complex, and sophisticated computer programs are required to model well the "blowdowns" to obtain discharge mass flow rates and fluid states. For example, depressurization shock waves have been observed to travel backwards along the pipe from the open end. Some programs are commercially available for dynamic simulation of pipeline operation and blowdowns; see Norris [32b, 32c].

In most release modeling applications, it suffices to make worst case estimates of release rates by applying the principles discussed above for holes. However, if detailed estimates for discharge from a (long) pipe are required, the methodology described in *API Recommended Practice 521, Guide for Pressure-Relieving and Depressurizing Systems* [13] can be a starting guide. (This reference is currently being revised. *[1995]*) Also, the pipe flow calculation methods contained in Perry's Sixth, Chapter 5 can be employed. Sometimes it is only necessary to find the operating discharge rate of a pump which feeds the pipe(s) of interest.

Two phase fluid flow, especially with liquid flashing involved, is even more complex than that for single phase flow mentioned above. Much work has been done over the years to develop understanding and design methods for systems involving flashing and two-phase flow of fluids through pipes.

Several methods for estimating flow rates of two-phase and/or flashing fluids through pipes are:

> Leung and Ciolek extended the former's 1992 correlation for flashing liquid flow through orifices to pipes [31]. The general model, which covers any extent of subcooling, requires the simultaneous solution of three transcendental equations. However, if the liquid is highly subcooled, the mass flux for a pipe segment is calculated by a simple, explicit function of stagnation pressure and temperature, vapor pressure at stagnation temperature, pipe length, pipe diameter, and the Fanning friction factor.
>
> Perry's Sixth, pages 5-44 to 5-45, summarizes a general computational scheme for this phenomena which assumes the liquid and vapor flow at equal velocities.
>
> The SAFIRE computer program [19] was developed under the auspices of the American Institute of Chemical Engineers, Design Institute for Emergency Relief Systems (DIERS) research program. SAFIRE contains several models, including one for homogenous equilibrium flow (no vapor/liquid velocity slip) and one with velocity slip. The development work was done primarily to improve methods for sizing pressure relief systems on pressure vessels such as reactors. References 17 and 18 also provide manual calculation methods.

> H.E.A. van den Akker [35,36] presents mathematical models for flashing, choked flow in pipes, based upon experimental data especially obtained for model development. The results from the model agree fairly well with the experiments, but that author notes that more experimental work and understanding of the phenomena is required.

Additional references, including some for experimental and development work, are given in the Chapter 3 section of the *References.*

Computer programs are commercially available for the design of safety relief systems; these can be used in a reverse manner to estimate flows through and from particular equipment configurations. Those of which the author is aware treat steady state operation only, and some can treat complex networks with bypasses, etc. These programs are often available from companies which market process flowchart simulation software.

Initial Jet Expansion

General Considerations

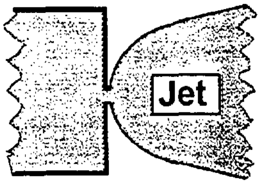

If a gas or two-phase fluid in Bernoulli (non-choked) flow exits a hole or valve to the atmosphere, the *initial* expansion will be small, if any, so the diameter of the jet stream will not differ significantly from the effective diameter of the hole. This diameter can be used directly for input to turbulent jet models for near field dispersion. On the other hand, as the vapor or vapor/liquid mixture in *choked flow* exits a hole or valve, it expands by doing work against the atmosphere which also causes it to cool. The *initial* expansion is extremely rapid. During this expansion, air is violently and rapidly entrained into the jet stream; they are usually called *turbulent jets.*

The initial expansion is extremely rapid and occurs in a short distance as observed with high speed photography of high pressure jets. Then, the rate of growth by air entrainment is seen to be not as rapid as initially. No experimental data has been found, or experimental methods devised, to investigate temperatures and concentrations within the initial expansion region, to the author's knowledge. Two models for initial expansion are presented below. Mathematical models for the following "entrainment region" usually are formulated with the rate of air entrainment to be proportional to the circumferential area of a differential slice through the jet perpendicular to its travel path. Thus for near field applications, where the concentration of released substance in the jet strongly depends upon the jet diameter, the initial jet diameter should be estimated as accurately as possible, for expanded diameters can be several times the throat diameter. The higher the reservoir pressure, the more will the area of the initially expanded stream differ from that of the outlet. For applications in which dispersed concentrations are of interest only in the far field, it may *not* be necessary to calculate the expanded jet diameter and other properties; this is because the amount of air entrained into the plume in the near field becomes negligible with respect to the total amount of air entrained over the whole path of the plume.

Initial Jet Expansion Models

This expansion process is actually irreversible, for the restoring force is the constant atmospheric pressure. However, the general practice has been use models that are, in some part, based upon the concept of reversibility. Two simple models are described below, then their advantages and drawbacks are discussed comparatively.

Model 1. The expansion process uses a control volume drawn around the stagnant reservoir, the orifice, and the initially expanded jet. Assume that no heat is transferred to or from the released stream with the air, and that there is no mixing with the air. The steady state process is assumed to be reversible and adiabatic, hence isentropic. Because it is assumed that liquid head (Δz), heat transfer (Q), and shaft work (Ω_{shaft}) effects are negligible, the first law Equation 44 reduces to

$$H_3 - H_1 = \Delta H = -\frac{1}{2} u_3^2 \tag{100}$$

for $u_1 = 0$ at the stagnant reservoir inlet to the orifice. Solving Equation 31 for the (expanded) jet area, A_3, substitution of the result into Equation 100, and rearranging gives

$$A_3 = \frac{w_{max}}{\rho_3 \sqrt{-2\Delta H}} \; . \tag{101}✧$$

Therefore, the expanded jet diameter is

$$D_3 = \sqrt{\frac{4A_3}{\pi}} \; . \tag{102}✧$$

Equations 100 and 101 constitute the initially expanded jet model. The atmospheric pressure is known★. For a vapor phase only system, the problem is to find the temperature (T_3) so the density and enthalpy can be found. For a two phase system, this temperature is the atmospheric boiling point, but then the fractions of vapor and liquid must be found so the enthalpies and specific volumes for each phase can be combined to find their bulk values, ΔH and v, respectively. A solution may be obtained by assuming that the process is isentropic. Then for gases, either ideal or real, the concepts used to develop Equation 52 can be used to obtain the temperature. For aerosols, the vapor fraction can be found by Equation 62.

Model 2. The cross-sectional area of the expanded jet is found by balancing the stream momentum *change* against the net pressure force on the expanding region of the jet's cross-sectional area.

$$w_{max}(u_3 - u_2) = A_2(P_2 - P_3) \; . \tag{103}$$

The left side of the preceding equation represents the momentum change of the stream on expansion to atmospheric pressure and the right side represents the force required for expansion; SI units-of-measure are newtons = [kg • m]/[s^2]. The geometrical concepts are shown in Figure 8. This equation may be rearranged to

---

★ Atmospheric pressure (P_3) usually can be that for mean sea level (MSL), 101325 Pa. For high elevations, this pressure can be taken from the definition of the Standard Atmosphere (Weast and Astle, [4-19]).

$$u_3 = u_2 + \frac{A_2}{w_{max}}\left(P_2 - P_3\right). \tag{104}✧$$

Thus, by Equation 31,

$$A_3 = \frac{w_{max}}{u_3 \rho_3}. \tag{105}$$

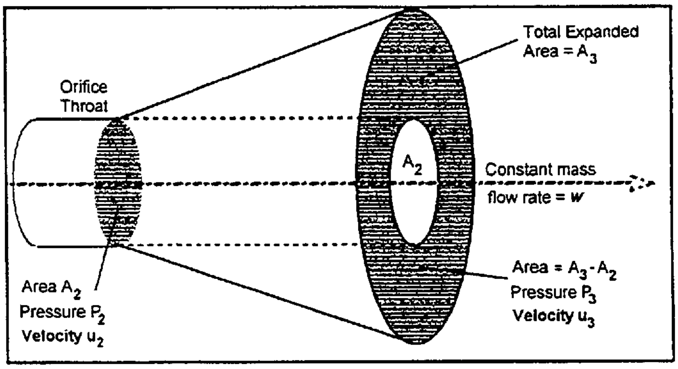

Figure 8. Expanding Jet Force Balance.

Now, although the expanded velocity has been found without resorting to thermodynamic functions, the density, ρ_3, must still be found. For this, the first law for a control volume around the orifice throat and the expanded jet plane can be used:

$$\Delta H_{2,3} = H_3 - H_2 = -\frac{1}{2}[u_3^2 - u_2^2]. \tag{106}$$

The total enthalpy for the expanded jet, H_3, is found from thermodynamic tables, charts, or appropriate computer routines at atmospheric pressure, with the throat velocity, u_2, being available from the throat calculations. Therefore, using u_3 from Equation 104, H_3 can be found from the preceding equation. Equation 65 gives the fraction vapor (substituting subscript 2 for subscript 1), which may then be used with the corresponding liquid and vapor specific volumes to calculate the bulk density for Equation 105. If the expanding jet is a non-condensing gas, H_3 from Equation 106 can be used to find the corresponding temperature at atmospheric pressure from thermodynamic tables, etc., which also provide the specific volume.

Comparison of Methods . Both methods conserve mass (e.g., Equation 105), and energy (Equations 100, 106). The *first method* is based directly on the First Law, as are the models for calculation of the choked mass flow rates. The calculations are simpler than for Method 2 because the throat parameters (e.g., velocity, temperature, etc.) need not be obtained. Because a third relationship is needed to define the process, isentropicity is assumed, which is consistent with the assumptions used to calculate the choked mass flow rate. However, this assumption is an idealization, for entropy change is always greater than zero. The *second method* balances pressure force against momentum, so the isentropicity assumption is not required to solve the problem.

We note that the AEROPLUME turbulent jet model of HGSYSTEM (version 3.0) uses Method 2 for the diameter of the expanded jet. However, for the vapor only example below, for which the physical orifice diameter is 1.00 cm, Method 1 gives an expanded jet diameter of 1.72 cm, while Method 2 gives a diameter of 0.80 cm.

Example Calculations

Vapor-only jet. The expanded jet diameter was calculated for Case 1 of the choked mass flow rate example for chlorine vapor presented on page 34. The input and derived quantities, along with references to equations used, etc., are presented in a stepwise manner in the following box. Chlorine was assumed to be an ideal gas.

Example: Expanded Jet Diameter for Chlorine Vapor Choked Flow

Parameter	Symbol	Units	Value	Reference
For the reservoir				
Temperature	T_1	kelvin	300	Page 35
Pressure	P_1	Pa		Page 35
Vapor heat capacity, const. pressure	C_{pv}	J/[kg·K]	60.9	Page 35
Heat capacity ratio	k		1.4	Page 35
Exit mass flow rate	w_{max}	kg/s	0.0872	Page 35
For atmospheric conditions				
Pressure	P_3	Pa	101,325	Mean sea level
Temperature	T_3	kelvin	189.4	By Equation 55
Gas density	ρ_3	kg/m^3	4.562	Gas law: = MP/[RT]
Enthalpy change	ΔH	J/kg	-6734.6	Eq. 50: = $C_p[T_3-T_1]$
Expanded jet area	A_3	m^2	2.329E-04	Equation 100
Expanded jet diameter	D_3	cm	**1.72**	Method 1
Expanded jet diameter	D_3	cm	**0.80**	Method 2

Note that the expanded "gas" temperature, T_3, was calculated to be 189.4 kelvin, whereas the normal boiling point of chlorine is 238.6 kelvin. Thus the implied assumption that the gas is non-condensible is wrong. A more correct way would be to calculate the expanded diameter by using the isentropic VLE Equation 63 to find the fraction vaporized at the normal boiling point, then continue as in the following example for flashing liquid flow. (This exercise has been omitted.)

Flashing Liquid Jet The example flow rate calculation for flashing liquid chlorine presented on page 45 is extended below to find the expanded jet diameter in the box on the following page.

Example: Expanded Jet Diameter for Flashing Liquid Chlorine Choked Flow

Parameter	Symbol	Units	Value	Reference
For the reservoir				
Temperature	T_1	kelvin	290	Given
Entropy of liquid	S_{l1}	J/[kg·K]	2016.8	Fitted data
Enthalpy of liquid	$H_{l1} = H_1$	J/kg	523,633	Fitted data
For the expanded jet				
Temperature (normal boiling point)	$T_3 = T_{NBP}$	kelvin	238.6	Tables
Entropy of liquid	S_{l3}	J/[kg·K]	1834.8	Fitted data
Entropy of vapor	S_{v3}	J/[kg·K]	3021.9	Fitted data
Fraction vapor	f_v		0.153	Equation 62
Fraction liquid	f_l		0.847	$= 1 - f_v$
Specific volume of liquid	v_{l3}	m^3/kg	6.434E-04	Fitted data
Specific volume of vapor	v_{v3}	m^3/kg	0.2742	Fitted data
Specific volume of aerosol	v_3	m^3/kg	0.2322	Equation 56
Density of aerosol	ρ_3	kg/m^3	4.307	$1/v_3$ (Equation 57)
Enthalpy of vapor	H_{v3}	kg/m^3	523,633	Fitted data
Enthalpy of liquid	H_{l3}	kg/m^3	234,833	Fitted data
Enthalpy of aerosol	H_3	kg/m^3	279,110	Eq'n 24; l = liq, vap
Enthalpy change	ΔH	J/kg	-14,779	$H_3 - H_1$
Mass flow rate	w_{max}	kg/s	0.3628	Page 45
Area of expanded cross-section	A_3	m	4.899E-04	Equation 100
Physical orifice diameter	D_2	m	0.010	Given
Expanded jet diameter	D_3	m	**0.025**	Method 1
Expanded jet diameter	D_3	m	**0.017**	Method 2 (AEROPLUME)

Note that the expanded diameters for the two methods are relatively greater than in the case of the gas only release example. This is expected because of the vaporization. Because of the enthalpy (per unit mass) of liquids are much greater than for vapors, at a given temperature, a particular increase in reservoir temperature should give higher expanded diameters compared with gas-only releases.

Evaporation

Introduction

Mass flow rates from the evaporation of "spilled" substances which form liquid pools on ground surfaces, and for floating contiguous liquid areas on water surfaces, depend upon a number of variables. These variables include the mass flow rate and chemical composition (properties) of the substance flowing onto the surface, energy sources and sinks involved in providing the net heat of evaporation, the shapes (e.g., area and depth) of the pools, and boundary layer variables affecting mass transfer into the atmosphere (e.g., wind speed). The estimated mass flow rates into the air are then used with appropriate dispersion models, as discussed elsewhere in this manual. In general, the process is time dependent. However, it may be possible to use initial, maximum evaporation rates for dispersion estimates in particular applications, or for screening purposes.

The evaporating *liquid* may be a pure- or multi-component mixture. Bulk properties can be found by methods referenced in preceding sections of this chapter, or as cited in the accompanying references; in certain cases, a direct reference is provided. Note that if the liquid is multicomponent; its composition and therefore bulk properties, will usually be dependent upon time.

The relevant mass and energy flows are depicted in *Figure 8*. The evaporation *flux* (mass flow rate per unit area) from the upper surface of a pool is determined by the net energy available for the phase change process. This process is usually treated as isenthalpic and reversible which assumes that the kinetic energy is negligible with respect to the heat energy required. Thus, the mass rate of evaporation is ultimately determined by the heat available divided the heat of evaporation. The net energy at any instant is affected by long and short wave radiation and by heat conduction from the air and ground (or water) surfaces. If the size of the pool is unknown or growing, it is common practice to assume that the spill spreads onto a perfectly level smooth surface of infinite area; the liquid area changes with time, perhaps to some upper limit. This areal limit may be defined by dikes around storage tanks or other barriers, by equating the total mass evaporation rate (flux • area) to the constant input liquid flow rate, or by other forces such as surface tension.

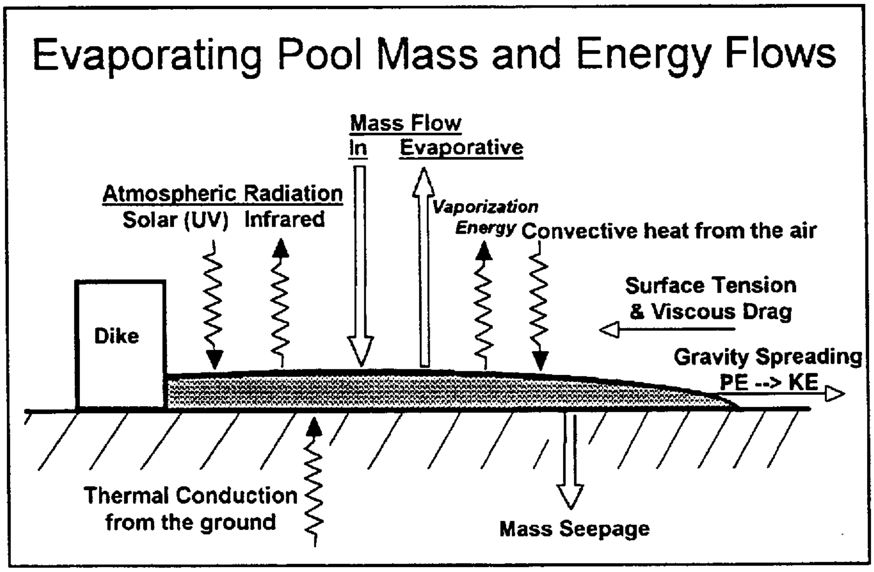

Figure 9.

Two evaporation *regimes* can occur: The *boiling pool* regime takes place if the boiling point of the liquid being spilled exceeds the temperature of the ground or water surface. In the case of a spill onto the ground, if the amount or rate of the spill is large enough, the temperature of the ground at the liquid interface will eventually approach the boiling point of the liquid, which reduces the heat transfer rate to very small values compared to other energetic processes. Thus in situations where conductive and radiative energy processes are small relative to the heat of evaporation, the *convection limited* evaporation regime is dominant. The principal factors controlling convective evaporation are the liquid vapor pressure and wind flow variables.

All the models discussed later assume that the evaporating pool is formed on a perfectly level, flat surface. The surface may have varying textures, and thus heat transfer coefficients. The area of the pools may or may not be limited by dikes (berms). The heat transfer rate from the ground is found by the "standard" semi-infinite slab model, wherein the ground is initially assumed to be uniform in temperature and homogeneous in thermal conductivity. At zero time, the initial pool surface contacts the smooth, flat surface of the slab; some models allow the initial cylinder to expand successively in surface areal increments as the pool grows circularly, possibly until a specified limiting radius is reached.

Following is a summary review of the more recent literature. These references were drawn upon to present the most applicable algorithms for modeling the various phenomena. Finally, a numerical example is given for the boiling pool regime. Scenario 8 in Chapter 6 is an example for the convection rate limited regime.

Evaporation Model Survey

The features of the more recent mathematical models for pool evaporation are summarized in *Table 3*. All of these models draw upon the work of others, and often the same algorithm or correlation for a "building block" is used by several authors. Unless otherwise noted, the models are based on the simultaneous solution of heat and mass transfer equations; numerical solution methods are usually required. The common heat conduction algorithm is the semi-infinite slab model which is described later. For the most part, the models all assume a homogeneous liquid pool with no leakage from its bottom. All models produce the evaporation rate, or flux as a function of time, with the exception of Fleischer's, which produces dispersed concentrations from a coupled Gaussian puff dispersion model as functions of time or for the steady state. Also, Kawamura and Mackay estimate point value evaporation fluxes only. The models, or modeling systems, are described in approximate chronological order. Distinctive features of these models are briefly described.

Wu and Schroy, 1979 [52]. This modeling program calculates the emission rate as a function of time from a continuously replenished, quiescent pool containing a pure component or a binary solution (e.g., water, volatile solute). Spill rate from a hole is calculated for flashing and non-flashing flow. The convective heat transfer coefficient is found by a relationship derived for cooling water ponds.

The documentation for this program is very limited. The user must supply all physical properties and conditions, including those associated with radiation and wind speed. This program was developed before suitable experimental evaporation flux data became available for validation. The computer program (Fortran) and documentation is available from the Monsanto Company at no charge, provided the user agrees to supply Monsanto with computer-readable copies of any modified program developed.

Table 3.

Summary of Evaporation Model Features

Subscript	Variable / Parameter description	Wu & Schroy	Fleischer	Shaw & Briscoe	Kawamura & Mackay	Webber & Brighton	Hesse	Cavanaugh, Siegell & Steinberg	Reynolds
	Reference	52	41	37,48	44	51	43	38, 39	57
	Pool Input								
	Multicomponent mixtures	Binary				*Model only estimates area of a liquid pool spreading on a liquid or solid substrate.*		Y	
	Physical properties methods/ Database		Y^2					Y	Y
	Release rate calculations	Y						Y	Y
	Aerosol from initial spill							Y	
	Mass and energy transfer								
solar	Short wave (solar) radiative heating	Y			Y		Y	Y	Y
rad	Long wave (infrared) radiative cooling	Y			Y		Y	Y	Y
air	Convective heat exchange from atmosphere	Y			Y		Y	Y	Y
sub	Conductive heat exchange with substrate	Y	Y	Y	Y		Y	Y	Y
dike	Conductive heat exchange with dikes							Y	
sens	sensible heat (mixing), includes feed stream	Y	Y		Y		Y	Y	Y
surf	Surface temperature for heat transfer				Y^5		Y	Y	Y
evap	Convective mass transfer	Y	Y	Note 3	Y	Note 7	Y	Y	Y
	Ice formation in wet ground heat transfer		Y						
	Water as substrate is treated	Y		Y				Y	
	Pool size parameters								Note 10
	Potential to kinetic energy balance for spreading			Y	*Model only estimates evaporative mass flux.*	Y	Y	Y	
	spreading momentum terms					Y			
	Viscous drag effects			Y^4		Y	Y		
	Water substrate inertia			Y^4		Y			
	Surface tension terms			Y^4		Y			
	Pool size limit	Y	Y	Y				Y	
	Solution methods								
	Numerical solution required	Y	Y	Y	Y^6	Y^8		Y	Y
	Public domain computer program available	Y	Y					Y^9	Y^{11}

Notes

1 Blanks indicate negative.
2 Corresponding states correlations
3 Blank entries indicate negative.
4 Only for water substrate model.
5 Two model forms available, one uses pool surface temperature (better), other uses bulk temperature.
6 Surface temperature model only.; bulk temperature model solution is direct.
7 Models assume the evaporative mass flux ("regression rate") is known.
8 The shallow layer model allows approximate analytic solutions.
9 Incorporated into HGSYSTEM version 3.0.
10 Either pool area or depth must be supplied by user; other parameter is calculated.
11 This is the PUDDLE submodel in the ALOHA accidental release simulation program.

Fleischer (1980) [41] developed the Shell Spills model before dense gas dispersion models became available, so the Gaussian puff model was used for time dependent dispersion. Dispersed concentrations as functions of space and time are output from the Fortran program. The algorithm is unique in that it treats the freezing of wet ground which affects conduction heat transfer rate. The program uses a liquid-to-air convective mass transfer correlation developed for distillation columns. This program was developed before suitable experimental evaporation flux data became available for validation.

Shaw and Briscoe (1978, 1980) [37, 48] presented general models for evaporation from land and water substrates for instantaneous (total amount) vs. continuous (finite liquid flow rate) situations. Approximate, integral solutions to the general models are also given and are several are presented below. For spreading on water, the evaporative mass flux must be externally supplied, while the spreading-on-land model equates the evaporative flux to the net excessive heat derived from conduction.

Kawamura and Mackay (1987) [44] focused on estimation of the evaporation flux on the basis of comprehensive heat balances. Some of the sub-model terms are based upon correlations based on their experimental work. The basic model uses the temperature of the upper surface of the pool for radiative heat transfer. A variant of the model eliminates the surface temperature to use the bulk pool properties. Comparison of the two models with experimental data indicates that the surface temperature form is better, but requires iterative numerical solution.

Webber and Brighton (1987) [51] were concerned with the fluid mechanics of determining the area of a pool spreading freely on a liquid or solid surface. Thus they assume the evaporative mass flux, or regression rate, is a known function. (This is complementary to Kawamura and Mackay's interest.) They note that surface tension effects can have significant consequences for an evaporating pool. As the liquid evaporates, the level cannot (in their model) drop below a minimum, surface (interfacial) tension controlled thickness. Therefore, once the pool as a whole reaches this minimum depth, then further evaporation implies that either the leading edge must retreat (shrinkage) or “holes” must appear in the middle.

Hesse (1992) [43] assumes the liquid spill occurs on a level, unobstructed substrate and that the free surface takes on a parabolic shape with the leading edge limited to a minimum depth determined by surface roughness.

Cavanaugh, Siegell and Steinberg (1992, 1994) [38, 39] of Exxon describe a fairly extensive spill modeling program (LSM90) which incorporates many of the algorithms heretofore described. The program treats boiling and non-boiling pools, multicomponent substances, water and land substrates, and dikes on land. Originally, the physical property calculations were coupled to the DIPPR database. However, the model has been placed into the public domain by incorporation into HGSYSTEM (version 3.0) where it has been interfaced with the common DATAPROP module physical and thermodynamic properties for multicomponent VLE calculations. The HGSYSTEM supervisory program prepares an intermediate input data file in the LSM90 format for execution. Bernoulli, flashing choked, and user-supplied flow rate calculations from holes to the pool are retained.

Reynolds (1992) [47]. The PUDDLE submodel contained within the fairly comprehensive ALOHA accidental release modeling program system assumes that either the pool area or pool depth are known, from which the unchanging pool area is derived. The model uses Kawamura and Mackay's methods for estimation of evaporation flux. Brighton's methods are used for calculating convective mass transfer based upon atmospheric boundary layer parameters. The puddle is approximated by a rectangle with five equally spaced point sources aligned along a center axis normal to the wind direction.

Spill Rates

If a vessel catastrophically fails by a major rupture or very large hole, the release can be treated as instantaneous. On the other hand, if the release is from a relatively small hole (such as a pipe, valve, or puncture), the total release flow rate will depend upon the parameters discussed in a previous section (*Flow Rate Estimation*). In all situations, it is necessary to specify the fraction of liquid which goes into the evaporating pool. If the atmospheric boiling point of released material is above ambient temperatures (which includes the ground or water surface), then the total amount or rate of liquid flow may be calculated from the vessel's liquid content or by the Bernoulli equation respectively. However, if the release involves a flashing liquid, then some or all of the liquid may remain suspended as an *aerosol* in the dispersing vapor cloud; only a fraction (if any) of the initially formed liquid phase falls to the surface to form a pool. Another situation could be the release of a saturated vapor, e.g., from a pressure relief valve on the the top of a distillation column. The initial liquid fraction can be estimated by Equations 62 or 63, but if the discharge is directly to the atmosphere, the liquid may be totally suspended as an aerosol. On the other hand, if the relief valve discharges to a flare relief gathering system, some of the effluent liquid phase could be removed by devices such as demisters and in knock-out drums.

Aerosol Formation

Methods for estimating the fraction of liquid remaining suspended as aerosol ($f_{aerosol}$)★ are very scarce. Fauske and Epstein [20] who refer to Bushnell and Gooderum [37b], state: *"It is now well established that if a liquid is heated to above its boiling point at atmospheric pressure and released into the atmosphere, it disintegrates into fine droplets in the 10-100 μm size range*[9]*. Such small droplets will become airborne as a result of the momentum of the release and the wind."* This statement is somewhat too all-inclusive, for many parameters govern how much of the theoretical liquid fraction formed in the initially expanded jet or cloud will fall to the ground, thus forming an evaporating pool. The following is an overview of the phenomena involved in causing (or preventing) liquid rainout, as well as of research in this area.

Governing Phenomena. When a superheated, flashing liquid is exposed to the atmosphere, the total substance (in the case of an instantaneous release) or the jet stream (in the case of a release from a hole) will attempt to establish thermodynamic equilibrium within itself and with its surroundings. In the initial expansion, before a significant amount of air can mix in, energy contained within the stream in excess of that required for vaporization can be used to form liquid droplets as well as kinetic energy; the gas formation-expansion process is disruptive. The energy required to form droplets, relative to a single volume of the liquid (low surface area) of the same total, equals the product of the surface tension times the surface area. For spherical droplets, the total surface area of N droplets of uniform diameter D can be calculated from the liquid density and the surface areas and volumes of spheres for a unit mass of liquid. Such calculations show that the energies required to form very small

---

★ Defined as the fraction of liquid remaining suspended basis the total liquid remaining *after* flashing.

droplets (e.g., 1 - 10 μm average diameter) are small fractions of the total enthalpy changes for flashing choked flow releases.

The settling velocities of particles (droplets) in *still air* are primarily a function of density, size and shape as well the density of air (Perry's Sixth, pp 5-63 to 5-68). Table 20-102 (Perry, p. 20-78) also shows the size ranges of common atmospheric dispersoids, such as clouds, fog, rain, mist, dust, etc. A particle dropped from a given height will travel given distance horizontally before it impacts; this distance depends upon the horizontal wind or jet velocity, and the turbulent flow regime of the air. In a general, particles of sizes less than 100 μm will tend to stay suspended for wind speeds greater than about 2 m/s if released at heights greater than 1 or 2 meters. Think of fogs and mists. Because of the forces described below, most jet releases will cause droplets larger than 100 μm to remain airborne.

Many other forces operate in the turbulent, flashing jet or in the instantaneously forming vapor cloud. Mechanical breakup forms aerosols through surface stresses as the stream flows through the atmosphere. The high turbulence generated within the expanding jet entrains air at a high rate. Depending upon the air temperature and other factors, heat will be exchanged with the vapor and liquid released substance. If the air is warmer than the initially expanded jet (the usual case), then droplet evaporation rates will be enhanced because of temperature and vapor phase dilution by air. Thus as the jet or cloud travels, the liquid droplet fraction will decrease. Also, because of surface tension, large drops tend to grow at the expense of small drops through collision. On the other hand, if a water miscible substance is released with high superheat, and the atmosphere is cool and humid, stable fogs can be formed in which the liquid droplets are aqueous solutions of the released substance(s). Of course, the ground surface temperature is important; cryogenic substances may instantly vaporize on impact (for relative small release rates/amounts). Melhem describes a model which comprehensively treats most of these, and other rainout phenomena (Fthenakis [45b]).

In field experiments of flashing liquids released through orifices, such as the *Desert Tortoise* test for ammonia and the *Goldfish* tests for hydrogen fluoride, all the liquid remained suspended ($f_{aerosol} = 1$). The AIChE Center for Chemical Process Safety (CCPS) has been sponsoring an aerosol research program since 1987. The first version of the 1989 CCPS RELEASE model is used in the Exxon LSM modeling program [38] for pure components. That program uses heuristic rules to estimate the amount of flashing liquid rainout. This preliminary model over predicts the liquid "rainout" and is applicable only to pure components. Research in this area is ongoing.

Rainout Algorithm. Considering the purposes of this manual, before-the-fact estimation of consequences from given release scenarios, the following stopgap algorithm is suggested for use on a worst case basis (T_1 is the storage or stagnation temperature, T_{NBP} is the normal or atmospheric boiling point temperature, and f_l is the fraction liquid from flashing):

A. Liquid is released:
   1. If $T_1 < T_{NBP}$, then $f_l = 1$ and $f_{aerosol} = 0$.
   2. If $T_1 > T_{NBP}$, then calculate f_l and,
      a. If f_l is small (e.g., less than 0.2) or the degree of superheat exceeds 10 degrees kelvin, then use $f_{aerosol} = 1$ (no pool formed),
      b. else, use f_l as calculated with $f_{aerosol} = 0$.

B. Saturated vapor is released:
— Calculate f_l and use $f_{aerosol} = 1$ (no pool formed).

Alternatively, the worst case downwind concentrations can be bracketed by assuming that all f_l of the substance goes into the pool on one hand, and that all the substance remains airborne with f_l liquid droplet fraction on the other hand.

Size and Shape of Pools

Concepts. If the input liquid flow to an evaporating pool is great enough compared with evaporative losses, the pool will grow until this flow stops (assuming no other losses). Otherwise, the pool can reach a steady state size governed by input flow rate matching total evaporation rate. If the release time is small compared with this spreading time, say less than a minute or two, and the maximum pool area can be specified, it may be adequate to assume the spreading as well as the release are essentially instantaneous. In that case, only the initial, total amount of liquid spilled over the given area is required to estimate the evaporation losses over time. On the other hand, and assuming that the pool is formed on a perfectly level, flat, impermeable surface, with or without a containment dike or berm, this growth will first consist of spreading in a radial direction, then, when the dike is encountered, the depth increases. In practice, some spill scenarios involve a circular storage tank placed in the center of a square area contained by a dike. For these purposes, the horizontal area of the tank can be subtracted from the total diked area, to give the available area for pool formation. Then, evaporation from the net equivalent circular area can be estimated by the methods discussed below.

The simplest models for liquid spreading are based on a kinetic vs. potential energy balance to obtain the volume as a function of time. If the substrate area is infinite in extent, then this simple model theoretically allows the pool to spread to an infinite radius with an infinitely small thickness, or depth. A better model, as shown by Webber and Brighton [51], considers surface roughness effects on viscous drag, and surface tension which controls the minimum thickness. For any model, if the spill is not contained by dikes, a minimum thickness should be invoked for the spreading calculations.

A General Model. A minimum set of equations for an evaporation model which treats spreading is as follows. The *overall mass balance* is

$$\frac{dW_{pool}}{dt} = w_{in} - G_{evap} A_{pool} \tag{107}$$

where W_{pool} is the total mass of liquid in the pool at time t, w_{in} is the mass flow rate of liquid into the pool, G_{evap} is the evaporation mass flux, and A_{pool} is the total top surface area of the pool. The overall *change in total enthalpy* for the pool is

$$\frac{dH_{pool}}{dt} = w_{in} H_{in} - G_{evap} H_{vapor} A_{pool} + A_{pool} \sum_j \zeta_j \tag{108✧}$$

where H denotes enthalpies per unit mass (or mole) for the terms on the right hand side, and ζ_j are radiant and conductive energy fluxes. For a level, cylindrical pool, the radius changes according to

$$\frac{dr_{pool}}{dt} = \sqrt{2gh_{pool}} \; . \tag{109}$$

The above three equations are to be simultaneously integrated over time, using appropriate initial values, and with additional relationships such as

$$V_{pool} = \pi r^2 h_{pool} \; . \tag{110}$$

and liquid density. Input variables can be arbitrary functions of time.

Approximate Models. By ignoring the evaporative loss term in the differential mass balance equation, Shaw and Briscoe treated mass and radius as independent variables to obtain the following integral solutions:

For a *spill at finite rate*, w_{in},

$$W_{pool} = \frac{4}{15} G_{evap} \left[8\pi g B \frac{w_{in}}{\rho_l} \right]^{1/2} t^{5/2} \tag{111}$$

where B is the buoyancy ratio, equal to 1 for ground substrate and equal to $(\rho_{water} - \rho_l)/\rho_{water}$ for water substrate. The corresponding pool radius is

$$r_{pool} = \sqrt{2/3} \left[8 g B \frac{w_{in}}{\rho_l} \right]^{1/4} t^{3/2} \; . \tag{112}$$

For an *instantaneous spill*, the total mass at any time is

$$W_{pool} = \pi G_{evap} \left(\left[\frac{2gBA}{\pi} \right]^{1/2} t^2 + r_o^2 t \right) \tag{113}$$

where A is the pool area and r_o is the initial pool radius, and,

$$r_{pool} = \left(\left[\frac{8gBA}{\pi} \right]^{1/2} t + r_o^2 \right)^{1/2} \; . \tag{114}$$

Shaw and Briscoe concluded that there was little difference between predictions of their full SPILL numerical code and the above approximate solutions for spills on water. However, they used a constant, experimentally derived value for the mass evaporation rate. On the other hand, those authors stated that the above approximate models are not sufficiently accurate for land applications, and therefore their full SPILL numerical model [similar to the set of equations, 111 to 114 above] must be applied in all cases.

The LSM90 program uses approximate models based on those of Shaw and Briscoe.

Model Components

The principal mass and energy flow "terms" or "components" currently used in evaporative source modeling, as mentioned in the General Model above (Equations 107 to 110), are summarized below and are intended to be representative, but not all-inclusive.

Evaporative Mass Transfer. If the pool temperature, or specific enthalpy, is externally specified, then the evaporative mass flux can be found by dividing the excess from the enthalpy balance equation by the heat of vaporization of the released material (assuming a liquid pool with homogeneous properties). However, if temperature or enthalpy is determined in the model, then the mass flux must be determined by another independent relationship.

Kawamura and Mackay use the convective mass transfer coefficient correlation developed by Mackay and Matsugu [45]:

$$k_c = 8.06E-06\, u_{wind}^{0.78}\, D_{pool}^{-0.11}\, N_{Sc}^{-0.67}, \quad m/s. \qquad (115)\diamond$$

For which the dimensionless Schmidt number is

$$N_{Sc} = \frac{\mu}{\rho_{surf}\mathfrak{C}} = \frac{\nu}{\mathfrak{C}}, \qquad (116)$$

where μ is the absolute and ν is the kinematic viscosity, ρ the density of the evaporating surface vapor film, and $\mathfrak{C}$ the molecular diffusivity for the vapor. The density is found by the ideal gas law is

$$\rho_{surf} = \frac{MP_{surf}}{RT_{surf}} \qquad (117)$$

in which M is the molecular weight, P_{surf} is the vapor pressure and T_{surf} is the temperature at the surface. The evaporative mass flux is then

$$G_{evap} = k_c \rho_{surf}\,. \qquad (118)\diamond$$

Kawamura and Mackay's *Surface Temperature Model* determines the pool's surface temperature, T_s, by numerically solving the overall energy flux balance equation for this variable. Their *Direct Evaporation Model* does not contain the surface temperature, the pool surface temperature is assumed equal to the air temperature. Solution of the latter model is direct and requires no iteration.

The LSM90 modeling program uses the above method for estimating evaporative mass transfer flux.

The Shell Spills Model by Fleischer [4] uses a dimensionless number correlation from Sherwood, Pigford and Wilke [49] (developed for distillation column design) to calculate the evaporative mass transfer coefficient. Using the Sherwood dimensionless number, the mass transfer coefficient is

$$k_c = N_{Sh} \frac{D_{pool}}{\mathfrak{C}} . \tag{119}$$

If the Schmidt number (Equation 116) is less than 0.5, the Sherwood number for air is calculated by

$$N_{Sh} = 0.664\, N_{Sc}^{1/3}\, N_{Re}^{1/2} , \tag{120}$$

otherwise,

$$N_{Sh} = 0.037\, N_{Sc}^{1/3}\, [N_{Re}^{0.8} - 15{,}200] . \tag{121}$$

The Reynolds number for air is

$$N_{Re} = \frac{u_{wind}\, D_{pool}}{\nu} . \tag{122}$$

This method is used for Scenario 8 in Chapter 6.

Evaporative Heat Flux. The heat flux (J/[m^2 •s] leaving the pool by evaporation is the product of mass flux (Equation 118) and the heat of evaporation:

$$\zeta_{evap} = G_{evap}\, \Delta H_{lv} . \tag{123}$$

Air to Pool Heat Transfer. If the evaporation rate is large, e.g. the pool is boiling, then the enthalpy flow is essentially one way, i.e., into the atmosphere. On the other hand, if the evaporation rate is relatively low, the pool can be warmed or cooled by the wind contacting the surface of the pool. For this, the air-pool convective heat transfer flux is

$$\zeta_{air} = \hbar_{air} (T_a - T_s) . \qquad (124)\diamond$$

By heat/mass transfer analogy, Kawamura and Mackay obtained the heat transfer coefficient (J/[s•K])

$$\hbar_{air} = k_c \rho_a C_{p,a} \left(\frac{N_{Sc}}{N_{Pr}} \right)^{0.67} . \tag{125}$$

The Prandtl number for air in the preceding equation is

$$N_{Pr} = \frac{\nu}{\rho \mathfrak{C}} \ . \qquad (126)$$

(See Perry's Sixth, page 3-254 for a table of Prandtl numbers for air vs. temperature and pressure.)

The LSM90 program uses this algorithm.

Solar Heating. The flux of solar shortwave radiation, perpendicular to the earth's surface, at the top of the atmosphere averages 1,353 W/m^2 (the solar constant [50, p. F-161]). On a clear day, about 75 % reaches the earth's surface after scattering and absorption by the atmosphere; this corresponds to about 1,000 W/m^2. The actual flux reaching a particular location (the evaporating pool) depends upon the declination angle the sun makes with the point on the surface (90 degrees = perpendicular). Raphael [46] gives the following equation for solar flux incident to a flat surface:

$$\zeta_{solar} = 1111(1 - 0.0071C_I^2)(\sin\phi_S - 0.1), \quad W/m^2, \qquad (127)$$

where the cloudiness index, C_I, is fraction of sky covered in tenths, i.e., $0 \le C_I \le 10$ (as reported on National Weather Service observational data reports) and ϕ_S is the ray incident angle which is a function of observer latitude, longitude, the time of the day, and the day of the year★. If $\sin\ \phi_S < 0.1$, the solar flux is zero. For most accidental release applications, the greatest daylight heat flux is when the incident angle is near 90 degrees, so for several hours, the worst case form of Equation 127 reduces to

$$\zeta_{solar} = 1000(1 - 0.0071C_I^2) \ . \qquad \text{(128)✧}$$

For screening purposes, the sky can be assumed clear ($C_I = 0$), thus $\zeta = 1000$ W/m^2. Raphael gives the detailed equations for calculating ϕ_S for a particular location and hour of the year; these are summarized and used by Reynolds in the ALOHA model.

The LSM90 modeling program uses a somewhat different form to calculate the solar flux. The sine of the incident angle is calculated as the time fraction of a 180 degree hemicircle for the sun's position since sunrise, the flux is directly proportional to the fraction of clear sky, and a fluid reflectance coefficient is used. For a clear sky with the sun directly overhead, the same results are obtained as above. The amount of light reflected from a pool (reflectance) for different liquid materials, different substrates, different colors, etc., will be less that 9-11%; this is incorporated into Equation 128. If the reflectance is zero and the sun is overhead, the LSM90 flux is the same as Raphael's. Otherwise, it appears that the LSM90 form has redundantly accounted for reflectance.

★ This can be exactly calculated by a DOS computer program, *MICA*, available from the U.S. Naval Observatory [53].

Radiative Cooling. The temperature difference between the pool and the atmosphere results in a net loss of energy from the pool by long wave infrared radiation. The net radiative flux loss *from* the pool can be approximated by

$$\zeta_{rad} = \sigma_{SB}\left[\epsilon_{\uparrow}T_{surf}^{4} - \epsilon_{\downarrow}T_{air}^{4}\right] \qquad (129)\diamond$$

in which the first term represents loss from the pool and the second term the gain from the air. The Stefan-Boltzman constant, σ_{SB}, for black body radiators equals 5.67E-08 W/[m^2 • K^4]. The pool surface temperature, T_{surf}, may be approximated by the bulk pool temperature in some models. The *emissivity* of the liquid ($\epsilon_{\uparrow}$) is usually not available for many chemicals; Raphael reports the average effective value for water is 0.97, and shows that the atmospheric emissivity ($\epsilon_{\downarrow}$) varies between about 0.7 to 0.9 for zero cloud cover for a range of humidities.

In the LSM90 model, the above equation is approximated by

$$\zeta_{rad} = \epsilon_{\uparrow\downarrow}\,\sigma_{SB}\left[T_{surf}^{4} - T_{air}^{4}\right], \qquad (130)$$

where $\epsilon_{\uparrow\downarrow}$ is the "average" emissivity. If the net long wave radiation exchange is small with respect to the other energies involved, a constant $\epsilon_{\uparrow\downarrow}$ value in the above range, say 0.8, could be used.

Heat Transfer from the Ground★. The commonly used model for conduction of heat from the ground into the evaporating pool assumes that before the pool contacts the flat, level ground, the ground everywhere below (one dimension, *z*) is at ambient air temperature T_a. After time $t = 0$, the ground surface is constantly maintained forever at the *constant* pool temperature, T_{pool}. After Carslaw and Jaeger [40], the general solution to the problem is

$$T(z) = T_a - (T_a - T_{pool})\, erfc\left(\frac{z}{2\sqrt{\alpha_T t}}\right) \qquad (131)$$

in which *erfc* is the complementary error function and α_T is the thermal diffusivity. The corresponding rate of the *ideal* heat flux into the pool at the ground-liquid interface is

$$\zeta_{ideal\ slab} = \frac{\lambda_T (T_a - T_{pool})}{\sqrt{\pi\alpha_T t}} \qquad (132)\diamond$$

where α_T is the thermal conductivity of the ground. *Figure 10* shows ground temperature (*T*) vs. depth (*z*) for several times *t*. This model does not allow the pool temperature to change (as for a boiling pool of a pure component), nor for heat transfer into the ground column below the pool from the adjacent ground at different temperatures. If these factors need be considered (e.g., the area of the pool is changing at constant boiling point, or the liquid in the pool is changing composition which changes the boiling temperature), then the original partial differential equation with associated

---

★ Heat transfer from water substrates is sparsely treated in this manual. See Shaw and Briscoe's reports [37,48] and that of Webber and Brighton [51].

boundary conditions upon which Equation 131 is based should be solved differently, probably by numerical methods. Equation 131 can be called the "instantaneous spread model;" it is used by the Shell Spills and ALOHA models.

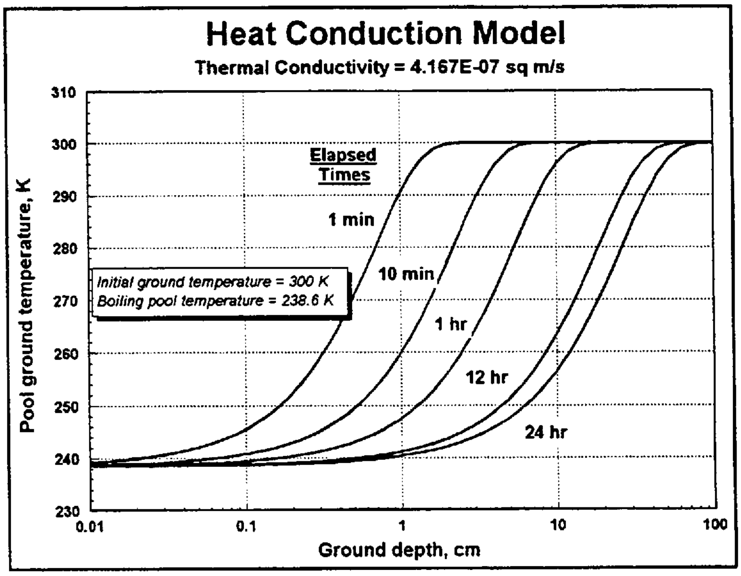

Figure 10.

Shaw and Briscoe stated that it was necessary to use thermal fluxes approximately three times greater than the theoretical values from Equation 131 to obtain agreement with experiments of the Japan Gas Association. Thus they used a *"surface roughness correction factor,"* X (= 3), "...which allows the [preceding] equation to be extended to other soils by changing the relevant thermal properties." Applying this factor to Equation 127 gives

$$\zeta_{cond} = \frac{X\lambda_T (T_a - T_{pool})}{\sqrt{\pi \alpha_T t}} \tag{133}$$

as the effective conduction heat flux. They also state that Equation 133 will over-predict the evaporation rate of a boiling liquid if the area over which the pool spreads is relatively large compared with the rate of the spill, i.e., the spreading time is significant. Hence, they presented the following model in which concentric annuli (adjacent cylinders) of radius r' and width dr' are exposed to the boiling, spreading liquid on their ground surface end. Let t′ be the time at which the liquid first reaches the annulus at r′, then, from Equation 128, the average heat flow rate from this annulus at time t is

$$\bar{q}(r') = \Theta \frac{2\pi r' dr'}{(t-t')^{1/2}} \tag{134}$$

where

$$\Theta = \frac{X k_s (T_a - T_{pool})}{\sqrt{\pi \alpha_T}} \tag{135}$$

and $(t-t')$ is the time that the boiling liquid has been present at this annulus. Therefore , the total heat flow rate for the whole pool area up to a radius r(t) is

$$q_{pool}(r) = 2\pi\Theta\int_0^{r(t)} \frac{r'}{(t-t')^{1/2}}dr' \; . \qquad (136)$$

This is the heat flow rate from the ground annulus into the boiling pool at time *t*; (W = J/s). Then Shaw and Briscoe use the preceding heat flow to calculate the evaporative *mass* flow, which assumes all other heat flows and exchanges for the pool are negligible; then the evaporative mass flux at time *t* equals

$$G_{evap} = q_{pool}(r)/\Delta H_{vap} \; . \qquad (137)$$

The model represented by Equation 136 is still only approximate, for heat conduction in the radial direction in the ground, with its associated boundary layer condition, is ignored. Arguably, it might be better to use a model based upon the full partial differential equations in depth, radius and time. However, in most before-the-fact modeling applications, the structure, homogeneity and properties of the underground will not be well known, if at all. Thus the much greater complexity of parameter and spatial distribution is generally not justified, considering the inherent scenario definition uncertainties.

Equation 136 can be approximated by a summation of finite differences using Euler's method:

$$q_{pool,n} = 2\pi\Theta\sum_{n=1}^{N}\left[\frac{r_{n-1}\Delta r}{(\Delta t)^{1/2}}\right] \qquad (138)\diamond$$

in which *n* denotes the time step index and *Δ* is the finite difference operator for the time and corresponding radius steps.

The preceding equation is essentially the same approach used in the LSM90 modeling program, except the geometrical shape of the spreading pool area is treated somewhat differently. In that program, if the spreading pool encounters a dike, conductive heat transfer from the dike walls is similarly treated. Also, the LSM90 model does not use the *X* surface roughness correction factor.

Because soil properties required for these computations are difficult to find, *Table 4* presents these parameters for a number of substrates. The data was taken from Table 4 of Shaw and Briscoe, and Table 2.2 of Reynolds (ALOHA).

Table 4.

Thermal Properties of Natural Materials

Material	*Remarks*	*Density* ρ kg/m^3	*Specific heat* C_p J/[kg•K]	*Thermal conductivity* λ_T W/[m•K]	*Thermal diffusivity* α_T m^s/s	*Reference*
Concrete		2300	961	0.92	4.16×10^{-7}	Shaw & Briscoe
Soil	Average	2500	836	0.96	4.59×10^{-7}	Shaw & Briscoe
Soil	Sandy, dry	1650	794	0.26	1.91×10^{-7}	Shaw & Briscoe
Sandy soil	Dry	1600	800	0.30	2.4×10^{-7}	Reynolds
Soil	Moist, 8% water, sandy	1750	1003	0.59	3.36×10^{-7}	Shaw & Briscoe
(40% pore space)	Saturated	2000	1480	2.20	7.4×10^{-7}	Reynolds
Clay soil	Dry	1600	890	0.25	1.8×10^{-7}	Reynolds
(40% pore space)	Saturated	2000	1550	1.58	5.1×10^{-7}	Reynolds
Peat soil	Dry	300	1920	0.06	1.0×10^{-7}	Reynolds
(80% pore space)	Saturated	1100	3650	0.50	1.2×10^{-7}	Reynolds
Snow	Fresh	100	2090	0.08	1.0×10^{-7}	Reynolds
	Old	480	2090	0.42	4.0×10^{-7}	Reynolds
Ice	0° C, pure	920	2100	2.24	11.6×10^{-7}	Reynolds
Water	4° C, still	1000	4180	0.57	1.4×10^{-7}	Reynolds
Air	10° C, still	001.2	1010	0.025	2.05×10^{-5}	Reynolds
Air	Turbulent	001.2	1010	≈ 125	≈ 10	Reynolds

Numerical Example

The following example, for an instantaneous spill (instantaneous pool formation) shows heat and mass flux for the convective and conductive terms discussed above. Chlorine and air properties were obtained from Perry's Sixth, and those for ground from the above table. The heat fluxes at the bottom of the table are the relative contributions for the 10 s elapsed time. Changing the time to 2 seconds changes the ground flux fraction from 0.457 to 0.65, and for 40 s this fraction becomes 0.30. Thus, as expected, the initial radiation contributions to the evaporation rate are negligible, but as the ground cools down, these terms become more and more important.

Example Rate Calculations for Evaporation

Physical and Thermodynamic Properties

Description	Symbol	Units	Value
For chlorine			
Molecular weight	M		70.91
Normal boiling point	T_{NBP}	K	238.55
Liquid density at NBP	ρ_l	kg/m^3	0.3108
Absolute viscosity in air	μ	Pa•s	0.1104
Kinematic viscosity in air	ν	m^2/s	0.0305
Molecular diffusivity of vapor in air	$\mathfrak{C}$	m^2/s	8E-06
Heat capacity of vapor in film	C_p	J/[kg•K]	405,710
Enthalpy of vaporization	ΔH_{vap}	J/kg	2.867E+08
For the atmosphere (no water vapor)			
Wind speed	u_{wind}	m/s	5.00
Air temperature	T_a	K	298.15
Absolute viscosity	μ_a	Pa•s	1.84E-05
Kinematic viscosity	ν_a	m^2/s	5.08E-06
Density (by ideal gas law at 1 atmosphere)	ρ_a	kg/m^3	3.62
Heat capacity at constant pressure	$C_{p,a}$	J/[kg•K]	1000
Solar angle	ϕ_s	degrees	45
Cloud cover			0
For the ground (concrete), see Table 4			
Thermal conductivity	λ_T	W/[ms]	0.92
Thermal diffusivity	α_T	m^2/s	4.16E-07
Initial uniform temperature (same as air)	T_a	K	298.15
Specified for the evaporating pool			
Surface temperature (assumed T_{NBP} + 5)	T_{surf}	K	243.55
Pool Diameter	D_{pool}	m	7.00
Pool area (from diameter)	A_{pool}	m^2/s	153.94
Average net emissivity for solar radiation	$\epsilon_{\downarrow\uparrow}$		0.8
Time after instantaneous spill	t	s	10

Calculated Quantities

Intermediate parameters	Symbol	Units	Equation	Value	Fraction of Absolute Total
Vapor film density	ρ_{surf}	kg/m^3	113	3.55	
Schmidt number for vapor film	N_{Sc}		112	0.63	
Reynolds number for air	N_{Re}		118	6.89E+06	
Prandtl number for air	N_{Pr}		122	0.71	
Convective mass transfer coefficient	k_c	m/s	111	1.68399E-05	
Evaporative mass flux	G_{evap}	kg/[m^{2}s]	114	5.976E-05	
Air-to-pool heat transfer coefficient	h_a	J/[Kt]	120	5.660E-02	
Heat fluxes					
Evaporative heat flux	ζ_{evap}	J/[m^2.s]	119	**-17,134**	**-0.516**
Solar heat flux	ζ_{solar}	J/[m^2.s]	124	**674**	**0.020**
	ζ_{rad}	J/[m^2.s]	125	**-199**	**-.006**
	$\zeta_{ideal\ slab}$	J/[m^2.s]	128	**15,167**	**0.457**
Sum of absolute values of heat fluxes:				**33,174**	**1.000**

CHAPTER 4

CHAPTER FOUR

Meteorology

Quick Reference

Meteorology is a very large and complex field of knowledge. However, the meteorological phenomena which primarily affect the dispersion of accidental releases of concern here are generally limited to a relatively small geographical area (say less than 20 kilometers in diameter), and from the surface of the earth to the upper limit of the atmospheric boundary layer (which altitude varies up to about 3,000 meters, depending upon the conditions). The science and art which deals with this limited scope is called *micrometeorology*; the following discussion presents the aspects of it which primarily govern accidental release dispersion modeling.

The nature of the local terrain, as well as man-made structures, can have significant effects upon the micrometeorological behavior of the atmosphere. The heating and cooling effects differ over water bodies compared with the land. Terrain features such as hills, mountains, lakes and valleys will cause different airflow than over a flat plain. Man-made structures, especially the larger groupings of them, such as urban centers and industrial plants, will cause the local general airflow to be altered in direction and to enhance mixing processes. *Figure 1* [Hosker, 4a] shows how complex the wind flows can be around even a simple cubic structure. In this figure, the wind flows from left to right, and the wind speed varies exponentially with elevation, as shown by the **INCIDENT WIND PROFILE** diagram. Meteorologists refer to terrain which is not relatively flat as *complex*. Special techniques such as computational fluid dynamics and physical modeling (*e.g.*, wind tunnel) are needed to model dispersion in complex terrain and around significant man made structures. This Manual treats only flat, or non-complex, terrain where the simpler similarity-type models are applicable.

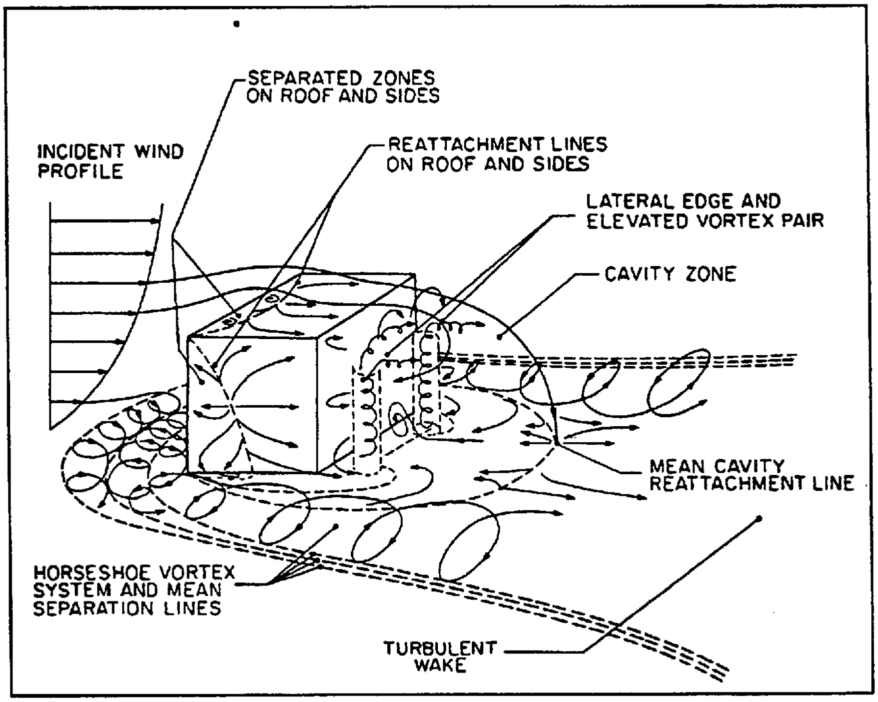

Figure 1.

Usually, about nine meteorological/atmospheric boundary layer parameters need to be specified for modeling vapor cloud dispersion. Following is a very brief overview of how these parameters relate to the phenomena involved.

Consider a vapor cloud from a release for which the observer is far enough downwind so only atmospheric dispersion processes predominate.. As the vapor cloud travels with the wind, ambient air will continuously be mixed into it, and it may rise, sink, or be of neutral buoyancy with constant average elevation. The following phenomena will affect the mixing of air *into* the vapor cloud:

1. Turbulence is mechanically induced in the horizontally flowing airstream by the presence of terrain features (grass, trees, hills, etc.) and structures. The rougher the terrain and the larger the structures (and their number), the greater the turbulence. This effect is characterized by the **surface roughness length parameter,**[★] z_r.
2. Convective turbulence in the air stream can be enhanced or reduced by variables that influence the heat input and output to/from the earth's surface. Thermal radiation from the sun (insolation) during the day cause vertical air flows which causes mixing of air parcels (turbulence); these effects are reduced by cloud cover. Meteorologists have developed a simplified turbulence classification scheme to make *a priori* dispersion modeling more tractable; this is the **stability class** concept.
3. The higher the horizontal **wind speed,** u, the more diluted the vapor cloud will become as a function of time. Since cloud dimensions increase with distance downwind because of the air being *entrained* into them by this mixing, the pollutant concentration will decrease.
4. The density of the dispersing cloud is determined by its initial values, the rate at which ambient air is mixed into it, and the properties of the air (**ambient temperature, barometric pressure, relative humidity**). Also, the **ground** or **sea temperature** may need to be considered. These variables are also affected by the heat input and output to/from the earth's surface, the surface roughness, and the wind speed.
5. The rate at which a cloud grows in vertical and horizontal directions is affected by the *relative importance of the initial cloud buoyancy versus the ambient mechanical turbulence.* The relative importance of the two variables affects the **release Richardson number,** Ri_*. When the release Richardson number is large, dense gas dispersion effects dominate and when the number is small, the cloud is positively buoyant. A different dispersion model may be required, depending upon whether the cloud is positively or negatively buoyant.

The modeling parameters of interest that influence jet releases and evaporating pools are identical to those discussed above, but with some different effects. For a jet release, the wind speed will affect the trajectory of a vertically directed vapor cloud. The greater the wind speed the less the initial rise. For an evaporating pool, the wind speed and properties of the pool will affect the emission rate. The following will provide additional discussion on each of the above highlighted parameters, as well as wind direction.

[★] The symbol z_o is more commonly used; z_r is used here to avoid conflicts with other usage.

Modeling Parameters

Boundary Layer

In fluid mechanical theory of the atmospheric boundary layer, the variation of wind speed (u_a) is related to the velocity measurement height above the surface (z) by an equation of the following form:

$$\frac{u_a}{u_*} = \frac{1}{k}\left[\ln\left(\frac{z}{z_r}\right) - \Phi\left(\frac{z}{\lambda}\right)\right]. \tag{1}$$

Where:

u_a = wind speed
u_* = friction velocity constant (empirically derived),
k = von Karman's constant (0.41),
z = measurement height,
z_r = surface roughness length parameter,
Φ = a function, *e.g.*, $4.7 \cdot (z/\lambda)$, and
λ = the Monin-Obukov length parameter (MOL).

The surface roughness parameter is related to the turbulence induced by surface structures and features; more on this later. The absolute value of Monin-Obukov length may be thought of as the depth of the mechanically mixed layer near the surface. For a given state of the atmosphere, Φ and λ are obtained by fitting the equation to the vertical wind speed profile. The value of λ is negative for unstable atmospheric conditions, positive for stable conditions, and approaches infinity for neutral conditions [2]. The values for u_*, λ, and z_r are determined by fitting the appropriate form of Equation 1 to experimentally observed wind speeds at various elevations, z, above the surface.

Dispersion models, such as are used for examples in this manual, internally use Monin-Obukov length, but this may not be stated explicitly in the users' manuals. To simplify modeling parameter specification for *a priori* purposes, many models use Golder's correlation [15] to obtain the MOL, given the stability class and roughness length. Golder's correlation is based upon a number of field experiments in which the maximum roughness length corresponded to desert covered with sagebrush (about 0.05 m). *Golder's correlation is extrapolated for higher roughnesses.*

For Equation 1, if the rightmost term containing the MOL is zero, as is generally true for neutral stability, then the equation reduces to

$$u_a = \frac{u_*}{k}\ln(z/z_r) \tag{2}$$

This is the well-known logarithmic wind speed profile law. It is the basis of a working approximation used in many U.S. Environmental Protection Agency (EPA) modeling programs [*e.g.*, 14] and is discussed further under *Wind Speed* below.

Roughness Length Estimation

Usually, the dispersion models of main interest here require that the user supply the roughness length for a dispersion simulation. There are several methods available for obtaining estimates of z_r ranging from field measurements to a simple lookup table [16]. In general, z is roughly proportional to the average height of the buildings or obstructions in an area. The proportionality constant typically ranges from 0.03 to 0.1. Unfortunately, an easily applied method for obtaining the proportionality constant is not available. Various researchers have put together tables of z_r versus site description; these are the basis of *Figure 2*. Use of these approximate values with an inspection of the site and surroundings is the most practical means of estimating z_r.

Figure 2 includes a range of surface roughness lengths that were measured during wind tunnel testing of an actual refinery model [17]. The observed range for z_r was 0.5 to 3 m, based on a limited set of experimental observations. Based on these results, however, it is recommended that the surface roughness length for large refineries be set at 1 m and for small refineries at 0.5 m.

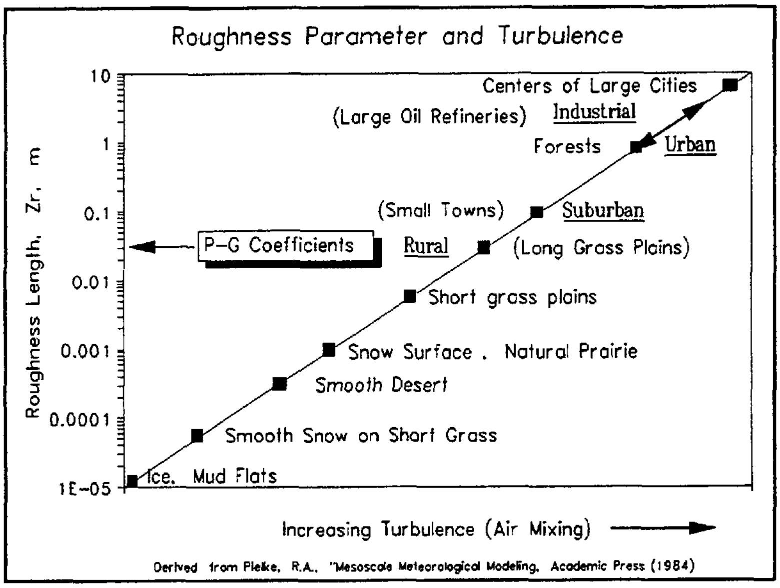

Derived from Pielke, R.A., "Mesoscale Meteorological Modeling, Academic Press (1984)

Figure 2. Roughness length versus site classification.

Some models have the capability to specify the surface roughness as a function of downwind distance. In this case, the area around the site should be separated into zones of different surface roughness using Figure 2. The highest concentrations will then occur for wind directions that have the lowest surface roughness.

If the dispersion modeling program to be used does not have the capability of varying the surface roughness parameter with downwind distance, the potential effects of this variation should be estimated by means of bounding simulations. For example, suppose a potential release could occur in an industrial plant area with $z_r = 1.0$ m and the surrounding offsite area is suburban with $z_r = 0.1$ m. Then modeling runs with the 1.0 m value can be used to estimate the dispersed concentrations at the plant fence line, and the concentrations from the 0.1 m runs will *conservatively* predict the values downwind of the fence line.

Because this scheme was proposed in 1978 before surface roughness came into use with accidental release models, the U.S. Environmental Protection Agency may recommend Auer's method [20] to determine whether a particular geographical area can be classified as *Urban* or *Rural* for regulatory purposes. This type of classification may also influence the selection of σ_y dispersion coefficients; see below.

Atmospheric Stability

For the purposes of simplifying model input, atmospheric stability is usually classified according to the Pasquill-Gifford (PG) stability classes defined in *Table 1* [13]. The winds speeds in this table *are for a 10 m measurement height*. The standard set of Gaussian plume model dispersion coefficients *(σ_y, σ_z)* associated with each stability class were developed on the basis of a number of different field experiments in which the averaging times varied from about 2 to 20 minutes with 3 minutes predominating. Also, the roughness parameter varied; a value of 0.03 m is generally used for rural applications.★

Table 1.

Definition of Pasquill-Gifford Stability Classes

10 m wind speed m/s	Daytime Insolation			Nighttime Conditions	
	Strong	Moderate	Slight	Thin overcast or >4/8 cloudiness	<3/8 cloudiness
<2	A	A-B	B		
2-3	A/B	B	C	E	F
3-5	B	B-C	C	D	E
5-6	C	C-D	D	D	D
>6	C	D	D	D	D

Stability Classes:
A Extremely unstable
B Moderately unstable
C Slightly unstable
D Neutral conditions
E Slightly stable
F Moderately stable

The stability categories range from **A** to **F** with **A** being unstable and **F** being stable. For unstable conditions a puff, or parcel, of air that is displaced vertically will tend to continue to move in the vertical direction, while for stable stratification that parcel will tend to settle back to its original position. Under neutral stratification, that parcel will tend to remain at the level to which it is displaced. These phenomena cause the most horizontal and vertical mixing in unstable atmospheres, moderate mixing for neutral conditions, and the lowest mixing (dispersion) for stable conditions. Similarly, plume widths and heights are largest under **A** stability and smallest under **F** stability.

On Gaussian Plume Models

Dispersion models which treat neutral buoyancy or trace gas releases by means of normal probability distributions with dispersion coefficient parameters σ_y, σ_z, (and σ_x for time dependent forms) are generally called "Gaussian models." They may apply to point, line, area and volume sources. In advanced model codes, the dispersion coefficients may be related to the roughness parameter and Monin-Obukov length via correlations. All use the logarithmic wind speed profile.

To simplify applications, and to speed program execution, many of the EPA's core Gaussian models do not use roughness or Monin-Obukov parameters; they are built into the dispersion coefficients. The Pasquill-Gifford dispersion coefficients for rural terrain are based upon experiments for which z_r was estimated to be 0.03 m. The McElroy-Pooler coefficients are based upon extensive field tests over urban and suburban areas.

*The term **"Gaussian plume"** model is used throughout this Manual to mean the basic EPA-type model for which the atmospheric boundary layer parameters (e.g., roughness length) are bundled-up into the dispersion coefficients and thus cannot be externally specified, except through rural vs urban coefficient set selection.*

An example of the most unstable class, **A**, would be a hot summer afternoon where cumulus clouds are building up; these are indicative of large vertical velocities and turbulence. The most stable class, **F**, occurs at night with low winds and no cloud cover. As can be seen in the table, neutral stability can occur under many conditions, and it will occur if the wind speed becomes high

---

★ Sometimes, the parameters associated with the Pasquill-Gifford stability classes are confused with the Prairie Grass field experiments in which the release durations and averaging times were both 10 minutes and the surface roughness parameter was 0.06 m.

enough under most atmospheric conditions. The most frequent stability class at most sites is **D**, which occurs mostly during the daytime. The "worst case," **F**, occurs a significant fraction of the winter nighttime hours at most sites unless the local wind speeds are high.

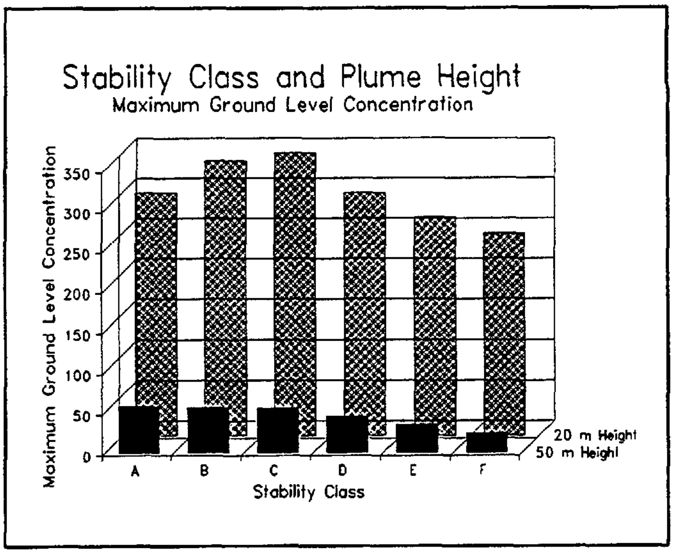

Figure 3.

For ground level releases of *constant rate*, the highest ground-level concentrations will generally occur under **F** stability. For vertically-pointing jet releases, the maximum ground level concentration can occur under any stability condition depending upon the initial properties of the jet, and of the height of the release above ground level. This is illustrated in *Figure 3*, which shows the maximum downwind distance concentration for a neutrally buoyant cloud, 20 m and 50 m plume heights, 1 m/s wind speed and 1 g/s release rate. This figure was prepared using the Gaussian dispersion model for the far-field [4]. The figure shows that for a 50 m plume height the critical stability (i.e., stability that will give the maximum ground level concentration) is **A** stability and for a 20 m plume height the critical stability is **C** stability. The critical stability will trend toward **F**, the lower the plume height. This simple example indicates that parametric sensitivity tests are required to determine the critical stability for jet releases directed in the vertical or nearly vertical direction. Table 1 must be used to define a wind speed range for each stability category or else the wind speed-stability class combination can be meaningless.

The PG classification scheme, with the associated sets of dispersion coefficients based upon *rural* data, is used by the dense gas dispersion models (as for the three systems used for example modeling here). For *industrial, urban and suburban* areas, dispersion is greater, as exemplified by the McElroy-Pooler (MP) dispersion coefficients [14]. Gaussian plume model calculations made with MP **F** stability coefficients give dispersion results comparable to calculations made with PG **E** stability coefficients. Also, because of significant atmospheric heating over refinery complexes, **E** should be the only *stable* class used for refineries which have urban areas adjoining.

These stability classification schemes do not treat *calms*. By definition, the atmosphere is called *calm* if the wind speed is less than 2 meters per second. Winds, if any, are so light and variable in speed and direction that these parameters are difficult to define on an average basis. A number of accidental releases with unfortunate consequences have occurred under calm, stable conditions.

Inversion layers above the ground act to trap vapor clouds released below them. Thus, if the release (*e.g.*, at ground level) is large enough and/or the height of the "lid" is low enough, then downwind dispersed concentrations will be significantly larger than for no inversion layer trapping. Most ground level, dense gas dispersion models such as HEGADAS, DEGADIS, and SLAB do not handle inversion layer effects. If the inversion layer effect is important, other models should be used. For example, to estimate concentrations at far-field downwind distances where a dense gas cloud would become diluted to essentially neutral buoyancy, the Gaussian plume model can be used. For this, the *user should ensure that the modeling calculations include the power series terms for both ground and inversion layer reflection.*

Wind Direction

For worst case analyses, it is always assumed that the *average* **wind direction** always blows directly toward the most sensitive, or critical, area with respect to the released material's toxic and/or flammable properties. Therefore, average wind direction, *per se*, usually need not be considered as an explicit, atmospheric variable. Consider concentration effects in all directions to downwind locations of interest, *i.e.*, radii. If the terrain is complex (which can include man-made structures) effects such as channeling in canyons or city streets, as well gravity flow of dense vapor clouds should be considered.

Wind Speed

Wind speed affects downwind concentrations by diluting the plume, by changing the plume rise for an elevated release, and by changing the rate of evaporation from a pool. For a ground-level horizontal jet release that is less dense than air or is the same density as air, concentrations generally tend to decrease in inverse proportion to the wind speed. For dense cloud releases and low wind speeds, ground level concentration may not so decrease proportionately to wind speed because spreading phenomena may predominate near the source. For calm wind conditions, the cloud spreads in a circular pattern about the release if on a level plane. The models used for example modeling herein do not treat the calm case; Post [II-6b] and Moser [II-20] describe modeling program based on accepted principles .

For vertically directed jet releases, the wind speed not only affects the dilution but also changes the plume trajectory. For low wind speeds, the initial plume rise due to jet momentum effects can be large. At higher wind speeds, the horizontal velocity of the air will act to reduce the momentum rise of the jet and cause the cloud to bend over. For a jet release forming a dense cloud, the jet may bend over. Depending upon the initial release height, wind speed and density of the material, the plume may sink to ground level. For neutrally buoyant or buoyant releases, the jet centerline will remain above ground level, but as the jet's vertical dimension grows, the expanding (in diameter) cloud may contact the ground. In general, a critical wind speed (*i.e.*, the speed at which the overall maximum ground-level concentration occurs) for a jet release directed vertically cannot be specified on an *a priori* basis. To find the critical wind speed, one should perform all initial calculations for the lowest speed that will occur for a given stability category in Table 1 (say **F** stability and 2 m/s or **D** stability and 4 m/s). Next, increase the wind speed until the maximum ground-level concentration starts decreasing with increasing wind speed. For evaporating pools, the higher the wind speed the higher the rate of evaporation, if the necessary heat is available to the liquid. This effect alone would act to increase concentrations, but the high wind speeds also act to dilute the cloud and thereby decrease concentrations. The critical wind speed for this type of release would also have to be determined on a trial and error basis as described for the vertical jet release. This effect is demonstrated in Scenario 8, presented later.

As noted above, wind speed increases logarithmically with height above the surface. The EPA models often use the *wind speed power law* as

$$u_a = u_{meas}\left(\frac{z}{z_{meas}}\right)^p \tag{3}$$

where subscript *meas* denotes the measurement value and exponent *p* is empirically derived. Meteorological data from the National Weather Service is based on z_{meas} = 10 m unless otherwise noted. Typical values of the exponent are shown in *Table 2*.

The stability category classification scheme in Table 1 is based on 10 m measurements heights. Wind speeds at lower heights can be significantly less than at 10 m. For example, a 10 m wind of 3 m/s gives 1.2 m/s for 1 m height by Equation 4-3 using the urban class **E** exponent of 0.40.

Table 2.

TYPICAL VALUES FOR p IN EQUATION 3

Stability Class	Terrain Type Urban	Terrain Type Rural
A	0.15	0.07
B	0.15	0.07
C	0.20	0.10
D	0.25	0.15
E	0.40	0.35
F	0.60	0.55

Ambient Temperature, Pressure, and Relative Humidity

These parameters affect the plume/cloud by their influence on ambient air density and are generally of lesser importance than the other parameters described in this chapter.

The relative density of a plume (or cloud) relative to air (ρ′) is defined as

$$\rho' = \frac{\rho_p - \rho_a}{\rho_a}, \tag{4}$$

where subscripts *p* and *a* refer to the densities of the plume and the atmosphere, respectively. Therefore, if the plume or cloud's relative density is near or less than zero, the effect of these three parameters on the dispersion results will be much larger than if the relative density is large (*e.g.*, > 0.2). This factor must be considered during the following discussions.

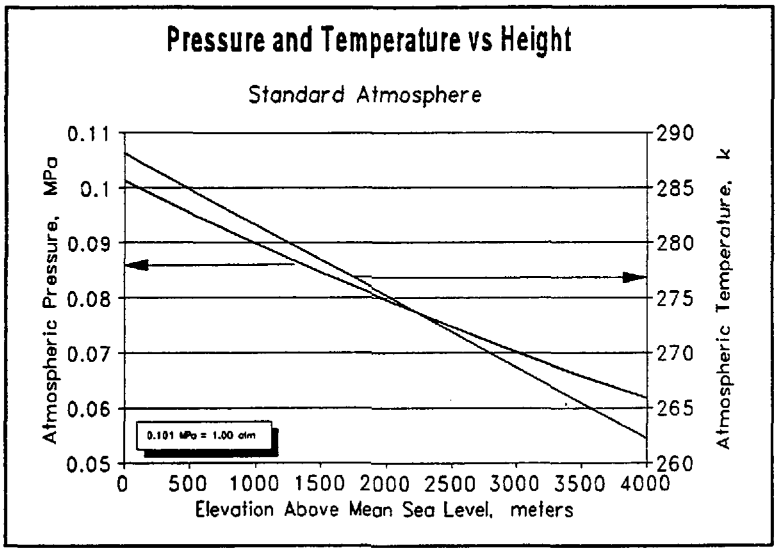

Figure 4.

The ideal gas law can be used to calculate relative densities for atmospheric temperatures and pressures to compare the relative importance of these parameters on plume/cloud buoyancies; this would be for constant relative humidity. For the *Standard Atmosphere* [7, 19], the variation of pressure and temperature with altitude are shown in *Figure 4*.

Figure 5 demonstrates the effect of relative humidity on relative density; these relationships were calculated by means of published water vapor pressure vs temperature functions [3-7] with the ideal gas law. Because this effect is relatively small, if the released fluid is inert, and if water condensation vaporization heat effects are low (no ice/liquid water/ water vapor phase changes), then using 50% relative humidity is recommended. Otherwise, the modeling scenarios should consider this effect.

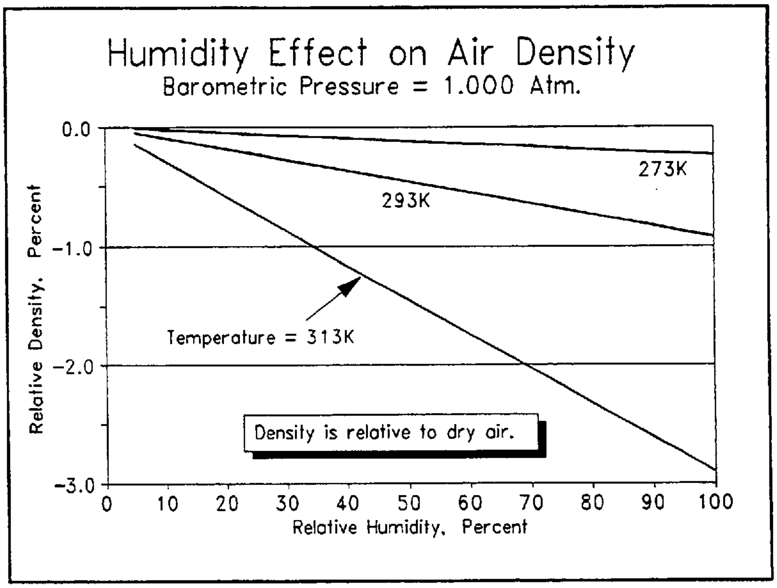

Figure 5.

Temperature and relative humidity values will vary from site to site in accordance with a region's climatology. Local climatological summaries provided by the National Weather Service may be consulted to estimate appropriate values for modeling. Alternatively, reasonable temperature and relative humidity values can be selected on the basis of local experience. For ambient pressures, the local elevation should be used in conjunction with Figure 3 to estimate the local pressure *at the temperature of the standard atmosphere at that elevation* [7,18]. Then use the ideal gas law to correct the pressure for the temperature used for modeling. These corrections are usually of minor importance unless extremes of temperature and/or ground altitude above sea level are involved. Note that some models do not allow the user to specify ambient pressure (i.e., 1.0 atm is fixed internally.)

Averaging Time

Averaging time (the time over which continuously-recorded concentrations are averaged) and *release duration* significantly affect concentrations of dispersed materials. Release duration will be discussed in the following section, but both parameters generally must be considered simultaneously by the modeler.

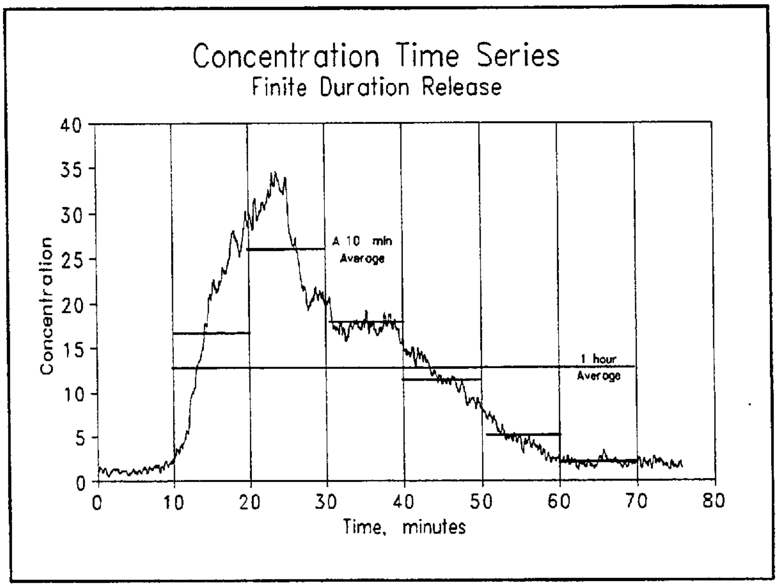

Figure 6.

Figure 6, for a cloud passing a receptor (recorded with a very fast response time sensor), shows the effect of 10- and 60- minute averaging times on a typical, continuously-recorded concentration curve. The 60-minute averaged values are much lower than the peak instantaneous value, and the maximum of the 10-minute concentration values is also less than the peak value. Note that only if this finite duration cloud passed the point and all other concentrations were zero, then an 8-hour averaged concentration would be about ⅛ that of the 60-minute value depicted.

If a material is emitted at a constant rate with an infinite duration (steady state), then the averaged concentrations would center about a mean value; the longer the averaging time, the closer will be the sampled mean concentration to the mean, based upon an infinite sampling time.

The averaging time basis for model concentration estimates depends upon the averaging time used for processing the original field data upon which the σ_y dispersion coefficients are based. The crosswind dispersion (the shorter the averaging time the less wind meander) is usually adjusted by means of the ***0.2 power law*** (Hanna *et al.* [2], Turner [13]) by:

$$C(t) = C(t_{avg})\left[\frac{t_{avg}}{t}\right]^{0.2} \tag{5}$$

where $C(t_{avg})$ is the concentration for some averaging time t_{avg}. For the standard Pasquill-Gifford dispersion coefficients, t_{avg} may be taken as 10 minutes. This equation is not appropriate for averaging times greater than about two hours (Turner [4]).

For model input purposes, a 10 s averaging time (or the shortest time allowed in a model) should be assumed for flammable vapor clouds. For toxic clouds, averaging times should be chosen according to criteria developed by health specialists. For examples in this manual, 1, 10 and 15 minute averaging time are often used for illustrative purposes only.

Release Duration

For a steady-state release (infinite travel time for constant conditions), only air entrainment around the circumference of the vapor cloud, normal to the downwind centerline path or axis, contributes to dilution of the released substance. However, if the release occurs for a finite time which is less than the travel time to given downwind receptors, then air will be entrained in the leading cloud surface, and into the trailing cloud surface after the release stops.

Therefore, if a release is short with respect to the travel time of interest, air entrainment into the front and back of the cloud will constitute a major portion of the dilution. On the other hand, as the release duration increases, this contribution will decrease so that, in the limit, the puff and steady state dispersed concentrations will be asymptotically matched.

Downwind concentrations from dispersion models, such as HEGADAS, SLAB, DEGADIS, and the Gaussian Plume, which assume *steady state* similarity relationships, can be adjusted for *constant release rates* of finite duration by multiplication with a *Finite Duration Factor* ("FDF"). This factor is a function of travel time and atmospheric parameters. Dispersion along the downwind axis is accounted for by σ_x, which is a function of downwind distance. This is used in a Gaussian form to obtain the FDF. McFarlane, *et al.* [4, Chapter 7, §7.4; Appendix 3, §6.3] discuss the algorithms used in HGSYSTEM, as well as their source and development. These authors state: "Literature data on σ_x as a function of the downwind distance are scarce and not very well established..." It is often desirable to use the FDF technique because the time and effort for a steady state dispersion simulation is always much less than for a time dependent simulation.

If a finite duration, constant rate release occurs for which the travel time is about twice the release duration, the concentrations at the downwind points must be corrected for downwind travel time averaging or a time dependent model should be used. Also, if the release is varying rapidly with time, and/or the release rate (and state of the stream) is an arbitrary function of time, a time dependent model must be used.

Plume Buoyancy Criteria

To choose the appropriate dispersion modeling method for a particular application, it may be necessary to decide if the source is generating a dense gas (negatively buoyant), neutrally buoyant, or lighter-than-air (positively buoyant) cloud. For continuous *low momentum*★ releases, the release Richardson number, Ri_*, can be used to characterize the potential cloud behavior [18]. This dimensionless number estimates the relative importance of plume buoyancy to the ambient mechanical turbulence,

$$Ri_* = \frac{plume\ buoyancy}{ambient\ mechanical\ turbulence} , \qquad (6)$$

which, for neutral buoyancy and dense gas clouds, can be calculated by

$$Ri_* = \frac{g(\pi/4)u_a D_p[(\rho_p - \rho_a)/\rho_a]}{u_*^2 u_a} . \qquad (7)$$

All the parameters are based on the just-released cloud conditions. For neutral atmospheric stability, the Equation 1 friction velocity, u_*, can be roughly approximated with

$$u_* = \beta\, u_a ; \quad \beta = 0.065 \qquad (8)$$

Panofsky and Dutton [5]. For estimation purposes, β for unstable and stable atmospheres can be roughly taken as 0.2 and 0.02, respectively.

Note that if the released fluid density (ρ_p) is greater than the atmospheric density (ρ_a), Ri_* will be positive; if it is greater than about 10, then the cloud will tend to sink towards the ground. If Ri_* is negative, the cloud *may* rise. If neither relation applies, the cloud may be treated as neutrally buoyant.

If it is thus estimated for a ground level source that the cloud or plume is dense, then a dense gas, ground level model should be used for dispersion calculations (*e.g.*, HEGADAS, SLAB, DEGADIS). If neutrally buoyant and the source area is small compared with the downwind dispersion distances of interest, then the Gaussian plume model can be used. If the source area is important, then the dense gas models can also be used. Also, if the mass flux from an area source is very low so that the rapid mixing with the atmosphere negates molecular weight effects (*e.g.*, a pool evaporating by convection), then either a ground level, dense gas model *or* the Gaussian model can be used

---

★ Momentum is the product of velocity times mass flow rate.

as needed. However, remember that the Gaussian model does not allow explicit external specification of the terrain roughness length parameter (but one can choose rural/urban).

The three modeling systems mentioned above cannot be used for lighter-than-air, *area* releases. However, the rigorous turbulent jet models correctly treat positively buoyant gases.

For releases with significant momentum, *i.e.*, turbulent jets, it is not possible to calculate *a single* Richardson number for dispersion model selection because of the intense air entrainment near the source and along the jet's path. The turbulent jet models use several criteria for determining when transition from jet regime to atmospheric advection should be made. For example, the HFPLUME and PLUME turbulent jet models in HGSYSTEM use three parameters to determine the transition point: excess velocity ratio, entrainment ratio, and relative buoyancy. For further information, see the HGSYSTEM User's Manual [II-6] and Hanna, Briggs, and Hosker [2].

CHAPTER 5

CHAPTER FIVE

Mitigation Countermeasure Modeling

Introduction

This chapter is concerned with modeling the effectiveness of countermeasures for reducing dispersed concentrations of toxic and/or flammable fluids from accidental releases. Countermeasures may be implemented by means of the plant design process, later addition of mitigation equipment and practices, and emergency response procedures.

Quick Reference

First, published studies addressed to the design and operation of methods for *after-the-fact* mitigation of vapor cloud concentrations are reviewed. Plume mitigation methods are for passive barriers, spray barriers, steam curtains and foams which involve dilution and/or removal of the released materials from the air. Secondly, methods are presented by which these mitigation techniques may be quantitatively incorporated into the dispersion modeling process by calculation of modified plume (vapor cloud) characterization parameters for the barrier location. The very important mitigation method of release duration minimization, as mentioned in the preceding chapter, is discussed further. *Scenario 7* of *Chapter 6* complements this discussion as an example of the methodology for modeling water spray barrier and release duration control mitigation of a ground level plume from a reactive hydrogen chloride release.

Many release mitigation methods, for both before- and after-the-fact are summarized by Prugh and Johnson [1]. The *Industry Cooperative HF Mitigation/Assessment Program* ("ICHMAP"), supported by 20 hydrofluoric acid producing and consuming companies, sponsored extensive research and development on HF vapor cloud dispersion and mitigation, as well as modeling. The work consisted of HF field releases, HF release - water spray tunnel studies, environmental wind tunnel studies (nonreactive flows), and source/dispersion mathematical model development; a great deal of the information developed can be extended to non-HF release situations. About twelve research reports were prepared [2] which are referenced below; these reports contain excellent literature reviews and full descriptions of all field and laboratory experimental work.

Scenario 7 in *Chapter 6* exemplifies the use of the release duration control and water spray barrier plume modification mitigation methodology discussed below.

Review of Plume Mitigation Methods

Passive Barriers

Physical obstructions to the flow of vapor clouds, such as process plant structures, specially designed vapor fences, and vapor boxes (rectangular, open-top boxes placed around a process unit), can alter the path and concentration of released material downwind of an obstacle. The ICHMAP work using environmental wind tunnels is summarized in one report [2]. Meroney *et al.* [3,4] developed some correlations for the near field dilution caused by various physical barrier types on the basis wind tunnel experiments. Petersen and Ratcliff, for ICHMAP [5,6], investigated several vapor fence and box barriers in grassland, moderately obstructed process unit, and heavily obstructed process unit environments. Barrier effectiveness results are presented graphically with the *concentration reduction factor (α)* as a function of downwind distances for a large experimental program in which the following parameters were varied: site configuration, barrier design, simulated-HF volumetric release rate, release duration, source gas specific gravity, wind speed, Richardson number, wind direction for asymmetric obstacles and environments, and barrier height. These references can be used to estimate values for *α*, required later for modeling passive barrier effects in the near field. The only apparently available correlation is that of Meroney [3] for vapor fences (presented later).

Active Barriers

Active barriers are defined for these purposes as plume mitigation devices or methods whose operational parameters can be controlled during plant operation (*e.g.*, on/off water mass flow rate). The released material may or may not react with or be absorbed by the sprayed fluid to be removed from the atmosphere. (Although the term "water spray curtain" is used below, the discussion is generally applicable to other aqueous liquids, *e.g.*, sodium bicarbonate solutions.) Because of space limitations, it is not possible to discuss all aspects of water curtain spray barrier design. Several aspects are mentioned, but a much more complete description of most design variables and their consequences are presented in the ICHMAP Summary Report [7].

Water Spray Curtains – No Removal. Meroney *et al.* [4,7] also mathematically modeled the dilution effects of nonreactive gas releases by water spray curtains; these were compared with published field and laboratory experiments. Water and other fluid "sprays" are turbulent jets which entrain relatively large amounts of air; they are essentially air "pumps." (Water spray devices were once used in coal mines as auxiliary ventilation.) Thus they can be useful for rapid dilution of inert materials (*e.g.*, LNG) to minimize cloud flammability near the release location. Atallah, Guzman and Shah [9] reviewed design and effectiveness of water spray barriers especially for dispersion of LNG vapor clouds. They concluded that spray barriers can be effective, but their effectiveness will decrease with increasing wind velocity and gas release rate. They developed guidelines for physical barrier design, recommending Moodie's correlation [10] for upward-pointing sprays, while McQuaid's correlation was recommended for downward-pointing sprays [11]. (These two correlations are given below.) Atallah *et al.* also strongly recommended that a portion of a designed spray curtain barrier be field-tested before proceeding with a large commercial installation.

Figure 1 is an example of dilution-only mitigation by a spray barrier which shows top hat concentration curves calculated by Meroney's SPRAY62 box model, using the parameters of the *Goldfish 1* hydrogen fluoride (HF) full-scale desert field test.

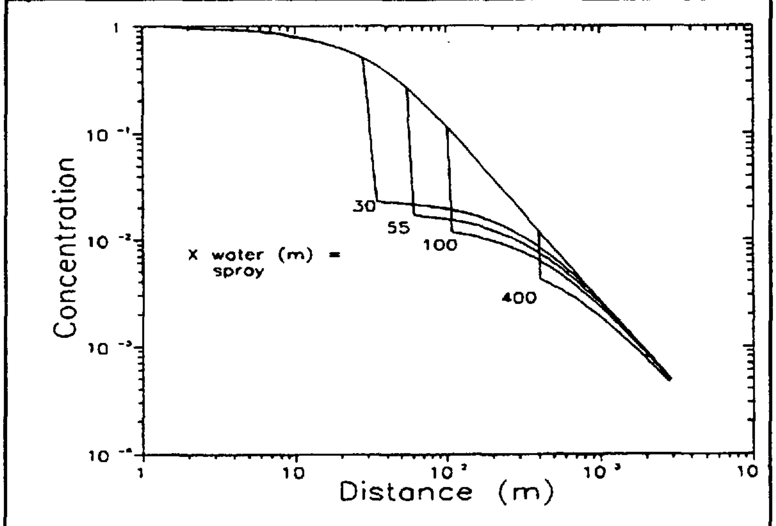

Figure 1. Spray Curtain Dilution by Entrainment (from Meroney [4])

In that test, HF was released as a horizontal jet 1.2 m above the ground with release rate = 28 kg/s for 125 s, wind speed = 5.6 m/s, and surface roughness = 0.0002 m. For this example, the HF removal function was turned off in the computer program so only additional air entrainment from the spray curtain was simulated. The spray curtains were located 30, 55, 100 and 400 m downwind from the release source as noted in the figure. *Note that both axes of the graph are logarithmic.* With passive barriers, the concentration curves return to the no-barrier values much closer to the source because the amount of additional air entrained is much smaller than for the sprays.

> *The reason for this remarkable effect is that as the downwind distance increases beyond the barrier, the amount of additional air caused to be entrained into the cloud by the barrier becomes insignificant with respect to the amount of air entrained by means of the atmospheric boundary layer processes.*

Blewitt, Petersen, Ratcliff and Heskestad [12] conducted extensive experimental studies in an environmental wind tunnel for the design of water spray curtains to mitigate simulated-HF (inert gas) releases from industrial facilities. Parameters varied for the spray curtain included: manifold geometry, nozzle type, nozzle orientation and nozzle spacing; also, HF release rate, release height, wind speed, wind direction with respect to the facility and release direction (along with the wind and into the wind). Two sensor grids downwind measured released gas concentrations. Visual effects of the sprays were recorded. Their principal conclusions were: 1) sprays from nozzles pointing directly inward (horizontally) were most effective, and 2) nozzle spacing had little effect on cloud behavior (within the ranges studied...Author).

Water Spray Curtains – With Removal. Extensive experimental studies were sponsored by ICHMAP to study the parameters affecting removal of HF from plumes by aqueous spray curtains [12, 13, 14, 15, 16]. These were conducted in a large, closed system for safety and material balance reasons, among others. When liquid HF (at ambient temperature) is released to the atmosphere, it flashes to form an aerosol. Very complex thermodynamics are involved, as well as rate limited processes such as evaporation and solution of the HF in the water drops, and the reverse. Considering these factors, the study investigated many parameters which influence the completeness of HF removal. Parameters studied included spray curtain configuration (see above) with upward and downward pointing nozzles, types of nozzles, one or two spray curtains in the plume path, wind speed, HF mass flow rate, liquid HF volumetric flow rate to spray water volumetric flow rate ratios, water spray droplet size distributions, and additives in the spray water. The principal result reported for each experiment was *scrubbing efficiency* (ε), defined as the ratio: [mass released HF removed]/[mass released]. *Figure 2* presents example results of the type which may be used for

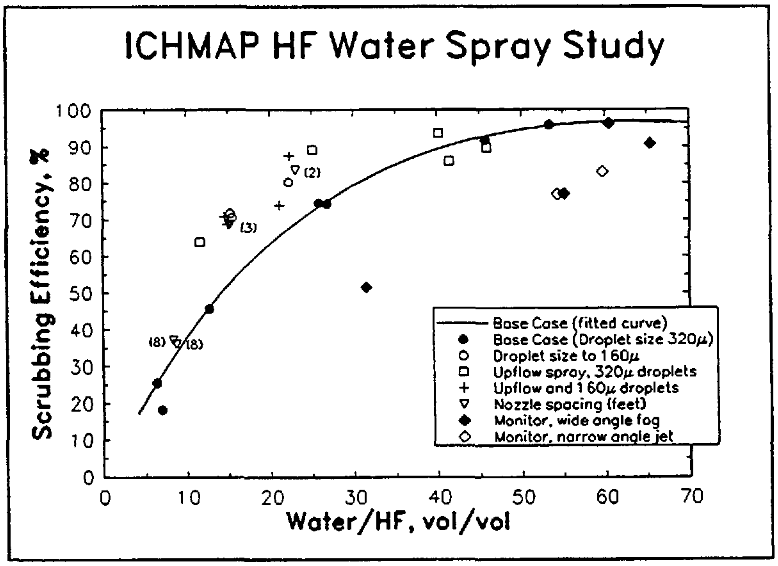

Figure 2.

design purposes; data in References 13 and 14 should be considered for actual spray curtain design.

For **removal only** barriers (which can exist only through mathematical modeling, for any plume interception device will induce some additional dilution), the dispersed concentration of released substance does *not* asymptotically approach the non-mitigated concentrations as the downwind distance beyond the barrier becomes large.★ *Figure 3* exemplifies how the concentration of a released material (very soluble in water) is *permanently reduced* when two spray curtains which have 80% scrubbing efficiency (ε), placed 100 and 300 m downwind, intercept a plume. For this graph, Meroney's modeling program had the barrier-enhanced air dilution inoperative. These types of results have been observed experimentally in wind tunnels and field tests [3]. Again, see *Scenario 7* for further examples.

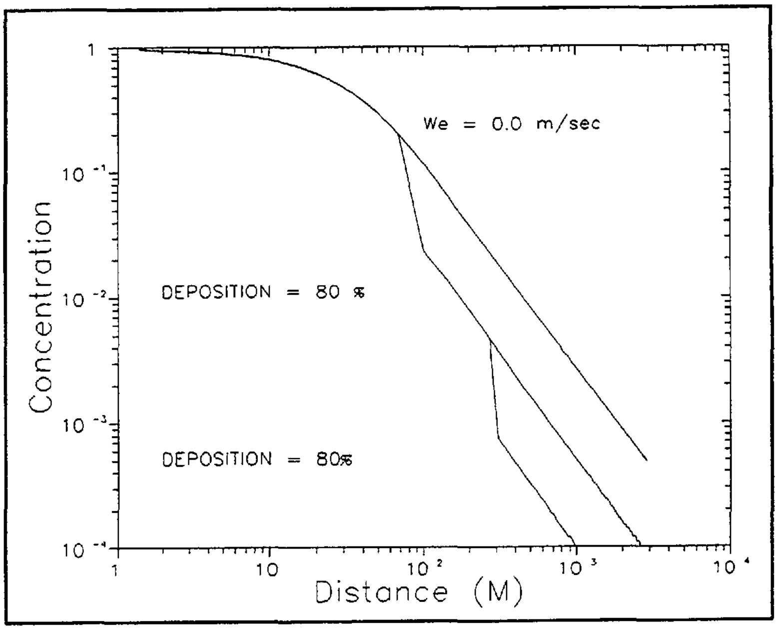

Figure 3. Spray Curtain Removal (from Meroney [4].)

Figure 4 illustrates the mitigation effect of ***both* spray barrier-enhanced air entrainment and removal** for the same Goldfish 1 basis. The upper curve is for no mitigation, the in-between curve is for an entrainment velocity of 6 m/s (no removal), and the lowest curve is for the same entrainment with removal. It follows that dilution-only barriers can be effective for reducing flammability of the vapor cloud in

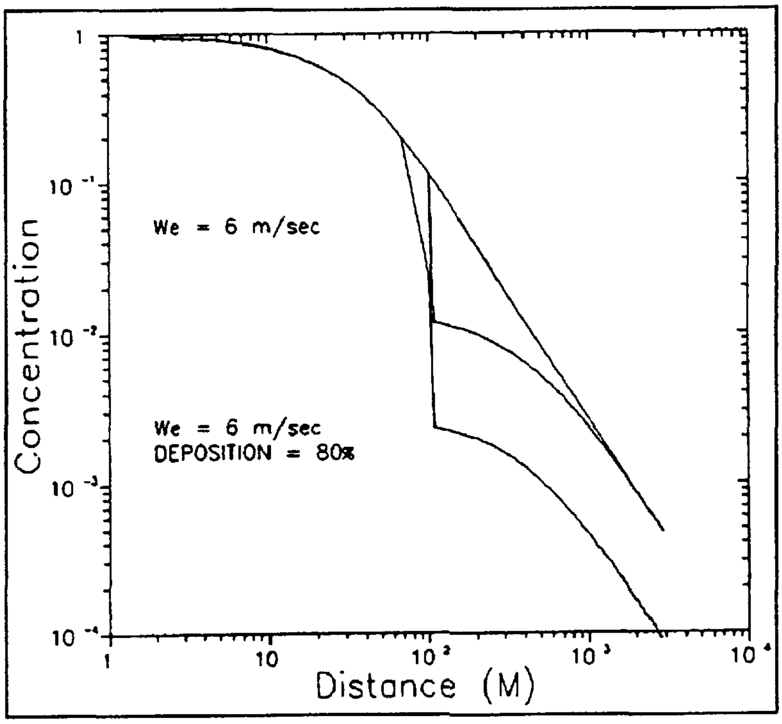

Figure 4. Spray Curtain Removal with Entrainment (from Meroney [4]).

★ Of course, the HF-water solution running off from under the spray curtain or monitor must be appropriately disposed of because it can be hazardous and/or corrosive. Also, if this solution is not neutralized nor removed from the surface, the HF will re-evaporate into the air.

the near field. They will not be very effective for reducing far-field concentrations of materials having toxic or undesirable effects.

> *Thus if a particular modeling application is only concerned with far field effects, only the removal of the released material (reduction in mass flow rate) by a curtain need be modeled. Also, at sufficiently far distances from the source, the manner in which the dispersed substance is released (e.g., jet vs evaporating pool) becomes immaterial, so the reduced mass flow rate calculated for a curtain can be "transferred" to the source location. In this case, the extra modeling effort required to restart the dispersion at a downwind curtain location is not required; use the simplest source modeling with appropriate emission rates.*

Fire Monitors. Blewitt, Petersen, Ratcliff and Heskestad [17] studied factors influencing the use of fire monitors (manually directed, large water flow rate, adjustable spray pattern "cannons") for mitigation of HF releases. The wind tunnel experiments, sponsored by ICHMAP, investigated essentially the same types of variables as for those authors investigated for spray curtains. Again, an inert HF simulant was used, so dilution rates, but not actual removal rates, were obtained. (However, the *Hawk* field tests which used actual HF, and showed that monitors could be effective for removal, is referenced). It was concluded from the wind tunnel study that monitors can be effective for release mitigation, if properly operated. Also, the ICHMAP water spray curtain tests referenced above included experiments for fire monitor HF removal. These various reports should be consulted to obtain design data.

Spray Removal of Non-Volatile Aerosols. No experimental data appears to exist for removal of non-volatile liquids (inert or reactive) from unconfined plumes. Capture of non-volatile particles by water or other liquids is collision dependent, and thus dependent on the gas-particle relative velocities, plus parameters such as particle size distributions, spray nozzle operation, direction of sprays vs gas flow, and overall spray liquid to gas volumetric flow rates. Industrial scrubbing towers generally use downward pointing sprays with the gas stream flowing upward to be cleaned. Perry's Chemical Engineer's Handbook [18] addresses many of the design considerations for spray chambers or towers, for vertical flows as well as for horizontal cross flow spray chambers. Design literature can often be obtained from vendors of closed system gas scrubbers.

Steam Curtains. Steam curtains operate similarly to water curtains, except that high jet velocity is traded for high mass flow in water curtains to obtain the momentum rates required for dilution. Steam curtains are usually designed to point upward so the hot vapor will heat dense clouds to enhance their buoyancy which, coupled with the high upward momentum of the steam, cause rapid dilution and the cloud to rise. As reported by Prugh and Johnson, steam supply requirements are considerable, requiring about 0.2 kg steam per kg of contaminant to reduce concentrations below the lower flammable limit. They also report that about 80 times the energy per unit length of barrier is required for steam curtains than for equivalent water curtains. Steam jets can generate static electricity ignition sources.

Hartwig [19,20] gives concentration reduction factors obtained in large-scale field releases mitigated with steam curtains. Experiments were made in calm and in windy conditions. Those authors caution that the results presented are applicable only to the particular operating conditions used. A correlation for design purposes is not presented. One important point made was that with wind present, steam plumes carrying contaminant can loop over to cause the lower part of the plume to be re-entrained into the initial part of the steam curtain, which markedly reduces its effectiveness. Steam curtains may be of particular advantage for situations where the released material reacts very quickly with steam to form less toxic materials, e.g. phosgene. No correlations were found by this author for estimation of dilution and removal parameters; this might be because of the application-specific nature of steam curtains.

Foams. Foams can be used to cover spills of evaporating liquids to reduce the evaporation, thus mitigating downwind air concentrations of the spilled material. The spilled materials can be cryogenic fluids which form boiling pools or non-boiling materials. For dispersion modeling, the mass transfer rate of the spilled material which makes its way through the foam to the atmosphere ("evaporation" rate) can be used directly for area source dispersion models. The effectiveness of foam-producing chemicals (usually made with water as a basis) depends upon many factors, among which are the chemical composition (mixtures, pure components), [water]/[foaming material] ratio, temperatures, chemical composition, and method of application. In general, a foaming material must be specifically selected (or designed) not to react with the spilled liquid to prevent degradation or prevention of the foaming material's performance.

Prugh and Johnson list a number of commodity and proprietary materials which can be used to cover specific substrates. Hartwig and Böke [21] also list a number of covering materials available in Europe. Hartwig also presents quantitative results for a number of small- and large-scale experiments performed to measure the effectiveness of various foams covering a number of evaporating liquids. Hiltz [22] also contains a number of references. Prime sources of application and effectiveness information are the manufacturers of the particular foam-producing and covering materials; Prugh and Johnson list a number of such suppliers.

Release Duration Control

Perhaps the best way to mitigate the effects of an accidental release is to stop it as soon as possible; the shorter the "on" time, the better. However, some time usually elapses before a release is detected, with more time being required to start shutdown and/or "quick dump" procedures for downwind devices such as spray curtains. As discussed in Chapter 4, two phenomena operate to decrease the time vs concentration effects of the released substance on downwind receptors: if the release duration is shorter the cloud is shorter, and thus the immersion time of receptors in the vapor cloud is smaller, which means the *average* concentration or *dose* (integral of concentration over time) is lower. In addition, the *peak* concentration will be lower due to increased air entrainment with respect to the downwind travel plume axis.

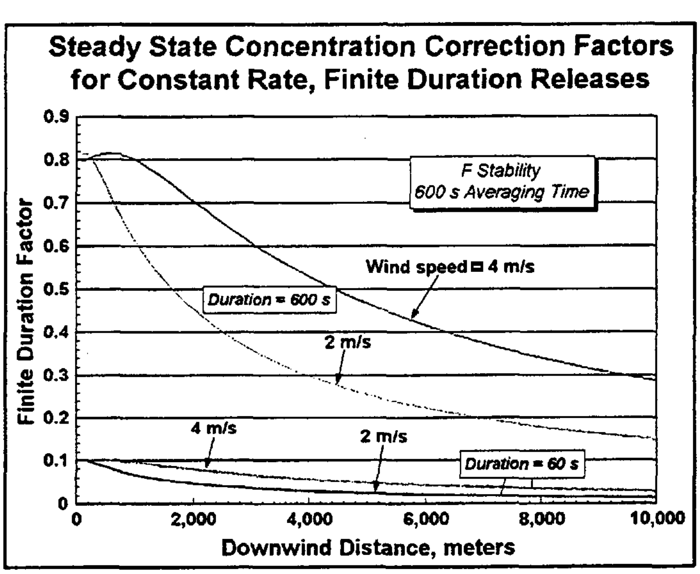

Figure 5.

Again, as mentioned in *Chapter 4*, "first-cut" dispersion modeling results can be obtained fairly quickly for screening purposes by using the finite duration factors to adjust steady state dispersion modeling concentrations for finite duration, constant mass flow rate releases. If the modeling program does not contain this algorithm internally (SLAB does [II-7]), the FDF correction can be applied to the steady concentration vs downwind distance results from a post processor program. *Figure 5* shows the FDF curves for F stability, 600 s concentration averaging time for two release durations and two wind speeds. Although the other variables have some effect on the magnitude of the FDF values, release duration is most important—and effective—as a control.

For example, the release rate and state from a pressurized vessel can be taken at the values for the initial flow to the atmosphere. Assume this rate release is constant for τ_{flow} seconds. Say the wind (= plume) velocity is u m/s; then the downwind distance to which steady state concentrations can be used is approximately the product of these two values. Beyond that distance, concentrations rapidly decrease below the steady state values because of longitudinal dispersion; these may be calculated by multiplying the steady state concentration at a given downwind location by the *finite duration factors*. The resultant concentration functions of downwind observer locations (*x, y, and z*) form envelopes containing the maximum concentrations which existed. Families of curves or surfaces can thus be developed to compare the relative effectiveness of various source reduction times (durations) with each other and the steady state results. If the leading edge of the vapor cloud arrives at the spray curtain position before the latter is turned on, then the source reduction is a two step process which is best simulated in a general manner by a time dependent dispersion model. Depending upon the relative timing of the two actions (source turn-off and spray activation), it may be possible to apply the steady state with a finite duration adjustment solution method to obtain rapid mitigation effectiveness estimates.

Estimation of Plume Modification Parameters

Scope

The following discussions assume that a vapor cloud is formed at ground level and flows with a finite wind along a definable path. Although the cloud variables such as temperature, concentration and average velocities will be distributed through the area of planar cross-sections normal to the downwind flow axis, it is assumed that the variables' values (*e.g.*, concentrations, temperature, and mass fluxes) are homogeneous. That is, the top hat assumption is valid. With this, parameters such as plume cross-sectional area, total and componential mass flow rates, temperature, etc. are scalars or can be converted to single values.

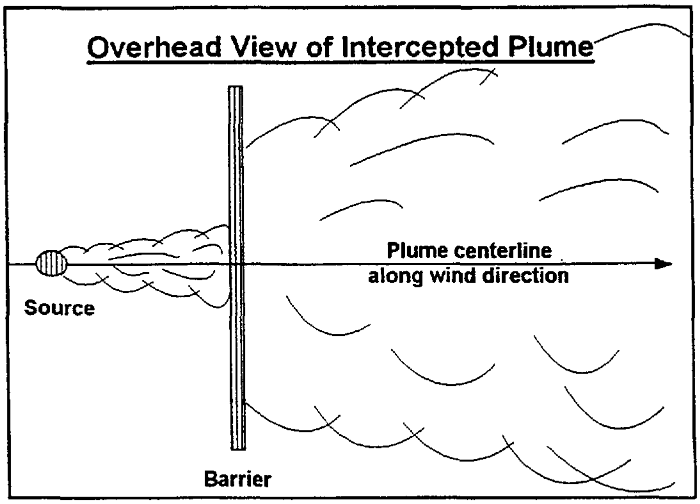

Figure 6.

Figure 6 is a conceptual view looking downward from over the traveling cloud. It is assumed that the barrier (passive or active) is large enough to completely intercept the plume in both the vertical and crosswind directions. Also, it is assumed that the thickness of the barrier is negligible with respect to downwind distances of interest. Therefore, given a set of parameters which characterize the concentrations, mass flows, and energies for the cloud cross section entering the barrier, these quantities can be redefined on the basis of given barrier-caused air entrainment rates plus the released substances' removal rates. This redefinition of the plume can be manually implemented as demonstrated in the *Chapter 7, Scenario 6* example, or, better, automated within a dispersion modeling program. *Appendix II* provides an overview of similarity-type dispersion modeling programs. The design of mitigation barriers is beyond the scope of this manual.

Air Entrainment Dilution Devices

General Relationships. Water spray and steam curtains as well as passive barriers dilute the vapor cloud by causing *entrainment* of air into the plume; this is in *addition* to that air caused to be entrained by atmospheric processes. The barrier-enhanced air entrainment velocity (u_e), is often needed for the equation

$$U_e = u_e \cdot A_s , \tag{1}$$

where U_e is the volumetric flow rate of the additionally entrained air from the barrier device, u_e is the entrainment velocity, and A_s is the projected interaction area of the spray with the plume. The concentration reduction factor (α) is usually available from the literature or from correlations,

$$\alpha = \frac{U_s}{U_{ns}} , \tag*{(2)$\Diamond$}$$

where U is a plume volumetric flow rate, subscript ns is for the plume entering the barrier (no spray), and s denotes the plume leaving the barrier (spray). The corresponding plume diameters for symmetrical deformation are

$$\frac{D_s}{D_{ns}} = \sqrt{\alpha} . \tag{3}$$

Within a dispersion program, the above entrainment velocity can be added to that for entrainment caused by normal atmospheric processes at the downwind distance corresponding to a specified downwind mitigation barrier location. Also, where the mass flow rate of released substance remains constant through the barrier and no energy is exchanged, material balance on the released component gives

$$U_s = U_{ns} + U_e , \tag{4}$$

or, by combining Equations 2 and 4,

$$U_e = U_{ns}(\alpha - 1) . \tag*{(5)$\Diamond$}$$

Meroney [3,4,7] defines the area for total air entrainment into the cloud passing through the spray barrier as

$$A_s = \frac{m \, \pi D_{si}^2}{4} , \tag{6}$$

in which

m = number of spray nozzles over the vapor cloud, and
D_{si} = spray impact circle diameter.

This diameter should be obtained from the spray manufacturer's design literature, for it will generally not be the projection of the spray cone onto the ground. If the nozzles are sufficiently high, the droplets will quickly attain terminal velocities. The interaction area implicitly defined in Equation 6 can be used for sprays pointing in directions other than downward. However, the basis upon which the concentration reduction factor has been measured or defined should be considered. For passive barriers, the cross-sectional area of the plume "impinging" upon the barrier can be used for A_s. Therefore, combining Equation 1 and 5 gives

$$u_e = \frac{U_{ns}(\alpha - 1)}{A_s} . \tag{7}$$

If the plume temperature is T_{ns} on entering the curtain, then Equation 7 can be found by

$$u_e = \frac{T_a}{T_{ns}} \cdot \frac{U_{ns}(\alpha - 1)}{A_s} , \tag{8}$$

where T_a is the atmospheric temperature and the value of U_{ns} can be obtained from dispersion model intermediate results. This equation assumes no phase changes (no aerosol) which affect energy balances significantly, nor humidity effects; it assumes that the before-dilution amount of air required is based on a given value of α for the new cloud mixture which attains ambient temperature on mixing. This is probably a good first approximation, because sprays are most likely to be close to ambient temperature and mixing is intense, and therefore fast heat exchange occurs. To be more exact, simultaneous heat and mass balances equations would have to be set up and solved to account for the initial vapor temperature, the entrained air, humidity changes, aerosol vaporization, etc. Rearranging Equation 8 yields

$$\alpha = \frac{u_e A_s}{U_{ns}} + 1 = \frac{U_e}{U_{ns}} + 1 . \tag{9}$$

If the temperature correction is used, multiply u_e by T_{ns}/T_a in Equation 9.

Water Sprays – Downward Pointing Nozzles. McQuaid's correlation [11] may be used for estimating dilution effects of spray curtains with downward pointing nozzles. For several *field* experiments, it was found that downward pointing sprays diluted dense gas concentrations to the levels predicted theoretically by the correlation, whereas upward pointing sprays were less effective in certain situations. A drawback of downward sprays is that the top spray header should always be higher than any potential plume to be mitigated. McQuaid's dimensionless group correlation parameter is defined as

$$\Phi = \frac{\rho_w^{1/2} F_N}{D_{si}^2} , \tag{10}$$✧

where

U_w = Total volumetric flow rate of water to sprays, m^3/s
ρ_w = Water density, kg/m^3
F_N = $U_w/P_w^{1/2}$, the nozzle flow number, $[m^3/s]/[(Pa)^{1/2}]$
P_w = Water pressure to nozzles, Pa
D_{si} = Diameter of spray impact area on the ground, m.

McQuaid's graphical correlation between the ratio U_e/U_w and Φ was fitted by the author, with an accuracy equal to the width of the plotted curve over the whole range shown, to:

$$ln\left(\frac{U_e}{U_w}\right) = a + b \cdot ln(\Phi) + c \cdot [ln(\Phi)]^2 , \tag{11}$$

for which a = 1.118309, b = - 0.7620935, and c = -0.0090127.

Water Sprays – Upward Pointing Nozzles. Upward flowing sprays must be able to project droplets of diameter greater than 500 µm higher than the height of any potential plume, but they do have an advantage in that overhead pipe header structures are not needed. In field tests with LNG, vertical upward sprays lifted the vapor plume sufficiently that downwind concentrations were less than 2%, the approximate lower flammability limit. As mentioned above, Atallah *et al.* recommended the correlation of Moodie [10] who defined

$$M = KF_N P_w / L \quad , \qquad (12)\diamond$$

for which

M = momentum flow rate per unit length of curtain, N/m
K = a nozzle-specific, empirically derived constant, $Ns/[m^3 \cdot Pa^{1/2}]$, (44.5 for an ideal nozzle 37.9 is a median value based on experiments)
F_N = $U_w/P_w^{1/2}$, the nozzle flow number, $[m^3/s]/[(Pa)^{1/2}]$
P_w = water pressure to nozzles, Pa, and
L = curtain length, m.

The momentum flow was correlated by Moodie with the concentration reduction factor (Equation 2) with

$$M = u_{1.25}^2 [0.65 e^{0.5\alpha} - 0.23]^2 \tag{13}$$

in which $u_{1.25}$ is the wind speed at 1.25 m elevation. From figures in Moodie's paper, it appears that the concentration ratio α (Moodie used the symbol CR) predicts $M^{1/2}/u_{1.25}$ to an accuracy of about a factor of 2 for *upward-pointing sprays*, but α is essentially uncorrelated for downward pointing sprays. Equation 15 may be rearranged to

$$\alpha = 2 \ln \left(1.539 \left[\frac{M^{1/2}}{u_{1.25}} + 0.23 \right] \right) . \tag{14}$$

This correlation can give α values ranging from 1/4 to 1/10 times those calculated by McQuaid's upward-pointing spray correlation.

Water Sprays – Other Orientations. Correlations for estimating air entrainment for water sprays which do not point directly up or down; *i.e.*, horizontally, apparently have not been published. Correlations for these orientations could be developed from the fairly large amount of data available in the literature.

Removal of Released Material

General. Experimentally, the removal effectiveness of a barrier is usually found by assuming that all the released material in the vapor cloud impacts the barrier, or the dispersed material concentrations are measured just before the device. Just after the device, arrays of sensors measure the concentration distributions. Numerical integration of the concentrations over the space grid gives average concentrations and defines the plume shape. The total mass flow rate of emitted material leaving the barrier can be calculated using the wind speed and other observed parameters. Thus, the *overall* effectiveness of the barrier may be characterized by the ratio of the released material mass flow rate entering the barrier (w_{ns}) to its mass flow rate leaving (w_s). Let

$$\kappa = \frac{w_{ns}}{w_s} . \tag{15}$$

The symbol κ is sometimes called the *concentration reduction ratio*, with its reciprocal, f_s, being the *fraction remaining* in the plume from a removal *process*. Sometimes the *scrubbing efficiency* ε is reported; this is the ratio of dispersed material remaining with respect to the material *entering* the barrier:

$$\varepsilon = 1 - 1/\kappa . \tag{16}$$

Scrubbing Efficiency of Spray Curtains and Firewater Monitors. Referring back, Figure 2 shows example HF scrubbing efficiencies from the ICHMAP-sponsored spray tunnel experiments drawn from Reference 13, Table 3.7-1. The fitted curve corresponds to their "base case" for which the experimental conditions and fitted equation parameters are from this reference. This report should be consulted for a particular application, because many more experimental conditions were used than for just the points shown in Figure 2. Note that the scrubbing efficiencies were reported on an overall inlet-outlet material balance basis; they *do not* include dilution effects caused by air entrainment induced by the water/solution sprays. For modeling use, κ can be found from the scrubbing efficiency and utilized with other information (see later) to modify the plume being modeled.

This scrubbing efficiency data for HF can be used for *other* released materials that are highly soluble in, or react with, water or other sprayed liquid (such as sodium bicarbonate solutions), if it can be assumed that the removal rate is mass transfer limited. Also, the partial pressure of the diffusing material as it is being absorbed into the droplets of spray water solution should be approximately no greater than that of HF.

> Consider the mass transfer rate defined by: MTR = $k_g A(\Delta c)$, where k_g is the mass transfer coefficient (mass per unit area), A is the droplet area available for mass transfer, and Δc is the difference in concentrations of the material being absorbed. The mass transfer rate, $k_g A$, is governed by the relative spray droplet-gas phase velocities and the Sauter mean droplet size for a particular spray curtain operation. This should be true for spray upflow, downflow, or other configurations. The remaining "driving force" term in the above rate expression depends upon the bulk gas and droplet concentrations less the interfacial partial pressure. Thus, as long as the driving force is equivalent for two substances (HF vs *other*), the mass transfer rates will be the same. For all cases involving fast chemical reactions which essentially go to completion, the interfacial partial pressure will be negligible. If ionic solution equilibrium is involved, such as acid-base neutralization or very high solubility, the reactions are generally very fast and the partial pressure can be made negligible if the neutralizing chemical in the spray solution is properly selected. Therefore, for all cases in which the partial pressure of the absorbed substance is, or can be made to be, essentially zero, efficiencies as illustrated in Figure 2 will be limiting.

Spray Barrier Removal Modeling Programs. Fthenakis developed the HFSPRAY modeling program [24, 25, 26] under ICHMAP auspices. The mathematical model simulates the mass, momentum, and energy interactions between multiple water sprays and an unconfined plume of HF in air; it predicts the flow fields of velocity, temperature, water vapor, and HF concentration in two-dimensional large geometries, for sprays in any direction. Modeling results compare favorably with HF spray tunnel experiments [23,26]. The program requires extensive computational resources, but has the best capability for detailed design of spray curtains and the estimation of the removal and dilution parameters where experimental data is not available or needs to be extrapolated. However, estimation of crosswind dependent effects depends upon external information. Fthenakis and Blewitt [23] used the HFSPRAY modeling program, along with data from ICHMAP-supported studies to investigate further the physical design of spray curtains. They concluded that, for a field HF process unit, a two-tier arrangement of horizontally-pointing nozzles is best, with effectivenesses (percent HF removed) ranging from 70% for high wind speeds (*e.g.*, 17 m/s) to 96% for average wind speeds (*e.g.*, 5 m/s). If the horizontal plume speed is too high, as caused by the wind or jet velocity, the plume can "punch through" the spray curtain to cause very poor removal effectiveness.

Jones [25] developed two simplified models for HF removal from plumes corresponding to upward and downward pointing water spray systems. The models are based on momentum balances, rates of mass transfer between water droplets and the HF stream, and phase equilibria of the mixture: HF, water, air. Water spray droplet size is a model parameter. The two dimensions are: *vertical* for the axis of the spray cone, and *horizontal* for the radius of the cone. Although the thermodynamic/ physical properties are specific to HF, the Fortran source code could be modified to handle other substances. Water spray-induced air entrainment appears to be ignored. The programs run fast enough for PC type computers. The models provide reasonable results when compared to the experimental results from the ICHMAP wind tunnel tests.

CHAPTER 6

CHAPTER SIX

Analysis and Simulation of Release Scenarios

Introduction

Scenario presentations are generally organized as follows:

1) The *Statement* section presents the scenario accompanying quantitative information needed to carry out the desired simulations. The *release attributes* sidebar shows the main features of the modeling problem.
2) The *Analysis* section discusses physical property and fluid mechanic (flow) parameters for characterization of the released fluid, selection of atmospheric and boundary layer parameters as well as the applicability of the modeling programs to the solution of the problem. Selection of specific modeling programs may be discussed if germane to parameter selection. A *RECAP* box summarizes the model input parameters used.
3) The *Simulation* section may discuss further specifics of the modeling program selection, followed by discussions of results obtained.
4) A *Discussion* part may be included, if deemed appropriate, for more general conclusions.

Because of the extensive calculations and the number of computer files generated in the course of any one "study" or scenario simulation, it is not possible to include them in this Manual. However, the important modeling parameters and other data germane to the problem are presented by means of appropriate tables and graphs. *If not mentioned, the appropriate default parameters discussed in Appendix I will have been used.*

The scenario discussions follow the classifications shown in ***Figures 2-1, 2-2 and 2-3.*** Pages, tables and figures are numbered according to *Sn-I*, where *n* is the scenario number and *I* is the local sequence number. For example, page *S8-3* denotes the third page for Scenario 8.

In some cases, isopleth shapes appear to be irregular. This is primarily due to the geometrically increasing downwind distance step size which cause large steps at longer distances. The plotting program used connects the points with straight lines, or by spline functions. Spline functions don't always work because strange looking oscillatory envelopes are generated, in which case straight line segments have been used. Considering the accuracies of the overall estimates, it was concluded that further smoothing was not justified.

Unless otherwise noted, 10 m measurement heights apply to the wind speeds quoted.

In the course of final editing in May 1996, the thermodynamically consistent assumptions and equations for initial expanded jet diameters presented in *Chapter 3* replaced a less accurate formulation used for the simulations in *Scenarios 3* and *6*. Thus, the present method will give somewhat different diameters than those presented in the tables. However, dispersion results, if calculated by the new expanded jet diameter formulation, should not produce significantly different values than those listed for the old formulation. This only applies to SLAB and DEGADIS examples; HGSYSTEM's PLUME internally calculated the expanded diameter.

Scenario 1: Hydrogen Sulfide from Unlit Flare Stack

Statement

This scenario demonstrates the dispersion effects of two important variable classes on the behavior of vertically-pointing turbulent jets (plumes):

Release Attributes

Material: . . . . *Sour Gas*
Method: . . . . *Stack*
Fluid state: . . . . *Vapor*
Chemical reactions? . . . . *No*
Release time type: . . . *Steady state*
Turbulent jet: . . . . *Vertical*
"Cloud" height: . . . *Initially elevated*
Roughness type: . . . . *"Mixed"*
Stability: . . . . *A,D,F*
Averaging time: . . . . *60 s*
Hazard: . . . . *Toxic*

- The *momentum*, which is the product of the initial fluid mass flow rate and its density,
- The *atmospheric conditions*, which govern the wind speed and air density.

For a hazard analysis, maximum ground level concentrations of H_2S are to be estimated for a range of potential pressure relief valve discharges of sour process gas from a 26.8 m-tall flare stack. Flared gas has greatly increased plume buoyancy as well as air dilution rates compared with the non-burned gas. Of concern is the possibility that the released gas is not ignited or that the flame goes out, thus causing potentially hazardous concentrations of H_2S at ground level.

The design maximum flow rate for the stack is 16 kg/s, the minimum flow rate is 1.6 kg/s, the flow regime is non-choked, and the stack exit temperature is 300 K. The exit diameter of the stack is 0.20 m. The chemical composition of the stack gas, which contains methane, ethane propane and hydrogen sulfide is given.

The process unit is in a small oil refinery surrounded by suburban and rural areas with trees.

Analysis

Stack Gas Physical Property Parameter Estimation

Modeling programs require single, or bulk, values for the stack *gas* specific heat at constant pressure (C_p) and its molecular weight (M). Given the nominal effluent gas composition as shown in *Table S1-1*, the molecular weight for the bulk gas is the sum of the individual component mole fractions times the corresponding molecular weight. The component specific heats were found from information in Chapter 3 of Perry's Sixth. Those heats for methane and ethane are finite difference approximations to the temperature derivatives of enthalpies at 300 and 350 K. This approach gave spurious values for propane, because 350 K is just under the critical temperature of 369.8 K, as found by plotting the enthalpies from 280 to 360 K. The more consistent C_p = 1.14 value shown in the box for propane is the finite difference derivative from enthalpies 300 and 310 K. The heat capacity for H_2S was calculated for 300 K by means of the equation in Table 3-181 of Perry's Sixth. With these componential values, the heat capacity for the bulk gas is the sum of the products of the weight fractions times the C_p values of the individual components. See page 3-15 for more aspects of calculating pseudo-pure componental properties.

Table S1-1.

STACK GAS COMPOSITION

Compound	Mole %	Weight %	Mol. Weight	C_p KJ/ kg•K
Methane	14.6	6.1	16.04	2.30
Ethane	10.6	8.4	30.07	1.86
Propane	71.6	82.8	44.09	0.99
H2S	3.2	2.7	32.02	1.08
Bulk values			**38.1**	**1.14**

Because the modeling programs do not "know" that the released "pure" gas is really for a multi-component system, modeled bulk gas concentration results (mole fraction = volume fraction) must be multiplied by 0.032 to obtain the H_2S concentrations.

Other Parameters

For ambient and gas temperatures of 300 K, the unlit stack gas-to-air density ratio is 1.38 (ideal gas equation: gas density = 1.61 kg/m^3), which indicates the emitted gas is denser-than-air. Depending upon the jet's momentum and the wind velocity, the plume can sink to the ground or remain elevated. Thus a vertically-pointing turbulent jet model should be used for the near-field. (Briggs' Plume Rise "EPA" model is inappropriate because it does not allow sinking.) For dispersion beyond the distances where the plume contacts the ground or remains elevated with essentially neutral buoyancy, ground-level dense gas or Gaussian-type dispersion modeling should follow the jet modeling, respectively.

The jet dispersion process is very nonlinear with respect to release rate. For large release rates, the initial momentum is high but turbulent jet air dilution is also very large. Low rates have low momentum but the jet dilution is also lower. Thus, the modeling should be done for the minimum and maximum design release rates of 16 and 1.6 kg/s, respectively, *as a start*. Since the flow is non-choked, initial jet expansion may be neglected, so the initial jet diameter is equal to physical stack diameter.

To exemplify atmospheric stability class effects on the plume behavior, classes **A**, **D**, and **F** (see Chapter 4 as well as the Appendix I recommended defaults) were selected with appropriate combinations of wind speeds and atmospheric temperature; see *RECAP* box. The temperatures are appropriate to the class, but more representative values should be obtained from local meteorological knowledge for a real application. The wind speeds for neutral stability of 4 and 8 m/s were selected to demonstrate the effect of doubling this parameter.

MODELING PARAMETER RECAP

Stack Gas	
Molecular weight	38.1
Specific heat, C_p, KJ/[kg.K]	1.14
Release rates, kg/s	1.6 to 16
Temperature, K	300
Stack diameter, m	0.20
Stack height, m	26.8
Roughness length, z_r, m	0.1
Atmospheric variables	
Stability **A**	
temperature, K	310
wind speed, m/s	3
Stability **D**	
temperature, K	300
wind speed, m/s	4, 8
Stability **F**	
temperature, K	273
wind speed, m/s	2
Relative humidity, %	50

Close to the jet source, surface roughness does not affect dispersion. However, as the transition is made into atmosphere-controlled dispersion, the roughness parameter, z_r, becomes important. For this example, assume the average roughness length is 0.1 m.

Simulation

The SLAB model was primarily used to demonstrate the effects of the variables of interest. Use of the other two models is discussed later. Note that the near-field and far-field situations, and the smooth transition between, are all automatically handled within the single SLAB program.

SLAB

Table S1-2 summarizes the main features for selected modeling results. Note that the H_2S concentrations shown were obtained by multiplying the released gas concentrations calculated by

Table S1-2.

SUMMARY OF *SLAB* RESULTS FOR SCENARIO 1
H2S in Gas from 26.8 m Flare Stack

1	2	3	4	5	6	7	8	9	10
			Ground Level		For Plume Centerline				
Case	Stab. Class	Wind Speed m/s	Amb-ient Temp. K	Release Rate kg/s	Max. H2S Conc'n ppm	DWD* for Max. H2S m	Maximum Height m	DWD for Max. Ht. m	Touch down at DWD = m
SLAB:									
1	A	3	310	16.0	3.5	456	75	109	572
2	D	4	300	16.0	3.1	1730	70	150	2490
3	D	4	300	1.6	1.5	701	31	15	1190
4	D	8	300	16.0	1.5	1610	52	130	2680
5	F	2	273	16.0	11.7	5140	99	818	5140
6	F	2	273	0.8	10.9	1000	31	17	1210
7	F	2	273	1.6	17.7	1060	34	34	1100
8	**F**	**2**	**273**	**3.2**	**105.6**	**5220**	**42**	**67**	**464**
9	F	2	273	6.4	17.5	2380	58	133	2300
DEGADIS:									
8	F	2	273	3.2	4.4	1796	41	136	2743
HGSYSTEM (PLUME ==> PGPLUME):									
8**	F	2	273	3.2	0.4	2200	32	48	500

* "DWD" = Downwind distance

** Wind speed measurement height = 1 m, all others: 10 m.

the model by 0.032, the mole (or volume) fraction of H_2S in the dispersed gas. *Figure S1-1* presents the calculated plume centerline trajectories ("paths") and some corresponding plume centerline, ground level concentrations are plotted in *Figure S1-2*. The concentrations become greater than zero at various distances downwind from the source in accordance with the path of the plume centerline and the vertical dispersion about it.

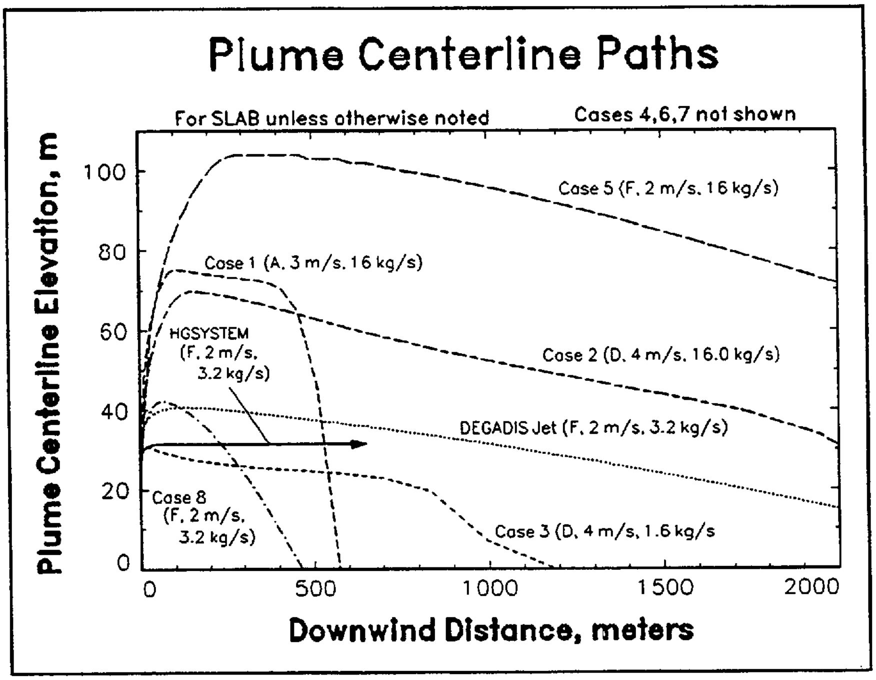

Figure S1-1.

The case for **A** stability (high vertical mixing) shows that the plume centerline "touches down" to the ground (Column 10) at a downwind distance fairly close to the source, but the maximum H_2S ground level concentration is less than 10 ppm. This near ground impact can be explained by the lower relative wind speed of Case 1 with respect to Case 2 (3 vs 4 m/s) and the higher relative density of the plume (air temperature 310 vs 300 K).

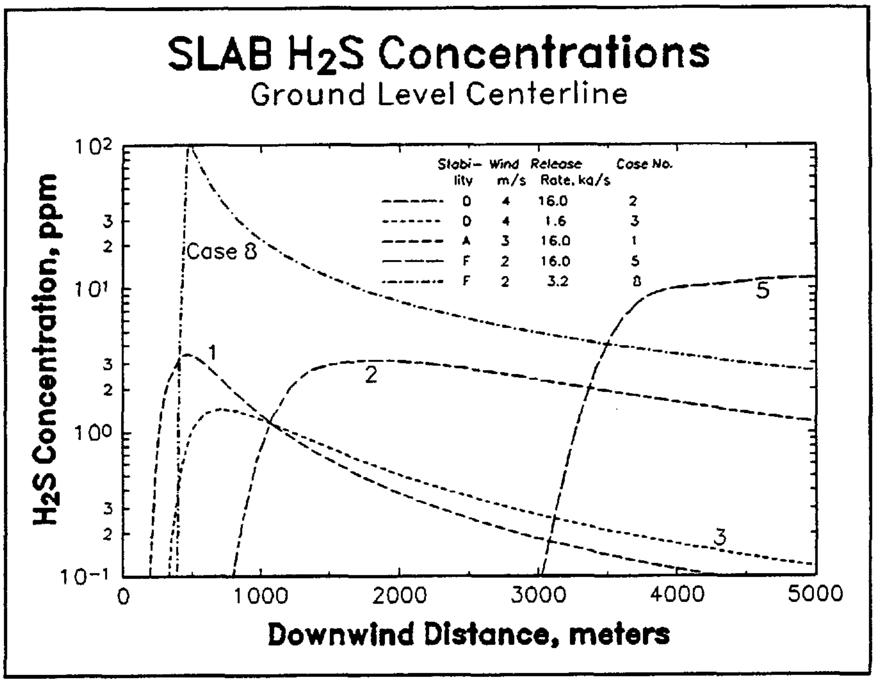

Figure S1-2.

Cases 2, 3, and 4 show results for two release rates and two wind speeds for neutral stability. For a 4 m/s wind, the lower 1.6 kg/s release touched down much closer to the source than did the 16 kg/s case. Note that the 1.6 kg/s plume (low momentum) rose to 31 m at a downwind distance of 15 m from the stack, whereas the 16 kg/s plume (high momentum) rose to 70 m at 150 m downwind. Yet the maximum ground level concentrations do not differ by very much! This is because the low momentum plume began sinking much closer to the stack and with less jet-induced turbulence than did the high momentum plume. Case 4 shows the inverse effect of wind speed on dispersed concentrations when compared with Case 2; the concentration was approximately halved.

Case 5 for F stability shows a significantly higher maximum ground level H_2S concentration than any of the cases listed above it. But the plume rise was higher than any of the preceding cases because the wind speed is very low, 2 m/s. Also, the plume did not touch down until 5 km downwind, whereas it touched down at about 2 km for Case 4 because the relative density of the plume was closer to the air density. But the rate of dispersion is significantly lower for this high stability, so the overall effect is to cause high ground level H_2S concentrations.

Cases 6 through 9 were made to search for the "critical" release rate which could cause the highest ground level concentration (for **F** stability and 2 m/s wind). The first sequence of release rates was planned to start at 0.8 km/s (half the lowest ever expected) and doubling each time. As can be seen in the table, 3.2 kg/s gave the highest H_2S concentration of about 20 ppm. This estimate could have been refined by making more runs within the 1.6 to 6.4 kg/s interval. However, this resolution is probably sufficient to address H_2S concentration concerns for the present purpose. Further studies might consider changing the stack height and/or gas exit conditions, then to repeat the modeling with the new parameters.

DEGADIS

SLAB's "optimum" Case 8 was modeled with DEGADIS, which resulted in markedly different results than the former model as shown at the bottom of Table S1-1. The maximum ground level concentration is about an order of magnitude lower and the touchdown point is about 4 km, whereas the comparable SLAB touchdown point is about 1 km. The concentrations reported were all from DEGADIS' JETPLUIN sub-program; the follow-on ground level dense gas model was implemented by the program.

HGSYSTEM

Case 8 of Table S1-2 was modeled with PLUME followed by PGPLUME. The former terminated normally at a downwind distance of 48 m with a plume centroid height of 32 m because the plume became essentially neutrally buoyant at the last position. Numerical solution difficulties first prevented normal termination when the 10 m wind speed measurement height was used; the program completed normally with a 1 m height. This parameter value leads to higher wind speeds at plume centerline height than result with the 10 m measurement height (*i.e.*, about 13 vs 3 m/s), which causes the plume to bend over earlier than for the original 10 parameter value. Because the plume was elevated, then leveled off, and became neutrally buoyant, PLUME automatically generated a file for input to PGPLUME, the Gaussian plume modeling program.

The plume path is shown in Figure S1-1 as the solid line. The arrowhead indicates that the plume centerline height remains constant at 32 m, because the Gaussian model uses a virtual point source at this elevation. PGPLUME results are shown in Table S1-2. Program PGPLUME provides its results in a different form than most other programs being used here. For each specified downwind distance, a two-way table of concentrations is produced, with columns for crosswind distances from the plume centerline and rows for receptor elevations above the ground. From these displays, it can be easily seen that concentration is very sensitive to receptor elevation until the plume becomes well mixed vertically in the far field.

Also, because the wind speed at plume centroid height is high, the centerline lowering effect of the wind is countered in the Gaussian model calculations in which concentration is inversely proportional to the wind speed. This explains the very low maximum value of 0.4 ppm H_2S shown in the table.

Scenario 2: Hydrogen Sulfide and Carbon Dioxide from a Safety Relief Stack

Statement

For a certain oil field located in a rural area, secondary recovery operations use carbon dioxide as the flooding agent. The separation plant produces a recycled stream containing about 1.3%v H_2S with the balance being essentially all CO_2 which is representative for discharges to a new safety relief stack being designed for the unit. The design maximum flow rate of 12 kg/s of this stream is to be used to estimate the required stack parameters of height above grade and exit diameter. For the diameter calculations, assume an internal pressure of 70 kPa (10 psig) at 275 K.

Release Attributes	
Material:	*H_2S in CO_2*
Method:	*Hole*
Fluid state:	*Vapor*
Chemical reactions?	*No*
Release time type:	*Steady state*
Turbulent jet:	*Vertical*
"Cloud" height:	*Initially elevated*
Roughness type:	*Rural*
Stability	*A, D, F*
Averaging time:	*60 s*
Hazard:	*Toxic*

For this example, assume that the ground level concentrations for H_2S and CO_2 concentrations should not exceed 10 ppm and 2.0 %v, respectively, on an averaging time basis of 60 s.

Analysis

Source/Release Parameters

Because the released gas is 98.7% CO_2, the physical properties of pure carbon dioxide were used for the stack gas. These, plus stated and derived quantities, are summarized in *Table S2-1*. The flow regime is non-choked because the pressure ratio, *r*, is greater than the critical pressure ratio, r_c (Equation 3-6). Therefore, sub-critical gas flow Equation 3-71 was rearranged to find

Table S2-1.

STACK DIAMETER SIZING PARAMETERS	
Specific heat ratio, k	1.3
Atmospheric pressure (P_3), Pa	101325
Inside stack pressure (P_1), Pa	170325
Pressure ratio, $P_3/P_1 = r$	0.595
Critical pressure ratio, r_c	0.546
Molecular weight	44.
Inside stack temperature, K	275.
Inside gas density, ρ, kg/m³	3.30
Adiabatic expansion coefficient, Υ	0.737
Required maximum flow rate, w, kg/s	12.0
Discharge coefficient, C_D	1.00
Calc'd. Bernoulli flow stack exit diameter, m	**0.175**

Table S2-2.

SOURCE/RELEASE PARAMETERS

1	2	3	4	5	6	7	8	9	10
Mass	Internal Stack			Vol. Flow		Expanded Jet			
Flow	Pressure		Density	Orif.	In Atmo	Area	Diam.	Density	Temp.
W	P_1		ρ_1	U_2	U_3	A_3	D_3	ρ_3	T_3
kg/s	Pa	atmo	kg/m3	m³/s	m³/s	m³	M	kg/m³	K
12.00	171243	1.690	3.297	3.640	5.450	0.03601	0.214	2.202	243.6
9.60	144673	1.428	2.785	3.447	4.533	0.03163	0.201	2.118	253.3
7.68	128491	1.268	2.474	3.105	3.727	0.02887	0.192	2.061	260.3
6.14	118451	1.169	2.280	2.694	3.038	0.02712	0.186	2.022	265.3
4.92	112224	1.108	2.160	2.275	2.461	0.02602	0.182	1.997	268.6
3.93	108239	1.068	2.084	1.887	1.985	0.02531	0.179	1.981	270.8
3.15	105751	1.044	2.036	1.545	1.597	0.02486	0.178	1.970	272.3
2.52	104151	1.028	2.005	1.255	1.282	0.02457	0.177	1.963	273.3
2.01	103120	1.018	1.985	1.014	1.028	0.02438	0.176	1.959	273.9
1.61	102475	1.011	1.973	0.816	0.824	0.02426	0.176	1.956	274.3
1.29	102063	1.007	1.965	0.656	0.659	0.02419	0.175	1.954	274.5
1.03	101795	1.005	1.960	0.526	0.528	0.02414	0.175	1.953	274.7

Stack exit (orifice) = 0.175 m. Stack exit gas temperature 275 K.

the required exit area; then, for the given flow rate of 12 kg/s total gas, the corresponding exit diameter was found to be 0.175 m.

Because the CO_2 flow rate varies from very low to 12.0 kg/s, *Table S2-2* was generated to obtain the *expanded jet parameters* required by the DEGADIS and SLAB dispersion models. For each given w, the stack gas internal pressure, P_1, must conform to the sub-critical gas flow Equation 3-71 using the 0.175 m stack exit diameter. Equations 3-71, 3-72, 3-73 and 3-18 were simultaneously solved for P_1 by a nonlinear solution algorithm feature of the spreadsheet program software. With the parameters of columns 1, 2 and 4, the expanded jet parameters of columns 5 through 10 were calculated by means of the appropriate equations from the set comprising Equations 3-97 through 3-102. Note that subscript 2 denotes the orifice ("throat"), and because the flow is not choked, $P_2 = P_1$ for the equations.

It can be seen in the rightmost columns of the table that the expanded jet temperature and density differ significantly from the internal stack "initial" conditions. Also not shown, the adiabatic expansion factor (Υ) significantly varied from 0.74 for the 12 kg/s flow to 1.00 for the 1.03 kg/s flow.

In a particular application, specific details of practical stack construction must be considered. However, for simplicity in demonstrating dispersion modeling effects, only the above physical diameter of 0.175 m is used.

Other Parameters

MODELING PARAMETER RECAP
(See also Table S2-1)

Stack Gas	
Molecular weight	44
Specific heat, C_p, KJ/[kg.K]	0.83
Release rates, kg/s	1.3 to 12
Temperature, K	Table S2-2
Expanded jet diameter	Table S2-2
Stack diameter, m	0.175
Stack height, m	(variable)
Roughness length, z_r, m	0.1
Atmospheric variables	
Stability A	
temperature, K	300
wind speed, m/s	2
Stability D	
temperature, K	300
wind speed, m/s	4
Stability E	
temperature, K	275
wind speed, m/s	2
Relative humidity, %	95

For elevated plumes, expected to be attained by choice of a sufficiently high stack, stable atmospheric conditions usually result in the highest ground concentrations of dispersed material. However, depending upon exit gas conditions and flow rate, unstable atmospheres can sometimes cause much vertical mixing near the stack, and perhaps lead to high concentrations. Also the higher wind speeds associated with neutral stability can sometimes lead to high concentrations because of plume bend-over, and since this stability class usually predominates in many geographical locations, it should always be considered. Therefore, initial simulations were made for **A**, **D** and **F** stabilities using the respective (default) wind speeds of 2, 4, and 2.

It was assumed the rural countryside had a number of trees, hedges, etc., to result in an average roughness length of 0.1 m. (Rural *grasslands* would have roughness lengths near 0.03 m.)

The total gas contains 1.3% H_2S; thus, 10 ppm H_2S corresponds to 0.077% total gas. Because this is less than the specified 2% maximum value for CO_2, only the ground level concentrations of H_2S predicted by the modeling programs are presented. Also, to obtain the *concentration of H_2S in parts-per-million* from the total, or bulk, dispersed gas concentration (mole fraction) reported by the models, the latter must be multiplied by the factor $[1.0 \bullet 10^6$ ppm/mf$]\bullet[0.013$ fraction $H_2S] = \mathbf{1.3 \bullet 10^4}$.

Table S2-3.

H2S Ground Level Centerline Concentrations
Initial DEGADIS Simulations for 5 m Stack Height

CO2 Release rate, kg/s	12.0	12.0	1.29
Stability class	D	F	F
Wind speed, m/s	4	2	2
Maximum ppm H2S	5	23	96
At downwind distance, m	307	500	82
First downwind distance for less than 10 ppm, m	406	1063	323

Simulation

DEGADIS was primarily used. The results from three preliminary simulations are shown in *Table S2-3* which shows much higher concentrations to be estimated for the **F** stability cases than for **D** stability. The plume paths for these simulations are shown in *Figure S2-1*. An **A** stability run for 12 k/s failed. However, on the basis of other experience, in addition to these results, it was concluded that **F** stability at 2 m/s wind speed should cause the highest ground level H_2S concentrations; these conditions were used for all further simulations. Therefore, a heuristic search was performed in which release rate and stack height were varied as shown in *Figure S2-2*. (The maximum ground level H_2S concentration [ppm] for each coordinate point representing a simulation is shown next to the circular point.) No ground level H_2S concentrations resulted for the last two simulations at 23 m stack height with 12 and 1.6 kg/s gas flows (top vector).

On the basis of these DEGADIS simulations, it could be concluded that an approximate stack height of 23 m and exit diameter of 0.175 meters should keep CO_2 and H_2S concentrations below the specified "levels of concern" for all atmospheric conditions given the maximum flow rate and maximum H_2S concentration in the release gas.

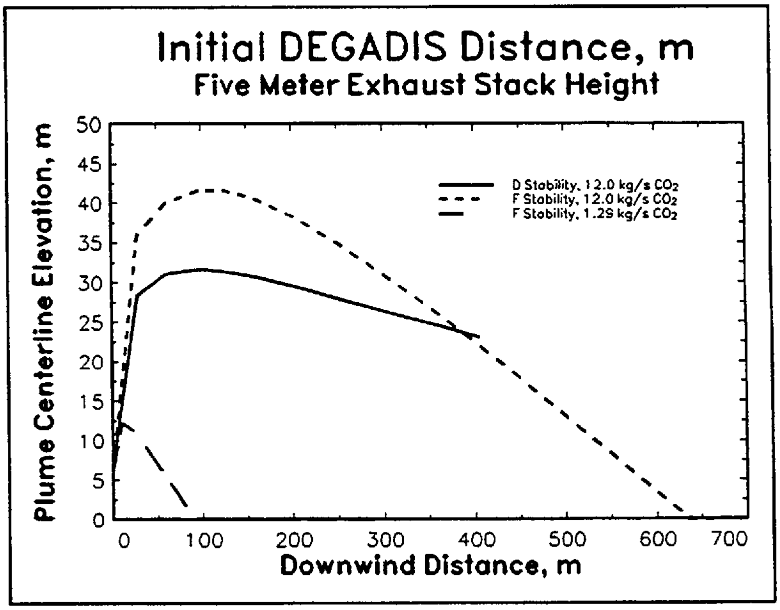

Figure S2-1.

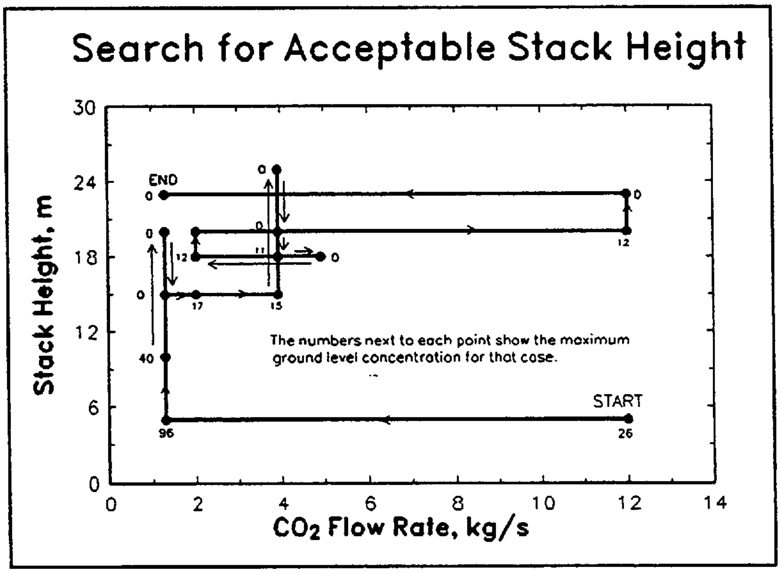

Figure S2-2.

Other Modeling Programs

SLAB was run for the same conditions and parameters as the final two DEGADIS runs described above. The maximum downwind concentrations and plume paths for these four runs are shown in *Figures S2-3 and S2-4*, respectively. Corresponding PLUME (HGSYSTEM) results could not be obtained; the program aborted because convergence could not be achieved by the nonlinear equation solver. However, the high (12 kg/s) flow rate solution was obtained to about 14 m downwind with the path still rising. The program-computed expanded jet temperature for this case was 263 K, which significantly differs from the 244 K value shown in Table S2-1.

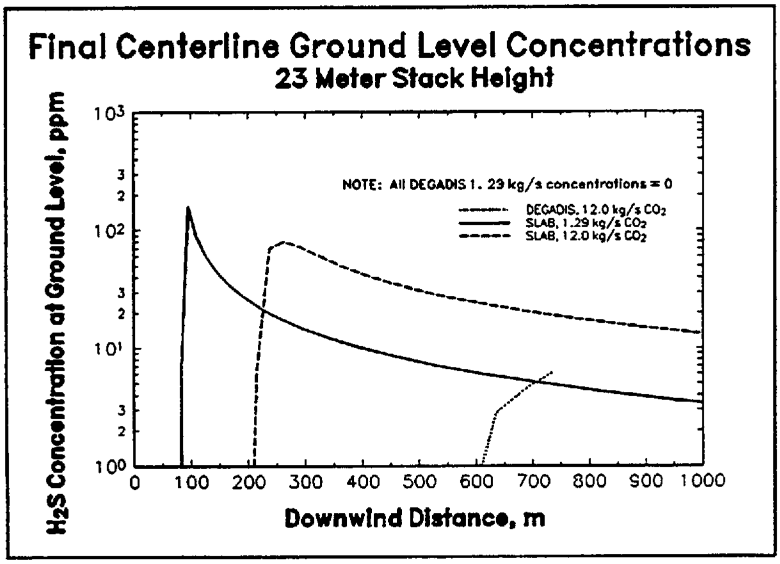

Figure S2-3.

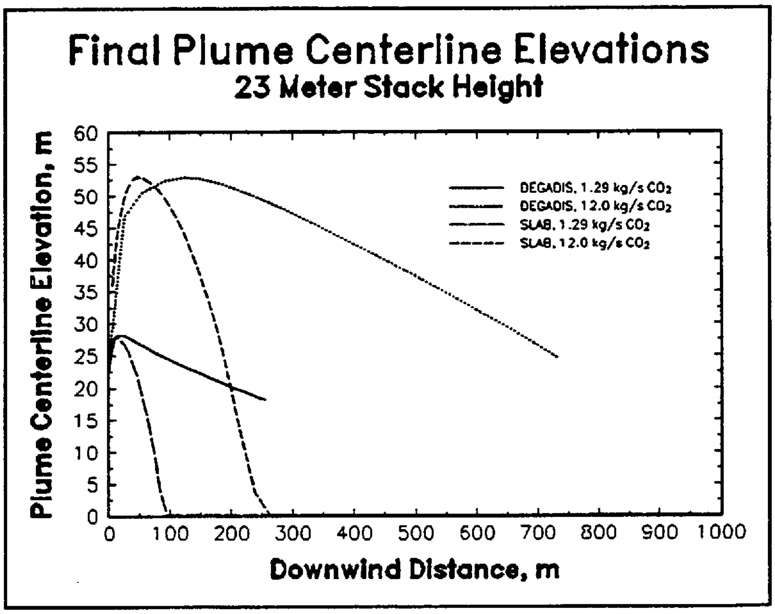

Figure S2-4.

Scenario 3: Supercritical Propane Pipe Hole Release

Statement

Supercritical propane at 340 K and 7.0 MPa is heated in a gas-fired process preheater to a temperature of 540 K. Assume that the pressure in the outlet line is the same as for the feed line, and that a 19 mm diameter hole can develop from some type of failure on either line. The holes are both about 3 meters above grade. How far downwind could a vapor cloud remain flammable? The most likely ignition source is about 15 m feet from the heater. Could the jet's vapor be ignited if it happened to be directly towards the ignition source?

Release Attributes

Material:	*Propane*
Method:	*Hole*
Fluid state:	*Supercritical fluid*
Chemical reactions?	*No*
Release time type:	*Steady state*
Turbulent jet:	*Horizontal*
"Cloud" height:	*Initially elevated*
Roughness type:	*Industrial*
Stability:	*D*
Averaging time	*10 s*
Hazard:	*Flammable*

Analysis

Source/Release Parameters

A single component chemical fluid is in the supercritical state if its temperature exceeds the critical temperature (369.85 K for propane) and/or its pressure exceeds the critical pressure (4.248 MPa). That is, separate liquid and vapor phases do not coexist; the fluid has a single set of physical properties. The pressure-temperature-density functions will not be those of an ideal gas, nor be those generally used for liquids. For example, the density of propane vapor at 300 K and 0.1 MPa (1 atm) is about 1.8 kg/m^3, and the density of many hydrocarbon liquids at ambient conditions is on the order of 800 kg/m^3. The densities of supercritical fluids usually lie somewhere between such typical values. Because of the very large pressure difference between the fluids and the atmosphere, choked flow would certainly occur. Before using the choked flow equation in Chapter 3 to estimate the release rate, the physical properties of propane in the temperature - pressure region of interest must be determined and used to estimate the flow rates through `the 19 mm hole for the two temperatures.

Table S3-1.

Propane Properties at 7.0 MPa

1	2	3	4	5	6	7	8	9
Tem-pera-ture	Fluid Density Real	Fluid Density Ideal	C_p	k = C_p/C_v	Sound Speed Real	Sound Speed Ideal	En-thalpy (H)	En-tropy (S)
K	mol/L	mol/L	J/mol*K	m/s	m/s	J/mol	J/mol*K	
300	11.479	2.806	115.3	1.556	809	246	-1224	197.6
320	10.815	2.631	123.1	1.588	691	254	1157	205.3
340	10.045	2.476	133.5	1.644	571	261	3717	213.0
360	9.094	2.339	149.7	1.757	448	269	6534	221.1
380	7.766	2.216	184.5	2.050	315	276	9820	230.0
400	5.552	2.105	246.6	2.566	209	283	14201	241.2
420	3.745	2.005	188.9	1.922	206	290	18657	252.1
440	2.983	1.913	151.4	1.522	228	297	21994	259.8
460	2.570	1.830	138.1	1.361	247	304	24867	266.2
480	2.297	1.754	132.8	1.277	263	311	27568	272.0
500	2.096	1.684	130.9	1.227	277	317	30201	277.3
520	1.939	1.619	130.8	1.193	290	323	32817	282.5
540	1.812	1.559	131.6	1.169	301	329	35440	287.4
560	1.704	1.503	133.0	1.152	312	335	38086	292.2
580	1.613	1.452	134.8	1.138	321	341	40764	296.9
600	1.532	1.403	136.7	1.126	331	347	43479	301.5

CRITICAL TEMPERATURE IS 369.85 K   CRITICAL PRESSURE IS 4.248 MPa

A "mol" is 1 gram-mole. Note that 1 mol/L = 1 mol/liter = 1 kg-mole/m^3
Ideal gas quantities were calculated here; others are from the NITSFLUIDS database.

Required thermophysical properties for propane were obtained from the NITSFLUIDS database on-line to the STN International network. This database was selected mainly because it gives C_v directly. Smoothed properties can be generated with reported accuracies of about 3 - 5%. *Table S3-1* lists the properties of interest, along with some derived values to be discussed later. (Note that over this temperature range, fluid densities differ markedly from ideal gas values; particularly for the low temperatures.) Also C_p and k go through a maximum near the critical temperature; a finer grid would show much larger values near that point than can be seen in the table.

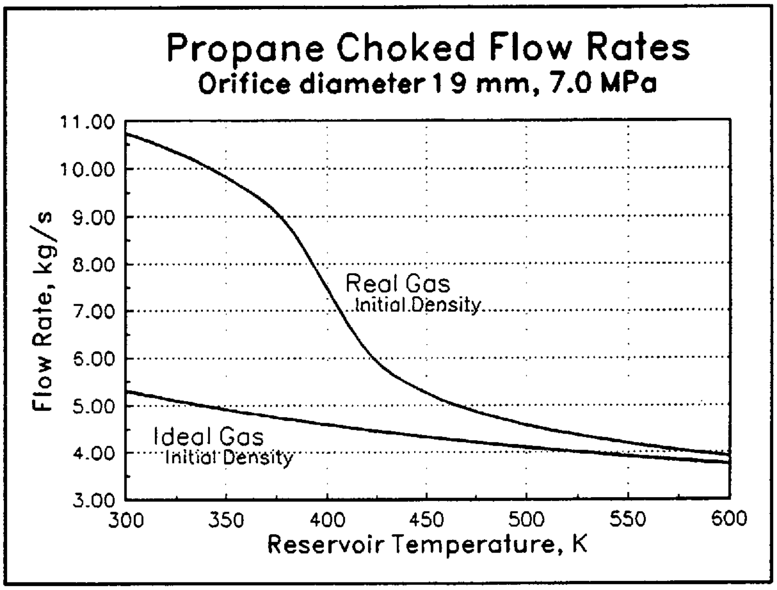

Figure S3-1.

Table S3-2.

SOURCE PARAMETERS AND MODELING RESULTS
Supercritical Propane Release

	Modeling Program Used			
Source Parameters	PLUME	SLAB	PLUME	SLAB
Reservoir temperature, K	340	340	580	580
Specific heat ratio (k)	**	1.14	**	1.14
Mass flow rate, kg/s	10.0	10.0	3.8	3.8
Throat temperature, K	318	318	542	542
Expanded jet temperature, K	**	202	**	345
Model input gas temp., K	318	202	542	345
Expanded jet diameter, cm	**	9.6	**	9.6
Input source diameter, c	1.9	9.6	1.9	9.6
Molecular weight of gas	44.09	44.09	44.09	44.09
C_p of gas, J/[(mol)(K)]	133.5	134.2	134.8	134.2
Modeling Results				
Percent (v) propane at 15m	1.9	2.0	1.0	1.6
Distance to 1.0%v propane	30	50	15	35
Distance to 0.5%v propane	81	117	26	82
Plume diameter at 15 m	4.9	8.5	5.1	8.2
Plume diam. at 1%v point	10.5	15.3	5.1	12.2
Plume diam. at 0.5%v	29.7	30.2	10.0	20.4
Pressure to the orifice, Mpa	8.4	NA	4.2	NA

** Not used for PLUME input, nor available in the output.
NA: Not Applicable

To estimate the release flow rates, it would be most accurate to use the *"rigorous"* method discussed in Chapter 3. However, since only approximate results are required, the ideal gas choked flow computations as presented in Chapter 3 were employed, but with some modification. *Figure S3-1* shows the choked flow rates for the *ideal gas* (Equation 3-69), compared with the use of Equation 3-68 with the *real gas* fluid densities from Table S3-1. The specific heat ratio, *k*, used for these calculations was 1.14. (Varying *k* showed that a change from 1.1 to 1.6 changed the mass flow rates by only 10% at the 340 K inlet temperature, using the real gas density.) Note that at the higher end of the temperature range, the densities (Table S3-1) differ by only about 10% and the flow rates (Figure S3-1) differ by about 5%. Because Equation 3-68 shows the correct effect of gas density (flow proportional to the square root of density), the flow rates and subsequent expansion calculations were made according to the "real gas" case in this figure. The results used for the models (and other source parameters) at the two temperatures are presented in *Table S3-2*.

The velocity at the throat *is* the speed of sound in the gas; this is shown as the sound speed in Table S3-1. Referring to that table, note that at the high temperatures, the ideal vs real sound velocities are close, which gives some confidence here. It must be kept in mind that *the dispersion results will only be first approximations* with respect to more rigorous flow rate calculations.

As indicated in Table S3-2, the PLUME model requires the physical diameter of the orifice and the temperature of the reservoir to which the orifice is "attached" because it performs the calculations for expanding the jet to atmospheric pressure. SLAB does not perform the jet expansion calculations, so these must be done by the user.

Atmospheric Parameters

MODELING PARAMETER RECAP

See *Table S3-2* for released fluid physical properties and expanded jet parameters.

Atmospheric/Boundary Layer

Roughness length, m	0.1
Stability Class	D
Relative Humidity	0
Wind speed, m/s	2
Air temperature, K	293
Averaging time, s	10

The *RECAP box* shows the common atmospheric boundary layer parameters used for the simulations. The averaging time was taken as 10 seconds because peak concentrations are of interest from the flammability standpoint. The roughness parameter is inoperative for turbulent jets; it is inapplicable because the source and effects are down within plant structure levels. The same applies to the stability class designator; values are required by the modeling programs. The low wind speed is essentially negligible with respect to the early jet speeds. The relative humidity was set at zero, for the PLUME program aborted with plume temperatures which were less than the freezing point of water. A humidity greater than zero was not tried with SLAB.

Simulation

Model Type

The fluid emitted from the hole will form a turbulent jet. If the jet is directed vertically, the plume would rise a significant distance before being bent over by the wind. This would be followed by sinking if the plume is denser than the ambient air. However, if the jet is pointed horizontally, this effect would be absent and higher centerline concentrations would occur at adjacent locations, such as ignition points (which can be expected to be somewhat near the ground). For this reason, it was concluded that a horizontal jet would be the "worst case." Since DEGADIS has only a vertical jet module, it could not be used. The turbulent jet module, PLUME, in HGSYSTEM, and SLAB, were used for the simulations.

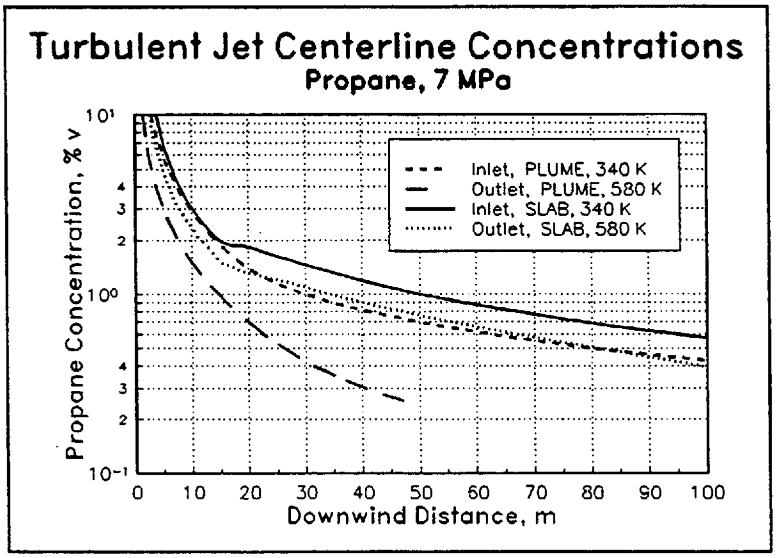

Figure S3-2.

Figure S3-2 presents the jet plume centerline concentrations vs downwind distance for the horizontal plumes. The model results showed that the centerline elevation remained essentially constant at 3.0 meters for all distances shown. Selected centerline concentrations and associated plume diameters are also shown in the lower part of Table S3-2.

As is characteristic of turbulent jets, the concentration of propane dropped very rapidly (below about 2%) in about 100 expanded jet diameters (0.096 m), roughly 10 to 20 meters.

Conclusions

The *flammability criteria* discussed in Chapter 1 states that, in lieu of other information and to be conservative, a model-estimated flammable fluid concentration in air must exceed 0.5 %v to be ignitable. Considering the uppermost three curves in Figure S3-2, it can be concluded that, since all centerline concentrations are estimated to be greater than 0.5%v pentane to 80 m downwind, the plumes would be flammable at that ignition source location. With respect to a release on the inlet side of the heater, SLAB predicts the concentration would drop through 0.5%v at about 118 m (beyond the right side of the graph) downwind, while PLUME predicts this flammability limit would be reached at about 80 meters. For the outlet side, SLAB estimates that the 0.5%v distance would be at about 80 meters also. These distances apply along the jet centerline, so the plume would, in theory, have to travel directly toward an ignition source located at the given, farthest-flammable distance. This assumes no obstacles or ground contact. Also, PLUME has a "top-hat" concentration distribution (a single average value across the cross-section), while SLAB calculates the normally-distributed concentrations normal to the plume axis, so off-axis concentrations decrease.

Actually, flammable jets, as being considered here, could impact adjoining structures, which may deflect the vapor or tend to trap it. Also, the fired part of the heater could be an ignition source if the release is near and/or oriented toward it. Depending upon the number and kind of structures in the area, the wind speed, wind direction, source/release conditions, and the release duration, a flammable cloud could build up as well as travel longer distances than mentioned above. Also, if the atmosphere is calm (which happens a significant amount of the time), a vapor cloud could build up and spread out in all directions until an ignition source is finally reached. These factors must be considered.

Scenario 4: Oil Well Blowout

Statement

The 0.35 m diameter well casing of a sour crude production well breaks off at ground level to cause a blowout which spews oil and gas vertically into the air at about 23,000 kg/hr. The temperature of the mixture just before discharge into the atmosphere is 316 K (108 F). It is expected that the discharge would continue at this rate for some time, perhaps several days, before it could be shut off. The crude assay analysis and flash calculation results of conditions are known. From these, the H_2S concentration in the vapor phase of the released fluid is about 12 %v.

Release Attributes

Material: .... *Sour crude oil*
Method .... *Hole*
Fluid state: .... *Flashing liquid*
Chemical reaction? .... *No*
Release time type: ... *Steady state*
Turbulent jet: .... *Vertical*
"Cloud" height: .... *Elevated per jet*
Roughness type: .... *Rural*
Stability: .... *Various*
Averaging time: .... *60 s*
Hazard: .... *Toxic*

Dispersion modeling is required to estimate "worst case" H_2S concentrations vs radii from the well. For example, what would be the radius from the source for which the H_2S concentration would always be less than 10 ppm, for all expected meteorological conditions?

The meteorological conditions typical for the area are hot, humid days with the atmosphere becoming very unstable during the day, with maximum instability occurring in the early afternoon. At night, the earth can cool enough to sometimes cause stable conditions. Daytime winds as well as cloud cover produce neutral stability.

Analysis

Source/Release Parameters

The release to be modeled is a two-phase (vapor/liquid) turbulent jet, and can be treated as steady-state. Because crude oils, in general, contain a large proportion of very low vapor pressure components, the jet would be rising into the air with vapor being disengaged from the liquid, which mostly falls to the ground. The fluid will be intensely mixed with the air in the near-field by the turbulent jet. The wind causes the vertical plume to "feather-out" (which our models cannot handle). Enough of the liquid should be distributed as an aerosol to cause the major part of the plume to sink to the ground. Also, because of their relative densities, the vapor and liquid phases would travel at different velocities ("slipping") with insufficient mixing time to allow phase equilibrium; this process starts in the well casing pipe. As the fluid is mixed with the air, the liquid and vapor phases will be constantly changing in composition due to evaporation of liquid droplets and mixing with air.

No modeling programs are available which adequately treat all these phenomena, so simplifying assumptions must be made. Therefore, assume that the vapor and liquid are in homogenous equilibrium. Given the *crude oil assay* for the composition of the oil, and the before-release temperature and pressure of the oil, a vapor/liquid equilibrium ("flash") calculation can be used to estimate the released phase compositions along with physical and thermodynamic properties. Typical information for a real situation was provided to the author for this example, *Table S4-1*.

However, the modeling programs being used for these examples cannot directly handle multi-component, multiphase mixtures. SLAB can handle simple phase equilibria for *single component (pure)* fluids. DEGADIS has been designed to handle fluid/air mixtures of arbitrary densities; data are "triples," each of which contains: mole fraction "contaminant" (basis a contaminant/air mixture), concentration of contaminant (kg/m^3), and total mixture density (see Appendix II). HGSYSTEM's HEGADAS can treat pure component evaporating aerosols, but the PGPLUME turbulent jet can only deal with ideal gases. Therefore, the initial modeling was done with SLAB, further simulations made with DEGADIS using the triples option, then HGSYSTEM was used for a vapor-only release.

Table S4-1.

```
              CRUDE OIL FLASH RESULTS - TWO-PHASE SUMMARY

                 Temperature:      315.5 K =   108.2 F
                 Pressure:     0.101325 MPa =     1 atm
                                                                  Cumula-
                                       Mole Percent Component      tive

Component       NBP,K Mol. Wt.    Liquid     Vapor     Total      Mass %
H2S                     34.15      0.49      11.63      6.59       2.47
CO2                     44.01      0.04       2.04      1.14       3.02
N2                      28.02      0.00       1.40      0.77       3.26
Methane                 16.04      0.18      41.78     22.98       7.31
Ethane            185   30.07      0.28      12.37      6.90       9.59
Propane           231   44.10      0.95      12.08      7.05      13.00
I-Butane          263   58.09      0.46       2.58      1.62      14.04
n-Butane          273   58.13      1.53       5.98      3.97      16.57
I-Pentane         302   72.16      1.48       2.46      2.01      18.17
n-Pentane         309   72.13      2.24       2.82      2.56      20.20
Hexanes       ca. 323   91.98      5.68       2.42      3.89      24.13
Heptanes      ca. 372  100.99     12.08       1.69      6.39      31.21
Octanes       ca. 399  112.99     11.97       0.57      5.72      38.32
Nonanes       ca. 424  129.98     10.83       0.18      4.99      45.45
Other                  212.00     51.81       0.00     23.42     100.00

    Total flow rates:
       Molal, kgmol/s             0.03199   0.03878   0.07076
       Mass, kg/s                 5.09867   1.34217   6.44084
       Volumetric, m^3/s          0.00642   1.00383   1.01025

    Phase attributes:
       Density, kg/m3             794.152     1.337     6.376
       Specific volume, m^3/kg    0.0013    0.7479    0.1569
       Mixture mole fraction      0.4520    0.5480    1.0000
       Mass fraction              0.7916    0.2084    1.0000
       Volumetric fraction        0.0064    0.9936    1.0000
```

Pseudo-Pure Component Properties Estimation

Referring to *Table S4-1*, note that essentially all of the low molecular weight compounds, H_2S through I-pentane, are contained in the vapor phase, with n-pentane distributed about evenly between the phases, while almost all of the higher molecular weight compounds are in the liquid phase at this release temperature and pressure. The lower part of the table shows parameters for the two phases as well as for the total mixture.

SLAB uses the pure-component equation for calculating the mass or mole fraction vapor presented in Chapter 3 to calculate the fraction vaporized:

$$f_v = \frac{C_{p,l}\Delta T}{\Delta H_{vap}} \quad . \qquad (3\text{-}67)$$

To obtain the constant heat of vaporization required by SLAB, the heats of vaporization for pentane, hexanes and heptanes were found in Perry's Sixth. These ranged from about 76 to 85 calories per *gram* at the normal boiling points, and 88 for all at 25 C; so 83 cal/g, which corresponds to 347.3 kJ/kg, was selected . Using the release temperature (T_l = 315.5 K) minus the normal boiling point (T_{NBP}) for ΔT, and C_{pl} = 2118 J/[kg•K], T_{NBP} was varied using the above equation so that f_v best agreed with the vapor mass fraction of Table S4-1, 0.208. A T_{NBP} value of 281 K yielded f_v = 0.210 at 315.5 K, and 0.128 at 302 K (the ambient temperature to be used). The latter fraction appears reasonable, considering the fraction of low boiling point compounds shown, and that actually some vapor will be in solution. Therefore, these parameters were used with SLAB. The initial liquid mass fraction was 0.792 (= 1 - f_v). The SLAB default option for using these input parameters with the Clausius-Clapeyron equation was used to calculate the equilibrium vapor pressure. Because the flash was made at atmospheric pressure and the given temperature, and the liquid phases constituted a large mass fraction of the total, the expanded jet diameter was set to the casing diameter, 0.35 m.

Atmospheric Parameters

Three sets of meteorological conditions were used for the SLAB two-phase simulations: 1) Pasquill-Gifford stability class **D** (neutral) with a 5 m/s wind speed and 75% humidity; 2) the very unstable class **A** with a 5 m/s wind to demonstrate the increased vertical mixing; 3) for nighttime conditions, stability **E** with a 2 m/s wind.

A "receptor" or *z*-plane height of 1.0 m was used unless otherwise noted. Near the source, ground level heights (z = 0) may be significantly lower than for a meter or two higher with elevated plumes. At far-field distances, the vertical mixing will tend to make concentrations insensitive to this variable.

MODELING PARAMETER RECAP

Pseudo-Pure Component Properties	
Molecular weight	34.6
Specific heat, C_p, KJ/[kg.K]	1.75
Normal boiling point, K	276
Liquid mass fraction	0.792
Heat of vaporization, KJ/kg	347.3
Liquid heat capacity, KJ/[kg•K]	2.12
Liquid density, Kg/m^3	794
Source	
Release rate, kg/s	6.44
Temperature, K	315.5
Well diameter, m	0.35
Release height	0
Atmospheric variables	
Stability **A**	
temperature, K	305
wind speed, m/s	5
Stability **D**	
temperature, K	305
wind speed, m/s	5
Stability **E**	
temperature, K	294
wind speed, m/s	2
Relative humidity, %	75
Roughness length, z_r, m	0.03
Receptor height, m	1

Simulation

Two-Phase Releases

Figure S4-1 presents the plume centerline concentrations for the three simulations described in columns (runs) 1, 2, and 3 of *Table S4-2* in which the rows under Estimated Values summarize the various distances to selected downwind concentrations as well as maximum plume path heights. As might be expected, the **A** stability case shows greater dispersion than the neutral case, as the distance from the source increases because of increased vertical mixing. Also as expected, the stable case **E** shows the highest concentrations. *Figure S4-2* compares the plume half- widths, defined ★ as

$$bbc = \sigma_y / \sqrt{3},$$

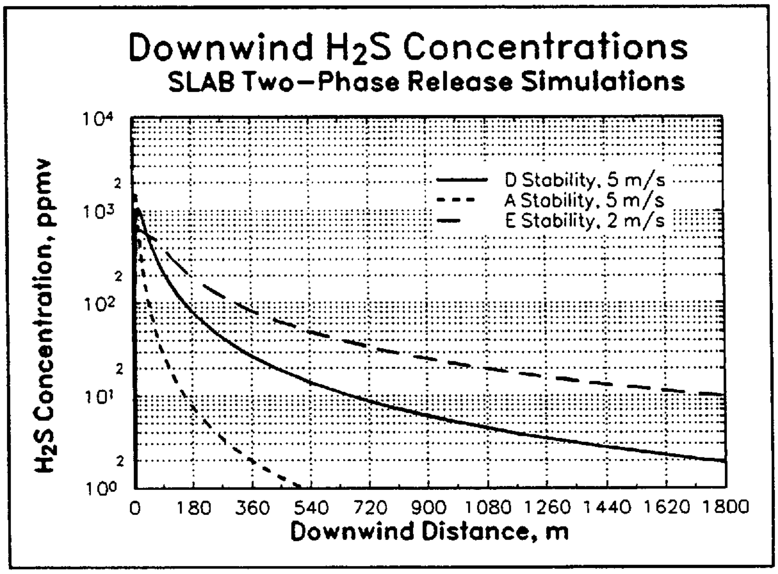

Figure S4-1.

★ In the output file column labeled *bbc* from SLAB. The relationship is strictly valid only beyond the downwind distance where gravity slumping becomes negligible.

for a 1 m receptor plane height for the three cases. The largest width shown for the **E** stability cloud can be ascribed to a combination of close-in plume impact with the ground, more initial gravity spreading and low wind speed. The large air entrainment and vertical mixing of the **A** stability case causes the cloud to be wider than that of the **D** stability case.

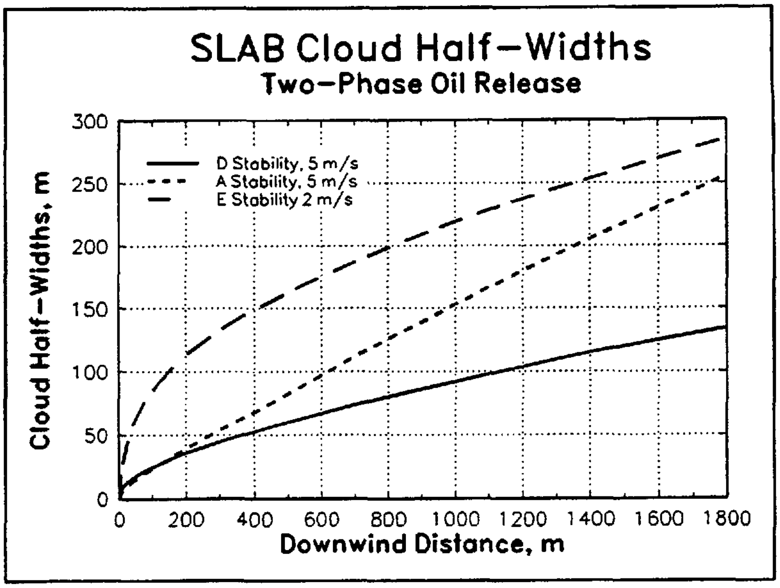

Figure S4-2.

Actually, considering SLAB's results with respect to plume height and spreading from a qualitative standpoint, most of the liquid in the released oil would fall to the ground and form a pool. Thus, additional emissions and dispersion will result from this area source, with the emission rate being controlled by the concentration of H_2S in the liquid and its rate of replenishment at the top surface by diffusion. General purpose programs which can model these phenomena do not appear to be publicly available.

DEGADIS Modeling

For the *triples* option, a spreadsheet was developed to calculate air/contaminant (released two-phase fluid) sets for air mole fraction ranging from zero to one in 30 equal steps. The released fluid properties were taken from the *Total* column of Table S4-1, and the air density was 1.15 kg/m^3 (300 K, no water vapor). Other parameters were as for SLAB above.

The DEGADIS program failed with an error message which indicated non-convergence of the numerical integration method. The program did run satisfactorily for the triples test case supplied with the program. Various convergence tolerances and initial step sizes were tried, but to no avail; therefore, this approach was abandoned.

Vapor-Only Release Modeling

Another way of estimating the downwind distance to which hazardous H_2S concentrations could travel is to assume that all of the vapor behaves as a single-phase vertical jet, with source diameter equivalent to the area which the vapor part of the liquid would occupy during HEM discharge. This would give, perhaps, an upper bound because the same intensive mixing occurs in the turbulent jet in the near field, but the far field would represent dispersion caused by atmospheric phenomena, not with the additional cloud spreading effect on dispersion. This was done, using all three modeling systems, using only the vapor properties and rates shown in Table S4-1. The simulations were made only for the neutral atmospheric case; results for the unstable and stable cases would be relatively similar to those for the two-phase cases.

The results are summarized in the right half of *Table S4-2,* and the downwind centerline concentrations are plotted in *Figure S4-3* (the two-phase curve from SLAB is also shown for comparison). Both SLAB and DEGADIS determined that the plume bent over and formed a ground level, dense

Table S4-2.

SUMMARY OF RESULTS FOR SCENARIO 4
Oil Well Blowout

Run No. ===>	1	2	3	4	5	6
Released phases	------ Liquid & Vapor ----			-------- Vapor Only --------		
Modeling system	SLAB	SLAB	SLAB	SLAB	DEGADIS	HGSYSTEM
PG stability class	D	A	E	D	D	D
Wind speed, m/s	5	5	2	5	5	5
Ambient temperature, K	305.4	305.4	294.3	305.4	305.4	305.4
Ambient temperature, F	90	90	70	90	90	90
Relative humidity, %	75	75	95	75	75	75
<u>Source Parameters</u>						
Release rate, kg/s	6.44	6.44	6.44	1.34	1.34	1.34
Orifice diameter, m	0.35	0.35	0.35	0.35	0.35	0.35
Orifice elevation, m	0.00	0.00	0.00	0.00	0.01	2.00
<u>Estimated Values</u>						
Meters* to 1000 ppm H2S	22(a)	14	None(b)	54	None	25/2.7**
Meters to 100 ppm H2S	158	48	310	205	214	540/1.3
Meters to 10 ppm H2S	669	157	1790	726	879	900/1.3
Max. plume path height,	3.4	2.6	1.0	1.9	4.5	4.0***
Meters to maximum height	1.0	1.0	1.0	3.2	28.0	8.0
Meters to 100% vapor	4.3	3.7	4.3			

* Downwind distance along the centerline. All concentrations are for z = 1.0.
(a) 34 m for z = 0. | The distances to 100 and 10 ppm were about the same as for
(b) 56 m for z = 0. | z = 1 for both runs 1 and 3.
** [Downwind distance]/[Elevation for the concentration]
*** Plume became neutrally buoyant at this height and distance.

<u>Common Parameters</u>

Roughness length Zr, meters	0.03	Wind speed measurement height, m	10
Averaging time, seconds	60	Orifice diameter, m	0.35

gas cloud. HGSYSTEM's PLUME determined that the plume remained elevated (centerline at about 4 meters), so it set up the partial input file for PGPLUME, which in turn estimates dispersion with the Gaussian plume model. The results from the latter are shown in Figure S4-3.

However, it was not possible to get PLUME to run with the source height at zero meters; the height of the source had to be greater that 1.5 m. The smooth curve in Figure S4-3 for HGSYSTEM was obtained by linear (x) - log (concentration) interpolation of PGPLUME results to obtain the 1 m z-plane values plotted.

Conclusions

Analysis of the **D** stability simulations indicates that predicted downwind distances to given H_2S concentrations do not differ significantly with respect to the modeling program used or the source characterizations of aerosol vs vapor only. From this example, it appears that the vapor-only release simulations gave adequate estimates compared with the aerosol simulations, and perhaps with a small extra safety factor. However, jets with different momentum, thermodynamic behavior, and other parameters might lead to markedly different conclusions.

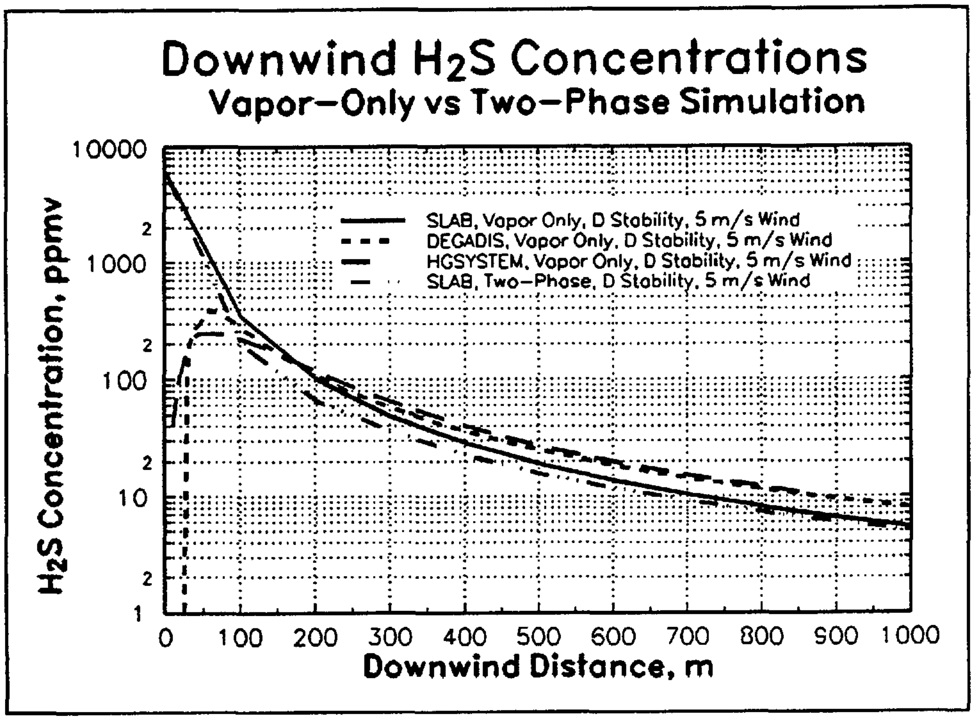
Downwind H2S Concentrations
Vapor–Only vs Two–Phase Simulation
SLAB, Vapor Only, D Stability, 5 m/s Wind
DEGADIS, Vapor Only, D Stability, 5 m/s Wind
HGSYSTEM, Vapor Only, D Stability, 5 m/s Wind
SLAB, Two–Phase, D Stability, 5 m/s Wind
H2S Concentration, ppmv
10000
2
1000
2
100
2
10
2
1
0
100
200
300
400
500
600
700
800
900
1000
Downwind Distance, m

Figure 3.

Scenario 5: Liquified Chlorine Tank Truck Accident

Statement

On an partly cloudy night with light winds, a tank truck filled with liquid chlorine to its full 16 metric ton capacity, jack-knifes, then overturns in tall grass adjacent to the highway. The tank ruptures and empties in 30 minutes in a manner so that the rapidly expanding fluid forms an aerosol as it enters the atmosphere. Assume that the internal tank storage temperature equals the ambient temperature, 303 K (86 F). For this locale in the Midwest prairie/farm country, forecasts call for daytime high temperatures of 303 K with winds from 4 to 8 m/s with moderate insolation and minimum nighttime temperatures near 293 K with winds ranging from calm to 3 m/s with < 3/8 cloud cover.

Release Attributes

Material:	*Chlorine*
Method	*Large hole*
Fluid state:	*Flashing liquid*
Chemical reactions?	*No*
Release time type:	*Finite duration*
Tank Rupture:	*Area source*
"Cloud" height:	*Ground level*
Roughness type:	*Rural*
Stability:	*C and E*
Averaging time:	*900 s*
Hazard:	*Toxic*

If a release such as exemplified here were to be made, and the appropriate monitoring instruments were available at the right places and times, a number of phenomena would be observed. At 4 m/s wind, the cloud from the 30-minute release would travel 7,200 m during that 30 minutes. Even if the wind direction and speed stayed constant for that long (within the averaging time concepts), then for longer times the cloud undoubtedly would start to change course along its path. Also, no terrain is completely plane, so the cloud, or parts of it, would be diverted by terrain features, trapped into low lying areas, etc. Then, if the period of interest included the transition from night to day, sun heating effects will change the surface temperature and winds, etc., so as to change the meteorological conditions from those postulated.

Analysis

Source Characterization

The fraction aerosol in the released mixture could be calculated for this pure component by Equation 3-52, which (along with other physical properties for the two phases) could initialize a boiling pool area source directly modeled by HEGADAS and SLAB. The triples input could be used with DEGADIS. However, experience from field tests and modeling indicates that aerosols are completely vaporized in less than 100 meters, so the distance error caused by assuming the source is initially all vapor should be negligible.

Therefore, for the worst case purpose of this scenario modeling, it should be adequate to model the source as a cloud at its boiling point being discharged over a relatively small ground area. If the specified area is small enough, the dense gas dispersion models will cause the cloud to spread out until the product of maximum take-up flux coupled with initial cloud surface area equals the discharge rate, thus providing a correct steady state source area size. It follows that the dense gas, area source dispersion models, HEGADAS, DEGADIS, and SLAB can be used directly.

Atmospheric Parameters

The given nighttime conditions indicate a PG stability class **E** (See Table 4-1); a 3 m/s wind was used because it is the minimum for the class under the < 3/8 cloudiness condition. Similarly, stability class **C** was indicated for an average wind speed of 4 m/s. These two sets of meteorological conditions should be representative enough to give the worst case estimates required.

The given rural terrain conditions indicate the roughness length parameter should be 0.03 m (Appendix I). An averaging time of 900 s was used.

MODELING PARAMETER RECAP

Released Gas	
Molecular weight	70.9
Specific heat vapor, C_p, KJ/[kg.K]	1.58
Release rates, kg/s	8.9
Source area input, m^2	20
Normal boiling point = gas temperature, K	239
Release duration, s	1800
Roughness length, z_r, m	0.03
Atmospheric Variables	
Stability **C**	
temperature, K	303
wind speed, m/s	4
Stability **E**	
temperature, K	293
wind speed, m/s	3

Simulation

Figures S5-1 and *S5-3* show the resulting centerline concentrations vs downwind distance, while *Figures S5-2* and *S5-4* show 1 ppm chlorine crosswind concentration isopleths. Because SLAB *always* averages the concentrations with respect to release duration, only one simulation was run for each of the two sets of meteorological conditions; the results are labeled "SLAB 1800 s" on the figures. To obtain the finite duration results for HEGADAS, it was necessary to run the steady-state HEGADAS-S program, then use the HSPOST post-processor program to time-average the results with respect to downwind travel time for the 1800 s release duration (curves labeled "HEGADAS 1800 s"). The steady state results for DEGADIS are not corrected for downwind travel time; as noted elsewhere, that requires an external program not currently available.

As expected, the models predict very long distances to the points where chlorine concentration falls below 1 ppm. Note in Figure S5-1 that the distance to 1 ppm chlorine for HEGADAS *without* correcting for release duration is about 100 km, whereas the *corrected* curve shows the distance to be about 46 km!

As expected, the chlorine concentration drops below 1 ppm at long distances, compared with distances where source modeling effects are important. For the **C** stability cases, the 1 ppm points are about 38 km downwind for both the corrected and uncorrected curves. Therefore, it can be concluded that more detailed source modeling is not justified for this case.

Discussion

Using these models to predict concentrations out to such long distances must be considered semi-quantitative, at best. The farther the distance from the source, the more uncertain the estimates will become. If simulations were to be made for **F** stability, the distances would have been much greater than for the **E** stability case shown here.

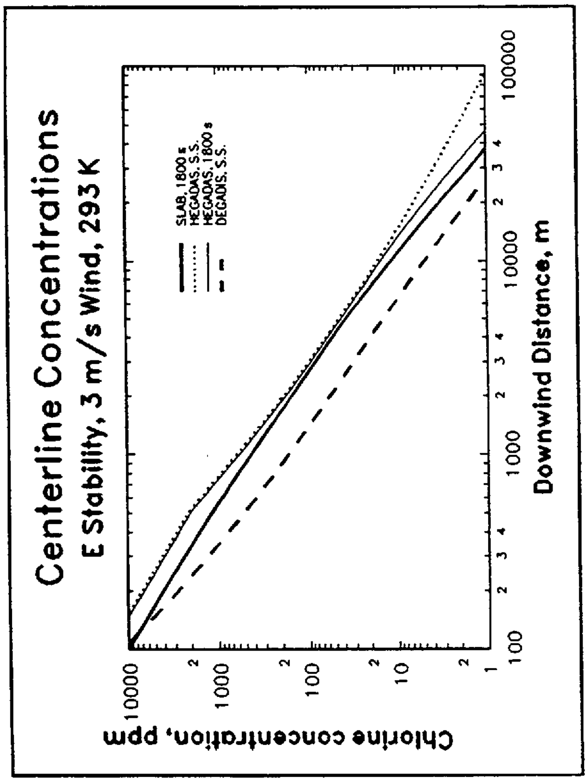

Figure S5-1

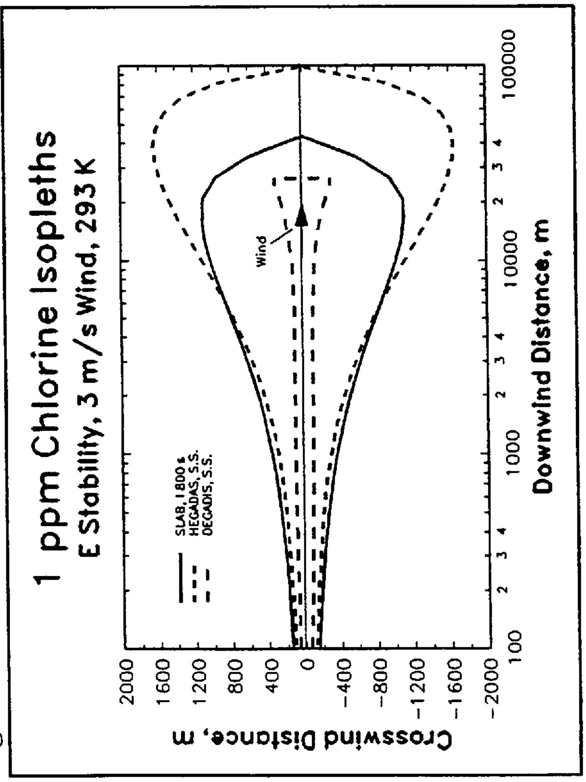

Figure S5-2.

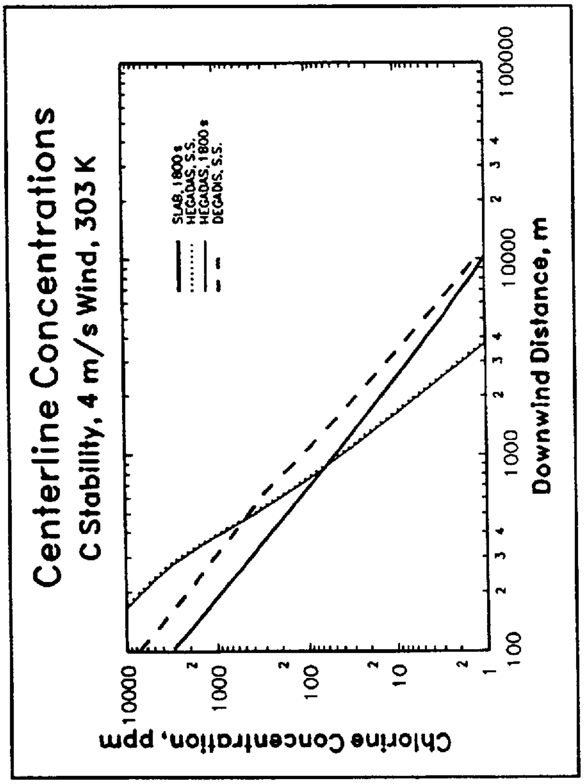

Figure S5-3.

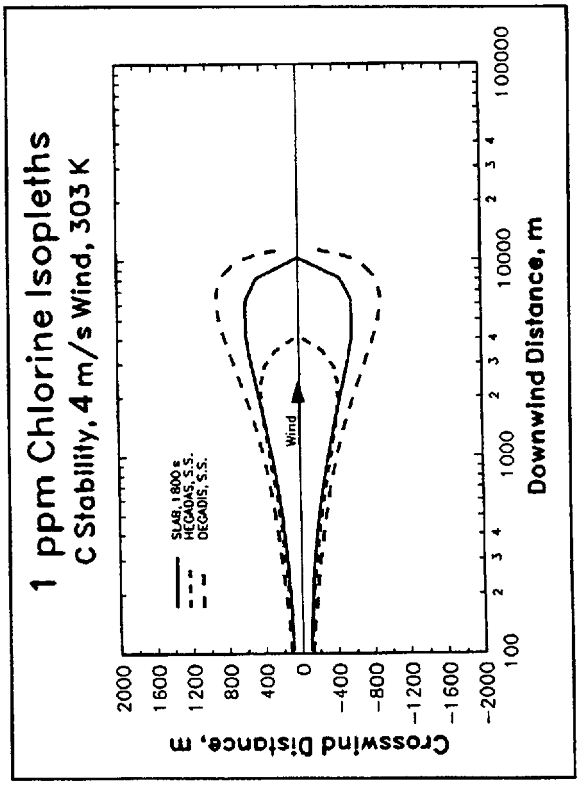

Figure S5-4.

Scenario 6: Ammonia Hose or Pipe Break

Statement

As part of a study on designing, the site of a new railroad tank car and tank truck ammonia loading facility for a very large refinery/chemical plant complex, hazard analyses indicated that possible consequences of hose breakage or accidental disconnection should be investigated. The hose end could whip around to discharge liquid ammonia in any direction, or the pipe to which the hose was connected could discharge the stream in any direction.

Release Attributes

Material: .... *Ammonia*
Method: .... *Hole*
Fluid state: ...... *Flashing liquid*
Chemical reactions? .... *Yes*
Release time type: Finite duration
Turbulent jet: .... *Horizontal*
"Cloud" height: .. *Initially elevated*
Roughness type: ...... *Industrial*
Stability: .... *D*
Averaging time: .... *Various*
Hazard:................. *Toxic*

Upstream automatic control systems are being designed so that if a release such as this occurs, flow can be stopped in a very short time (several minutes or less). To assist the control system designers and management in deciding the design maximum automatic shut-off time, from a safety and best technology standpoint, a modeling study has been requested to estimate the effect of this variable on maximum dispersed concentrations from potential, accidental ammonia releases from the planned facility.

Assume the ammonia in the pressure vessels is in temperature equilibrium with the surroundings, and that the pipes and hoses have inside diameters of 5 cm.

Demonstrate how different release durations and associated averaging times can affect dispersed concentrations.

Analysis

Thermodynamic Considerations

Ammonia is hygroscopic with a heat of solution of roughly 30 kJ/mol, thus this energy may need to be considered when anhydrous ammonia contacts humid air. Also, the vapor pressures of ammonia - liquid water solutions are very non-ideal with respect to the ammonia concentration. Therefore, the release of anhydrous ammonia could possibly involve significant thermodynamic effects not considered by any of the modeling program systems being used here for demonstration purposes. Wheatley [2,.3, 4] extensively studied the phenomena involved in the discharge of liquid ammonia into humid air; this included the complete, realistic simulation of the source thermodyamics followed by dispersion. From the various figures in the first report cited, and particularly Figures 8, 16, and 24 there, it can be concluded from his TRAUMA modeling that relative humidity (range: 0 - 80%) has no significant effect on the prediction of dispersed concentrations. Therefore, the ammonia - liquid water solution effects can be ignored for this modeling.

To simulate releases of fluids which form vapor/liquid aerosols, SLAB requires the normal boiling point temperature, the heat of vaporization (constant), vapor and liquid heat capacities (constants), the liquid density, and constants for the vapor pressure function of temperature. Because NH_3 is non-ideal in its thermodynamic behavior, published data (Perry's Sixth, page 3-170) was plotted and fitted to functions appropriate for use with SLAB. *Figure S6-1* shows that the log of the vapor pressure plotted against reciprocal absolute temperature over the range of interest gives a straight line. SLAB [II.7, page 63] uses the equation

$$\frac{P_{sat}}{P_3} = \exp\left[SPA - \frac{SPB}{(T+SPC)}\right] \tag{1}$$

where *SPA*, *SPB* and *SPC* are constants and *T* is the local temperature. Because the SPC constant is zero here (no curvature, Figure S6-1), taking logarithms of both sides of the preceding equation results in the linear equation:

$$\ln\left(\frac{P_{sat}}{P_3}\right) = SPA - SPB\left(\frac{1}{T}\right) . \tag{2}$$

This was fitted to published data by linear regression with a spreadsheet program. For Equation 2, the slope of the left-hand-side quantity with respect to reciprocal temperature, SPB, can be related to the heat of vaporization by the Clausius-Clapeyron equation (3-2), thus

$$SPB = \frac{\Delta H_{vapor}}{R} . \tag{3}$$

The value of SPB found by regression was –2795 K. The value of SPA is not input to SLAB because the program calculates it from Equation 1 given SPB and the normal boiling point, T_{nbp}.

By Equation 3, the fitted heat of vaporization is 23 MJ/kgmole (R = 8313 J/kgmole). By subtracting the liquid enthalpy from the vapor enthalpy at 300 K *(Figures S6-4 and S6-3*, respectively), the heat of vaporization is about 20 MJ/kgmole. This difference is acceptable considering other inaccuracies in the overall modeling; the fitted model was used here (converted to the mass basis).

The liquid density and enthalpy were fitted by regression to quadratic functions of temperature; these are the continuous lines shown in *Figure S6-2* and Figure S6-4. Resultant function-calculated values for 300 K were input to SLAB. Because the modeling programs require constant vapor heat capacities, $C_{p,r}$ this value was found as the slope of the straight line fitted to the vapor

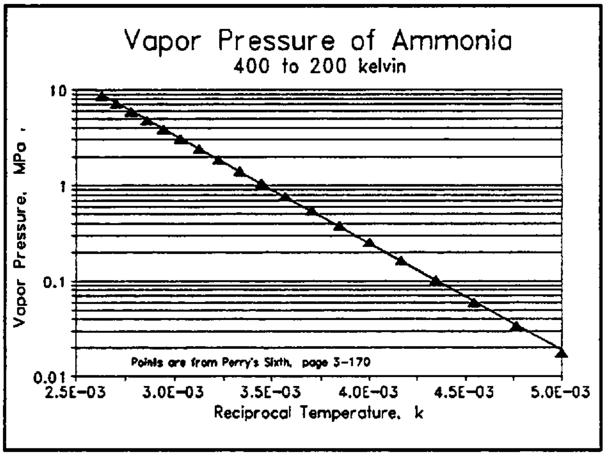

Figure S6-1.

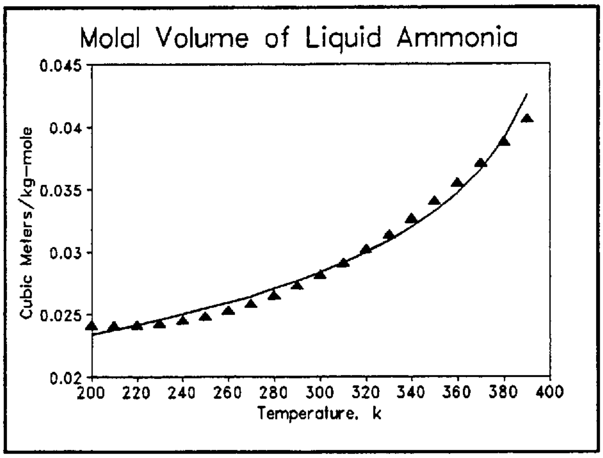

Figure S6-2.

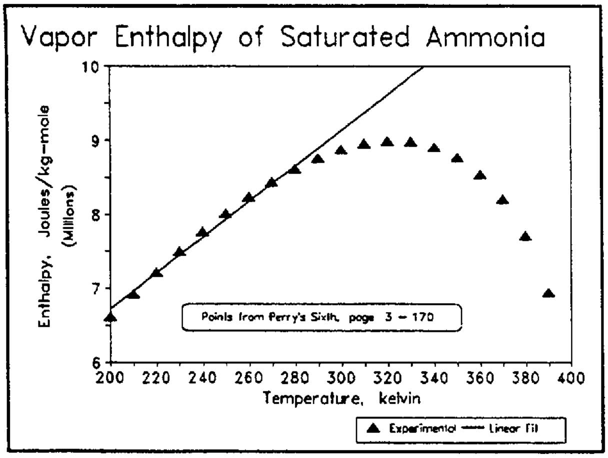

Figure S6-3.

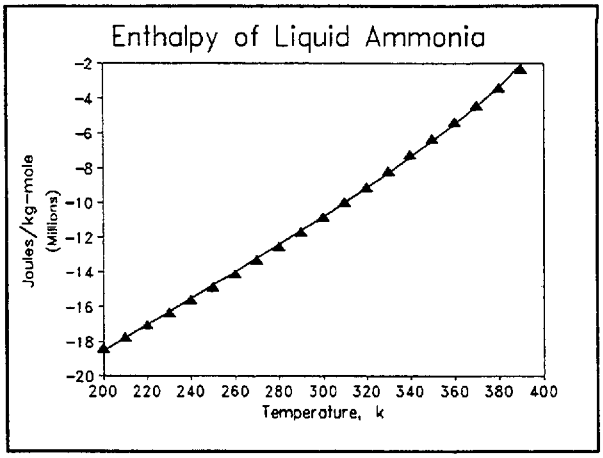

Figure S6-4.

enthalpy as shown in *Figure S6-3.* The mass release rate of 11.67 kg/s NH_3 (Leung-Epstein correlation for flashing liquid choked flow) and expanded jet diameter of 0.0167 m^2 were calculated by the methods of Chapter 3.

A summary of these *thermodynamic* parameters used for modeling are shown in *Table S6-1* for an example SLAB input file. (The program had been modified by the author to carry through the identification information shown in addition to the parameter values and symbols.) Lines starting with an asterisk are comments.

Other Parameters

Horizontal jet releases (1 m above the ground) were simulated because they will result in the highest ground level concentrations in the near and far fields compared with vertical releases. Because the releases are for an industrial complex, $z_r = 0.35$ m is conservatively intermediate between about 1 and 0.1. For simplicity, only one value was used for release rate, jet angle, roughness parameter and atmospheric conditions; see *RECAP* box.

MODELING PARAMETER RECAP

Released fluid properties	**Table 6-1**
Orifice diameter, m	0.05
Initial jet orientation	horizontal
Initial jet elevation, m	1
Ammonia release rate, kg/s	11.7
Roughness length, m	0.35
Atmospheric stability class	D
Ambient temperature, K	300
Wind speed, m/s	4
Release durations	Steady state and 10, 60, 120 s
Averaging times, s	10, 60, 600, 900

Of the three modeling systems, only SLAB has been designed to cope with horizontal and vertical jet discharges of pure component vapor/liquid aerosols. DEGADIS treats only vertical jets, but the information for VLE with varying air content must be calculated externally. HGSYSTEM's PLUME for turbulent jets cannot handle aerosols. Therefore, SLAB was used for most of the modeling, followed by vertical release examples for both SLAB and DEGADIS.

Table S6-1 shows the base case (steady state) set of remaining input parameters for SLAB.

Simulation

Figure S6-5 shows the predicted effects of ammonia release rate duration on downwind *maximum* centerline concentrations for four release durations varying from infinite (steady state) to 10 seconds; the averaging time was held constant at 10 seconds. Note that *SLAB reports the* *maximum concentration of all passing "peaks" by using finite duration release correction to steady state concentrations.* At any particular downwind distance, the program averages the concentration passing by that point with respect to time, noting that dispersion is taking place along the downwind path (σ_x). Thus the longer the distance from the source, the more dispersion along the x-axis occurs. For example, if the release duration is 60 s and the wind speed is 4 m/s, a "puff" will travel 240 m downwind in the 60 seconds. Beyond the 240 m point (not shown on the graph), a pulse will be observed at further distances; the pulse broadens with respect to downwind distance as that distance increases. Thus, the shorter the initial, square-wave pulse (duration of release), the less material will be available for dispersion, so the *maximum* concentrations will decrease with release duration as shown in this Figure. *Figure S6-6* shows the corresponding travel times for peak maxima vs downwind distance.

Table S6-1.

```
                     BASE CASE INPUT FOR SLAB

SLAB Run: Scen. 6. SS, D, 4 m/s, 300K, Tav= 10s, Ht.= 1m
File name:   ASSG01L.SLI
*    (Data column is width = 12.)
* Miscellaneous
*
           2 idspl = spill type (HORIZONTAL JET = 2)
           1 ncalc = sub-step multiplier
*
* Release Gas Properties
*
   0.01703   wms   = molecular weight of source
    1413.4   cps   = vapor heat capacity, Cp, (J/kg-K)
    239.75   tbp   = boiling point temperature
    0.7426   cmed0 = liquid mass fraction
1.3682E+06   dhe   = heat of vaporization (J/kg)
    4310.4   cpsl  = liquid heat capacity (J/kg-K)
     600.2   rhosl = liquid source density (kg/m3)
2794.69      spb   = saturation pressure constant (K)
       0.0 spc     = saturation pressure constant (K)
   239.75    ts    = temperature of source gas (K)
*
*  Spill Characteristics
*
     11.67 qs      = mass source rate (kg/s)
    0.0167   as    = source area (m2) - EXPANDED JET
   20000.0 tsd     = continuous source duration (s)
       0.0 qtis    = instantaneous source mass (kg)
       1.0 hs      = source height (m)
*
* Field Parameters
*
      10.0 tav     = concentration averaging time (s)
   10000.0 xffm    = maximum downwind distance (m)
       0.0 zp(1)   = concentration measurement height (m)
      1.00 zp(2)   = concentration measurement height (m)
       0.0 zp(3)   = concentration measurement height (m)
       0.0 zp(4)   = concentration measurement height (m)
*
* Boundary Layer & Meteorological Conditions
*
      0.35 z0      = surface roughness height (m)
      10.0 za      = ambient measurement height (m)
      4.00 ua      = ambient wind speed (m/s)
     300.0 ta      = ambient temperature (K)
       50. rh      = relative humidity (percent)
       4.0 stab    = atmospheric stability class value
       0.0 ala     = inverse Monin-Obukhov length (1/m)
         0          END OF INPUT PARAMETERS
```

Figure S6-7 illustrates the effect of various averaging times for a constant ammonia release duration of 60 s. Here, as the averaging time increases, an observer at a downwind location will "see" a passing peak, and if the averaging time is long enough, many very low (and/or zero) concentrations will contribute to the averaged concentration, thus effecting lower average values the longer the averaging time.

Finally, SLAB and DEGADIS were run to simulate the ammonia release for a vertical jet at the same release height (1 m) for the time conditions shown in *Figure S6-8.* A detailed comparison of the SLAB curve with the corresponding horizontal release curve in Figure S6-1 showed that the horizontal case gave higher concentrations over the whole distance shown. The DEGADIS curve differs from the SLAB curve by a factor of about 2. The relative effects of release durations and averaging times would be the same as for the horizontal jet cases. As noted in Appendix II, DEGADIS does not provide the facility to calculate averaging time effects with respect to downwind distance; this must be calculated externally by the user. Because the DEGADIS results have not been corrected for averaging times at downwind distances, the separation between the two curves in Figure S6-8 is confounded with averaging times and differences.

(Figures S6-5 through S6-8 follow.)

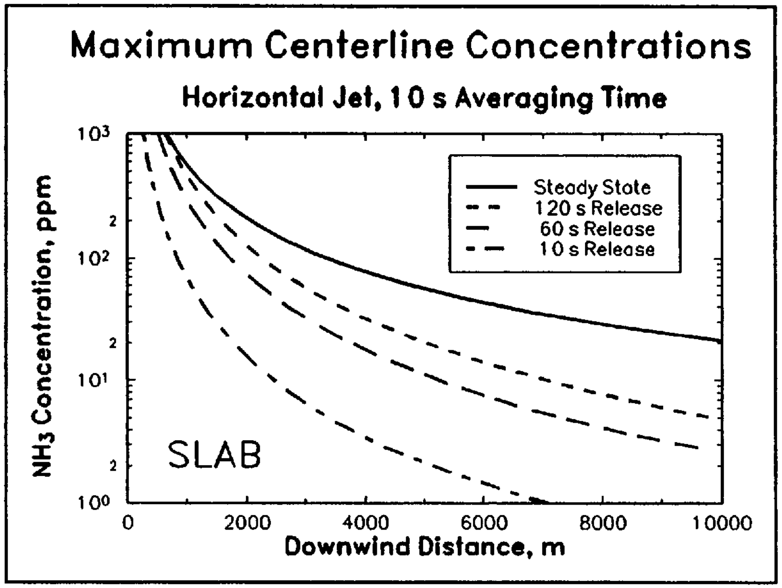

Figure S6-5.

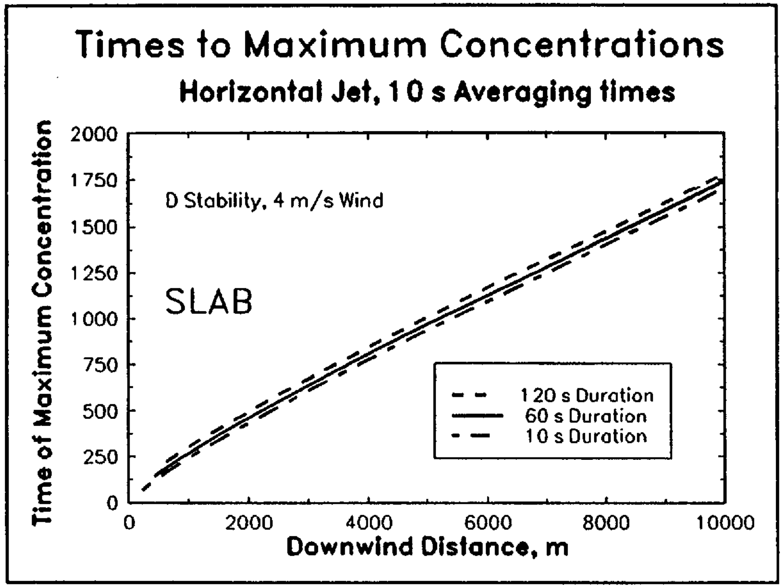

Figure S6-6.

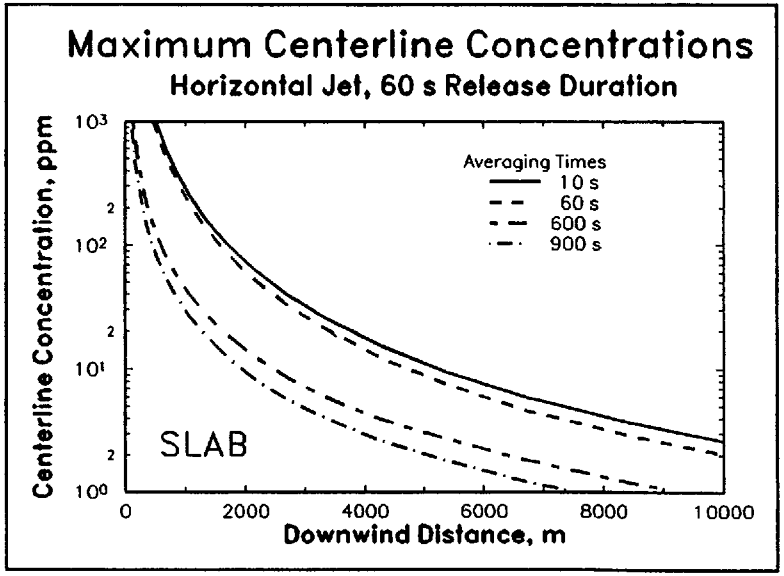

Figure S6-7.

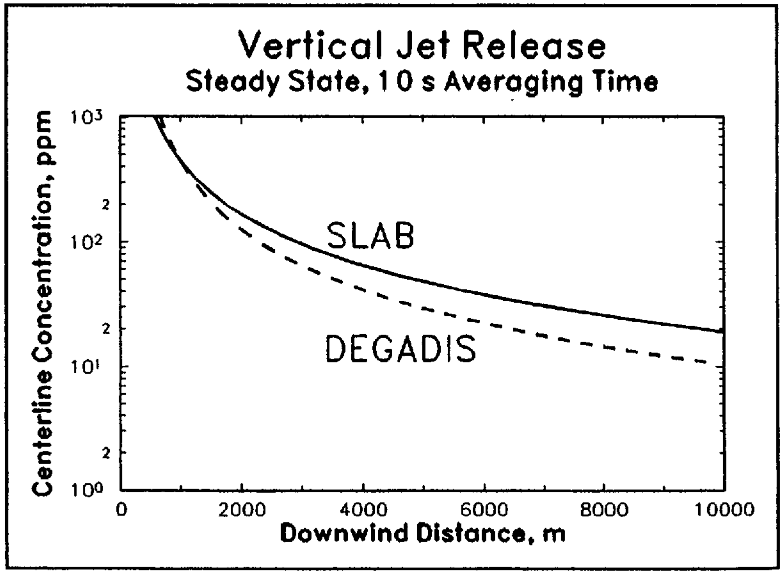

Figure S6-8.

Scenario 7: Hydrogen Chloride Pipe Break

Introduction

This exercise demonstrates typical procedures that may be used to model water spray barrier mitigation effects by means of a ground level hydrogen chloride plume release. The presentation differs from other scenarios in this chapter in that it is a step-by-step presentation of methods, rather than an analysis and solution of a given problem. These methods are, in general, applicable to the removal of other chemicals and/or other barriers (*e.g.*, steam curtains, vapor fences) provided their specific effects can be quantified.

Scenario Objectives

1. *Demonstrate modeling of water spray barrier mitigation effects on an HCl vapor cloud.*
2. *Show how the parameters for the mitigated plume are calculated from pre-barrier plume parameters for restarting the dispersion modeling after the barrier location.*
3. *Show how results from time-dependent modeling can be bounded by steady state modeling.*

Using the general concepts presented in Chapter 5, unmitigated and water-spray-barrier mitigated finite duration HCl jet releases are modeled with HGSYSTEM (see Appendix II). The individual spray barrier effects of spray-induced air entrainment and/or removal of HCl from the plume are compared. Parameters for the spray barrier operation were calculated by McQuaid's downflow correlation presented in Chapter 5. HGSYSTEM was used for the modeling because it contains a horizontal turbulent jet model (PLUME), and the parameters of the plume can be externally redefined downwind of the release point. The germane model input files, and the output file from PLUME (needed for plume parameter redefinitions) are listed in Appendix III. Modeling results are presented graphically following this text.

The parameter values used in the "design" of the water spray barrier should not be considered as typical for other applications, for the purpose of this presentation is to demonstrate a *methodology* for modeling the effects of barriers on plume dispersion.

Scenario Description

Anhydrous hydrogen chloride is released from the vapor space of a pressure vessel through a 2.54 cm hole (*e.g.*, a broken pipe) to form a turbulent jet plume flowing horizontally; the hole is 1.0 m above the ground.

Parameters for the release from the vessel as well as environmental parameters are given in *Table S7-1*.

The sequence of events after the release begins is:

1. A water spray curtain, which fully intercepts the plume, is turned on 90 s after the start of the release.
2. The constant rate release is stopped at the source 270 s after it begins.

Estimates of maximum HCl concentrations downwind of the release are required as a function of time and distance. Also, a recommendation is sought for the down-

Table S7-1.

RELEASE PARAMETERS	
Hydrogen Chloride Properties	
Molecular weight	36.46
Normal boiling point, C	-85
Heat Capacity = C_p, J/[mol•K]	29.08
Heat capacity ratio, C_p/C_v	1.41
Source:	
Vessel contents	
Temperature, C	26.9
Pressure, kPa	800
Hole diameter, mm	2.54
Horizontal jet height, m	1.0
Discharge coefficient	1.0
HCl mass flow rate, kg/s	***1.06***
Release duration, s	270
Atmospheric Boundary Layer:	
P-G Stability Class	E
Wind speed, m/s	3.0
Wind speed height, m	10
Ambient temperature, K	273
Relative humidity, %	75
Roughness length, m	0.5
Averaging time, s	"Instantaneous"

wind distance to the spray curtain. HCl concentrations less than 1 ppm are not of immediate interest.

Source and Spray Curtain Parameters

Release Rate

Because the vessel pressure is greater than about twice atmospheric, flow through the hole is choked, or critical. Equation 3-69 for choked flow of an ideal gas was use to calculate the mass flow rate of 1.06 kg/s using the properties for HCl shown in Table S7-1. The properties were taken from Perry's Sixth. A discharge coefficient of 1.0 was used to be conservative.

Turbulent Jet Simulation

The PLUME turbulent jet model for inert gases in HGSYSTEM contains a submodel which calculates the expanded jet parameters given the fluid stagnation temperature, orifice diameter, mass flow rate, gas molecular weight, and gas specific heat. The model assumes an ideal gas expands adiabatically (cf. Equations 3-103 to 3-106). The PLUME input data file is listed in *Appendix III*, which also shows other parameters required. Note that the DURATION value serves the only purpose of causing a partial input file for HEGADAS to be produced in addition to the jet simulation results file. The relative humidity had to be set to zero, otherwise the low temperature below the freezing point of water caused the program to halt with messages to the effect that this was an illegal situation.

A water spray curtain must be physically designed and located so that all of any anticipated plume is totally intercepted, and efficient mass transfer of the released material to the liquid water droplets obtained. The curtain should be located far enough away from the process equipment to avoid punch-through of the plume by momentum processes, yet as near as possible to the equipment to minimize costs associated with barrier size and water flow capacity. Also, spacing concerned with maintenance and vehicle access are among the variables to be considered.

The jet simulation output file from PLUME (listed in Appendix III) show a table of plume parameters as a function of downwind distance (Column 1). Note that the program found a flash temperature of -59 C (top right corner of the listing), whereas the correct temperature should be the normal boiling point of HCl, (-85 C), because the vapor is saturated at the storage temperature. This discrepancy is caused by use of the ideal gas equation for the adiabatic expansion. If the expanded gas temperature had been taken as -85 C, then the fraction vaporized according to Equation 3-52 could be found. However, the versions of PLUME and HEGADAS employed do not treat aerosols. This approximation of using all vapor release instead aerosol for the expanded jet and initial stages of downwind dispersion should not cause significant errors for the *far field* concentration estimations. On the other hand, significant underestimates could be incurred for the *near field* with this use.

Referring to the tabular part of the PLUME output, Column 4 shows that the jet's velocity has dropped to about 10 percent of its original value (wind speed at 1 m height is about 2 m/s), Column 6 shows that the temperature (15.3 C) is close to ambient (15.0C), the mole percent HCl in the homogeneous cross-section (Column 7) has dropped to about one percent., and the plume density of 1.23 kg/m^3 is the same as the ambient air. Thus, it might be assumed that a curtain barrier located at 12 m from the release source is acceptable; this downwind distance was used for the simulations.

Water Spray Curtain Plume Modification Parameters

Downward pointing water sprays were assumed, with appropriate spray water droplet size and flow rates to give an HCl scrubbing efficiency $\varepsilon = 93$ %. Items 9–14 of *Table S7-2* shows other parameters used for the sprays. Item 15 was found by dividing the plume diameter by the nozzle spacing. Item 17 was calculated by Meroney's Equation 5-6, and Item 18 by Equation 5-16. With the water flow rate per nozzle of 0.005 m^3/s (Item 19), McQuaid's correlation (Equations 5-10 and 5-11) was used to obtain the concentration reduction ratio α = 2.76 which corresponds to a dilution factor $1/\alpha$ = 0.363. Using this information, the three characterizing plume parameters, effective plume diameter, mean concentration, and total mass flow rate of released material in the plume (D, β, and E^{br}), were calculated for the plume leaving the barrier.

Table S7-2.

Development of Spray Curtain Plume Mitigation Parameters

	Parameter Description	Symbol	Value/Units
	Parameters from HGSYSTEM's PLUME		
1	Release rate of material at source	E_{br}	1.06 kg/s
2	Downwind distance of curtain from source	x	12.00 m
3	Horizontal plume diameter (top hat)	D	4.64 m
4	Horizontal plume velocity	U_{plume}	7.03 m/s
5	Temperature of plume	T_{plume}	15.30 C
6	Released material concentration	β	1.03 % vol
7	Density of plume	ρ	1.23 kg/m^3
8	Total mass flow rate of the plume	$dmdt$	83.00 kg/s
	Spray curtain parameters:		
9	Curtain is downward pointing water sprays.		
10	Water pressure to nozzles	P_w	551,000 Pa
11	Diameter of spray cross-section on ground	D_{spray}	4.00 m
12	Horizontal nozzle spacing	L_{nozz}	1.00 m/nozzle
13	Density of liquid water	ρ_w	1,000 kg/m^3
14	Scrubbing efficiency of spray curtain	ε	93 %
	Dependent parameters:		
15	No. of nozzles to just cover plume width	N_{pwnoz}	4.64
16	Pre-spray plume volumetric flow rate	U_{ns}	67.48 m^3/s
17	Meroney's cloud area for air entrainment	A_s	58.31 m^2
18	Mass fraction material remaining in plume	f_s	0.0700 fraction
	From McQuaid's correlation		
19	Water flow rate (per nozzle)	U_w	0.005 m^3/s
20	Nozzle flow number	F_n	6.376e-06
21	Correlating parameter	Φ	1.331e-05
22	Ratio ex correlation	U_e/U_w	5,106.12
23	Entrained air volumetric flow rate (1 nozzle)	U_{el}	25.53 m^3/s
24	Entrained air to plume	U_e	118.46
25	Concentration reduction ratio	α	2.76
26	Dilution factor	$1/\alpha$	0.36
27	Post-barrier plume diameter	D'	7.70m
28	Spray air entrainment velocity	u_e	2.03 m/s

The above-mentioned three parameters from PLUME's output at 12 m downwind (two leftmost columns of *Table S7-3*), must be redefined for input to HEGADAS. These must be mapped into the HEGADAS input parameters shown (rightmost two table columns) by multiplying the values of the PLUME parameters by the factors shown in the center column of the table. (This mapping is done automatically in HGSYSTEM for non-mitigated plumes.)

Table S7-3.

Parameter Symbols, and Conversion Factors from PLUME to HEGADAS

PLUME	Symbols	Factor	HEGADAS	Symbols
Plume diameter, m	$D = D^{PL}$	0.4165	Effective cloud half-width, m	$BEFF = b = b_{eff}$
"Top hat" concentration	$beta = \beta = C^{PL}$	0.0141	Centerline ground-level mole fraction emitted gas	$CONC\,S_{br} = c_A = y_{wg}$
Total mass flow rate	E^{br}	1	Total mass flow rate emitted gas, kg/s	E^{br}

HEGADAS Air Dispersion Simulations

To illustrate the various modeling concepts, principles, and phenomena involved in the release scenario, the HEGADAS-S dense gas modeling program was used for steady state modeling of the 1.06 kg/s HCl release as well as the release rate of (1-0.93)(1.06) = 0.0745 kg/s rate for HCl removal from the plume. The concentration results were adjusted for the several combinations of release durations by finite duration factors as discussed in Chapter 5. The scenario was also simulated with the time dependent version of the program, HEGADAS-T. Output from both programs were further processed by the author's Pascal object-based programs which optionally adjust steady state concentrations to finite duration release bases by finite duration factors, and which convert the results (centerline concentrations, x vs y concentration isopleths given z, and x vs y vs concentration surfaces) into files formatted for input to commercial plotting programs.

Steady State and Finite Duration Simulations

Six cases were simulated with the steady state dispersion program:

- ***Steady state.*** HCL mass flow rate = 1.06 kg/s, no mitigation, infinite release duration (line 1 of *Table S7-3*)
- ***No barrier, 270 s release.*** As above, but steady state results adjusted for 270 s duration
- ***No barrier, 90 s release.*** As above, 90 s duration
- ***Spray air only, 90 s release.*** Parameters per line 2 of Table S7-3, 90 s duration
- ***Spray curtain removal only, 90 s release.*** Parameters per line 3 of Table S7-3, 90 s duration
- ***Spray curtain removal and spray air injection.*** Parameters per line 4 of Table S7-3, 90 s duration

Table S7-4 presents the parameter values in reference the steady state *Base Case* used in the HEGADAS-S input files for the simulations. The Base Case input file is listed in Appendix III. The listing has been annotated to show the parameters changed for the subsequent simulations★. All steady simulations used the "instantaneous" averaging time defined in HGSYSTEM.

★ If an averaging time (AVTIMC) less than or equal to 18.75 is assigned, both HEGADAS programs use that as a flag to assign "instantaneous" averaging times; if AVTIMC > 18.75, the actual value is used for the averaging time.

Table S7-4.

Vapor Cloud Characterization Parameters for Spray Curtain Barrier Mitigation Simulations

Description		Spray Curtain Barrier		Common	From PLUME		For HEGADAS	
Line	Mitigation Action	Removal ε	Spray Air $1/\alpha$	HCl Flow E^{br}	Diameter D	Conc. β	Half-Width BEFF	Conc. CONCS
1	Unmitigated Base Case (no spray curtain)	0	0	1.064	4.64	1.03	1.933	0.01452
2	Spray curtain air entrainment only	0	0.363	1.064	7.702	0.3738	3.208	0.00527
3	Removal only by spray curtain	93%	0	0.0745	4.64	0.0721	1.933	0.00102
4	Removal and entrainment	93%	0.363	0.0745	7.702	0.0262	3.208	0.00037

Plume volume reduction for released material removal is assumed to be insignificant.

Resultant cloud centerline concentrations are shown in *Figure S7-1*. (All figures follow this text.) As can be seen, the steady state (infinite duration) release gives the highest concentrations. The second highest curve, for the same release rate but of 270 s duration, has essentially the same concentrations in the near field for downwind distances less than about 1,100 m. The third highest curve (which joins the other two below 1,100 m) shows the important effect of reducing the release duration to 90 s. The last curve in the group, denoted by the △ symbols, shows the near field effect of additional water spray air injected into the cloud at the barrier location; as expected, the HCl concentrations merge with the no-air cases in the far field. The lowest two curves show the permanent effect of 93 % removal of HCl from the plume by the spray curtain. The full mitigation effect curve (★ symbols) shows that the spray air injection reduced the near field concentration below the flammability limit, and that the HCl removal lowered its maximum downwind concentration to less than about 100 ppm beyond 1200 m.

Simulations based on steady state modeling programs, as exemplified here, can be used for quickly screening proposed mitigation procedures. These results will be compared with time dependent modeling results below.

Time Dependent Simulation

HEGADAS-T was used to simulate the combined release duration and spray curtain mitigation effects for the above scenario. Referring to the input file listing in Appendix III, the constant parameters for HCl physical properties and the environment are the same as for the steady state simulations. In the TRANSIT data block, BRKDATA records were input for 5 s time steps with each record of *BEFF*, *CONCS*, and E^{br} according to the scenario action times and parameter values in lines 1 and 4 of Table S7-4. The time dependent solution uses LaGrangian observers, with observed cloud properties obtained as functions of travel time and downwind distances, all based upon solutions of the steady state HEGADAS model. For each specified observation time (TSTAR, see the CALC data block), the program produces a "snapshot" matrix of cloud variables (essentially the same as from HEGADAS-S) where the centerline concentration and other parameters are functions of the downwind distance. The first point for each curve is determined by the program according to sampling time restrictions or by the specified minimum centerline concentration of interest (CAMIN). For the latter, 1 ppm HCl was used.

Figure S7-2 presents the family of centerline concentration vs. downwind distance functions obtained for the specified snapshot times. The curve for 150 s shows that a portion of the cloud had passed by the barrier when the water spray was turned on at 90 s elapsed time; the distance traveled for the front of the cloud at that time was about (90 s) x (2 m/s) = 180 meters. This corresponds to the maximum on that curve.

Because of the specified instantaneous averaging time, the vapor cloud has a very sharp "front." The points 25 m beyond the rightmost ends of the 200 s through 400 s curves fell below 1 ppm, as recorded in the HEGADAS output file. A second maximum appears which was caused by the shut off of the source at 270 s. Finally, as the travel time becomes greater, more dispersion in all three distance axes caused the maxima to merge into one, with concomitant reduction in peak concentrations.

One can envision an "envelope" curve which slopes down diagonally and just touches the rightmost maxima on the time dependent concentration curves of Figure S7-2. *Figure S7-3* is a composite of the preceding figure and three finite duration curves from Figure S7-1. The 270 s release, no barrier effect curve forms a downwind envelope boundary for all of the time dependent curves, with the maxima for the longer time curves tend to approach the 90 s release, no barrier curve. This is reasonable because some of the cloud had passed the barrier before the spray removal process was initiated. Also, the second, lower maxima tend to approach the 270 s release, barrier on curve before dispersion becomes so great that the concentration transition zone within the cloud disappears.

Figure S7-4 is similar to the preceding one, but the averaging time for the time dependent simulation is 300 seconds. There is not much difference in the time dependent curves, except at the observation times longer than 400 s, the maximum concentrations are somewhat lower. However, the differences for the two averaging times is not significant considering the inherent modeling uncertainties.

Conclusions

Time-dependent modeling can be used to estimate the effectiveness of mitigation techniques in the near field and to provide guidance on the approximate downwind locations beyond which the simpler far field procedures can be used. Critical parameters for the applicability of the time dependent modeling are the rapidity with which the source is varying in time, the averaging time, and the downwind distances of interest. For flammability questions, the averaging time should essentially be "instantaneous" (as defined by the modeling program), and the distances will be fairly close to the source. For toxic exposures, the averaging time usually will be defined externally and be specific for the released material. Downwind distances may be very large because of very low "critical" concentration limits.

For *far field* modeling applications, the specific release mechanism (*e.g.*, turbulent jet, evaporating pool, point source), as well as the effect of barrier-induced scenario air entrainment, eventually become negligible; therefore, only mass transfer removal effects and/or source reduction effects need be modeled. But the distances beyond which these effects become immaterial should be established by appropriate steady state and time-dependent modeling.

To estimate concentration bounds over the distance of interest, the steady state centerline concentration vs downwind distance curves, corrected and uncorrected for travel time averaging, may be able to provide quick, approximate bounds on downwind peak concentrations. Wind speed can be used to roughly estimate how far the concentrations from the highest release rate can travel. But only the time dependent concentration curves can be used to estimate integrated concentration exposures.

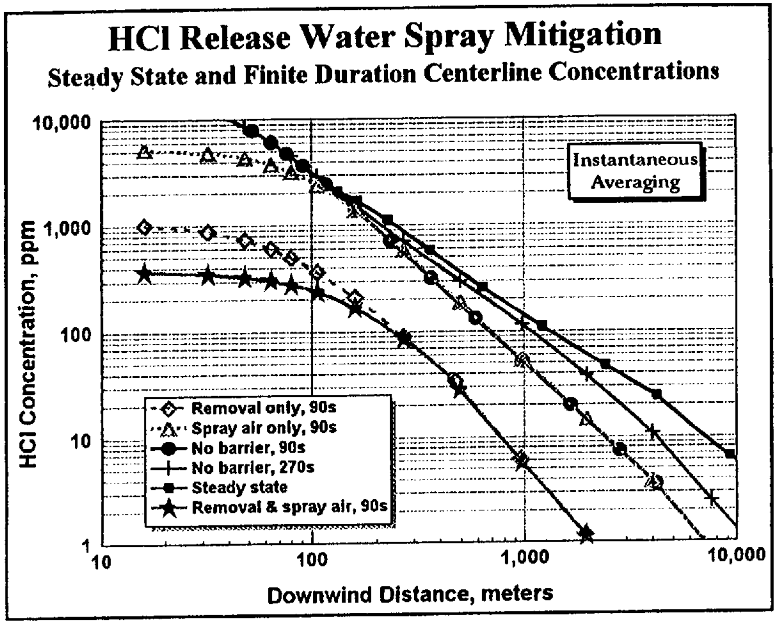

Figure S7-1.

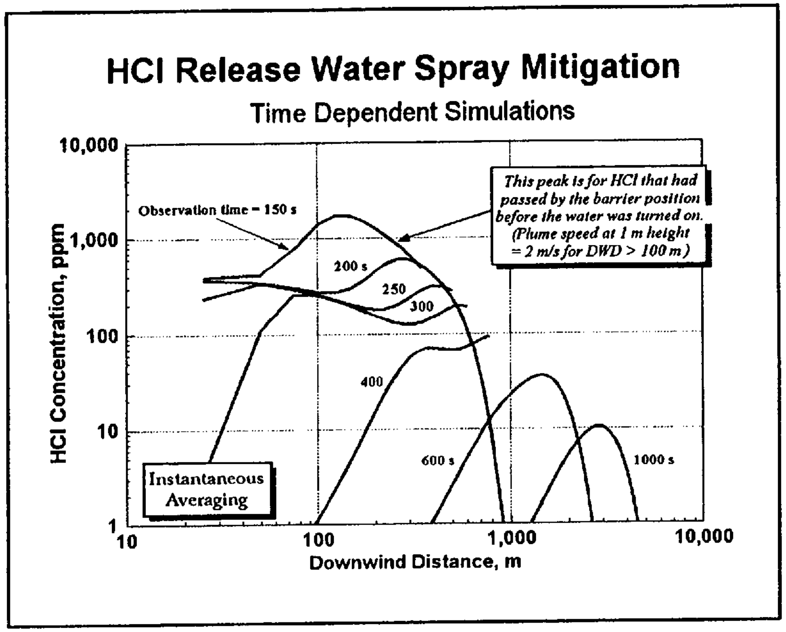

Figure S7-2.

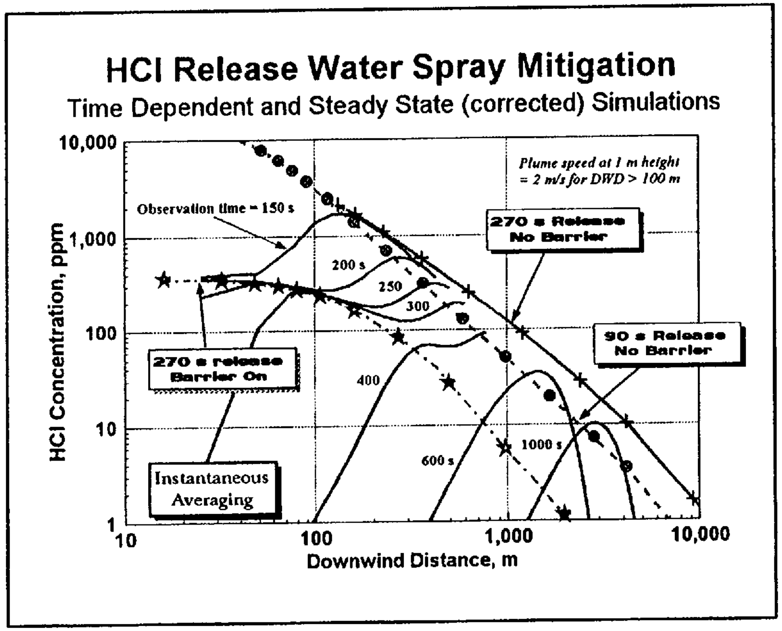

Figure S7-3.

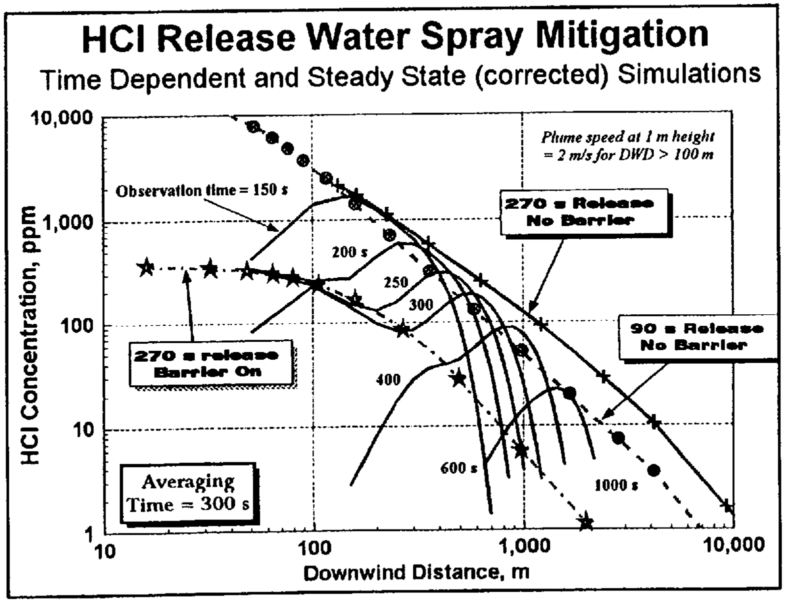

Figure S7-4.

Scenario 8: Evaporating Pool of Liquid Benzene

Statement

During construction operations, an outlet line on the bottom of a benzene storage tank is sheared off. The discharge continues for 30 minutes before it is stopped. The diked tank is located in the tank farm of a large refinery/chemical plant complex surrounded by urban and suburban populated areas. The minimum distance from this particular tank through the complex to the company fence line is 195 meters. Tank size and information needed for discharge rates as well as dike dimensions are given.

Release Attributes	
Material:	*Benzene*
Method:	*Evaporating pool*
Fluid state:	*Liquid*
Chemical reactions?	*No*
Release time type:	*Steady state*
"Cloud" height:	*Ground level*
Roughness type:	*Industrial/Suburban*
Stability:	*D*
Averaging time:	*10 min.*
Hazard:	*Toxic*

Assume the potential release could occur in the morning of a warm day with full cloud cover.

Required are estimates of downwind maximum concentrations of benzene as well as comparative plume areas shown by 1 and 50 ppm benzene concentration isopleths. The effect of wind speed is also of interest. Use a 10 minute averaging time for all concentration estimates.

Analysis

Source/Release Parameters

Because the normal boiling point of benzene, 353 K, is below any possible ambient temperature, the evaporation from the liquid pool formed by the release will be by convective mass transfer into the wind. The mass transfer rates were therefore calculated using Equations 3-119 through 3-122 to find the evaporative mass transfer coefficient for the constant area pool. Physical properties required for these calculations were obtained from Chapter 3 of Perry's Sixth; see *Table S8-1.*

Table 8-1.

BENZENE PROPERTIES	
Normal boiling point, K	353.25
Molecular weight	78.11
(Following are for 300 K)	
Liquid density, kg/m^3	871.8
Kinematic viscosity of vapor in air, m^2/s (v)	1.53E-05
Molecular diffusivity of vapor in air, m^2/s ($\mathcal{D}$)	7.70E-06
Vapor pressure, Pa	1.382E+04

Table 8-2.

STORAGE TANK PARAMETERS Liquid Benzene Release	
Tank diameter, m	8.0
Tank height, m	5.5
Initial liquid level, m	5.0
Square diked area side, m	11.6
Height of dike, m	3.3
Discharge pipe diameter, cm	7.62
Dike area less tank area, m^2 (area for evaporation)	84.3
Temperature of contents, K	300

The various tank and dike dimensions, along with the liquid level in the benzene tank, are given in *Table S8-2.*

The pressure corresponding to the liquid head 5.0 m was calculated to be *43.18 kPa* (= 5.0m•871.8 kg/m^3 • 9.80665★ m/s^2/1000). Using the liquid orifice Equation 3-74 for the flow from the 7.62 cm discharge pipe, the mass flow rate is 39.57 kg/s. This gives a volumetric flow of *0.04539 m^3/s.*

The liquid volume discharged in the 30 minutes is 81.7 m^3 or 71,228 kg, which corresponds to a pool depth of

---

★ This is the gravitational constant. Also, more significant figures are shown than can be justified so the calculations can be "tracked."

0.97 m. However, the time required to just cover the floor of the diked area with liquid would be very small, so steady state dispersion models were used.

For wind speeds *(u)* of 4.0 and 8.0 m/s (see later), the evaporation fluxes are $1.868 \cdot 10^{-3}$ and $3.421 \cdot 10^{-3}$ kg/[$m^2 \cdot s$], respectively, using the convective mass transfer equations. For the pool area of 84.3 m^2, these values give corresponding total emission rates of 0.157 and 0.288 kg/s.

Other Parameters

The specified atmospheric conditions indicate neutral stability, Class **D**. With this the principal wind speed used was 4 m/s, and to demonstrate the effect of a higher value, 8 m/s was also used.

Two roughness parameter values were used. For the plant complex area, z_r = 1.0 m was used with HEGADAS to the 195 m distant fence line, then z_r = 0.1 for the urban/ suburban area beyond. To show upper concentration bounds, a constant z_r = 0.1 m was also used with this model. Because this parameter must be constant with SLAB and DEGADIS, z_r = 0.1 m was used.

MODELING PARAMETER RECAP

Source Information	
Benzene properties	**Table S8-1**
Storage tank data	**Table S8-2**
Liquid discharge rate, kg/s	39.6
Liquid discharge rate, m^3/s	0.04539
Liquid discharge time, s	1800
Volume discharged, m^3	79
Release rates, kg/s	
4 m/s wind speed	0.157
8 m/s wind speed	0.288
Source area, m^2	84.3
Evaporation fluxes, kg/[$m^2 \cdot s$]	
4 m/s wind speed	$1.87 \cdot 10^{-3}$
8 m/s wind speed	$3.42 \cdot 10^{-3}$
Atmospheric Conditions	
Stability Class	D
Wind speeds, m/s	4, 8
Ambient temperature, K	300
Averaging time, s	600
Roughness Lengths, m	
HEGADAS (plant/surroundings)	
Breakpoint case	1.0/0.1
Uniform case	0.1/0.1
DEGADIS and SLAB, all cases	0.1

Simulation

HEGADAS, DEGADIS, and SLAB steady state model versions, with the above area source parameters, were used to estimate the benzene dispersion for the five cases noted in the legends in the figures. It was not necessary to correct the concentrations for downwind travel time averaging, because with a release duration of 30 minutes and a 4 m/s wind, the distance traveled by a cloud section is 7,200 m compared with the largest downwind distance of interest of about 1,500 m.

Figure S8-1 presents cloud centerline (maximum) concentrations vs downwind distances for the five cases, with corresponding plots for 1 ppm benzene isopleths in *Figures S8-2* and *S8-3*. In the first graph, the HEGADAS curve for the 1.0/0.1 z_r case is significantly lower than for the constant z_r = 0.1 m case; roughly half as large throughout the downwind distances.

Note that the 4 and 8 m/s curves for HEGADAS do not differ much although the release rate for 8 m/s is about 1.8 times that of the lower wind speed. The small difference between the curves is explained by the compensating inverse effect of wind speed on dispersed concentration.

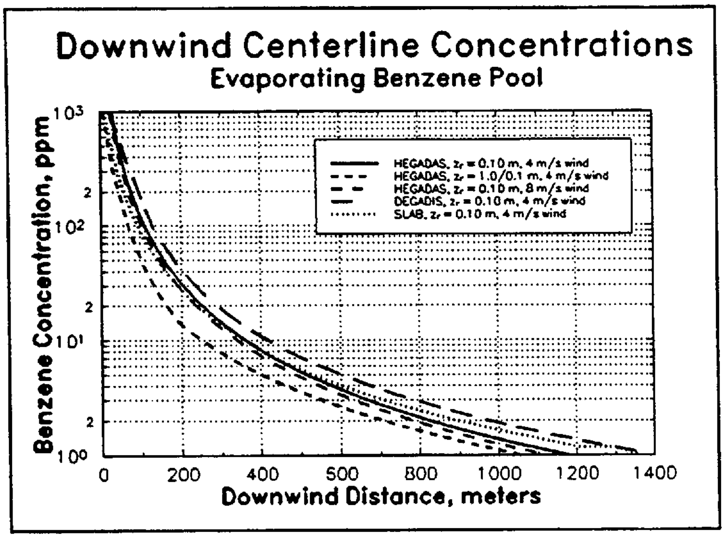

Figure S8-1.

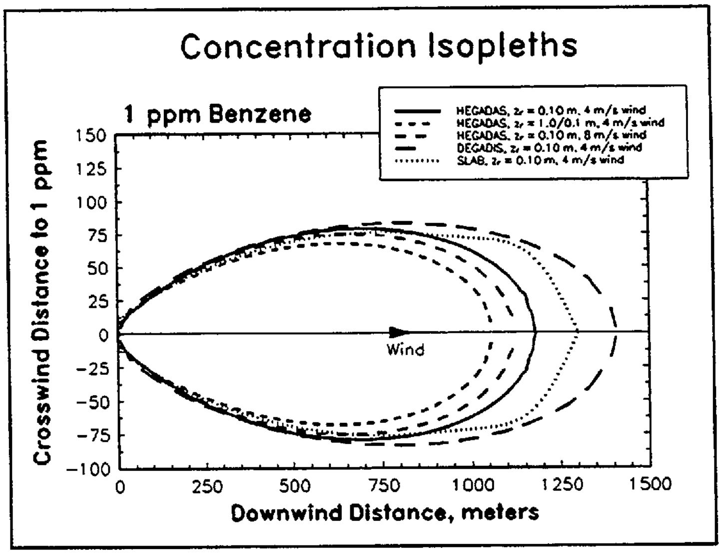

Figure S8-2.

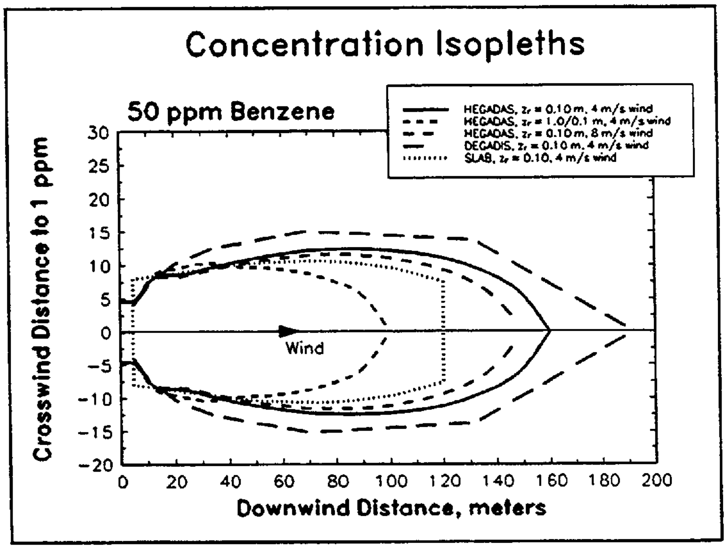

Figure S8-3. Corners and straight segments are caused by connecting the models' output points with straight lines without smoothing.

REFERENCES

REFERENCES

The selected references are organized by Manual chapter and subject.

(Many references are made to **Perry, R.H. and Green, D.W., and Maloney, J.O.**, *Perry's Chemical Engineers Handbook*, 6th edition, McGraw-Hill Book Company, New York (1984). For simplicity, this handbook will also be called: "Perry's Sixth.")

Chapter 3: Source Modeling

Thermodynamics and Physical Properties

1. **American Institute of Chemical Engineers**, Publications Sales, Dept. 345 East 47th Street, New York, NY 10017, Telephone 1-800-AICHEME
2. **American Petroleum Institute,** Publications Catalog, (see latest annual edition), REFINING section, Characterization and Thermodynamics, Petroleum Products, *Techical Data Book - Petroleum Refining, and Technical Data Book Documentation Reports Subsection,* 1220 L Street NW, Washington, DC 20005. Telephone (202) 682-8375
3. **Danner, R. P., and Daubert, T.E.,** *Manual for Predicting Chemical Process Design Data,* Design Institute for Physical Property Data, American Institute of Chemical Engineers, 347 East 47th Street, New York, New York 10017 (1987)
4. **Design Institute for Physical Property Data (DIPPR),** See references 8, 9, 10.
5. **Gess, M. A., Danner, R P., and Nagvekar, M.,** *Thermodynamic Analysis of Vapor-Liquid Equilibria: Recommended Models and a Standard Data Base.* Design Institute for Physical Property Data, American Institute of Chemical Engineers, 347 East 47th Street, New York, New York 10017 (1991)
6. **Perry, R.H. and Green, D.W., and Maloney, J.O.,** *Perry's Chemical Engineers Handbook*, 6th edition, McGraw-Hill Book Company, New York (1984)
7. **Reid, R. C., Prausnitz, J. M., and Poling, B.E.,** *The Properties of Gases and Liquids,* McGraw-Hill, 4th Edition, 800 pages (1986)
8. **Smith, J.M., and Van Ness, H.C.**, *Introduction to Chemical Engineering Thermodynamics,* 4th Edition, McGraw-Hill Book Company, New York (1987)
9. **STN International**, c/o Chemical Abstracts Service, 2540 Olentangy River road, P.O. Box 3012, Columbus, Ohio 43210-0012, Telephone (614) 447-3600 or 1-800-732-4227
10. **Technical Database Services, Inc. (TDS Numerica™)**, 135 West 50th Street, New York, New York 10020-1201. Telephone (212) 247-0587

Flow Rate Estimation

11. **Abdollahian, D., Healzer, J., Janssen, E., and Amos, C.,** *Critical Flow Data Review and Analysis,* Report No. NP-2192, Electric Power Research Institute, 3412 Hillview Avenue, Palo Alto, California 94304 (1982)

12. **American Institute of Chemical Engineers**, *SAFIRE Computer Program (Tape) and Documentation,* Marketing Department, 345 East 47 Street, New York, New York 10017 (1991 Publications Catalog)

13. **American Petroleum Institute,** *Guide for Pressure-Relieving and Depressuring Systems, API Recommended Practice 521 (Second Edition),* 1220 L Street NW, Washington, DC 20005 (September 1982)

14. **American Petroleum Institute,** *Recommended Practice 521: Guide for Pressure-Relieving and Depressuring Systems*, Third Edition (1990), 1220 L Street NW, Washington, DC 20005, Telephone (202) 682-8375

15. **American Petroleum Institute,** *Recommended Practice 520: Sizing, Selection, and Installation of Pressure-Relieving Devices in Refineries*, 1220 L Street NW, Washington, DC 20005, Telephone (202) 682-8375

16. **Coker, A.K.,** *Size Relief Valves Sensibly,* Chemical Engineering Progress, pp 20-27 (August 1992), *Part 2*, ibid., pp 94-102 (November 1992)

16b. **Simpson, L.L.,** *Estimate Two-Phase flow in Safety Devices,* Chemical Engineering, pp 98-102 (August 1991)

17. **Design Institute for Emergency Relief Systems (DIERS)**, *Emergency Relief System Design Using DIERS Technology*, 538 pp., American Institute of Chemical Engineers, 345 East 47th Street, New York, NY 10017 (1992)

18. **Design Institute for Emergency Relief Systems (DIERS)**, *Emergency Relief Systems for Runaway Chemical Reactions and Storage Vessels, (A Summary of Multiphase Flow Methods)* 200 pp., American Institute of Chemical Engineers, 345 East 47th Street, New York, New York 10017

19. **Design Institute for Emergency Relief Systems (DIERS)**, *SAFIRE Computer Program (Tape) and Documentation (A Computer Program for the Design of Emergency Pressure Relief Systems)*, American Institute of Chemical Engineers, 345 East 47th Street, New York, New York 10017

20. **Fauske, H.K., and Epstein, M.,** *Source Term Considerations in Connection with Chemical Accidents and Vapor Cloud Modeling,* Journal of Loss Prevention in the Chemical Process Industries, 1, pp 75-84 (1988)

21. **Fletcher, B.**, *Flashing Flow Through Orifices and Pipes,* Chemical Engineering Progress, pages 76-81 (March 1984)

22. **Hall, D. G., and Czapary, L.S.,** *Tables of Homogeneous Equilibrium Critical Flow Parameters for Water in SI Units,* Report No. EGG-2056, EG&G Idaho, Inc. (September 1980)

23. **Henry, R.E., and Fauske, H.K.,** *The Two-Phase Critical Flow of One-Component Mixtures in Nozzles, Orifices, and Short Tubes,* Transactions of the ASME Journal of Heat Transfer, pp 179-187 (May 1971)

24. **Henry, R.E., and Fauske, H.K.,** *Source Term Considerations in Connection with Chemical Accidents and Vapor Cloud Modeling, pp 251-271,* Proceedings of the International Conference on Vapor Cloud Modeling, Cambridge, MA (1987), CCPS, American Institute of Chemical Engineers, 345 East 47th Street, New York, New York 10017

25. **Hesson, J.C. and Peck, H.E.,** *Flow of Two-phase Carbon Dioxide Through Orifices,* AIChE Journal, **4**, No. 2, pp. 207-210 (June, 1958)

26. **Johnson, R.C.,** *Calculations of the Flow of Natural Gas Through Critical Flow Nozzles,* Transactions of the ASME Basic Journal of Engineering, pp 580-589, (September 1970)

27. **Johnson, R.C.,** *Tables of Critical-Flow Functions and Thermodynamic Properties for Methane and Computational Procedures for Both Methane and Natural Gas,* Scientific and Technical Information Office, National Aeronautics and Space Administration, Washington, DC (1972)

28. **Leung, J.C.,** *Simplified Vent Sizing Equations for Emergency Relief Requirements in Reactors and Storage Vessels,* AIChE Journal, **32**, No. 10, pp 1622-1634 (October 1986)

29. **Leung, J.C.,** *A Generalized Correlation for One-Component Homogeneous Equilibrium Flashing Choked Flow,* AIChE Journal, **32**, No. 10, pp 1743-1746 (October 1986)

30. **Leung, J.C.,** *Size Safety Relief Valves for Flashing Liquids*, Chemical Engineering Progress, pp 70-75 (February 1992). ***Corrections:*** CEP, p. 108 (March 1992)

31. **Leung, J.C., and Ciolek, W.H.,** *Flashing Flow Discharge of Initially Subcooled Liquid in Pipes,* Journal of Fluids Engineering, Transactions of the ASME, **116**, pp 643-645 (September 1994)

32. **Leung, J.C., and Grolmes, M.. A.,** *A generalized Correlation for Flashing Choked Flow of Initially Subcooled Liquid,* AIChE Journal, **34**, No. 4, pp 688-691 (April 1988).

32b **Norris, H.L. III and Puls, R.C.,** *Single a-Phase or Multiphase Blowdown of Vessels or Pipelines*, Paper SPE 26565, 68th Annual Technical Conference and Exhibition, Society of Petroleum Engineers, Houston, Texas (3-6 October 1993)

32c **Norris, H.L. III,** *Hydrocarbon Blowdown of Vessels and Pipelines*, Paper SPE 28519, 69th Annual Technical Conference and Exhibition, Society of Petroleum Engineers, New Orleans, Louisiana (25-38 September 1994)

(Note for the preceding two references. Mr. Norris is now with Scandpower, Inc., 11490 Westheimer, No. 270, Houston, TX 77077. The international company markets the OLGA suite of pipeline dynamic simulation programs.)

33. **NTIS Published Search:** *Critical Multiphase Flow* (1970 - April, 1983) - Citations from the NTIS Data Base, NTIS Access No. PB83-863951, National Technical Information Service, U.S. Department of Commerce, Springfield, Virginia.

34. **NTIS Published Search:** *Critical Multiphase Flow* (1970 - April, 1983) - Citations from the Energy Data Base, NTIS Access No. PB83-863986, National Technical Information Service, U.S. Department of Commerce, Springfield, Virginia. (As of 3/25/91, no later NTIS Published Searches on this subject are listed.)

35. **Van den Akker, H.E.A., and Bond, W.M.,** *Discharges of Saturated and Superheated Liquids from Pressure Vessels. Prediction of Homogeneous Choked Two-Phase Flow through Pipes,* Symposium on the Protection of Exothermic Reactors and Pressurized Storage Vessels, Institute of Chemical Engineers Symposium Series No. 85 (1984)

36. **Van den Akker, H.E.A., Snoey, H., and Spoelstra, H.,** *Discharges of Pressurised Liquefied Gases through Apertures and Pipes,* Fourth International Symposium on Loss Prevention and Safety Promotion in the Chemical Industries, Institute of Chemical Engineers Symposium Series No. 80, pp E23-35 (1982)

Evaporation

37. **Briscoe, F., and Shaw, P.,** *Spread and Evaporation of Liquid,* Prog. Energy Comb. Sci., **6**, pp 127-140, Pergamon Press Ltd (1980).

37b. **Bushnell, D.M., and Gooderum, B.B.,** J. Spacecraft and Rockets, **5**, pp 231-232 (1968)

38. **Cavanaugh, T.A. II, Siegell, J.H., and Steinberg, K.W.,** *Simulation of Vapor Emissions from Liquid Spills,* Paper 92-155.09, Air and Waste Management Association, Pittsburgh, Pennsylvania. (1992) (Also see the technical documentation for HGSYSTEM, version 3.0.)

39. **Cavanaugh, T.A. II, Siegell, J.H., and Steinberg, K.W.,** *Simulation of Vapor Emissions from Liquid Spills,* J. Hazardous Materials, **38** pp 41-63 (1994) (See also Reference 38)

40. **Carslaw, H.S., and Jaeger, J.C.,** *Conduction of Heat in Solids,* Clarendon Press, Oxford (1959)

41. **Fleischer, M.T.,** *An Evaporation/Air Dispersion Model for Chemical Spills on Land,* Shell Development Co., Westhollow Research Center, Houston, Texas. Available through NTIS: Document Access No. PB 83109470, Computer Program Access No. PB 83109181 (Large magnetic tape) (1980)

42. **Hanna, S.R., and Drivas, P.J.,** *Guidelines for Use of Vapor Cloud Dispersion Models,* American Institute of Chemical Engineers, 347 East 47th Street, New York, New York 10017 (1987)

43. **Hesse, David J.,** *Dynamic Model for Liquid Pool Vaporization,* Proc. 1992 Process Plant Safety Symposium, American Institute of Chemical Engineers - South Texas Section, c/o Houston Engineering and Scientific Society, 3121 Buffalo Speedway, Houston, Texas 77098-1823 (February, 1992)

44. **Kawamura, P.I., and Mackay, D.**, *The Evaporation of Volatile Liquids*, Journal of Hazardous Materials, 15, pp 343-364, Elsevier Science Publishers B.V., Amsterdam (1987)

45. **Mackay, D., and Matsugu, R.S.**, *Evaporation Rate of Hydrocarbon Spills on Water and Land*, Canadian J. of Chemical Engineering, **5**, p 434 (1973)

45b. **Fthenakis, V.M.**, (Editor) *Prevention and Control of Accidental Releases of Hazardous Gases*, Van Nostrand Rheinhold, New York, 115 p (1993)

46. **Raphael, J.M.** *Prediction of Temperature in Rivers and Reservoirs*, pp 157-165, Journal of the Power Division, American Society of Chemical Engineers (1962)

47. **Reynolds, R.M.**, *ALOHA™ (Areal Locations of Hazardous Atmospheres) 5.0, THEORETICAL DESCRIPTION*, NOAA Technical Memorandum NOS ORCA-65, National Oceanic and Atmospheric Administration, Hazardous Materials Response and Assessment Division, 7600 Sand Point Way NE, Seattle, Washington 98115, (1992). The ALOHA program is available from: National Safety Council, P.O. Box 558, Itasca, IL 60143-0558, Telephone: 800-621-7619

48. **Shaw, P, and Briscoe, F.**, *Evaporation from Spills of Hazardous Liquids on Land and Water*, Report SRD R 100, Safety and Reliability Directorate, U.K. Atomic Energy Authority, Wigshaw Lane, Cuclcheth Warrington, WA3 4NE (May 1978) (Reference 37 is the condensed paper.)

49. **Sherwood, T.K., Pidgford, R.L., and Wilke, C.R.**, *Mass Transfer*, McGraw-Hill, New York (1975)

50. **Weast, R.C., and Astle, M.J.**, *CRC Handbook of Chemistry and Physics, 63rd Edition*, CRC Press, Inc., Boca Raton, Florida (1983)

51. **Webber, D.M., and Brighton, P.W.M.**, *An Integral Model for Spreading, Vaporising Pools*, Report SRD R 3900, Safety and Reliability Directorate, U.K. Atomic Energy Authority, Wigshaw Lane, Cuclcheth Warrington, WA3 4NE (August 1987)

52. **Wu, J.M., and Schroy, J.M.**, *Emissions from Spills*, presented at Air Pollution Control Association Specialty Conference: "Control of Specific (Toxic) Pollutants," Gainesville, Florida, February 13-16 (1979). Contact: J.M. Schroy, Monsanto Chemical Company, 800 N. Lindbergh Boulevard, St. Louis, Missouri 63137. Telephone: 314-694-1000.

53. **Astronomical Applications Department**, *MICA for DOS, 1990-1999, version 1.0*, U.S. Naval Observatory, 3450 Massachusetts Ave., NW., Washington, DC 20392-5420. Available from NTIS, PB93500163, $US 55

Chapter 4: Meteorology

General:

1 **EPA,** *Guideline On Air Quality Models (Revised),* EPA Report No. EPA-450/2-78-027R, NTIS Report No. PB86-245248, United States Environmental Protection Agency Office of Air Quality Planning and Standards, Research Triangle Park North Carolina 27711 (July 1986)

2. **Hanna, S.R., Briggs, G.A., and Hosker, R.P. Jr.,** *Handbook on Atmospheric Diffusion,* Technical Information Center, United States Department of Energy, Report No. DOE/ TIC-11223 (1982). [Page 33, equation 4.15.]

3. **Smith, M.,** *Recommended Guide for the Prediction of the Dispersion of Airborne Effluents,* ASME Committee on Air Pollution Controls, The American Society of Mechanical Engineers, New York (1968)

4. **Turner, D.B.,** *Workbook of Atmospheric Dispersion Estimates,* Environmental Protection Agency, North Carolina (1974)

4a. **Hosker, R.P., Jr.,** *Methods for Estimating Wake Flow and Effluent Dispersion Near Simple Block-Like Buildings,* NOAA Technical Memorandum ERL, ARL-106, Air Resources Laboratories, Silver Spring, Maryland (May 1981)

Atmospheric boundary layer and diffusion:

5. **Panofsky, Hans A., and Dutton, John A.,** *Atmospheric Turbulence,* John Wiley & Sons, New York (1984)

6. **Pasquill, F., and Smith, F.B.,** *Atmospheric Diffusion,* Third Edition, Ellis Horwood Limited, Publishers, John Wiley & Sons, New York (1983)

Atmospheric properties and meteorological measurements:

7. **ASHRAE,** *Psychrometrics,* Chapter 6, 1989 ASHRAE Handbook, Fundamentals, SI Edition, American Society of Heating, Refrigerating and Air Conditioning Engineers, Inc., Atlanta, Georgia (1989)

8. **EPA,** *On-Site Meteorological Program Guidance for Regulatory Modeling Applications,* EPA Report No. EPA-450/4-87-013, United States Environmental Protection Agency Office of Air Quality Planning and Standards, Research Triangle Park, North Carolina 27711 (June 1987)

9. **EPA,** *Guideline On Air Quality Models (Revised),* EPA Report No. EPA-450/2-78-027R, NTIS Report No. PB86-245248, United States Environmental Protection Agency Office of Air Quality Planning and Standards, Research Triangle Park, North Carolina 27711 (July 1986)

10. **Hanna, S.R., Briggs, G.A., and Hosker, R.P. Jr.,** *Handbook on Atmospheric Diffusion,* Technical Information Center, United States Department of Energy, Report No. DOE/ TIC-11223 (1982). [Page 33, Equation 4.15.]

11. **Smith, M.**, *Recommended Guide for the Prediction of the Dispersion of Airborne Effluents,* ASME Committee on Air Pollution Controls, The American Society of Mechanical Engineers, New York (1968)

13. **Turner, D.B.**, *Workbook of Atmospheric Dispersion Estimates,* Environmental Protection Agency, North Carolina (1974)

14. **Wackter, D.J., and J.A. Foster,** *Industrial Source Complex (ISC) Dispersion Model User's Guide - Section Edition -- Volume I,* TRC Environmental Consultants, Inc., prepared for Office of Air Quality Planning and Standards, U.S. Environmental Protection Agency, Research Triangle Park, North Carolina 27711 (June 1986)

PG Stability Class, Roughness Length and Monin-Obukov Length parameters:

15. **Golder, D.,** *Relations Among Stability Parameters in the Surface Layer,* Boundary Layer Meteorology, 3, pp 47-58 (1972)

Roughness Parameter:

16. **Pielke, R.A.,** *Mesoscale Meteorological Modeling,* Academic Press (1984)

17. **Moser, J.H., Blewitt, D.N., Steinberg, K.W., and Petersen, R.L.,** *HF-HEGADAS Simulation of Dense Gas Dispersion from a Wind Tunnel-Modeled Oil Refinery,* Proceedings of the International Conference and Workshop on Modelling and Mitigating the Consequences of Accidental Releases of Hazardous Materials, May 20 - 24, 1991, New Orleans, Louisiana. American Institute of Chemical Engineers, 347 East 47th Street, New York, New York 10017

Richardson Number Criterion:

18. **Hanna, S.R., and Strimaitis, D.,** *Workbook of Test Cases for Vapor Cloud Source Dispersion Models,* Center for Chemical Process Safety, American Institute of Chemical Engineers, 347 East 47th Street, New York, New York 10017.

Standard Atmosphere:

19. **Weast, R.C., and Astle, M.J.,** *CRC Handbook of Chemistry and Physics, 63rd Edition,* p. F-164, CRC Press, Inc., Boca Raton, Florida (1982)

Geographical Area Classification:

20. **Auer, A.H., Jr.,** *Correlation Land Use and Cover with Meteorological Anamolies,* J. Applied Meteorology, v. 17, pp 636-643 (1978)

Chapter 5: Mitigation Countermeasures

1. **Prugh, Richard W. and Johnson Robert W.,** *Vapor Release Mitigation,* Center for Chemical Process Safety, New York, 1988.

2. **Industry Cooperative HF Mitigation/Assessment Program,** *Vapor Barrier Assessment Program for Delaying and Diluting Heavier-than-Air Hydrogen Fluoride Vapor Clouds,* Summary Report, June, 1989. Available from NTIS.

3. **Meroney, R.N., Neff, D.E., Shin S.H., *et al.*,** *Analysis of Vapor Barrier Experiments to Evaluate Their Effectiveness as a Means to Mitigate HF Concentrations, Fluid Mechanics and Wind Engineering Program,* Colorado State University, Fort Collins, Colorado (1988)

4. **Meroney, R.N.,** *Numerical Simulation of the Mitigation of HF Cloud Concentrations by Means of Vapor Barriers and Water Spray Curtains,* Proceedings of the International Conference on Modeling and Mitigating the Consequences of Accidental Releases of Hazardous Materials, pp. 431–442, American Institute of Chemical Engineers, 345 East 47th Street, New York (May 1991)

5. **Industry Cooperative HF Mitigation/Assessment Program,** *Vapor Barrier Assessment Program for Delaying and Diluting Heavier-than-Air Hydrogen Fluoride Vapor Clouds,* Volume I — Detailed Report (June 1989). Available from NTIS Report No. EEG 10617-1052

6. **Industry Cooperative HF Mitigation/Assessment Program,** *Vapor Barrier Assessment Program for Delaying and Diluting Heavier-than-Air Hydrogen Fluoride Vapor Clouds,* Volume II — Figures and Tables for the Detailed Report (June 1989). Available from NTIS Report No. EEG 10617-1053.

7. **Industry Cooperative HF Mitigation/Assessment Program,** Water Spray Committee, *Effectiveness of Water Spray Mitigation Systems for Accidental Releases of Hydrogen Fluoride,* Summary Report, (June 1989). Available from NTIS.

8. **Meroney, R.N., Neff, D.E.** *Numerical Modeling of Water Spray Barriers for Dispersing Dense Gases,* Boundary Layer Meteorology, **31**, pp. 233-247 (1985)

9. **Atallah, S., Guzman, E., Shah, J.,** *Water Spray Barriers for LNG Vapor Mitigation,* report prepared for Gas Research Institute Report GRE-89/0008, November, 1988.

10. **Moodie, K.,** *The Use of Water Spray Barriers to Disperse Spills of Heavy Gases,* Plant/Operations Progress, **4, No. 4**, pp. 234-241 (1985)

11. **McQuaid, J.,** *The Design of Water-Spray Barriers for Chemical Plants,* Proceedings of the 2nd International Loss Prevention Symposium, Heidelberg. DECHEMA, Postfach 9701 46 Theodor-Heuss-Allee 25, D-6000, Frankfurt, Germany (1977)

12. **Blewitt, D.N., Petersen, R.L., Ratcliff, M.A., Heskestad, G.,** *Evaluation of Water Spray Mitigation System for an Industrial Facility,* Proceedings of the International Conference and Workshop on Modeling & Mitigating the Consequences of Accidental Releases of Hazardous Materials, New Orleans, LA, American Institute of Chemical Engineers, 345 East 47th Street, New York (May 1991)

13. **Industry Cooperative HF Mitigation/Assessment Program,** Water Spray Committee, *Effectiveness of Water Spray Mitigation Systems for Accidental Releases of Hydrogen Fluoride,* Volume I — Detailed Report (June 1989). Available from NTIS: Report No. EGG--10617/DE90 007138.

14. **Industry Cooperative HF Mitigation/Assessment Program,** Water Spray Committee, *Effectiveness of Water Spray Mitigation Systems for Accidental Releases of*

Hydrogen Fluoride, Volume II — Appendices A - D (June 1989). Available from NTIS: Report No. EEG--10617-1036/DE90 007135.

15. **Industry Cooperative HF Mitigation/Assessment Program,** Water Spray Committee, *Effectiveness of Water Spray Mitigation Systems for Accidental Releases of Hydrogen Fluoride,* Volume III {Title pages missing, contains detailed chemical analysis results for the experiments.} (June 1989). Available from NTIS: Report No. UCRL--21214 (Vol 3)/DE90 001099

16. **Industry Cooperative HF Mitigation/Assessment Program,** Water Spray Committee, *Effectiveness of Water Spray Mitigation Systems for Accidental Releases of Hydrogen Fluoride,* Volume V—In Situ Aerosol Measurements 001098. Available from NTIS: Report No. UCRL--21214 (Vol 5)/DE90 001098

17. **Industry Cooperative HF Mitigation/Assessment Program,** Water Spray Committee, *Effectiveness of Water Spray Mitigation Systems for Accidental Releases of Hydrogen Fluoride,* Volume IX and X; *Wind Tunnel Modeling of Fire Monitors for HF Vapor Cloud Mitigation,* Volumes I and II (May 1992). Available from NTIS

18. **Perry, R.H., Green, D.W., and Maloney, J.O.,** *Perry's Chemical Engineers Handbook,* 6th Edition, McGraw-Hill Book Company, New York, (1984). (pp. 5-12 to 5-14 for choked flow).

19. **Hartwig, S.,** *Disaster Mitigation in Process Plants by Water and Steam Curtains,* Proc. 1992 Process Plant Safety Symposium, American Institute of Chemical Engineers - South Texas Section, c/o Houston Engineering and Scientific Society, 3121 Buffalo Speedway, Houston (February 1992)

20. **Hartwig, S. and Barth, U.,** *Der Wirkungsgrad von Dampfvorhängen zur Verdunnung von Schwergasschwaden bei Störfallfreisetzungen {Experimental Investigation of Steam Curtains as Technical Precautions for the Mitigation of Dense Vapor Clouds in a Disturbance Free Setting},* Chem.-Ing.-Tech. 63, No. 10, pp 1026-1027 (1991)

21. **Hartwig, S. and Böke, J.,** *Disaster Mitigation in Process Plants by Application of Foam,* Proc. 1992 Process Plant Safety Symposium, American Institute of Chemical Engineers - South Texas Section, c/o Houston Engineering and Scientific Society, 3121 Buffalo Speedway, Houston, Texas (February 1992)

22. **Hiltz, Ralph H.,** *The Potential of Aqueous Foams to Mitigate the Vapor Hazard from Released Volatile Chemicals,* presented at the International Symposium on Preventing Major Chemical Accidents, Washington, DC (1987)

23. **Fthenakis, V.M. and Blewitt, Doug N.,** *Mitigation of Hydrofluoric Acid Releases: Simulation of the Performance of Water Spraying Systems,* J. Loss Prev. Process Ind., 6(4): pp209-218 (1993)

24. **Fthenakis, V.M.,** *Modeling of Water Spraying of Toxic Gas Releases,* Ph.D. Thesis, Dept. of Applied Science, New York University (1991)

25. **Industry Cooperative HF Mitigation/Assessment Program,** *Effectiveness of Water Spray Mitigation Systems for Accidental Releases of Hydrogen Fluoride,* Volume VII — Computer Programs (June 1991). Available from NTIS.

26. **Fthenakis, V.M. and Zakkay, V.,** *J. Loss Prev. Process Ind.,* 3: p197 (1990)

Chapter 6: Analysis and Simulation of Release Scenarios

Scenario 1:

1a **Hanna, S.R., Briggs, G.A., and Hosker, R.P. Jr.,** *Handbook on Atmospheric Diffusion,* Technical Information Center, United States Department of Energy, Report No. DOE/TIC-11223 (1982). [Page 28, Table 4.1]

1b. **Leahey, D.M. and Davies., M.J.E.,** *Observations of Plume Rise from Sour Gas Flares,* Atmospheric Environment, **18, No. 5**, pp 917-922 (1984)

Scenario 6:

2. **Wheatley, C.J.,** *A Theoretical Study of NH_3 Concentrations in Moist Air Arising from Accidental Releases of Liquefied NH_3, using the Computer Code TRAUMA,* Report No. SRD/HSE/R 393, Safety and Reliability Directorate, U.K. Atomic Energy Authority, Wigshaw Lane, Culcheth, WA3 4NE, England (1987)

3. **Wheatley, C.J.,** *Discharge of Liquid Ammonia to Moist Atmospheres - Survey of Experimental Data and Model for Estimating Initial Conditions for Dispersion Calculations,* Report No. SRD/HSE/R 410, Safety and Reliability Directorate, U.K. Atomic Energy Authority, Wigshaw Lane, Culcheth, WA3 4NE, England (1987)

4. **Wheatley, C.J.,** *A Users Guide to Trauma - A Computer Code for Assessing the Consequences of Accidental Two-Phase Releases of NH_3 into Moist Air,* Report No. SRD/HSE/R 394, Safety and Reliability Directorate, U.K. Atomic Energy Authority, Wigshaw Lane, Culcheth, WA3 4NE, England (1987)

Other:

5. **(Editor),** *One-step Method Determines Sour Water H2S Hazard,* Oil and Gas Journal, pp 55 - 58, (February 24, 1986)

6. **Moser, J.H.,** *H_2S Hazard Analysis for Sour Water Spills: Method Development,* Shell Development Co., Westhollow Research Center, P.O. Box 1380, Houston, TX 77001 (1986)

Appendix II: Modeling Programs

DEGADIS

1. **Havens, J.,** *A Dispersion Model for Elevated Dense Gas Jet Chemical Releases,* Volumes I and II, U.S. Environmental Protection Agency, Report No. EPA-450/4-88-006 (April, 1988)

2. **Havens, J. and Spicer, T.O.,** *Development of an Atmospheric Dispersion Model for Heavier-Than-Air Gas Mixtures,"* U.S. Coast Guard, Final Report No. CG-D-23-85, USCG HQ, Washington, DC (May, 1985)

3. **Spicer, T.,** *Implementation of DEGADIS v2.1 on a Personal Computer,* American Petroleum Institute, 1220 L Street, NW, Washington, DC 20005.

HGSYSTEM

4. **McFarlane, K., Prothero, A., Puttock, J.S., Roberts, P.T. and Witlox, H.W.M.,** *Development and Validation of Atmospheric Dispersion Models for Hydrogen Fluoride. Part I: Technical Reference Manual,* Thornton Research Centre, Shell Research, Ltd. (1990) [Superseded by Reference 6b following.]

5. **Roberts, P.T., Puttock, J.S., and Blewitt, D.N.,** *Gravity Spreading and Surface Roughness Effects in the Dispersion of Dense Gas Plumes,* American Institute of Chemical Engineers Health and Safety Symposium, Orlando, Florida (March 18-22, 1990)

6. **Witlox, H.W.M., McFarlane, K., Rees, F.J., and Puttock, J.S.,** *Development and Validation of Atmospheric Dispersion Models for Hydrogen Fluoride. Part II: HF System User's Manual,* Thornton Research Centre, Shell Research, Ltd. (1990) [Superseded by Reference 6b following.]

6b. **Post, L.** (Editor), HGSYSTEM 3.0. *Technical Manual TNER.94.059 and User's Manual TNER.94.058,* Shell Research Limited, Thorton Research Center, P.O. Box 1, Chester, United Kingdom. Program discs and manual may be ordered from:

HGSYSTEM Custodian
Shell Research Ltd.
Shell Research Centre Thornton
PO Box 1, Chester, CH1 3SH, UK, or by E-mail:
HGSYSTEM@msmail.trctho.simis.com

The handling and shipping charge is £UK 126.50 per copy. U.S. price is about $200; some credit cards are accepted.

SLAB

7. **Ermak, D.L.,** *User's Manual for SLAB: An Atmospheric Dispersion Model for Denser-Than-Air Releases,* Atmospheric and Geophysical Sciences Division, Physics Department, Lawrence Livermore National Laboratory, Livermore, California 94550 (June 1990)

8. **Ermak, D.L., and Chan, S.T.,** *Recent Developments on the FEM3 and SLAB Atmospheric Dispersion Models,* Proceedings of the IMA Conference on Stably Stratified Flows and Dense-Gas Dispersion, Chester, England (1986)

9. **Ermak, D.L., Chan, S.T., Morgan, D.L., and Morris, L.K.,** *A Comparison of Dense Gas Dispersion Model Simulations with Burro Series LNG Spill Test Results,* Journal of Hazardous Materials, **6**, pp 129-160 (1982)

Calm Air Dispersion Dispersion Modeling:

11. **Hanna, Steven R., and Drivas, Peter J.,** *Guidelines for Use of Vapor Cloud Dispersion Models,* American Institute of Chemical Engineers, 345 East 47th St., New York, New York 10017, pp. 58-75, (1987)

12. **Eidsvik, Karl J.,** *A Model for Heavy Gas Dispersion in the Atmosphere,* Atmospheric Environment, **14,** p. 769 (ca. 1980)

13. **Byggstoyl, S., and Saetran, L.R.,** *An Integral Model for Gravity Spreading of Heavy Gas Clouds,* Atmospheric Environment, **17,** No. 9, p. 1615 (1983)

14. **Fay, James A., and Ranck, Dale A.,** *Comparison of Experiments on Dense Gas Cloud Dispersion,* Atmospheric Environment, 17, No. 2, p. 239 (1983)

15. **de Nevers, Noel,** *Spread and Down-Slope Flow of Negatively Buoyant Clouds,* Atmospheric Environment, **18,** No. 10, p. 2023 (1986)

16. **Havens, Jerry A., and Spicer, Thomas O.,** *Development of an Atmospheric Dispersion Model for Heavier-than-Air Gas Mixtures: Volume II - Laboratory Calm Air Heavy Gas Dispersion Experiments,* Report No. CG-D-23-85, U.S. Dept. of Transportation, U.S Coast Guard, Final Report May, 1985. NTIS Accession No. AD-A171-523.

17. **Colenbrander, G.W., and Puttock., J.S,** *Dispersion of Releases of Dense Gas: Development of the HEGADAS Model,* Appendix B in the User's Guide for the HEGADAS™ Heavy Gas Dispersion Program, National Technical Information Service Access No. PB89-164522 (1988)

18. **Puttock, J.S.,** *A Model for Gravity-Dominated Dispersion of Dense-Gas Clouds,*, Proceedings of the IMA Conference on Stably Stratified Flow and Dense Gas Dispersion, Chester, England, Oxford University Press (April 1986)

19. **McQuaid, J.,** (Editor), *Heavy Gas Dispersion Trials at Thorney Island,* Elsevier, New York (1985)

20. **Moser, James H.,** *CADM: A Computer Program for Modeling the Dispersion of Heavy Gas in Calm Air,* Proceedings of the International Conference and Workshop on Modelling and Mitigating the Consequences of Accidental Releases of Hazardous Materials, May 20 - 24, 1991, New Orleans, Louisiana. American Institute of Chemical Engineers, 347 East 47th Street, New York, New York 10017.

Other

21. **S.R. Hanna, J.C. Chang and D.G. Strimaitis,** *Hazardous Gas Model Evaluation with Field Observations,* Atmospheric Environment 27A(15): pp 2265-2285 (1993)

APPENDIX I

RECOMMENDED DEFAULT/STARTING VALUES FOR MODELING PARAMETERS

DEFAULT VALUES FOR MODELING PARAMETERS *

Recommended if, and only if, better estimates cannot be obtained for a particular modeling application.

Parameter Name	Subclass	Remarks	Recom-mended Value	Units of Measure	Text Reference Page(s)
Roughness Length	Industrial	Large refinery/chemical plant complexes	1	m	4-3
	Urban	"Built-up" areas (See Figure 4-2)	0.1		to
	Rural	Agricultural areas, sparse trees and buildings	0.03		4-4
PG Stability Class	Unstable	Warm/hot days, much insolation	A		4-4
	Neutral	Day or night with cloud cover and/or high winds	D		to
	Stable	Cold nights, clear sky, low wind, RURAL	F		4-6
		Cold nights, clear sky, low wind, URBAN	E		
Wind Speed	Stability A	Daytime, high insolation,	2	m/s	4-6
	Stability D	Overcast, "high" winds	4	m/s	
	Stability F	Cold nights, clear sky, low wind, RURAL	2	m/s	
	Stability E	Cold nights, clear sky, low wind, URBAN	3	m/s	
Ambient Temperature	Stability A	Use stability class maximum for locality.		K	4-8
	Stability D	Use stability class mean for locality.			
	Stability F	Use stability class minimum for locality.			
Relative Humidity		Non-reactive fluids, no phase change heat	50	%	4-8
Barometric Pressure		Altitude < 1000 meters, use 1 atmosphere:	101,325	Pa	4-7,8
		Altitude > 1000 m, see Figure 4-4	See Figure 4-4		4-7,8
Wind Direction		Not an input parameter; assume it always blows towards the most sensitive area.			
Wind Speed Measurement Height			10	m	4-7
Receptor Height			0	m	
Averaging Time		For flammability use: (According to health criteria for toxics)	10	s	4-9
Jet Angle		For near- and far-field estimates	Horizontal		See
		For far-field estimates	Vertical		scenarios
Jet Elevation			1	m	
Cp/Cv Ratio		Use only if not available!	1.4		3-13
Orifice Discharge Coefficient			0.6		3-32
Ideal Gas Law Constant (R)		Units: Pascal-kelvin-kilograms-meters (Joules)	8313	SI	
Other source parameters such as release rate and state, thermodynamic and physical properties must be obtained or calculated according to the modeling application.					

These parameter default values should be considered as starting values upon which to base a particular modeling study.

---

* During the final editing of this Manual (June 1996), the U.S. Environmental Agencies promulgated the final Clean Air Act Risk Management Program Rule [40 CFR Part 68, paragraph 112 (r)]. This rule specifies the values of a number of the above default paramenters for rule-defined worst case modeling. In particular, Paragraph 68.22 of this regulation should be consulted if the release modeling application is covered by the rule.

APPENDIX II

OVERVIEW OF SCENARIO MODELING PROGRAMS

Overview of Scenario Modeling Programs

To demonstrate recommended principles and usages for guidance in release/dispersion modeling, three well-known, publicly available computer program systems were used for simulation of the representative scenarios presented in Chapters 2 and 6: HGSYSTEM [4,5,6], SLAB [7,8,9], and DEGADIS [1,2,3]. Although a number of other programs are available, both publicly and from commercial sources (*e.g.*, Hanna, *et al.* [21]), it is believed these three provide good illustrations of the best methods (including judgment issues) to guide modeling applications. For most scenarios, the applicable submodels of each of the three systems were used if possible. However, the type and capabilities of their submodels differ, so it was not always possible to use a particular system for a given scenario. In the one scenario (7), in which the vapor cloud simulation must be redefined externally during the course of solution, only HGSYSTEM provided the necessary handles. A brief overview of the general capabilities and (input) requirements of the modeling program systems is given below, in which important differences are pointed out. Please refer to the *References* section under *Appendix II* for sources of further, detailed technical descriptions of the modeling programs, user's manuals, etc., and to the appropriate user's manuals for detailed use (including the exact composition of input and output files) of the programs.

Models Used

Program	Version
HGSYSTEM	1, Nov90
SLAB	April 1990
DEGADIS	2.1, Dec. 1990

At the time of final editing, May 1996, a new version of HGSYSTEM has been released which has markedly increased capabilities with respect to the version used for this manual. A description of its additional capabilities is at the end of this Appendix and program ordering information is given in Reference II-6b; to the best of the author's knowledge, no later versions of either SLAB or DEGADIS are pending.

Submodels

Table 1 shows the various submodels contained within each of the three modeling systems of interest. Note that only the HFSPILL module in HGSYSTEM contains calculations for the discharge rates and states of either liquid or gas from a pressurized vessel, and currently it handles only HF. These special cases for HGSYSTEM are discussed with the corresponding release modeling scenarios. For materials other than HF, external procedures must be used for these source calculations; see Chapter 3.

Table 1.

Comparison of Modeling System Features

Submodel Type	HGSYSTEM	SLAB	DEGADIS
Time-dependent tank discharge?	Only for HF	No	No
Flow rate through orifice?	Only for HF	No	No
Turbulent Jet?	Yes	Yes	Yes
Jet can point (in a plane perpendicular to the ground):	Any angle	vertically or horizontally	Vertically only
Expanding jet calculations?	Yes	No	No
Dense gas, ground level dispersion?	Yes	Yes	Yes
Elevated plume for far-field dispersion?	Yes	Yes	Yes
Aerosol thermodynamics?	HEGADAS only	Yes	Externally
Pool evaporation models for:			
Boiling on a water surface?	Flux from user	No	No
Boiling on a land surface?	No	No	No
Mass transfer limited on land?	Spreading pool only	No	No

Turbulent Jets and Far-Field Plumes

The three modeling systems contain the optional capability of simulating turbulent jets. Turbulent jets are formed when a fluid is discharged into another fluid (the air, here) with enough momentum to cause intensive mixing for a significant distance down the jet's axis. The mixing occurs very intensely and the rate of air entrainment increases with the energy of the discharged stream. In the near field, before atmospheric dispersion processes become important, many experiments have shown that, for all practical purposes, the jet's properties are circularly symmetrical in the plane normal to the jet's longitudinal axis. In addition, any time-averaged property, such as concentration, temperature and velocity are normally distributed with respect to radial distance from the axis. The original fluid's concentration along the longitudinal axis decreases exponentially; within roughly 50 to 100 initial jet diameters down-axis, the concentration (or other property) will drop to less than say, one to two percent of its initial value.

The jet, or initial plume models of the three systems are generally based on the original work of C. Ooms. Such models employ a set of simultaneous, nonlinear, ordinary differential equations in distance (the longitudinal axis) with mass, momentum and thermal energy balances. Entrainment of air into the jet is effected by means of the *entrainment velocity* concept which is based upon experimental work. Thus they are steady state; time is handled throughout the velocity function if the jet model is used with a following time dependent dispersion model. Some applications require that the fluid's discharge rate (and perhaps composition and properties) be varied with time, thus the jet model was used in the *quasi-steady state* manner in which all properties along the jet change instantly with time. That is, no capacitive effects are treated in transient applications of the jet model.

The principal input to a jet model is the emitted substance's total mass flow rate, its initial temperature, initial diameter, and other parameters by which the fluid's density and other properties (such as air-fluid enthalpies) can be calculated. (A later section describes how the thermodynamic properties are treated by the three systems.) Except for HGSYSTEM, the input, *initial jet parameters should be calculated for the expanded jet at atmospheric pressure by the methods of Chapter 3*. This will give the best estimates for plume rise or fall, and near field concentrations.

The jet models in HGSYSTEM, PLUME (for non-reacting or inert fluids) and HFPLUME (for HF) are designed to simulate jets pointing at any angle to the ground plane (including directly downwards). However, the User's Manual recommends against pointing the jet upwind because of numerical difficulties in solving the model. (The author could not get solutions with the jet pointed directly downward.) Also, if the exit gas velocity is low with respect to the wind speed, and the gas is relatively dense, then solutions may not be reached for vertical jets. The program usually signals this condition with "Stack Downwash" error messages. HFPLUME performs a flashing liquid, choked flow calculation for HF flashing liquid releases, and both models do the expanding jet calculations based upon mass, momentum and enthalpy balances. Also, these two jet models decide whether or not the plume will impact the ground plane or remain elevated, according to criteria of plume density, relative wind speed, release height and angle, etc. If the model impacts the ground, a partial input file will be generated for HEGADAS which contains coupling information so that mass, momentum and energy balances will be maintained for the plume-to-dense cloud (at ground level) transition. If the plume remains elevated, a similar partial input file will be generated for PGPLUME which models far field dispersion by means of the Gaussian model with Pasquill-Gifford dispersion coefficients. The near field models are of the top-hat form, in that only the average concentration in a circular cross-section is output as a function of any downwind distance.

If a normal distribution cross-section is required, the user would have to do these calculations externally, supplying the cross-axis dispersion parameters.

The turbulent jet model in SLAB simulates a jet which may point either straight up from the ground or parallel to the ground. If the jet is vertically-pointing, the plume may remain elevated above the ground or impact the ground as in HGSYSTEM. In the former case, the program internally performs the smoothly continuous mass, momentum and energy balance relationships into far-field Pasquill-Gifford dispersion. Otherwise, transition is made to the ground level dense gas model. All transitions between submodels are made automatically within the single SLAB program; only one input parameter file needs to be input for any applicable release simulation. The basic "stream" input to SLAB is for a circular area source, pointing vertically or horizontally. The initial jet diameter and temperature to be specified are those for the expanded jet. Whether or not the emitted fluid has sufficient velocity and momentum to become airborne (a jet), to generate a dense, slumping cloud at ground level, or to generate a neutral buoyancy cloud at ground level, is determined by the program by means of the input parameters.

The jet model in DEGADIS only points vertically and is essentially based on Oom's model with mass, momentum and thermal energy balances. If the plume remains airborne, a smooth transition is made into the Gaussian dispersion model with Pasquill-Gifford coefficients.★ Otherwise, a transition based upon a mass balance and plume width is made into the ground level, slumping, dense gas dispersion model. The DEGADIS system is composed of a number of stand-alone subprograms wherein the file output of one is linked to the next by means of intermediate files. For ground level area sources, program DEGINP may be used to interactively prepare a DOS BAT file for simulation execution. If a vertical jet is the source batch program, JETPLUIN reads a parameter file to produce a BAT file for the simulation.

The basic output from these jet models is usually the emitted fluid's concentration along the jet axis as well as temperature, diameter, density and angle of the path to the horizontal plane. The plume path locus is usually reported on the basis of Cartesian coordinates for which ground level is zero height and the release point normal plane is the origin for downwind distance.

Dense Gas Models

Generally, the submodels for initial spreading (or slumping) of dense source gas, followed by dispersion along the ground in the direction of the wind, are based upon the same concepts. In HGSYSTEM, the dense gas model is HEGADAS; this submodel is not specifically named in either DEGADIS or SLAB. For the initial condition, the user specifies the initial dimensions of the area source and the total emission rate or flux. If the emitted gas is dense relative to air, and its initial flux is less than that which can diffuse into the wind (the "maximum take-up flux"), then the cloud will spread out. If a steady-state model is used, then the cloud will spread until the total emission rate matches the (cloud area) • (maximum take-up flux) product. In this case, the initial area is immaterial as long as it is small enough to allow spreading, and numerical solution difficulties are not encountered. For a time dependent simulation in which a fixed amount of fluid is released for a finite (generally short) time, the choice of the initial source area could possibly have an important effect upon the calculated dispersion results.

★ At the time of this writing it appeared that only the PG coefficients for **D** stability are used. Also, experiments to simulate less-dense-than-air jetted plumes produced very erroneous results.

All three modeling systems provide for heat transfer from the ground to the (colder) cloud. In SLAB, this function always operates, while in HEGADAS and DEGADIS it is optional.

Concentration isopleth data (crosswind and vertical distances to specified concentrations vs downwind distances) are contained in the standard output files from HEGADAS and DEGADIS, but not from SLAB.

The SLAB output file contains a section which gives the equations and coefficients required to calculate a concentration at any [x,y,z] location and time on the basis of parameters tabulated for each step of downwind distance. These explicit equations involve a number of *error functions* and must be done by an external program which is not supplied. Thus concentration isopleths may be generated for both steady-state and time dependent solutions. Since the equation is explicit in concentration, iterative methods must be used to generate concentration isopleths.

Also, the SLAB output contains crosswind concentrations (volume fraction = mole fraction, $= f_{rm}$) at six normalized crosswind distances (*y/bbc*) for each downwind distance (*x*). The plume half-width, *bbc*, is output along with these concentrations. It turns out that the crosswind dispersion coefficient for the plume is

$$\sigma_y = bbc/\sqrt{3} \tag{1}$$

at downwind distances sufficiently beyond the initial pool spreading for the plume crosswind concentrations to be normally distributed. (This is usually true at distances for which isopleths are of interest.) Therefore, for a constant *x* and *z*, the mole fraction of released material at a given **y** can be calculated by

$$f_{rm}(y) = f_{rm}(0) \cdot exp\left[\frac{-y}{\sqrt{2}\cdot\sigma_y}\right]^2 . \tag{2}$$

The values for $f_{rm}(0)$ are found in the SLAB output column for $y/bbc = 0$. Dropping the subscript *rm*, it may be shown that the crosswind distance, *y*, to a specified released material concentration, **f(y)**, can be found from Equation 7-2 by

$$y = \left[-2\sigma_y^2 \, ln\left(\frac{f(y)}{f(0)}\right)\right]^{1/2} . \tag{3}$$

The above equation was used to calculate concentration isopleths in the far field from SLAB in several scenario simulations presented in this Manual.

Evaporation Submodels

As noted above, only HGSYSTEM among the three systems contains an evaporation rate modeling capability as shown in Table 1.

The SLAB User's Manual often uses the phrase "Evaporative Source Model." However, this means that the discharge mass flow rate and the circular area for the discharge have been determined by some external calculations (if the jet submodel is not employed).

For DEGADIS, as well as for SLAB, the initial mass flow rate and area must be specified.

Time Dependent Modeling

The methods for handling time-varying sources depends upon the modeling system. The transient computations all use the "0.2 Power Law" with Pasquill-Gifford dispersion coefficients (σ_y) to estimate crosswind averaging time effects, but treatments of the additional downwind, travel time effect varies with the system.

If a steady state simulation is performed to model a finite duration, but constant rate release, the travel time to a downwind location (as determined by the wind speed) must be considered with respect to the duration of the release. As the travel time (and therefore downwind distance) to a location increases beyond the release duration time, dispersion in the downwind direction increases.

The above phenomena are managed somewhat differently in the three systems, as discussed below.

SLAB

One can specify a cylinder of dense gas at atmospheric pressure, a cylinder at greater-than-atmospheric pressure (which will expand: an "explosion") or a constant flow rate, evaporating pool source with a finite duration, as input to this model. On starting, the program will begin by spreading of the initial cylinder, or by first expanding, then by spreading for the explosion, or by maintaining the emission rate constant for the specified duration, after which the rate is set to zero. Sets [time value, emission mass flux, release area] for an evaporating pool source cannot be input as can be done for the other two models.

Treatment of averaging time in the downwind direction is accomplished directly in the program by use of a downwind dispersion coefficient, σ_x, coupled with computations of average concentrations at downwind locations according to cloud travel times. For example, the results output for a finite duration release will have been adjusted for averaging time with respect to both the crosswind and downwind distances.

As mentioned above, concentration isopleths can be generated as a function of space and time by an external (user-supplied) program from the standard program output. Also, an *envelope* of concentration isopleths can be generated by utilizing the cloud parameters output as functions of time and distance.

HGSYSTEM

The time dependent version of HEGADAS will accept time-varying input in terms of arbitrary [time value, emission mass flux, release area] sets. These sets apply only to a ground level, evaporating pool type of release which cannot be coupled with a preceding *time varying* turbulent jet. If the simulation involves a constant flow rate, but *finite duration* turbulent jet source (modeled by either the PLUME or HFPLUME steady state models), the jet model may be semi-automatically coupled to the time dependent, ground level, dense gas cloud HEGADAS-T at the point where the plume sinks to ground level. The output from the time dependent program has an "instantaneous" averaging time along the downwind axis but with concentrations averaged according to the specified averaging time with respect to the crosswind axis. A specified averaging time less than or equal to 18.75 seconds is read to mean "instantaneous" by the program. Crosswind averaging times are specified with program input. Concentration averaging time corrections for downwind travel time can be treated by the post-processor programs, HSPOST, HTPOST, for steady state and time dependent HEGADAS programs, respectively. Scenarios 6 and 7 provide further discussions of techniques for time dependent modeling with HGSYSTEM.

If only downwind concentrations are required for a *finite duration* release, but corrected for averaging time in the *downwind direction* (crosswind averaging time is fixed by HEGADAS input), the HSPOST post-processor program can be used to correct the steady state HEGADAS-S output. This will save an inordinate amount of computer and manpower time. See also Chapters 4 and 5. As for the transient case, the desired averaging time must be used for the HEGADAS-S steady-state dispersion calculations.

DEGADIS

The time dependent version of DEGADIS will accept time-varying, area source input in terms of arbitrary [time value, emission mass flux, release area] sets, as for HEGADAS. These sets apply only to a ground level, evaporating pool type of release which cannot be coupled with a preceding turbulent jet. No provision is made for simulations in which a vertical jet, varying with time, couples to the dense gas, ground level cloud dispersion model.

The output from the time dependent program must be considered as instantaneous along the downwind axis. The program suite does not provide for adjustment of dispersion at downwind locations according averaging time; this must be done by an external program (not provided).

Thermodynamic and Physical Properties

DEGADIS, SLAB, or HGSYSTEM all treat air as an ideal gas, and handle water (vapor and liquid) by means of built-in thermophysical property functions; the user specifies the relative humidity.

If a non-reacting, vapor-only release is modeled, the thermodynamic properties of the cloud are calculated by assuming that the released vapor is an ideal gas of given molecular weight and with constant heat capacity. If a multicomponent gas is released, then it can be treated as a pseudo-pure component by appropriately calculating these averaged-value parameters externally (see Chapter 3). However, if the release involves a two-phase fluid (aerosol), then each of the modeling systems operate differently. Three-phase systems are not directly treated by any of the three systems, *e.g.*, simultaneous existence of vapor, released chemical and water liquid, and solid chemical and ice.

SLAB treats a two-phase release in a straightforward manner in which thermodynamic equilibrium is assumed at any instant. The initial liquid mass fraction, an average heat of vaporization, the normal boiling point, liquid and vapor heat capacities, liquid density, and the constants for the saturated vapor pressure function are provided by the user. Thus at any instant (cross-section of the cloud) the concentration of released material in the vapor phase, the concentration of liquid (basis the total vapor and liquid), the temperature, and the bulk density are directly computed. The initial liquid mass fraction can be obtained by means of the methods given in Chapter 3.

HGSYSTEM handles HF by unique, built-in thermodynamic routines which calculate the thermodynamic properties of the cloud by chemical reaction and vapor-liquid equilibria methods. Only the HEGADAS modules have provisions for user input of thermodynamic parameters for pure component, vapor/liquid phase equilibria (aerosols).

DEGADIS uses an externally defined function to treat non-ideal gas and aerosol behavior in its jet and dense cloud models. Input is a set of triplets, each containing:

1) The mole fraction of the released fluid/ambient air mixture.
2) The concentration of total released fluid basis the volume of the total mixture (kg release fluid/m^3).
3) The bulk density of the mixture.

The ordered triplets must go from 100% *ambient* air to pure released fluid; the number of triplets should be sufficient to define the curve for use by linear interpolation. Thus this input data must be generated by an external program, say a spreadsheet, or a special Vapor-Liquid Equilibrium (VLE) program which does the isenthalpic flash calculations for the [released fluid, ambient air] mixtures. Note that DEGADIS uses its isothermal modes, so jet or cloud temperatures must be obtained from the external calculations for the triplets. Thus, the water in the ambient air can most likely be neglected, considering the accuracy of the modeling.

Program Output

For the most part, each of the three modeling systems output the same kind of dispersion information as a function of downwind distance and/or time. This includes centerline concentration, cloud or plume width, temperature, density, etc. With HEGADAS and DEGADIS, the user can specify two concentrations for which horizontal isopleth distances from the centerline are output. In addition, HEGADAS will output vertical isopleths from the ground at the centerline for these two concentrations. SLAB provides concentrations at up to four distances (z) above the ground, and five concentrations at equal interval, normalized distances perpendicular to the centerline.

All three systems provide information in their output files so that point concentrations as a function of downwind, crosswind and vertical distances may be calculated externally.

The forms of the output files are such that they can be imported to other programs (*e.g.*, spreadsheets) for further manipulation and for plotting. HGSYSTEM contains post-processor programs that facilitate combination and preparation of output files for output to plotting programs, etc.

New Version of HGSYSTEM

Version 3 of HGSYSTEM★ was released in late 1995 and has many sorely needed capabilities for accidental release modeling; see Post [II-6b]. (At the time of this final editing, May, 1996, the author is not aware of any new developments for SLAB and/or DEGADIS.) The major, "visible" improvements are:

★ Version 1.0 was used for this manual; Version 2 was never issued.

- A generalized, multicomponent, two-phase *thermodynamic-physical properties subsystem* now provides the physical property and thermodynamic parameters for all source and dispersion submodels. This DATAPROP subsystem currently contains about 30 compounds such as water, inorganic inert gases, lower molecular weight hydrocarbons, hydrogen fluoride (detailed polymerization chemistry), and two fluorohydrocarbon refrigerants. Thus, *flashing single- and multi-component substances are now treated by all of the release rate, turbulent jet, and atmospheric dispersion submodels.*
- The hydrogen fluoride (HF) chemistry and thermodynamic submodel has been extended to handle water, HF, and *inert gas.*
- An initial dense gas, gravity slumping model, HEGABOX, has been made available. This model can be used for *calm air dispersion* on a plane.
- An *evaporating pool* release rate model, LPOOL, has been integrated into the program system. This model is based on Exxon's LSM90 model, of which several features have been noted in the *Evaporation* section of Chapter 3.
- Notable new features added to the time dependent dense gas dispersion model, HEGADAS-T, are:
  - Dry and wet deposition of particles from the plume
  - If the cloud becomes positively buoyant, it can lift off of the ground surface
  - A meteorological preprocessor to better estimate input meteorological parameters (stability, Monin-Obukov length, etc.)
  - Multiple values of the roughness length parameter can be specified for various downwind distances
  - Improved treatment of concentration fluctuations and averaging times
  - Plume confinement by channeling structures (large buildings), and terrain features such as canyons
  - Concentration estimates near upwind and downwind faces of structures, and from sources on buildings, plus other building effects.

APPENDIX III

HGSYSTEM FILE LISTINGS FOR SCENARIO 7

HGSYSTEM File Listings for Scenario 7

In reading the output listings, note that all HGSYSTEM programs ignore any characters to the right of an asterisk (*); these are comments. Blank records are also ignored.

The listings have been annotated to highlight and/or explain items discussed in the Chapter 6 text. Boxes have been added, and ***all comment text is in this format.***

Input file HCLJET.PLI for HGSYSTEM'S PLUME Turbulent Jet Modeling Program

```
TITLE   Base Case Horizontal Jet

GASDATA                   * PHYSICAL PROPERTIES OF GAS
                          *
   TEMPGAS  =  26.85      * CELSIUS        TEMPERATURE OF POLLUTANT
   MFGAS    =  100.0      * PERCENT        MOLE FRACTION OF POLLUTANT
   MFH2O    =  0.0        * PERCENT        MOLE FRACTION OF WATER
   MWGAS    =  36.46      * g/mol          MOLECULAR WEIGHT POLLUTANT
   CPGAS    =  29.08      * J/mol/C        ISOBARIC SPECIFIC HEAT
                          *
PIPE                      * PIPE EXIT-PLANE (CHOKE-FRONT) CONDITIONS
                          *
   DMDT     =  1.064      * KG/S           DISCHARGE RATE
   DEXIT    =  0.0254     * M              EFFECTIVE ORIFICE DIAMETER
   ZEXIT    =  1.00       * M              HEIGHT ABOVE (LEVEL) GROUND
   PHISTK   =  0.000      * DEGREES        RELEASE DISCHARGE ANGLE Zero= Horizontal
   DURATION =  90.        * S              RELEASE DURATION (<0 FOR STEADY)

AMBIENT CONDITIONS        * ATMOSPHERIC AMBIENT CONDITIONS
                          *
   ZO       =  10.0       * M              REFERENCE HEIGHT
   UO       =  3.0        * M/S            WIND VELOCITY AT HEIGHT ZO
   AIRTEMP  =  15.0       * CELSIUS        AIR TEMPERATURE
   AIRPRESS =  1.00       * ATMOSPHERES    AMBIENT PRESSURE
   RHPERC   =  0.0        * PERCENT        RELATIVE HUMIDITY
                          * Can't solve if RH > 0  because of condensation, freezes
DISP                      * DISPERSION DATA
                          *
   ZR       =  0.1        * M              SURFACE ROUGHNESS PARAMETER
   PQSTAB   =  E          *                PASQUILL STABILITY CLASS
                          *
TERMINAT                  * JET/PLUME DEVELOPMENT TERMINATION CRITERIA
                          *
   SLST     =  200.       * M              LAST REQD. DOWNWIND DISP.
   BETLST   =  1E-7       * PERCENT        LAST REQD. POLLUTANT CONCENTRATION
                          *
MATCH                     * MATCHING CRITERIA FOR HEGADAS/PGPLUME
   *   Default Values     *
   RULST    =   .1        *                LAST REQD. ABS. VALUE OF UJET/UAMB-1
   RELST    =   .3        *                LAST REQD. JET/(JET+HEG) ENTRAINM.
   RGLST    =   .3        *                MAX. BUOYANCY EFFECT FOR ADVECTION
   RNLST    =   .1        *                MAX. BUOY. EFF. FOR PASS. DISPERSION
```

Output file HCLJET.PLI from HGSYSTEM'S PLUME Turbulent Jet Modeling Program

```
Output from PLUME      Version NOV90           Title:    Base Case Horizontal Jet             Date: 26/12/93  Time:12:36

 Orifice conditions:                            Atmosphere conditions:                        Flash conditions:

 orifice temperature: 26.85C;                   data reference height: 10.00m;                flash temperature:-59.02C


 orifice pressure: 4.60atm;                     atmosphere temperature: 15.00C;               flash pressure: 1.00atm;
 orifice diameter: 0.03m;                       atmosphere pressure: 1.00atm;                 gas-jet velocity:482.48m/s;
 orifice height: 1.00m;                         relative humidity:  0.00%;                    flash density:   2.07kg/m3;
 orifice mass-flux 1.06kg/s;                    ambient wind-speed: 3.00m/s;                  flash diameter: 0.04m;
 pollutant mass-flux:  1.06kg/s;                atmosphere density: 1.23kg/m3;
 release inclination:  0.00deg;                 surface roughness: 0.1000m;
                                                Pasquill/Gifford class: 'E'.

 Gas Composition:                              Interpretation:                          Interpretation:

 mole-fraction water-vapour: 0.00E-01%;        x:   horizontal displacement (m);        beta:  pollutant mole-concentration(%);
 mole-fraction dry-air: 0.00E-01%;             z:   plume-axis height (m);              r:     jet mean density (kg/m3);
 mole-fraction pollutant gas: 1.00E+02%;       D:   plume effective diameter (m);       c:     pollutant concentration (kg/m3);
 exit-plane relative humidity: 0.00E-01%;      u:   mean plume velocity (m/s);          xx:    mass-fraction pollutant (-);
 pollutant molecular weight:  36.    g/mol;    phi: plume axis inclination (degrees);   hmd:   plume relative humidity (%);
 pollutant specific heat: 0.80    kJ/kg/C;     T:   mean plume temperature (C);         y H2O: plume relative humidity (%);

                                                                                (Column 11, hmd was all zeroes, so it was deleted.)
  1         2         3         4          5          6        7         8         9          10         12  (Columns numbered for text.)
  x         z         D         u         phi         T       beta       r         c         dm/dt       xx

 1.000     1.00     0.353      65.7     -9.853E-04   20.3     11.0      1.24      0.166      7.95      0.134
 2.00      1.00     0.676      34.7     -1.984E-03   18.1     5.61      1.23      8.536E-02  15.3      6.934E-02
 3.00      1.00     1.01       23.6     -2.996E-03   17.0     3.72      1.23      5.683E-02  23.0      4.622E-02
 4.00      1.00     1.34       17.8     -4.016E-03   16.4     2.76      1.23      4.215E-02  31.0      3.430E-02
 5.00      1.000    1.69       14.3     -5.042E-03   16.1     2.17      1.23      3.319E-02  39.4      2.701E-02
 6.00      1.000    2.05       11.9      5.762E-03   15.8     1.77      1.23      2.714E-02  48.2      2.209E-02
 7.00      1.00     2.43       10.4      0.320       15.7     1.53      1.23      2.350E-02  55.6      1.913E-02
 8.00      1.01     2.86       9.39      0.722       15.6     1.37      1.23      2.105E-02  62.1      1.713E-02
 9.00      1.03     3.30       8.60      1.07        15.5     1.25      1.23      1.924E-02  67.9      1.566E-02
 10.00     1.05     3.75       7.98      1.32        15.4     1.16      1.23      1.783E-02  73.3      1.452E-02
 11.0      1.07     4.20       7.46      1.48        15.4     1.09      1.23      1.669E-02  78.3      1.359E-02

 12.0      1.10     4.64       7.03      1.57        15.3     1.03      1.23      1.574E-02  83.0      1.282E-02
  Location of spray curtain barrier

 13.0      1.13     5.08       6.67      1.60        15.3     0.973     1.23      1.494E-02  87.5      1.216E-02
 14.0      1.16     5.52       6.34      1.56        15.3     0.925     1.23      1.421E-02  92.0      1.157E-02
 15.0      1.18     5.91       6.06      1.45        15.2     0.885     1.23      1.359E-02  96.2      1.106E-02
```

```
  16.0     1.21      6.29      5.81     1.39      15.2     0.849     1.23    1.303E-02  100.      1.061E-02
  17.0     1.23      6.68      5.59     1.35      15.2     0.815     1.23    1.252E-02  104.      1.019E-02
  18.0     1.25      7.07      5.38     1.32      15.2     0.785     1.23    1.206E-02  108.      9.815E-03
  19.0     1.28      7.45      5.20     1.31      15.2     0.757     1.23    1.163E-02  112.      9.465E-03
  20.0     1.30      7.84      5.03     1.29      15.1     0.731     1.23    1.123E-02  116.      9.141E-03
  21.0     1.32      8.23      4.87     1.28      15.1     0.707     1.23    1.086E-02  120.      8.841E-03
  22.0     1.34      8.61      4.73     1.27      15.1     0.684     1.23    1.051E-02  124.      8.560E-03
  23.0     1.37      8.99      4.59     1.26      15.1     0.663     1.23    1.019E-02  128.      8.298E-03
  24.0     1.39      9.37      4.47     1.25      15.1     0.644     1.23    9.890E-03  132.      8.053E-03
  25.0     1.41      9.75      4.35     1.24      15.1     0.625     1.23    9.607E-03  136.      7.822E-03
  26.0     1.43      10.1      4.24     1.23      15.1     0.608     1.23    9.340E-03  140.      7.605E-03
  27.0     1.45      10.5      4.14     1.22      15.1     0.591     1.23    9.088E-03  144.      7.400E-03
  28.0     1.47      10.9      4.05     1.21      15.0     0.576     1.23    8.850E-03  148.      7.206E-03
  29.0     1.49      11.3      3.96     1.19      15.0     0.561     1.23    8.625E-03  152.      7.023E-03
```

(Intermediate rows were deleted by the author.)

```
  96.0     2.49      33.1      2.24     0.618     14.8     0.203     1.23    3.114E-03  419.      2.537E-03
  97.0     2.50      33.4      2.24     0.614     14.8     0.200     1.23    3.082E-03  424.      2.510E-03
  98.0     2.51      33.7      2.23     0.609     14.8     0.198     1.23    3.050E-03  428.      2.484E-03
  99.0     2.52      33.9      2.22     0.605     14.8     0.196     1.23    3.019E-03  433.      2.459E-03
 100.0     2.53      34.2      2.22     0.601     14.8     0.194     1.23    2.988E-03  437.      2.434E-03
 101.      2.54      34.5      2.21     0.597     14.8     0.192     1.23    2.958E-03  442.      2.410E-03
 102.      2.55      34.8      2.21     0.594     14.8     0.190     1.23    2.929E-03  446.      2.385E-03
 103.      2.56      35.1      2.20     0.590     14.8     0.189     1.23    2.899E-03  451.      2.362E-03
 104.      2.58      35.4      2.20     0.586     14.8     0.187     1.23    2.871E-03  455.      2.338E-03
 105.      2.59      35.7      2.19     0.583     14.8     0.185     1.23    2.842E-03  460.      2.315E-03
 106.      2.60      36.0      2.19     0.579     14.8     0.183     1.23    2.815E-03  464.      2.293E-03
 107.      2.61      36.3      2.18     0.576     14.8     0.181     1.23    2.787E-03  469.      2.270E-03
 108.      2.62      36.6      2.18     0.572     14.8     0.180     1.23    2.760E-03  473.      2.248E-03
 109.      2.63      36.8      2.17     0.569     14.8     0.178     1.23    2.734E-03  478.      2.227E-03
 110.      2.64      37.1      2.17     0.566     14.8     0.176     1.23    2.708E-03  482.      2.205E-03
 111.      2.65      37.4      2.17     0.563     14.8     0.174     1.23    2.682E-03  487.      2.184E-03
 112.      2.65      37.7      2.16     0.559     14.8     0.173     1.23    2.656E-03  492.      2.164E-03
 113.      2.66      38.0      2.16     0.556     14.8     0.171     1.23    2.632E-03  496.      2.143E-03
 114.      2.67      38.3      2.15     0.553     14.8     0.170     1.23    2.607E-03  501.      2.123E-03
 115.      2.68      38.6      2.15     0.550     14.8     0.168     1.23    2.583E-03  506.      2.104E-03
 116.      2.69      38.9      2.15     0.548     14.8     0.166     1.23    2.559E-03  510.      2.084E-03
 117.      2.70      39.1      2.14     0.545     14.8     0.165     1.23    2.535E-03  515.      2.065E-03
 118.      2.71      39.4      2.14     0.542     14.8     0.163     1.23    2.512E-03  520.      2.046E-03
 119.      2.72      39.7      2.14     0.539     14.8     0.162     1.23    2.489E-03  525.      2.028E-03
 120.      2.73      40.0      2.13     0.537     14.8     0.160     1.23    2.467E-03  530.      2.009E-03
 121.      2.74      40.3      2.13     0.534     14.8     0.159     1.23    2.444E-03  534.      1.991E-03
 122.      2.75      40.6      2.13     0.532     14.8     0.158     1.23    2.423E-03  539.      1.973E-03
 123.      2.76      40.8      2.12     0.529     14.8     0.156     1.23    2.401E-03  544.      1.956E-03
 124.      2.77      41.1      2.12     0.527     14.8     0.155     1.23    2.380E-03  549.      1.938E-03
 125.      2.78      41.4      2.12     0.524     14.8     0.153     1.23    2.359E-03  554.      1.921E-03
 126.      2.79      41.7      2.12     0.522     14.8     0.152     1.23    2.338E-03  559.      1.904E-03
 127.      2.79      41.9      2.11     0.520     14.8     0.151     1.23    2.325E-03  562.      1.894E-03
 127.      2.79      41.9      2.11     0.520     14.8     0.151     1.23    2.325E-03  562.      1.894E-03
```

Input File BASECASE.HSI for HEGADAS-S Steady State Modeling

```
TITLE Base Case -- No mitigaton
 CONTROL * HEGADAS Control Flags Datablock.
   ICNT=   0              * flag controlling contour generation (-).
   ISURF=   2             * flag for no plume/ground heat transfer (-).
 AMBIENT * Ambient Atmosphere Datablock.
   ZAIRTEMP=  1.00        * height of temperature measurement (m).
   AIRTEMP=   15.0        * ambient (air) temperature (C).
   Z0=        10.0        * height of wind-speed measurement (m).
   U0=        3.00        * ambient wind-speed (m/s).
   RHPERC=   0.0          * atmosphere relative humidity (%).
   TGROUND =  15.0         * C earth's surface temperature
 DISP * farfield/heavy-gas dispersion Data.
   ZR=       0.100        * surface roughness height (m).
   PQSTAB=     E          * Pasqill/Gifford stability class.
   AVTIMC=    10.0        * concentration averaging time (s).

 GASDATA * Released gas Datablock.
   THERMOD=    1          * thermodynamic model flag (-).
```

```
    GASFLOW=    1.064        * HF mass flow-rate dry gas (kg/s).
```

Text Symbol is E^{BR}. Reduced to 7 % of this value for spray removal runs.

```
   CPGAS=     29.08       * specific heat of gas (J/mol/C).
   MWGAS=     36.46       * molecular weight of gas (g/mol).
   GASFRAC=   1.00        * mole fraction pollutant in released gas (-).
   HEATGR=    20.0        * ground heat transfer factor (-).
   WATGAS=   0.0          * mole-fraction water in released gas (-).
   TEMPGAS=  -59.0        * gas temperature immediately upon release (C).
 TRANSIT * PLUME/HEGADAS Transition Datablock.
```

The parameters in these two boxes below were changed according to Table S7-4 of the Chapter 6 text. (DISTS = 12.0)

```
  DISTS=    127.          * downwind distance from release point (m).
     CONCS=   2.139E-03      * center-line ground-level molar gas fraction (-).
     WS=      -17.4          * heavy-gas plume half-width (signed flag) (m).
```

DISTS = 12.0 for finite duration releases.
This is the parameter CONCS, changed per mitigation case.
This is the negative value of the parameter BEFF.

```
CLOUD * Output control datablock.
   DXFIX=    4.0          * arithmetic progression step length (m).
   NFIX=     20           * maximum number of (arithmetic) steps (-).
   XGEOM=    1.20         * scale factor for geometric series (-).
   XEND=    10000         * last required downwind distance (m).
   CU=      1.49E-04      * inner contour concentration (kg/m3).
   CL=      7.45E-06      * outer contour concentration (kg/m3). = 100ppm
   CAMIN=   7.40E-06      * last required gas concentration (kg/m3). = 5 ppm
```

Input File SCENARO7.HTI for HEGADAS-T Time Dependent Modeling

```
TITLE   Zr = 0.1m, Spray on 90s, HCl stopped in 270s, AVTIMC = 10S, 2/16/95

  CONTROL * HEGADAS Control Flags Datablock.

    ICNT=     0             * flag controling contour generation (-).
    ISURF=    2             * Flag indicating plume/ground heat transfer .

  AMBIENT * Ambient Atmosphere Datablock.

    ZAIRTEMP=  1.00         * height of temperature measurement (m).
    AIRTEMP=   15.0         * ambient (air) temperature (C).
    Z0=        10.0         * height of wind-speed measurement (m).
    U0=         3.00        * ambient wind-speed (m/s).
    RHPERC=   0.0           * atmosphere relative humidity (%).
    TGROUND =  15.0          * C earth's surface temperature

  DISP * Pasquill/Gifford Dispersion Data.

    ZR=      0.100          * surface roughness height (m).
    PQSTAB=    E            * Pasquill/Gifford stability class.
    AVTIMC=    10.          * concentration averaging time (s).

  GASDATA * Released HF-gas Datablock.

    THERMOD=     1          * thermodynamic model flag (-).
    CPGAS=      29.08       * specific heat of gas (J/mol/C).
    MWGAS=      36.46       * molecular weight of gas (g/mol).
    GASFRAC=    1.00        * mole fraction pollutant in released gas (-).
    HEATGR=     20.0        * ground heat transfer factor (-).
    WATGAS=    0.0          * mole-fraction water in released gas (-).
    TEMPGAS=   -59.0        * gas temperature immediately upon release (C).

  CALC * Output times Datablock.

      TSTAR=     150.        * Observer output times (s).
      TSTAR=     200.        * Observer output times (s).
      TSTAR=     250.        * Observer output times (s).
      TSTAR=     300.        * Observer output times (s).
      TSTAR=     400.        * Observer output times (s).
      TSTAR=     600.        * Observer output times (s).
      TSTAR=    1000.        * Observer output times (s).
      TSTAR=    2000.        * Observer output times (s).
```

These are the specified times for the concentration vs. downwind distance "snapshots" to be recorded in the output file.

```
CLOUD * Output control datablock.

    XSTEP=    25.           * (fixed) output step-length (m).
    CU=       1.49E-04       * inner contour concentration (kg/m3). = 100ppm
    CL=       7.45E-06       * outer contour concentration (kg/m3). = 5 ppm
    CAMIN=    1.49E-06       * last required gas concentration (kg/m3). 1 ppm

TRANSIT                *       Plume - cloud transition data block

  DISTS=       12.0    *       Downwind distance for the transition

TIMEDATA      0, 2     *       Time dependent data block

TSTPOOL =         0    *       Start time, s (Time to 15 m neglected.)
TSTEPR           5     *       Time step size, s

*
* BRKDATA records are [Effective half-width, Centerline HF mole fraction,
*    HF mass flow rate through the transition plane] per ITYPBR = 2.

*          BEFF        CONCS        Ebr       *    Time,s    Number
 * Initial Release:
BRKDATA = 1.9326     1.4523e-02     1.0640        *    0     1
BRKDATA = 1.9326     1.4523e-02     1.0640        *    5     2
BRKDATA = 1.9326     1.4523e-02     1.0640        *    10    3
BRKDATA = 1.9326     1.4523e-02     1.0640        *    15    4
BRKDATA = 1.9326     1.4523e-02     1.0640        *    20    5
BRKDATA = 1.9326     1.4523e-02     1.0640        *    25    6
BRKDATA = 1.9326     1.4523e-02     1.0640        *    30    7
BRKDATA = 1.9326     1.4523e-02     1.0640        *    35    8
BRKDATA = 1.9326     1.4523e-02     1.0640        *    40    9
BRKDATA = 1.9326     1.4523e-02     1.0640        *    45    10
BRKDATA = 1.9326     1.4523e-02     1.0640        *    50    11
BRKDATA = 1.9326     1.4523e-02     1.0640        *    55    12
BRKDATA = 1.9326     1.4523e-02     1.0640        *    60    13
BRKDATA = 1.9326     1.4523e-02     1.0640        *    65    14
BRKDATA = 1.9326     1.4523e-02     1.0640        *    70    15
BRKDATA = 1.9326     1.4523e-02     1.0640        *    75    16
BRKDATA = 1.9326     1.4523e-02     1.0640        *    80    17
BRKDATA = 1.9326     1.4523e-02     1.0640        *    85    18
BRKDATA = 1.9326     1.4523e-02     1.0640        *    90    19
*  Following 3 records for smoother transition to help convergence
BRKDATA = 2.2515     1.0985e-02     8.1663e-01    *    95    21
BRKDATA = 2.5703     7.4460e-03     5.6925e-01    *    100   22
BRKDATA = 2.8892     3.9075e-03     3.2188e-01    *    105   23
*  Spray curtain turned on:                       *          24
BRKDATA = 3.2080     3.6900e-04     7.4500e-02    *    110   25
BRKDATA = 3.2080     3.6900e-04     7.4500e-02    *    115   26
BRKDATA = 3.2080     3.6900e-04     7.4500e-02    *    120   27
```

This BRKDATA section specifies the vapor cloud source parameters as an arbitrary function of time. The TRANSIT block above shows that these parameters take effect at a distance of 12 meters downwind of the actual source (center) location.

Each record specifies the effective cloud half width, the centerline mole fraction of HCl, and the HCl mass flow rate for elapsed time.

```
BRKDATA = 3.2080      3.6900e-04      7.4500e-02      *     125  28
BRKDATA = 3.2080      3.6900e-04      7.4500e-02      *     130  29
BRKDATA = 3.2080      3.6900e-04      7.4500e-02      *     135  30
BRKDATA = 3.2080      3.6900e-04      7.4500e-02      *     140  31
BRKDATA = 3.2080      3.6900e-04      7.4500e-02      *     145  32
BRKDATA = 3.2080      3.6900e-04      7.4500e-02      *     150  33
BRKDATA = 3.2080      3.6900e-04      7.4500e-02      *     155  34
BRKDATA = 3.2080      3.6900e-04      7.4500e-02      *     160  35
BRKDATA = 3.2080      3.6900e-04      7.4500e-02      *     165  36
BRKDATA = 3.2080      3.6900e-04      7.4500e-02      *     170  37
BRKDATA = 3.2080      3.6900e-04      7.4500e-02      *     175  38
BRKDATA = 3.2080      3.6900e-04      7.4500e-02      *     180  39
BRKDATA = 3.2080      3.6900e-04      7.4500e-02      *     185  40
BRKDATA = 3.2080      3.6900e-04      7.4500e-02      *     190  41
BRKDATA = 3.2080      3.6900e-04      7.4500e-02      *     195  42
BRKDATA = 3.2080      3.6900e-04      7.4500e-02      *     200  43
BRKDATA = 3.2080      3.6900e-04      7.4500e-02      *     205  44
BRKDATA = 3.2080      3.6900e-04      7.4500e-02      *     210  45
BRKDATA = 3.2080      3.6900e-04      7.4500e-02      *     215  46
BRKDATA = 3.2080      3.6900e-04      7.4500e-02      *     220  47
BRKDATA = 3.2080      3.6900e-04      7.4500e-02      *     225  48
BRKDATA = 3.2080      3.6900e-04      7.4500e-02      *     230  49
BRKDATA = 3.2080      3.6900e-04      7.4500e-02      *     235  50
BRKDATA = 3.2080      3.6900e-04      7.4500e-02      *     240  51
BRKDATA = 3.2080      3.6900e-04      7.4500e-02      *     245  52
BRKDATA = 3.2080      3.6900e-04      7.4500e-02      *     250  53
BRKDATA = 3.2080      3.6900e-04      7.4500e-02      *     255  54
BRKDATA = 3.2080      3.6900e-04      7.4500e-02      *     260  55
BRKDATA = 3.2080      3.6900e-04      7.4500e-02      *     265  56
BRKDATA = 3.2080      3.6900e-04      7.4500e-02      *     270  57
```

The three cloud parameters are set to zero by the program for all times after 270 seconds.

INDEX

INDEX

Note: Appendices I and III are not indexed

232pp

11963C1P

American Petroleum Institute

1220 L Street, Northwest
Washington, D.C. 20005
202-682-8000
http://www.api.org

Order No. I46280